Systems Analysis of an Astrophysics Mission Utilizing Electric Propulsion

by

Bhavesh T. Patel

B.Eng., Aerospace Systems
University of Southampton (UK), 1993

Submitted to the Department of
Aeronautics and Astronautics in Partial Fulfillment of
the Requirements for the Degree of

MASTER OF SCIENCE
in Aeronautics and Astronautics

at the

MASSACHUSETTS INSTITUTE OF TECHNOLOGY

September 1995

Signature of Author .....
Department of Aeronautics and Astronautics
August 21, 1995

Certified by .....
Professor Manuel Martinez-Sanchez
Department of Aeronautics and Astronautics
Thesis Supervisor

Accepted by .....
Professor Harold Y. Wachman
Chairman, Departmental Graduate Committee

Systems Analysis of an Astrophysics Mission Utilizing Electric Propulsion

by

Bhavesh T. Patel

Submitted to the Department of Aeronautics and Astronautics
on August 21, 1995 in partial fulfillment of the requirements for the
degree of Master of Science in Aeronautics and Astronautics

Abstract

The Energetic Transient Array (ETA) is a mission, proposed by the Center for Space Research (CSR) at MIT, to set up an interplanetary constellation of six microsatellites for Gamma Ray Burst (GRB) astrometry. The microsatellites will be deployed into distinct heliocentric orbits by a carrier spacecraft which will be propelled by a stationary plasma (SPT-70) electric thruster.

This thesis documents the analysis carried out for the ETA constellation design. It addresses ETA system design from the systems engineering standpoint, with emphasis on constellation and propulsion system issues. Beginning with scientific requirements, the most important of which is GRB localization accuracy, systems engineering tools are applied to define trade options, system requirements, architecture and interfaces. Requirements flowdown to the constellation level enables an assessment of propulsion options through a top level trade study. This has resulted in the selection of the SPT-70 propulsion system for the carrier spacecraft. Constellation analysis, consisting of trade studies, includes consideration of design aspects such as number of microsatellites, SPT-70 thrusting direction and duration. A figure-of-merit, which is directly related to GRB localization accuracy, has been used to assess trade options. Results of trade studies have been synthesized into a mission scenario for ETA. The carrier spacecraft will deploy the six microsatellites over an 11 month period interspersed with SPT thrusting. Retrograde SPT thrusting provides rapid constellation development for commencement of scientific operations two years after launch. This thrusting strategy also results in closer proximity of the spacecraft to the Sun, simplifying spacecraft design, specifically of the power system. The impacts of constellation design on the system are identified by an overview of carrier, microsatellite and ground system designs. Programmatic issues such as cost, schedule, risk and management are discussed to complete the ETA systems analysis. The system level perspective allows an appreciation of system inter-relationships through assessment of constellation design impacts on other system elements.

This study has developed a mission scenario for the ETA mission as well as addressing the top level system design problem from a systems engineering perspective.

Thesis Supervisor : Manuel Martinez-Sanchez
Title : Professor of Aeronautics and Astronautics, MIT

Acknowledgments

My arduous but enlightening trek, from the inception to culmination of this project, has been facilitated by a lot of people. I would like to take this opportunity to express my gratitude to everyone for enabling me to accomplish this task. This thesis is as much yours as mine.

Professor Manuel Martinez-Sanchez for having faith in my abilities and giving me the opportunity to work on this project. Your friendly, helpful nature as well as your plethora of knowledge have made this a wonderful learning experience for me.

Dr. George Ricker, program manager of ETA, for allowing a "rookie" to be part of a team of "seasoned professionals". I have thoroughly enjoyed working on ETA. Thanks for coming up with such a unique space mission!

"It is the supreme art of the teacher to awaken joy in creative expression and knowledge"

- Attributed to Albert Einstein.

It has been a privilege for me to have been mentored by Professors with a phenomenal amount of knowledge, experience and achievements. Professor Stanley Weiss for advancing my knowledge of Systems Engineering. Visiting Professor Bob Lovell for teaching a budding engineer how to "get the right rocks" for his manager! My sincere gratitude to you both, Sirs, for providing guidance on my future and enabling career directions I could never have dreamed of. Professor Richard Battin for stimulating my interest in Astrodynamics and giving advice on the trajectory analysis carried out in this thesis. Professor Amedeo Odoni, my academic advisor, for guiding me through the course at MIT.

Thanks are also due to all members of the ETA team for making this a memorable initiation into Space Systems engineering for me. John Doty, Francois Martel and Kevin Hurley for your time and patience. Sandy Alexander for being such a great person to work with and teaching me the practical aspects of microspacecraft engineering. Dennis Tilley for providing material for the thesis. Special thanks to you both for taking the time to review the thesis as well.

"Wherever you are, it is your own friends who make your world"

- William James in "The Thought and Character of William James"

I have had many friends to share the highs and lows of life at MIT. Stacy Weinstein for being such a great friend ever since we worked on the Pluto mission two years ago. Thank you for encouraging me to study at MIT and being there when I needed advice. Graham

Swinerd for introducing me to Spacecraft Systems Engineering. It's great fun "doing all those good things!". Jec Gone for helping me settle down when I arrived at MIT and being very supportive since then.

A most rewarding experience at MIT has to be getting to work with highly motivated and extremely helpful friends and colleagues. My quest for knowledge has been spurred on by very intelligent classmates. Susanne Schroll and Mike Violet for assisting with the thesis and showing me how to work hard. Amir R. Amir for the friendship and support ever since I have been here. Cary Gumbert and Graeme Shaw for discussing things as diverse as Link Budgets and Soccer at weird hours of the night! It has been great fun learning with all of you folks. Thanks also to the "Chicos" for introducing me to softball and providing hours of "slugging" pleasure!

My family has always been there for support at all times. Many a time when I have been bogged down with one problem or another, the rays of hope have emanated from the cute smiles of my niece, Vaishali, and nephew, Meghal. Your efforts are highly appreciated! Here's to hoping that you become fascinated by the realm of space and the spacecraft that traverse its expanse!!

My sisters have pitched in with affection and words of encouragement whenever I have been down in the dumps. Thanks for making me feel so important and putting up with me all this time!

This work is dedicated to my Mother and my Father as a meagre token of appreciation for the love and blessings they continually shower upon me. Thank you for backing me all the way to realizing my dream.

"Life's battle doesn't always
go to the stronger or faster man,
but sooner or later the man who wins
is the man who thinks he can"

Table of Contents

List of Figures

List of Tables

List of Acronyms

AO	Announcement of Opportunity
ATF	Inter-Agency Transfer of Funds
AU	Astronomical Unit
AXAF	Advanced X-ray Astrophysics Facility
BACODINE	BATSE Coordinate Distribution Network
BATSE	Burst And Transient Source Experiment
BER	Bit Error Rate
C_3	Launch Energy (square of hyperbolic excess velocity)
CCD	Charge Coupled Device
c.g	center-of-gravity
CGRO	Compton Gamma Ray Observatory
CSR	Center for Space Research, MIT
DC	Direct Current
DCU	Digital Control Unit
D/NAR	Design/Non-Advocate Review
DOD	Department Of Defense
DSN	Deep Space Network
ΔV	Velocity Difference
EIRP	Equivalent Isotropic Radiated Power
EP	Electric Propulsion
ETA	Energetic Transient Array
FY	Federal Year
GEO	Geostationary Earth Orbit
GNC	Guidance, Navigation and Control
GRB	Gamma Ray Burst
G/T	Gain over Temperature (Receiver Figure of Merit)
HETE	High Energy Transient Experiment
HST	Hubble Space Telescope
ICD	Interface Control Document
I/O	Input/Output
IPN	Inter-Planetary Network
IR	Infra-Red
ISEE-3	International Sun-Earth Explorer 3
I_{sp}	Specific Impulse
ISTI	International Space Technology Inc.
L_1, L_2	Lagrange or Libration Points
LEO	Low Earth Orbit
LeRC	NASA Lewis Research Center
LNA	Low Noise Amplifier
MIL-STD	Military Standard
MSTI	Miniature Sensor Technology Integration
MIT	Massachusetts Institute of Technology
MOC	Mission Operation Center

MODA	Mission Operations and Data Analysis
MOU	Memorandum Of Understanding
NASA	National Aeronautics and Space Administration
N^2	N-squared
NRAO	National Radio Astronomy Observatory
OGAL	Orbit Going Around a Libration point
PDU	Power Distribution Unit
PI	Principal Investigator
PM	Program Manager
PMA	Propellant Management Assembly
PMT	Photo Multiplier Tube
PPU	Power Processing Unit
PVO	Pioneer Venus Orbiter
R&D	Research and Development
RF	Radio Frequency
RPM	Revolutions Per Minute
RSM	Radiation Storm Monitor
SDC	Science Data Center
SE	Systems Engineering
SEP	Systems Engineering Process
SERT	Space Electric Rocket Test
SOCC	Spacecraft Operations Control Center
SOHO	Solar and Heliospheric Observatory
SPT	Stationary Plasma Thruster
SPT-70	Stationary Plasma Thruster with 70 mm diameter discharge chamber
SPT-100	Stationary Plasma Thruster with 100 mm diameter discharge chamber
SRM	Solid Rocket Motor
SS/L	Space Systems Loral
TCM	Trajectory Correction Maneuver
TCS	Thermal Control System
TOA	Time-Of-Arrival
TSU	Thruster Selection Unit
UV	Ultra-Violet
VLBI	Very Long Baseline Interferometry
WWW	World Wide Web
XFC	Xenon Flow Controller
XIPS	Xenon Ion Propulsion System

Chapter 1

Introduction

> *"Gamma Ray Bursts (GRB's) are a deep and abiding mystery. Despite 20 years of intense study by observers and theorists, no one knows for sure what they are, where they come from, or even whether they are a single phenomenon.....accurate localization of GRB's provides a powerful means of attacking the question.....the concept of measuring GRB positions from times-of-arrival at independent spacecraft separated by interplanetary distances is an obvious choice." [1, 2]*

> *"Utilization of solar powered electric propulsion offers advantages over competing propulsion systems for a number of deep space missions. These advantages can include increased payload, reduced flight time, increased observational time at target, and utilization of smaller launch vehicles." [3]*

The synergistic alliance of these thoughts has resulted in the Energetic Transient Array (ETA) mission, an astrophysics mission proposed by the Center for Space Research (CSR) at MIT [4]. ETA promises to not only break new ground in the study of Gamma Ray Bursts (GRB's), but also blaze the trail for the effective amalgamation of electric propulsion and microspacecraft technology for deep space missions.

This report is the result of the analysis and design carried out by the author to support the development of mission and system concepts for ETA. The thesis involved a systems analysis of the ETA system, together with the design of the constellation deployment and subsequent development scenario for ETA. This chapter provides an overview of the ETA mission, which then leads onto the context in which the research was carried out and what the objectives for the thesis were. The order of presentation of material in this report is laid out in the thesis outline.

1.1 Mission Overview

The Energetic Transient Array (ETA) is a low cost, multiple microsatellite mission, proposed by the Center for Space Research (CSR) at MIT, to set up a dedicated interplanetary network for Gamma Ray Burst (GRB) astrometry [4]. Six microsatellites, each equipped with 4 GRB detectors, will be deployed into ~1 AU heliocentric orbits by a carrier spacecraft which will be propelled by a stationary plasma electric thruster (SPT-70). The constellation will develop within 2 years to provide sufficient baselines for localizing GRB's with unprecedented accuracy and frequency.

The distance, origin and nature of GRB's are issues which have remained unresolved ever since the first GRB measurements were made in the late 1960's, making them one of the most enduring and perplexing scientific mysteries of the latter half of the 20th century. Accurate GRB source localization and timely dissemination of data are instrumental in determining whether GRB's repeat and whether GRB counterparts exist at other wavelengths. Such information is necessary to test models and theories of GRB sources. Moreover, the identification of GRB counterparts would allow more powerful resources such as the Compton Gamma Ray Observatory (CGRO) and Hubble Space Telescope (HST) to be committed to the search for GRB sources.

The positions of GRB's are determined by measuring their times-of-arrival at independent spacecraft separated by interplanetary distances. Measurements onboard interplanetary spacecraft like Ulysses and Pioneer Venus Orbiter (PVO) have been both inaccurate and infrequent, primarily due to mismatched detector sensitivities as well as sub optimal interplanetary spacings. Over a period of 2 years, the dedicated ETA will localize about 800 GRB's to higher accuracies than previously achieved by any other observations, including both interplanetary spacecraft and Earth orbiting observatories and satellites. Accuracies of up to 1 arcsecond will be achieved, compared to 1 arcminute from the best current GRB astrometry systems. Thus, ETA will provide the scientific community with more accurate data on more GRB's than was previously possible.

The ETA space segment is set up in such a way as to provide the baselines necessary for accurate GRB localization, while facilitating dissemination of data in near real-time for follow-on observations by other observatories.

The times-of-arrival of GRB's at the microsatellites will be measured by the process of template matching. When a GRB occurs, the detectors on the microsatellites will be triggered and GRB data will be stored in the onboard solid state memory; storage capacity to accomodate more than a full day's worth of data will be provided. Two "trigger" satellites, in orbits within close proximity of Earth (0.02-0.04AU), will have sufficiently high datarates to downlink the full burst profile in real-time. The purpose of this is twofold: first, this allows a near real-time alert capability to direct more powerful Earth-based observation assets towards the GRB localization zone to search for GRB counterparts; secondly, this will minimize the downlink datarate requirements on the rest of the microsatellites which may be as far away as 2 AU. Ground processing will determine which of the burst profiles downlinked by the trigger satellites is interesting and a GRB template will be pre-

pared for uplinking to the other microsatellites. Template correlation will be carried out onboard to determine the times-of-arrival and only this data and a correlation confidence factor need then be telemetered back to Earth. This method of data acquisition thus avoids the need to downlink large amounts of data over distances approaching 2 AU, thereby simplifying the design of the microsatellites.

The constellation of 6 microsatellites needs to be deployed in an optimal manner to achieve the minimum distribution necessary for science activities to commence in the time specified by program requirements. In order to achieve this, the microsatellites will require large velocity differences (ΔV) relative to each other to achieve the constellation "spread". This, in unison with the cost limit (and hence mass limit) imposed on the program, requires a propulsion system with a high specific impulse (I_{sp}) for the deployment spacecraft (carrier spacecraft), in order to maximize ΔV while minimizing launch mass. Electric propulsion (EP), with its inherently high I_{sp} , is an ideal candidate for the mission. The preconceived notion of the immaturity of EP technology does not apply here since the carrier spacecraft will be propelled by the Russian-developed Stationary Plasma Thruster (SPT-70), a highly reliable and flight proven system. More than 50 SPT's have been flown on Russian spacecraft and over 10,000 hours of ground testing have already been accumulated in the US. The utilization of the SPT-70 and flight proven microspacecraft technology enable mission objectives to be achieved with the Delta-Lite launch vehicle, a smaller version of the Delta II.

The Delta-Lite launch vehicle will place the spacecraft stack (carrier and microsatellites) on an escape trajectory with a small injection energy (C_3). After a coasting phase of 85 days, the SPT-70 is fired for a period of 30 days before deployment of the first two microsatellites together, the orbits of which go around the Sun-Earth L_1 and L_2 libration points. These "trigger" satellites are always within 0.04 AU of Earth, enabling high rate communications. The rest of the microsatellites are deployed after thrusting times of 50-70 days between deployments, with shorter thrusting times as the carrier spacecraft mass decreases with each deployment. The sixth and final microsatellite is deployed about 11 months after launch. The retrograde (anti-velocity) direction of SPT-70 thrusting causes the constellation to develop within the inner reaches (inside Earth's orbit) of the solar system. This is advantageous in terms of quicker constellation development and positive impacts on spacecraft issues such as power generation.

The constellation will develop into a ~120° spread after 2 years, ~180° spread after 3 years and almost ~360° spread after 4 years. This scenario will provide over 2 years for routine high quality GRB astrometry. The space segment will be supported by a ground network including MIT's Haystack Antenna, the National Radio Astronomy Observatory in West Virginia and the Goldstone facility of the Deep Space Network (DSN).

ETA is scheduled for launch in the year 2000. The mission is estimated to cost under $70 million, which includes 20% contingency. The program will be managed in the Principal Investigator (PI) mode. Coordination of the multitude of universities, NASA centers, government laboratories and industrial contractors participating in the ETA program will be

managed by CSR/MIT, which has extensive experience in the management of space missions. Program risk is managed in a variety of ways. Technical risk is mitigated through the use of flight proven and reliable SPT technology and heritaged spacecraft designs. Accurate cost estimation based on previous CSR flight project experience and the incorporation of contingency in the overall program cost will minimize the chances of cost overruns. The mission is not constrained by any stringent launch window requirements. Schedule delays will be avoided through the inclusion of formal time contingencies in the mission schedule. Long lead-time items such as the development of Western electronics for the SPT-70 propulsion system are already underway.

ETA is unique in that it will unravel the secrets of GRB's, one of the most heralded mysteries of astrophysics, through a low cost mission which provides the opportunity to demonstrate electric propulsion, microspacecraft technology and distributed system concepts in an interplanetary setting.

1.2 Thesis Objectives

The current conceptual design phase of the ETA program allows one to maintain a system-wide perspective to appreciate the systems engineering implications, while performing analysis and design for a specific system element. It is thus possible to study the inter-relationships between a number of interesting engineering disciplines in the context of the mission.

The author was part of a team of professional scientists and engineers developing various aspects of the mission. Even though the primary responsibilities were in the areas of constellation design and SPT-70 implementation issues, the program provided an environment in which the author, from the perspective of academic research, was able to study the practical aspects of the following subject areas:

- **Systems Engineering**
  The design, development and operation of a complex system such as ETA requires a systematic approach which can enable system optimization against a variety of constraints. Because ETA is in the early phases of development, it was possible to apply systems engineering methodologies from the top level to lower levels of the system and assess the impact of driving system requirements. Requirements and interfaces could be derived from the functional characterization of the system for subsequent flowdown to lower levels in order to conduct trade studies and design the system. Consideration with regard to programmatic, budgetary and schedule constraints was also necessary.

- **Constellation Deployment/Development**
  The constellation has to be deployed in an optimal way with regard to a large number of requirements and constraints based on scientific measurement strategy, mission timelines, launch vehicle performance, electric thruster performance characteristics, data downlink strategy,

microsatellite design and so forth. The constellation analysis therefore provides an ideal focal point for the systems analysis presented in this thesis. Furthermore, the optimization of the deployment and subsequent development of the constellation provided an interesting problem in astrodynamics since the essentially Keplerian-type orbits of the microsatellites are coupled to the low-thrust trajectory of the carrier spacecraft. The orbit design for the near-Earth trigger satellites was another interesting issue that had to be considered.

- **Implementation of the SPT-70 electric thruster**
  The flight proven Russian Stationary Plasma Thruster (SPT-70) will provide the propulsion required by the carrier spacecraft to deploy the microsatellites. ETA will be the one of the first space missions to test Electric Propulsion technology in an interplanetary setting. The invaluable experience gained will pave the way for deep space missions which were previously unfeasible. This study focused on the applications aspects of the SPT-70, and issues related to hardware, spacecraft/ thruster interactions and thruster operation strategies were to be addressed.

- **Microsatellite/Carrier Spacecraft Design**
  ETA has the potential to provide a benchmark for future low cost, multiple microsatellite missions. The design of the microsatellites is challenging in that there are severe constraints on power, antenna gain, available mass and volume. Interface and contamination issues have to be addressed when integrating the SPT-70 with the rest of the carrier spacecraft. The author assisted the prime contractor in the design of the carrier spacecraft and microsatellites, through the provision of design input and feedback from the perspective of the constellation and electric propulsion analysis. This allowed the author to learn about the practical aspects of spacecraft design.

The project therefore permitted the study and application of systems engineering, astrodynamics, electric propulsion, microspacecraft design and general spacecraft systems engineering in an integrated context. The "real-world" program environment provided project experience as well as an understanding of other issues such as program management, cost, schedule and risk.

In light of the fact that this report would serve the dual purpose of documenting the study as well as providing a system-wide overview of the ETA mission, the following objectives were defined for this systems thesis:

> This study is a systems analysis of the ETA mission. The emphasis will be on applying the methodology of systems engineering to the mission, identifying and flowing down system requirements, interfaces and constraints to the constellation level and assessing the

impact of changing these due to various scientific, hardware (SPT-70 and spacecraft) and program management related issues. The focus for the study will be the constellation analysis since it provides an area for detailed design analysis and a central point of the system for studying systems engineering aspects. It will also fulfill the reseacher's responsibilities as a member of the ETA design team. The implementation aspects of the electric propulsion system will be addressed. A secondary objective of the thesis is to produce a report presenting a system-wide overview of the ETA mission.

1.3 Thesis Outline

The order of presentation of material in this report is outlined in Figure 1-1. Even though the process of analysis and design is iterative, an effort has been made to impart some sort of logical flow to the thesis. The iterative nature of the process will manifest itself as presentation of details before they are formally discussed. The overall content of the report is geared towards the systems perspective of this thesis, with the focus being the constellation analysis and design presented in Chapter 6. Discussions prior to that primarily set the stage in terms of defining requirements and constraints which impact the constellation design. The constellation itself identifies other constraints and derived requirements which have an effect on other system elements such as the spacecraft designs; these discussions are presented after the constellation analysis.

Chapter 2 introduces the scientific problem that ETA will address. The mission concept and science requirements will form the basis for applying systems engineering methodologies in a more formal manner in Chapter 3. This chapter presents the methodology and application of systems engineering principles to the ETA mission. The reader familiar with systems engineering methodologies can move directly to the applications section which comes after the discussion on methodology. The results of this chapter constitute definition of the system architecture and a set of system requirements which will provide inputs to later design sections. The first part of Chapter 4 will flow down the system requirements to the constellation level. A number of propulsion options, capable of meeting system requirements, will be identified for the carrier spacecraft. A top level trade study will be presented to select the propulsion system, the details of which will be presented in Chapter 5. It is necessary to discuss the propulsion system first since it imposes constraints that directly influence the design of the constellation, elaborated upon in Chapter 6. The impact of constellation design inputs on system design will be addressed in Chapter 7 where an overview of the current system design is given. Once the mission and system concepts have been defined, it is possible to delve a bit into the discussion of program level issues such as cost, schedule and risk; this is done in Chapter 8. Chapter 9 completes the report with conclusions drawn from the study, a summary of the baseline mission scenario, indication of pertinent hardware development issues and identification of areas which warrant further work.

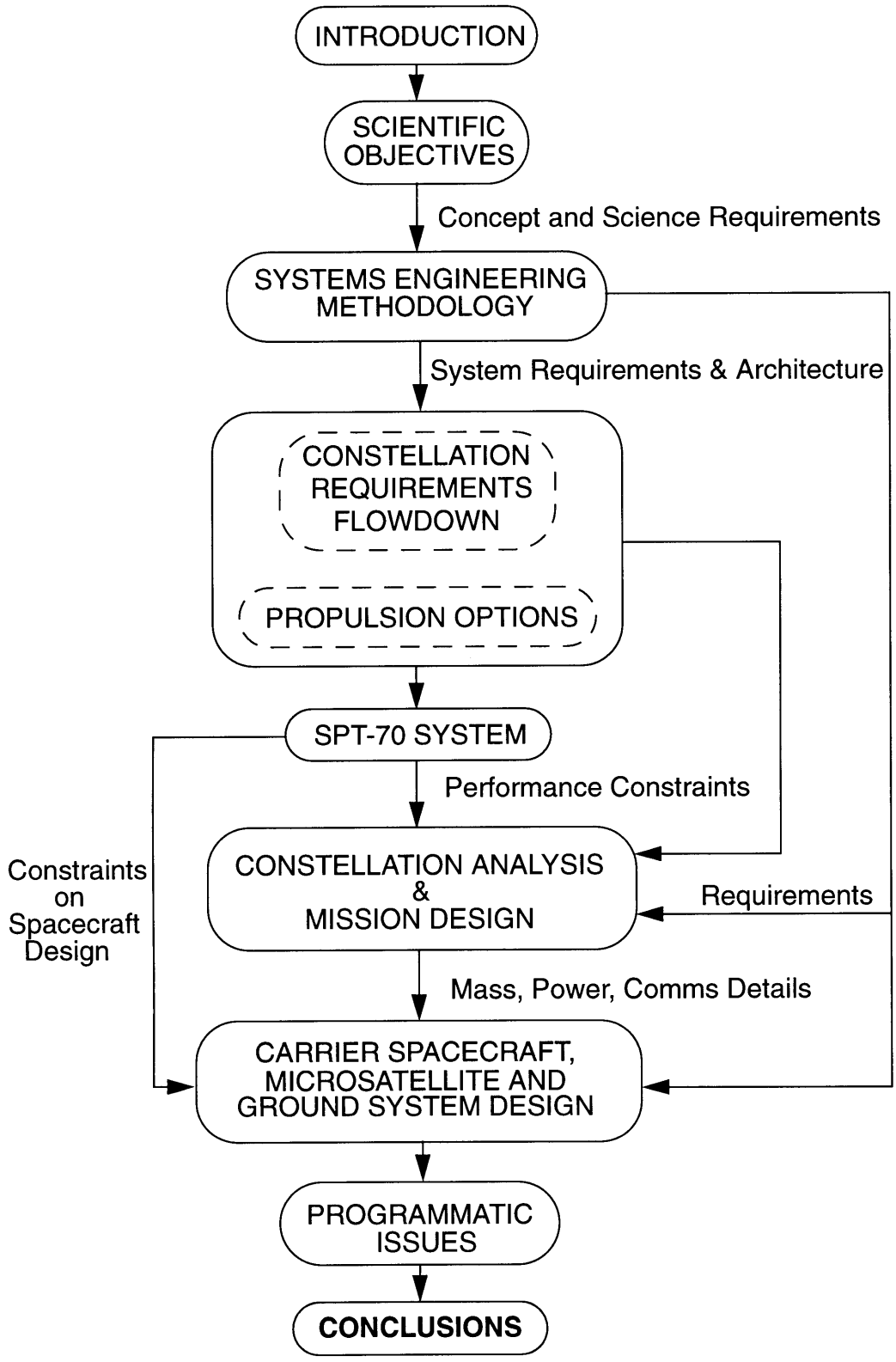

Figure 1-1: Thesis Flow

Chapter 2

Scientific Requirements

> *"Twenty years after their discovery (GRB's), source identifications and the distance scale to bursters remain contentious. Precise localizations of burst sources can help identify counterparts and constrain source models. Correlations between error boxes and unusual astrophysical objects would present a breakthrough, but even if no such correlations are found, it may be possible to place faintness limits on possible counterpart galaxies to help constrain cosmologically distant source models. While about a thousand bursts are at present localized to an accuracy of several degrees, only a few dozen source locations have an accuracy of several arc-minutes or better." [5]*

The paragraph above aptly sums up the rationale behind the need to acquire more accurate GRB localization data in order to gain insights into the baffling phenomenon of Gamma Ray Bursts (GRB's). Before scientific objectives and requirements can be defined, it is helpful to gain a fundamental understanding of the GRB phenomenon and current GRB astrometry techniques and limitations. Starting off with a brief introduction to GRB's, this chapter then goes into the techniques, accuracy requirements and performance capabilities of current systems. The concept of using a constellation of dedicated microspacecraft, which will achieve the required accuracies, is discussed next and a set of scientific requirements is established to set the stage for the system design of ETA.

2.1 The GRB Enigma

The mystery surrounding Gamma Ray Bursts continues to fascinate the astrophysics community. This section attempts to describe the enigma of the GRB, summarizing the current understanding of the phenomenon, theories of GRB sources and identifying the type of information scientists require to unlock the secrets of GRB's. No attempt is made to describe the astrophysics in detail; the interested reader is directed to the references for

more information on the subject.

2.1.1 Background

Gamma Ray Bursts are intense gamma-ray transients with energies hundreds of thousands or even million times greater than photons of visible light. GRB's were first discovered accidentally in the late 1960's by scientists at the Los Alamos National Laboratory. The Vela military satellites, which were being used to detect nuclear tests by sensing high energy radiation, detected short bursts of gamma rays, the sources of which could not be attributed to Earth, Sun or other solar system bodies [6]. The identity of the sources of such highly energetic GRB's continues to elude us more than 20 years later.

GRB's typically occur as bursts of intense radiation for short durations before lapsing into quiescence for years. Perhaps the most intriguing and frustrating point about GRB's is the apparent lack of associated radiation in other parts of the electromagnetic spectrum. This has prevented scientists from observing the phenomenon at visible, infra-red (IR), ultra-violet (UV) and X-ray wavelengths, accurately localizing the sources and establishing from the correlation, the distance to the GRB sources. Without knowing the distance to the GRB source, the intrinsic energy of a single outburst is impossible to determine. A multitude of theories have been proposed to explain the origin of GRB's. These range from galactic sources to extragalactic events occuring deep in space outside the Milky Way. Thus, establishing the distance to the source, possibly by identifying a counterpart, will go a long way towards solving the mystery of where GRB's originate from and how they are generated.

2.1.2 GRB Characteristics

GRB's have typical energies of 10-100 keV which puts them in the transition zone between high energy X-Rays and low energy Gamma rays. A variety of GRB classification schemes have been proposed. Two distinct classes have been identified, based on their short time variability [7]. Figure 2-1 shows typical profiles of short and long bursts.

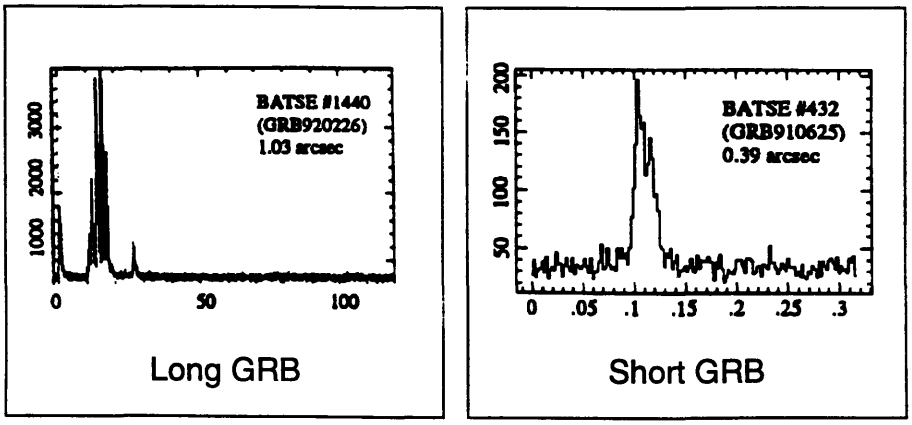

Figure 2-1: Typical GRB Profiles

Table 2-1 summarizes the characteristics of Type I (long) and Type II (short) bursts. The majority of GRB's detected thus far are of the longer duration type with soft spectra. The spatial distribution of GRB's is an important determinant in distinguishing theories of GRB sources [8].

Table 2-1: Classification of GRB's (pre-BATSE) [7]

Type I (~80% of bursts)	Type II (~20% of bursts)
Smooth	Variable
Long (0.3-1000 sec)	Short (0.01-10 sec)
Softer Spectra	Harder Spectra
Most are not uniformly distributed in space	Most are uniformly distributed in space

2.1.3 GRB Theories

The lack of understanding of the GRB phenomenon is underlined by the fact that more than 100 GRB models have appeared in peer-reviewed journals [9]. Scientists are currently divided, roughly equally, into two major lines of thought with regard to GRB sources:

- **Galactic Sources**
  In this concept, potential sources are neutron stars within an extended halo of our galaxy, the Milky Way. Light curves and energy spectra of GRB's seem to indicate that the sources must be small, dense and have intense magnetic fields; neutron stars have all these characteristics. However, one discrepancy with galactic theories is the fact that GRB's seem to come from all parts of the sky whereas known neutron stars are principally located in the galactic disk [10]. Some of the theories proposed to explain this discrepancy include Oort cloud models, extended galactic halo models, and local disk models [11]. Neutron starquakes, thermonuclear explosions, accretion and collisions are some of the processes thought to generate GRB's. The lack of a counterpart would favor the galactic theory.

- **Cosmological Sources**
  The proponents of these theories argue that GRB's could be caused by cataclysmic collisions between neutron stars, generating high energy bursts. The uniform spatial distribution of GRB's supports the cosmological model as well. However, such energetic events would be expected to emit energy at other wavelengths but no GRB counterparts have been detected to date. The other argument against this theory is how to explain GRB repetition. How can GRB repetition be explained by single cataclysmic events? In response, the idea of gravitational

microlensing has been proposed. Scientists argue that a GRB originating from an extragalactic source could pass through clusters of galaxies. The gravitational forces of these massive objects would "bend" the essentially straight line trajectories of gamma rays. As a result of this bending, the trajectories vary in length and hence radiation would arrive at the observer at different times, giving the impression of repeating GRB's [5,9]. It should be added that there is no compelling evidence currently to support this idea in the context of GRB's.

The above discussion only sheds light on some of the numerous arguments and ideas that are being proposed in the tussle between these paradigms. Lack of information is clearly one of the reasons for this mystery and future space missions are required to answer the questions raised by GRB research so far, some of which are:

- **Do GRB counterparts exist?**
  One of the quickest solutions to the GRB problem would be the identification of a counterpart [12]. Furthermore, discovery of counterparts at other wavelengths would enable the utilization of more powerful observation assets such as radio, IR, UV, and X-ray telescopes. The lack of counterparts would severely constrain cosmological models.

- **Do short GRB's come from the same sources as long GRB's?**
  As mentioned before, the number of short GRB's detected so far is substantially lower than long GRB's. One possible explanation of this could be the dead-time bias of current instruments against detecting short bursts. The question then arises as to whether there are more short bursts and if they come from the same sources as long GRB's [4].

- **Do GRB's repeat?**
  There is evidence which suggests that GRB's repeat. If it could be shown beyond doubt that they do indeed repeat, then this would favor the arguments for galactic models which predict repetition. In addition, repetition would severely constrain cosmological models [1,4,6,13].

- **Does gravitational microlensing occur?**
  Detection of microlensing would provide one of the strongest arguments for cosmological models [4,6,13].

Insight into most of the above issues can be provided by the accurate localization of GRB's. Current systems do localize GRB's but the measurements are not accurate enough to resolve the above questions convincingly. It is thus informative to first understand the methods, capabilities and limitations of current astrometry systems, before initiating the design of a system that would localize more GRB's with unprecedented accuracies.

2.2 GRB Astrometry

This section describes GRB astrometry in terms of detectors, standard techniques and their limitations. The discussion will assist in identifying what is required of a new astrometry system.

2.2.1 GRB Detector

The motivation for including a brief discussion on the detector is primarily to understand the requirements and constraints imposed on both scientific measurements and spacecraft design. The primary objectives of current GRB detector designs have been to [14]:

- attain lowest possible detection threshold in order to provide nearly bias-free statistical analysis of a large sample of GRB's
- have good energy resolution for better delineation of spectral features
- have accurate event time information for precise determination of source direction
- record maximum number of energy spectra in the shortest possible integration time to capture fast spectral variability.

Of course, the design of a particular detector will hinge upon specific mission requirements and constraints. Figure 2-2 illustrates a typical GRB detector; this is the one developed for the ETA mission and is derived from the BATSE detectors onboard CGRO [4]

.

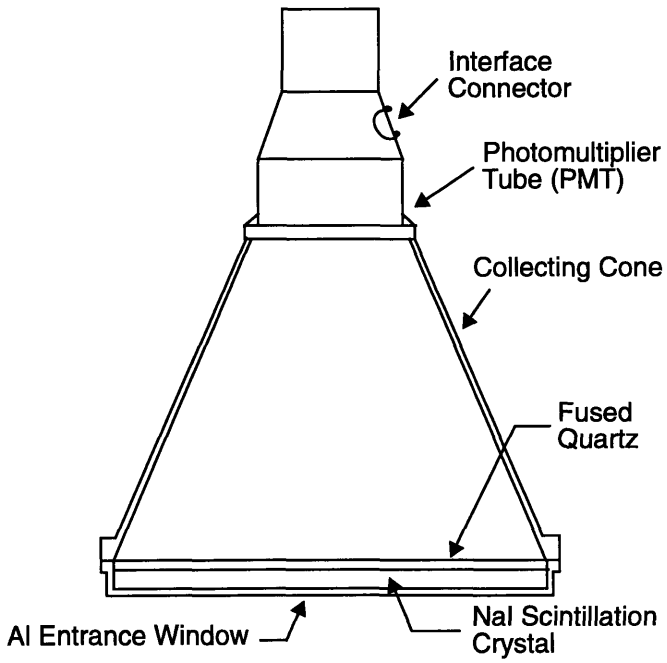

Figure 2-2: GRB Detector [4]

Gamma rays enter through the Aluminium (Al) window and a pulse is generated by the Sodium Iodide (NaI) crystal. The collecting cone directs the photons onto the Photo Multiplier Tube (PMT) for detection. The GRB detector is designed to minimize cost while providing high efficiency.

Each of the ETA microspacecraft platforms will have 4 such detectors, two pointing towards each ecliptic pole. The inclusion of two detectors to view each hemisphere, while increasing the observing area, also provides redundancy in both hemispheres. Moreover, this configuration enables the rejection of charged particle events which could corrupt GRB measurements. The detectors will be mounted on the North-South faces of the spacecraft to provide the required hemispherical fields-of-view. Such a placement will shield the detectors from direct exposure to the Sun which can also emit gamma radiation. This is especially important in light of the fact that the ETA mission will be operational during a period of high solar activity [4]. Table 2-2 summarizes the main features of the GRB detector.

Table 2-2: Characteristics of GRB Detector [4]

Scintillator	NaI
Collecting Area (cm^2)	324
Sensitivity (ct $cm^{-2}sec^{-1}$)	0.1
Energy Range (keV)	50 - 300
Maximum Count rate (sec^{-1})	10^5
Field of View	180^o
Detector Size	23 cm diam. x 25 cm
Detector Mass (kg)	3.80
Power Consumption (mW)	250
Power Interface	5 V DC
Payload Electronics Size	23 x 23 x 13 cm
Mechanical Interface	22 cm bolt ring

North-South face placement of the detectors however means that the system's accuracy will be maximum at the ecliptic poles and minimum in directions parallel to the ecliptic plane. A cosine law governs the amount of radiation incident to the detector and is the main reason for this variation in system accuracy with respect to ecliptic latitude.

The high voltage power supplies and power electronics will use standard bus voltages. Interfaces with the spacecraft are well defined to provide a self-test capability [4]. Each

detector will weigh 3.8 kg and nominally consume 0.25 W at 5 V DC.

2.2.2 Astrometry Techniques

The most crucial aspect of GRB astrometry is the localization of sources to an accuracy better than a few arcminutes [5,6], especially from the perspective of searching for GRB counterparts. Also, it is desirable to disseminate GRB positions in near real-time so that other observation systems with narrower fields-of-view can be committed to observing the GRB in a fading or quescient state [12].

A commonly used method of localizing GRB's is "arrival-time analysis", which is essentially a triangulation type of technique [6]. The principle is illustrated in Figure 2-3

.

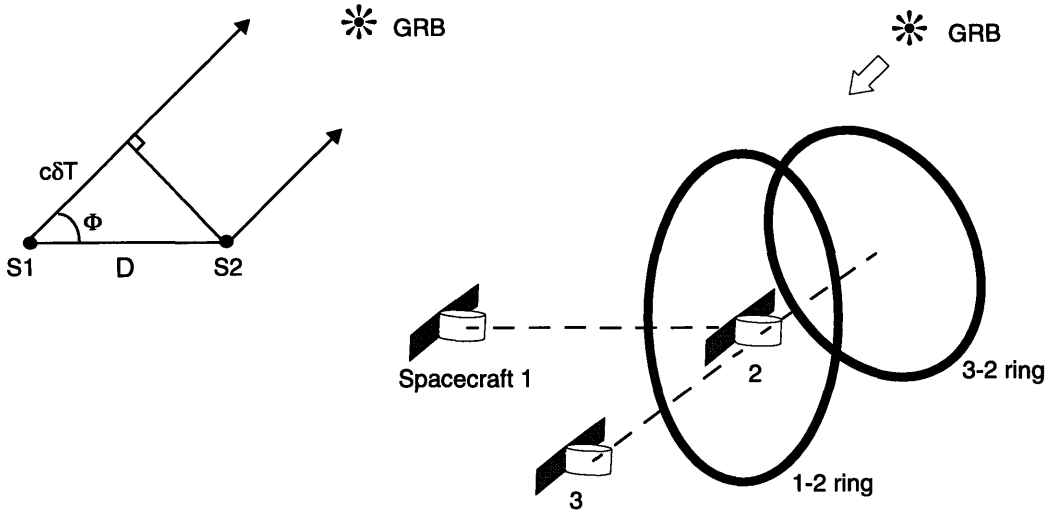

Figure 2-3: Arrival-Time Analysis (adapted from [6])

The basic idea is to time the arrival of the GRB at two widely separated spacecraft, constraining the GRB source to lie within a narrow ring on the sky, centred on the line connecting the spacecraft. Using a third spacecraft provides another such ring to further constrain the direction of the GRB to the points of intersection of the rings. The ambiguity is resolved by a fourth spacecraft. Thus, a minimum of four spacecraft are required to provide three annuli for unambiguously localizing the GRB. A four spacecraft system will enable detection of the presence of a timing error but will not be able to identify the errant spacecraft in question. A network of five spacecraft will not only detect system error but will also identify the spacecraft that is in error.

The half angle Φ of the annular ring , as shown in Figure 2-3, is given by

$$cos\,\Phi = \frac{c\,\delta T}{D} \qquad \text{Eqn (2-1)}$$

where c is the velocity of light, δT is the time difference of burst arrivals and D is the distance or baseline between the spacecraft. It can be shown by differentiating Eqn (2-1) that the width of the annulus, $d\Phi$, and hence one dimension of the resulting "error box", is [15]

$$\Delta\Phi = \frac{c\sigma(\delta T)}{D sin\Phi} \qquad \text{Eqn (2-2)}$$

where $\sigma(\delta T)$ is the uncertainty associated with the time delay.

The accuracy of the localization, as specified by the error box size, is a function of the timing uncertainty, inter-spacecraft baseline and the burst ecliptic latitude (for spacecraft in the ecliptic plane). For example, for a timing uncertainty of 0.5 milliseconds and baseline of 2 AU, a GRB originating from the direction of the ecliptic poles would have an error box of about 0.1 arcseconds. The timing uncertainty comprises two components [15,16]: statistical and systematic errors. Systematic errors are system related and can be minimized through design.

Assuming the spacecraft are in the ecliptic plane, it is clear that the sensitivity of the system will degrade for bursts closer to the ecliptic plane. For multiple pairs of spacecraft with similar values of $c\sigma(\delta T)/\sin\Phi$, the pair with the longest baseline will have the smallest error box.

It is important to realize that the strategy to locate GRB sources is dual pronged in that, not only is it important to accurately localize the burst, but it is also vital to disseminate the location data as soon as possible so that the GRB can be observed by other observation systems in the search for a counterpart.

In the context of the implications of the strategy on the design of the physical system itself, the following issues are crucial:

- **Accurate Timing**
  There are several aspects that contribute to overall timing uncertainty, the most important of which are [4,15] :
  - size and shape of burst profile
  - detector size
  - spacecraft subsystem uncertainties such as detector response time and clock errors
- **Spacecraft Location Accuracy**
  This translates into timing uncertainty but places requirements on the spacecraft tracking components of the system, namely the ground stations.
- **Dissemination of Localization Data**
  The system should, if possible, have the capability to disseminate GRB localization data as rapidly as possible so that powerful telescopes can be directed to search for counterparts. As [13] puts it, "catching the cul-

prit in the act should give us enough evidence for a conviction"!

The concept of time-arrival analysis is best exemplified by the interplanetary network (IPN) systems that have been set up in the past. An important point to note is that the IPN's were realized essentially by interplanetary spacecraft which were carrying out their core missions and were only incidentally equipped with "piggy back" GRB detectors. Some of the Earth-orbiting systems also have the capability to disseminate localization coordinates in near real-time. These systems are discussed next in order to appreciate their capabilities and limitations.

2.2.3 Current Systems

GRB astrometry has been carried out aboard many spacecraft over the years. Some of these include the Compton Gamma Ray Observatory (CGRO), ISEE-3, Solar Maximum, Pioneer Venus Orbiter (PVO), Venera and IPN's set up with various interplanetary spacecraft such as Ulysses and PVO. Only BATSE, HETE and IPN's are discussed here.

BATSE

The Burst And Transient Source Experiment (BATSE) onboard CGRO consists of a suite of 8 detectors located at the corners of the spacecraft [10]. Launched in 1991, BATSE has detected over 1,000 bursts to accuracies of about 7^{o}. The weakest bursts are localized to about 13^{o} while the strongest ones are detected more accurately to about 3^{o}. Note that these measurements are nowhere near the sub-arcminute accuracies required. BATSE, however, has the BATSE Coordinate Distribution Network (BACODINE), which rapidly transmits burst positions to observatories for follow-up observations. BATSE has also been included as part of an IPN. The disadvantage with Earth orbiting systems like BATSE is that 100% temporal coverage is not possible since the spacecraft goes through eclipse periods. It is vital to have 100% temporal coverage if the question of GRB repetition is to be answered convincingly.

HETE

The High Energy Transient Experiment (HETE) is a CSR/MIT managed astrophysics mission scheduled for launch in late 1995 or early 1996. The X-ray instrument onboard will provide 10 arcminute positions for 30 GRB's annually in real-time (up to 5 seconds after trigger) [4]. Best accuracies could approach 10 arcsec if UV photons are detected but it is unclear right now if GRB's emit UV photons as well. These error boxes are still not small enough to avoid source confusion [4].

Interplanetary Networks (IPN's)

GRB detectors onboard interplanetary spacecraft have been used to gather data for time-arrival analysis. An example is the 2nd IPN which consisted of Venera 13 &14, PVO, ICE, and Solar Maximum, and was in operation between 1981-1984. About 270 bursts were detected with best accuracies of several arcminutes [5]. Clock accuracy was 1 msec, ephemeris data was accurate to 1000 km and baselines were between 0.5-1.5 AU. So far, the inability to derive highly accurate GRB localizations from IPN's has stemmed from the following problems:

- insufficient spacecraft which also had sub-optimal spacings
- variability in detection and signal processing techniques led to differences in accuracy. Detectors were designed independently.

It is evident from the current capabilities of systems that what is required is a dedicated system which has not only the baselines typical of IPN's but is also optimized in terms of spacecraft locations and matched detectors. In order to effect the dual-pronged strategy of accurate localization and rapid trigger alert for counterpart searches, the system should ideally have a real-time or near real-time alert capability. The concept which could accomplish this with a single system is introduced next.

2.3 The Constellation Concept

The idea of setting up a dedicated constellation of spacecraft in heliocentric orbits was first suggested by George Ricker of CSR/MIT [1]. A number of microspacecraft with GRB detectors would be deployed into distinct ~1 AU orbits. The constellation would develop over time to set up the baselines typical of IPN's. Identical detector designs would minimize mismatch errors and the technique of onboard template matching to determine times-of-arrival would minimize telemetry rates, thereby simplifying the spacecraft design.

Such a system would, as a result of optimal spacings and matched detectors, provide significantly more accurate data and detect a larger number of GRB's than previously possible. To further enhance the concept, one or a few of the spacecraft could be deployed into orbits in the vicinity of Earth to provide high datarates and add on a near real-time alert capability. These orbits would have to be close enough to Earth to support high rate communications but at the same time, should not be too close to preclude these "trigger" satellites from providing 100% temporal coverage.

2.3.1 Concept

The concept would work as follows. A propulsion stage(s) would deploy the constellation by successively giving ΔV's to each spacecraft. Orbit dynamics would take over and develop the "spread" of the spacecraft. When a GRB occurs, it would trigger the detectors onboard the spacecraft which would store the time-tagged profiles. The "trigger satellites" (satellites in the vicinity of Earth) would downlink the whole GRB profile to Earth. A template of the GRB of interest would be prepared and uplinked to the rest of the constellation. The template would be correlated with stored profiles by onboard processing to determine the time-of-arrival of the GRB at a given microsatellite. This small amount of data and a correlation confidence factor would then be telemetered back to Earth for time-arrival analysis. If need be, the full profile could be downlinked later for subsequent analysis. The small datarates would simplify spacecraft design and onboard storage capacity for more than a day's worth of data would be provided.

The feasibility of such a concept would hinge on propulsion and microspacecraft technol-

ogy. Cost would obviously be of prime concern and the benefits of using a small launch vehicle would be substantial. The rate of "spreading" of the constellation is highly dependent on the differential velocities imparted to each microspacecraft. A quick spread would require high ΔV's, indicating high I_{sp} systems. The selection of the propulsion system is therefore crucial and utilization of Electric Propulsion, with its inherently high I_{sp}, would allow more microsatellites on a smaller launch vehicle.

The effectiveness of the entire concept can be lumped into a single metric or Figure of Merit, taking into account factors associated with the GRB, the detector and the baseline provided by the constellation.

2.3.2 Figure of Merit

In order to quantify the effectiveness of the constellation concept, a Figure of Merit, has been derived [17]; this would facilitate optimization of the various system elements. The system Figure of Merit, η_{sys}, is given by

$$\eta_{sys} = C_{burst} A_{det} \eta_{const} \qquad \text{Eqn (2-3)}$$

where C_{burst} (cm^{-2} sec^{-2}) is a factor determined by burst characteristics, A_{det} (cm^2) is the effective area of the GRB detector and η_{const} (sec^2) is a measure of the "spread" of the constellation. The objective should be to maximize the value of η_{sys}. This study focuses on the maximization of the constellation figure-of-merit,η_{const}, towards maximization of system figure-of-merit.

The maximization of the detector area is constrained by the available space on the spacecraft. On the other hand, the constellation spread may be maximized over the mission lifetime by appropriate deployment strategies; this will be dealt with in detail in Chapter 6. The Figure of Merit provides a convenient metric to assess the effectiveness of various options when conducting trade studies during the design process.

The ETA mission adopts the constellation concept in its entirety. Before realizing this concept into a physical system, it is necessary to define what the scientific objectives of the mission are and what scientific requirements these translate into. These would form the basis for the definition of technical system requirements, based on which the system would be designed.

2.4 ETA Scientific Requirements

The ETA system will be based on the dedicated constellation concept described previously and shall have the following scientific objectives [4]:

- search for existence of GRB counterparts
- determine the number and characteristics of short GRB's

- determine if GRB's repeat
- detect gravitational microlensing if it occurs (secondary objective)

In summary, ETA will attempt to provide insights into all the big questions that puzzle GRB researchers. In order to accomplish these objectives, the ETA mission has the following scientific requirements:

- detect a sufficiently large number of GRB's with accuracies of 1-100 arcsec. The exact number will depend on GRB characteristics and is necessary for statistical analysis to derive GRB positions. The ETA system will need to detect between 800-1,000 GRB's over its mission lifetime.
- provide a rapid trigger alert for ground-based and Earth-orbiting observatories
- provide accurate burst profiles
- ensure a constellation of at least 4 operational spacecraft over mission lifetime
- provide 100% temporal and 4π steradian coverage of the sky over mission lifetime.

The system has to be designed to conform to these scientific requirements. Definition of scientific requirements and system concept assists in approaching the design problem from a systems engineering perspective.

Chapter 3

Application of Systems Engineering Methodologies

> *"Systems engineering is a branch of engineering that concentrates on the design and application of the whole as distinct from the parts.....looking at a problem in its entirety, taking into account all facets and variables." [18]*

> *"Systems Engineering is an attitude of mind, once adopted and practised which causes things to fall into place in the correct order much more easily than they do if all individuals pursue their tasks in their independent ways." [19]*

The role of Systems Engineering (SE) in the design, development, manufacture, test and deployment of complex systems cannot be overemphasized. This chapter presents the application of the Systems Engineering Process (SEP) to ETA. The goal is to develop system requirements to support ETA scientific objectives, establish the system architecture and its interfaces and understand the inter-relationships between various system elements in terms of key characteristics or trade parameters. The result of the process is a better understanding of the system and associated trade space as well as the flowdown of system requirements to enable the design of the system.

The chapter starts off with an introduction to Systems Engineering, outlining its importance and characterizing the overall concept. The Systems Engineering Process, which is a subset of Systems Engineering, is elaborated upon, showing its relation in the overall context of Systems Engineering. Tools used in the SEP are then described before applying them to the ETA mission. Functional analysis and requirements flowdown are presented. The reader familiar with Systems Engineering methodologies can progress directly to the sections on the application of SEP tools to the ETA mission.

3.1 Introduction

This section provides an introduction to Systems Engineering, outlining specifically the Systems Engineering Process and the tools available for application to a given problem.

3.1.1 Background

Systems Engineering in the Aerospace industry was pioneered in the fleet ballistic missile programs that Lockheed Missiles and Space Company undertook in the 1950's. As systems became more and more complex, encompassing numerous engineering disciplines and technologies, it became more difficult not only to keep track of system requirements and interfaces but also to manage the entire program. A methodical approach to the whole problem was clearly required. Out of the experience accumulated over the years, the field of Systems Engineering has blossomed from being a fledgling discipline, frowned upon, into an expertise that is a critical element of any project today. Although originally created to assist with the development of complex weapons systems, the elements of Systems Engineering are applicable at all design levels and to all kinds of applications.

Systems Engineering (SE) considers all phases of the system lifecycle in order to identify obstacles that may potentially cripple the program downstream in the lifecycle. This "upfront system-wide" approach, which is a reversal of the natural tendency to "run off and do things right away", is crucial in avoiding the cost and schedule overruns that are typical today.

The complex inter-relationships between system elements requires the systems engineer to be a "system thinker", with the ability to appreciate problems from a system-wide perspective. In that respect, SE can be thought of as a "way of thinking". The application of SE is thus not constrained to a particular field but manifests itself in all sorts of human endeavors. From the perspective of engineering, SE is practised, just to cite a few examples, in the aerospace, computer, electronic and automotive industries.

Because of the widespread application of SE, there exist a multitude of definitions of the concept. Even though they differ based on the context of application area, there are common threads running through all which illustrate the most important aspects of this rapidly developing field of engineering.

3.1.2 Systems Engineering

Defining Systems Engineering is no easy task since it means different things to different people. It is, however, informative and interesting to compare a few of the number of definitions that exist, so that the common issues of the SE paradigm can be extracted.

The Department of Defense (DOD) defines Systems Engineering, in MIL-STD-499A, as follows [20]:

> *"Systems Engineering is the application of scientific and engineering efforts to*

- *transform an operational need into a description of system performance parameters and a system configuration using an iterative process of definition, synthesis, analysis, design, test and evaluation;*
- *integrate related technical parameters and ensure compatibility of all physical, functional and program interfaces in a manner that optimizes the total system definition and design;*
- *integrate reliability, maintainability, safety, survivability, human and other such factors into the total engineering effort to meet cost, schedule and technical performance objectives."*

MIL-STD-499B provides a complementary definition [20]:

> *"Systems Engineering is the management and technical process that controls all engineering activities throughout the lifecycle in order to achieve an optimum balance of all system elements to ensure satisfaction of system requirements, while providing the highest degree of mission success. It has two main activities:*
> - *interpreting the customer's needs and translating them into a set of requirements that can be met by individual design and specialty disciplines;*
> - *validating that the system satisfies the customer's needs through analysis, simulation and testing."*

The management aspect is elaborated upon in the following definition [21]:

> *"Systems Engineering is both a technical and management process. The* ***Technical*** *process is the analytical effort necessary to transform an operational need into a system design of the proper size and configuration and its documentation in requirements specifications. The* ***Management*** *process involves assessing cost and risk, integrating the engineering specialties and design groups, maintaining configuration control and continuously auditing the effort to insure that cost, schedule and technical performance objectives are satisfied to meet the operational need."*

The main points of the previous definitions are echoed clearly in [21]:

> *"Systems Engineering is a philosophy (or methodology) with which any project can be approached - even outside of engineering. Its chief characteristic is harmony. This means all parts work in unison (integration and interfaces), each part has its place (requirement traceability), the finished product is what you wanted (mission definition, specifications, verification), you know what you've done (documentation), you keep things in control (cost, schedule, design) and you make sure you're really doing the right thing (design*

reviews, working groups)."

Figure 3-1 attempts to incorporate the salient aspects of Systems Engineering that were identified in the previous definitions.

Although portrayed separately in the figure, the technical and management aspects of the program are generally integrated; the separation is for ease of understanding. Product development is an iterative process and there would be feedback between levels, that has not been depicted here for the sake of clarity. The analyses and discussions presented in this thesis are primarily focused on the technical aspects associated with Systems Engineering, although management issues are briefly addressed in a later chapter.

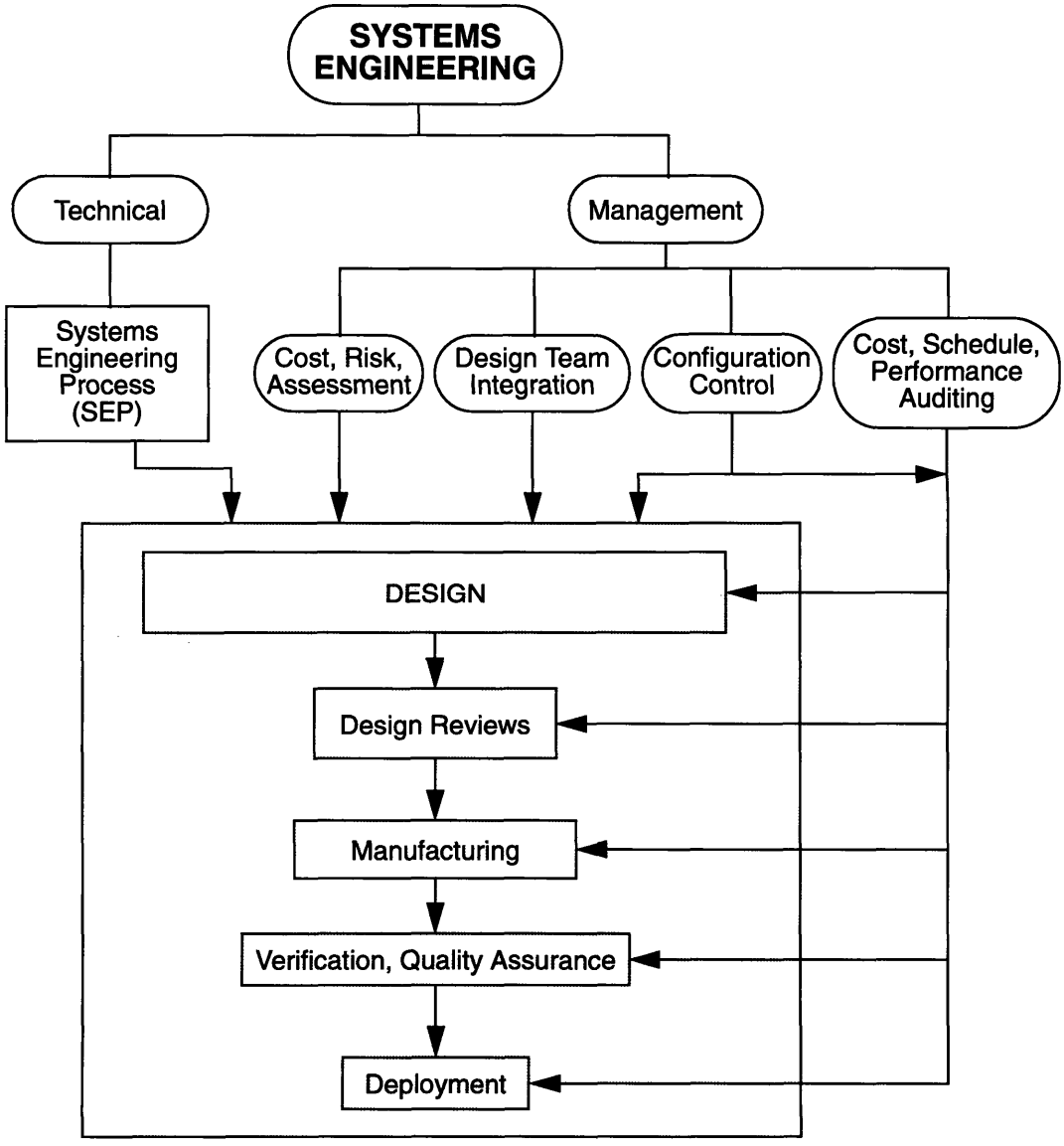

Figure 3-1: Systems Engineering

The technical portion of Systems Engineering is largely included in what is formally termed the "Systems Engineering Process"(SEP). It is important to note that the SEP is only a subset of the overall concept of Systems Engineering.

3.1.3 The Systems Engineering Process

> *"The Systems Engineering Process is the means by which a set of objectives is transformed into an operational system. This process is an iterative one which develops requirements and allocates them to succeedingly lower levels. A design concept is developed concurrently to provide a framework for the allocation, and to 'test' the allocation against what may be really achieved. The objective is to completely define the capability needed while minimizing cost and risk." [21]*

The Systems Engineering Manual 1-1, from the USAF Aeronautical Systems Division [20], goes further, saying

> *"The Systems Engineering Process is the integrated sequence of activities and decisions that transform a defined need into an operational, lifecycle-optimized system that achieves an integrated and optimal balance of its components. The Systems Engineering Process produces initial, intermediate and final products (data, equipment, trade study reports). The main tasks are*
>
> - *Requirements Analysis*
> - *Functional Analysis*
> - *Synthesis*
> - *Allocation*
> - *Trade Studies."*

Figure 3-2 illustrates the Systems Engineering Process. Four main sections constitute the SEP, namely

- Mission Requirements Analysis
- Functional Analysis
- System Synthesis
- Requirements Allocation and Flowdown.

These activities are enabled through various trade studies and the end result of the SEP is a baseline design and set of system requirements which are documented in a series of specialized documents and formats. These documents are then used extensively by specialty engineers to design the system.

The prime input to the SEP is a set of customer requirements. The details of the main sec-

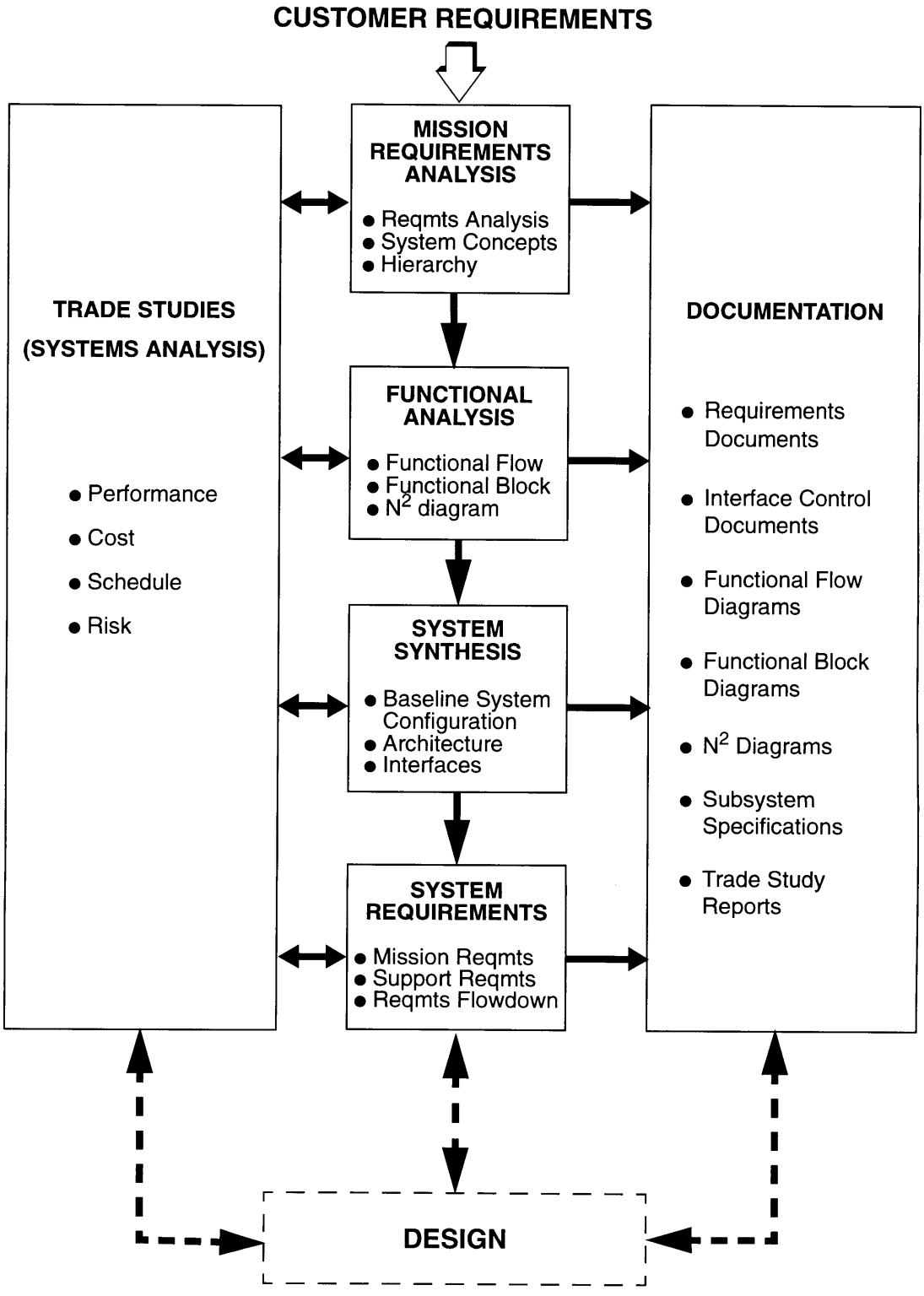

Figure 3-2: The Systems Engineering Process

tions of the SEP are outlined below. Note that these tasks may overlap with each other, giving an integrated, concurrent sense to the whole process.

- **Mission Requirements Analysis**
  This process consists of 3 major elements, namely

  - Requirements analysis, the objective of which is to define and refine all customer needs in terms of performance requirements and primary functions that must be performed
  - Establish system concepts
  - Define the system hierarchy

  Mission analysis examines those requirements that are payload related.

- **Functional Analysis**
  The primary goal of this analysis is to define the system requirements necessary to support the accomplishment of customer objectives. Tools such as functional flow diagrams and functional block diagrams are used to identify support requirements, interfaces and trade options. Some of these tools are described in a later section. Functional analysis provides a means of establishing requirements on all supporting elements of the system by examining its detailed operation and interactions.

- **System Synthesis**
  Building on from the work done in the functional analysis, the synthesis task involves defining the architecture necessary to establish the capability to satisfy system requirements. A baseline system configuration is arrived at and the interfaces and other inter-relationships between system elements are characterized. Tools such as N^2 charts and inter-relationship diagrams are utilized during this phase. Interfaces are especially important and managing them is vital since they provide the greatest leverage in systems architecting [18].

- **Requirements Allocation**
  Having defined the system architecture and a set of mission and support requirements, it is then possible to allocate the requirements to system elements. This is a task carried out during the requirements allocation phase of the SEP. The system requirements are allocated or flowed down to the lower levels to produce segment, element and component specifications. Requirements allocation facilitates design of the system to the lowest level. Moreover, it enables the traceability of requirements so that if a requirement is changed, it is easy to determine which system components are affected; requirements traceability also assists the process of fault diagnostics.

Trade studies form the core of the technical analyses that are performed during the SEP. They are conducted during all phases and at all levels of the SEP. The trade studies component of SEP is sometimes referred to as "Systems Analysis" [21] and is used to select between design options that arise. These alternatives can be in terms of requirements, functional options identified by functional analysis, interface options or even options that arise during the requirements allocation process. Metrics or figures-of-merit are usually defined in order to assess trade options objectively with regard to system requirements and program philosophy. The metric is a quantifiable parameter that is directly tied to system requirements in terms of performance, cost, schedule, risk and other important system characteristics. More often than not, a single metric is not sufficiently adequate in representing system capabilities and multiple metrics are necessary.

The selection of a metric depends on the type of system and is a task which requires careful consideration of driving system attributes. For example, a metric relevant to a system such as a Global Mobile Communications System is cost per billable minute. This metric incorporates both cost and revenue aspects of the system and is hence an appropriate metric for a commercial company whose main goal is to develop a profitable service [22]. For a scientific mission like ETA, the metric has to be related to scientific performance in some manner. Since the ETA system seeks to localize GRB's to unprecedented accuracy, it is logical to define a metric or figure-of-merit which is directly related to system accuracy.

The concept of trade studies using metrics is demonstrated in a later chapter involving constellation design of ETA. Trade studies form the crux of the Systems Engineering process and are an essential component for the methodical assessment of the variety of options that emerge out of any complex system concept.

The results of trade studies and all other analyses have to be documented for future reference. Documentation forms an integral portion of the SEP and is essential during the design process. Documents are updated systematically to provide design engineers with all the information they need. Some of the major kinds of documentation generated by the Systems Engineering Process include [21]

- System Requirements Documents
- Interface Control Documents
- System specifications
- Functional flow diagrams, Functional block diagrams
- System Block diagrams
- N^2 diagrams for interfaces
- Inter-relationship diagrams
- Timelines
- Performance Budgets.

When applying the SEP to the ETA mission, the focus will primarily be on the Functional Analysis. However, note that the top level aspects of the Mission Requirements Analysis were carried out in Chapter 2 where customer (or science) requirements were refined into performance parameters and a system concept was identified. The later chapters of the the-

sis present the systems analysis or trade studies in more detail. The major aspects of System Synthesis and Requirements Allocation are dealt with in this chapter after the Functional Analysis. Before going into the analysis, it is necessary to discuss the various SEP tools in the level of detail that is necessary to use them in the analysis that follows.

3.1.4 Systems Engineering Process Tools

This section outlines the major features of some of the techniques and tools associated with the Systems Engineering Process; the list is by no means exhaustive. The discussion serves to introduce the reader to the tools before they are applied in the rest of this chapter.

- **Functional Flow Diagrams**
  As shown in Figure 3-3, the purpose of the functional flow diagram is to indicate the sequential relationship of all functions which must be accomplished by a system.

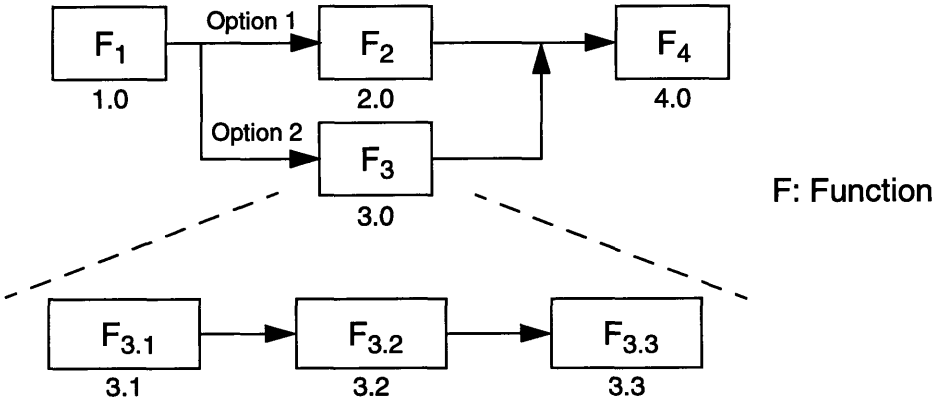

Figure 3-3: Functional Flow Diagram

The entire approach is functionally oriented and not equipment oriented. Functional flow diagrams are useful in that they can be used to develop requirements and identify trade study options. Because the overall mission operation may be long and complicated, it is more appropriate to develop the functional flow diagrams in a series of increasingly detailed functions. Starting off with a very simplified top level flow, the diagram is developed by expanding the functions within each block; this ensures that details are not omitted. The blocks are usually numbered for easy reference. It is likely that feedback will exist between various functions and these would be shown as appropriate; feedback paths are not shown in the figure above for the sake of clarity.

- **Functional Block Diagrams**
  Having developed functional flow diagrams for the system to varying levels of detail, functional block diagrams are drawn up to identify the hardware and software elements required to perform the functions. Figure 3-4 shows a typical functional block diagram.

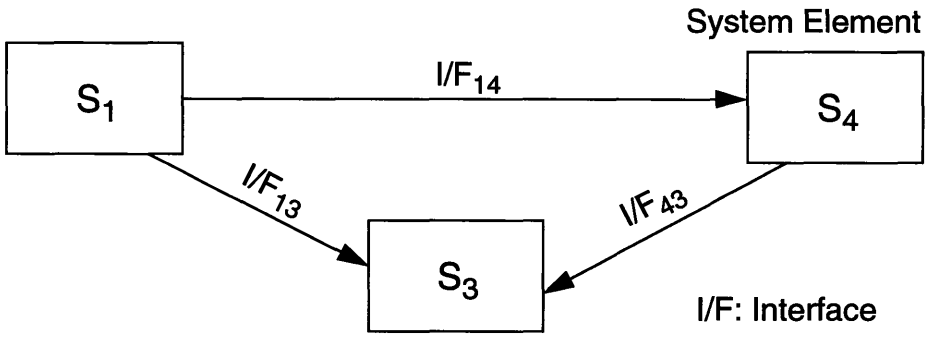

Figure 3-4: Functional Block Diagram

Interfaces between the system elements are identified. Each block within the top level functional block diagram can be further expanded, specifying the hardware/software for lower levels of the system. Functional block diagrams are also used for the construction of system reliability models [21].

- **Architecture**
  This is a specialized version of the system functional block diagram, albeit without the interfaces. The various elements making up the entire system are organized in a hierarchical manner as shown in Figure 3-5.

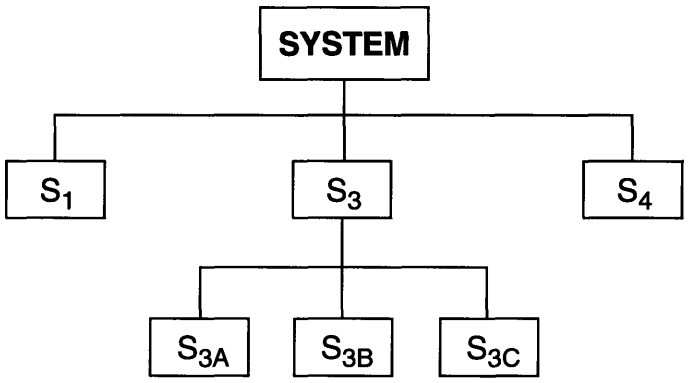

Figure 3-5: System Architecture

The architecture is useful for the organization of documentation such as requirements and interface control documents. It is especially useful for system synthesis and provides a compact hierarchical representation of the entire system.

- **N^2 Diagram**

  Even though the N^2 diagram has been used to develop data interfaces in software areas, it can be used to develop hardware interfaces as well. When used in conjunction with the functional block diagram, the N^2 diagram provides a neat and organized way to map interfaces between system elements. Figure 3-6 is an example of an N^2 diagram.

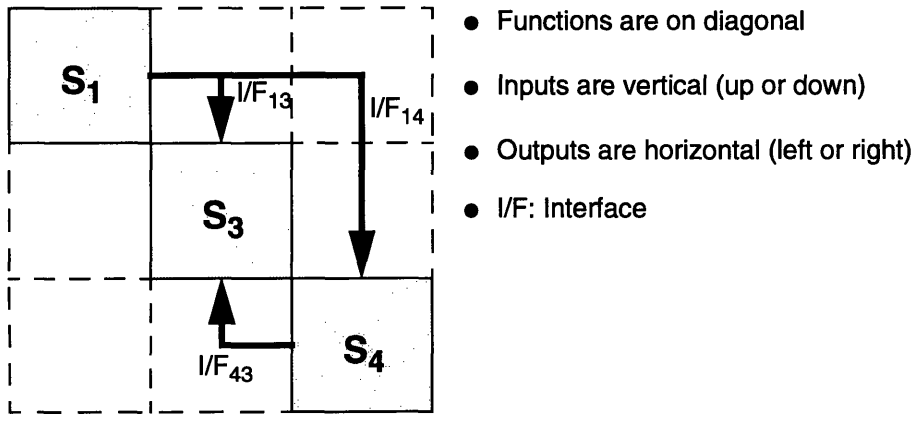

Figure 3-6: N^2 Diagram

An N x N matrix is set up with the N system elements placed in the N diagonal boxes. The interfaces are mapped based on the simple rule that inputs are vertical and outputs are horizontal. Potential interface management problems can be identified and resolved using N^2 diagrams.

- **Inter-Relationship Diagram**

  The inter-relationship diagram is a variant of the N^2 diagram in that it maps out the inter-relationships between system elements in terms of requirements, element attributes, system capabilities and constraints, performance/design parameters and so forth [23]. Figure 3-7 illustrates the concept

  The system elements are in the shaded diagonal boxes. Attributes (A) in the diagonally opposite boxes are inter-related. For example, Attribute $A_{1.6}$ of system element S_1 is related with attribute $A_{3.5}$ of system element S_3. The inter-relationship diagram can be used as a basis for determining the impact of a certain system attribute on the entire system. Furthermore, it is useful for the requirements flowdown process..

S1	1) $A_{1.1}$ 2) $A_{1.3}$ 3) $A_{1.6}$	
1) $A_{3.3}$ 2) $A_{3.1}$ 3) $A_{3.5}$	S3	1) $A_{3.2}$ 2) $A_{3.5}$
	1) $A_{4.5}$ 2) $A_{4.1}$	S4

Figure 3-7: Inter-relationship Diagram

- **Requirements Allocation**
  The flowdown of system requirements to lower levels is based upon the hierarchical system architecture and incorporates information gleaned from the inter-relationship diagrams as well. For the purposes of allocation and flowdown, system requirements can be classified into [21]

  - allocable parameters
  - non-allocable parameters.

  Allocable parameters are those which can be apportioned to system elements. Non-allocable parameters are those requirements which are applicable to all system elements. A good example of a non-allocable requirements is system lifetime. Examples of allocable parameters include pointing error, mass and power budgets. Allocable requirements are further distinguished, depending on whether they can be directly allocated or have to be converted into performance measurables through a derivation analysis and thus allocated indirectly. Pointing error requirements are directly allocable to elements which contribute to overall error. The error box size requirement for the ETA system is an indirectly allocable requirement since it has to be converted into performance measurables such as timing uncertainties and ranging errors. The flowdown of this important system requirement is performed in a later section of this chapter.

The techniques and tools discussed above can be used for analyzing both intra-level and inter-level issues. The implementation of these tools for the ETA mission is by no means complete. Incorporation of all details, such as spacecraft manufacturing, testing and so forth, was not within the scope of the study. The primary purpose of the effort was to apply the Systems Engineering Process to the mission and illustrate the unique attributes of the process that assist the design of complex systems like ETA.

3.2 ETA Functional Analysis

This section presents the functional analysis for the ETA mission. The Functional Flow diagram is developed progressively, showing trade options. The Functional Block diagram is derived from the flow diagram with major interfaces shown.

3.2.1 Functional Flow Diagrams

Figure 3-8 is the Functional Flow diagram for the overall ETA system. Starting off with a simple flow diagram, each block has been progressively expanded to develop the functionalities to finer details. The most important phases of the overall scenario are

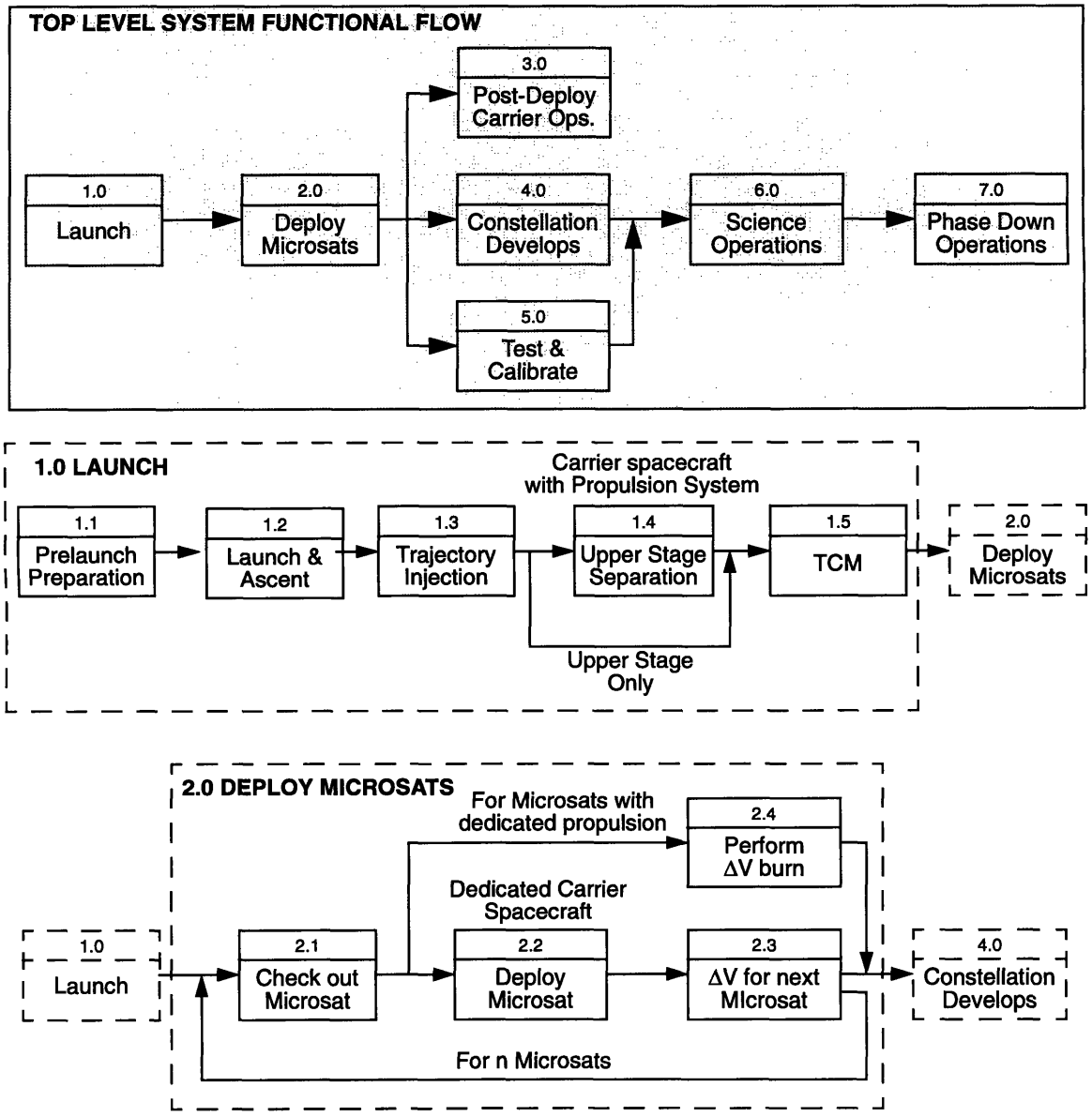

Figure 3-8: ETA System Functional Flow Diagram

- Launch
- Deployment of the microsatellite constellation
- Science operations.

The detailed flow for each of these phases is developed further. The flow diagram for the most functionally important phase of the mission, the science operations, is presented in Figure 3-9. Utilization of a numbering scheme is seen to facilitate the presentation and understanding of what can be a very detailed system functional flow.

Prior to initiation of the scientific activities, the system will be tested and calibrated with flight data (Function 5.0), which will also enable the verification of system software. The utility of the carrier spacecraft after the deployment of the microsatellites is undecided as of now (Function 3.0). Potential post-deployment scenarios include using the platform for a larger scientific instrument [2]. If an electric propulsion system is employed, the platform would be ideal for experiments to accumulate electric propulsion data and experience in the deep space environment. The post-deployment function of the carrier spacecraft is a top level trade which incorporates not only technical issues but also necessitates careful consideration of fiscal, programmatic and political issues. International cooperation would introduce cost-sharing which could substantially contribute to lowering costs from the standpoint of a single organization.

Scientific operations will continue, depending on the constraints placed essentially on the availability of funding. System lifetime of the hardware is not a driver here even though the system will have degraded over the nominal lifetime.

The launch phase (Function 1.0) will include separation from the upper stage of the launch vehicle if a dedicated carrier spacecraft is used for deployment of the microsatellites. A separation will not be required if the launch vehicle upper stage will be utilized in some fashion to deploy the microsatellites. Trajectory Correction Maneuvers (TCM) will be necessary to negate injection errors.

An interesting trade, revealed by the expansion of the deployment phase (Function 2.0), concerns the alternatives available to provide the necessary ΔV to place each microsatellite into a distinct heliocentric orbit. The options include using an upper stage compatible with the launch vehicle, a carrier spacecraft with a propulsion system, or even dedicated propulsion systems for each of the microsatellites. This trade is analyzed in more detail in Chapter 4.

The scenario for microsatellites with dedicated propulsion systems would include separation followed by the ΔV burn using the propulsion system, which may be a Solid Rocket Motor (SRM) or a liquid monopropellant system. The dedicated carrier spacecraft concept would involve separation from the launch vehicle and initiation of the deployment process after TCM. Prior to deployment, each microsatellite will be checked out. The carrier will then perform the burn to provide the necessary ΔV to the next microsatellite before its deployment. The process will continue until the last microsatellite has been deployed.

The science operations (Function 6.0), as laid out in Figure 3-9, involve using the trigger microsatellites, which are closer to Earth, in a different functional mode from the rest of the microsatellites.

When a GRB occurs, the detectors aboard the microsatellites will measure the GRB profile and store the time-tagged data within the onboard memory. Real-time downlinking of

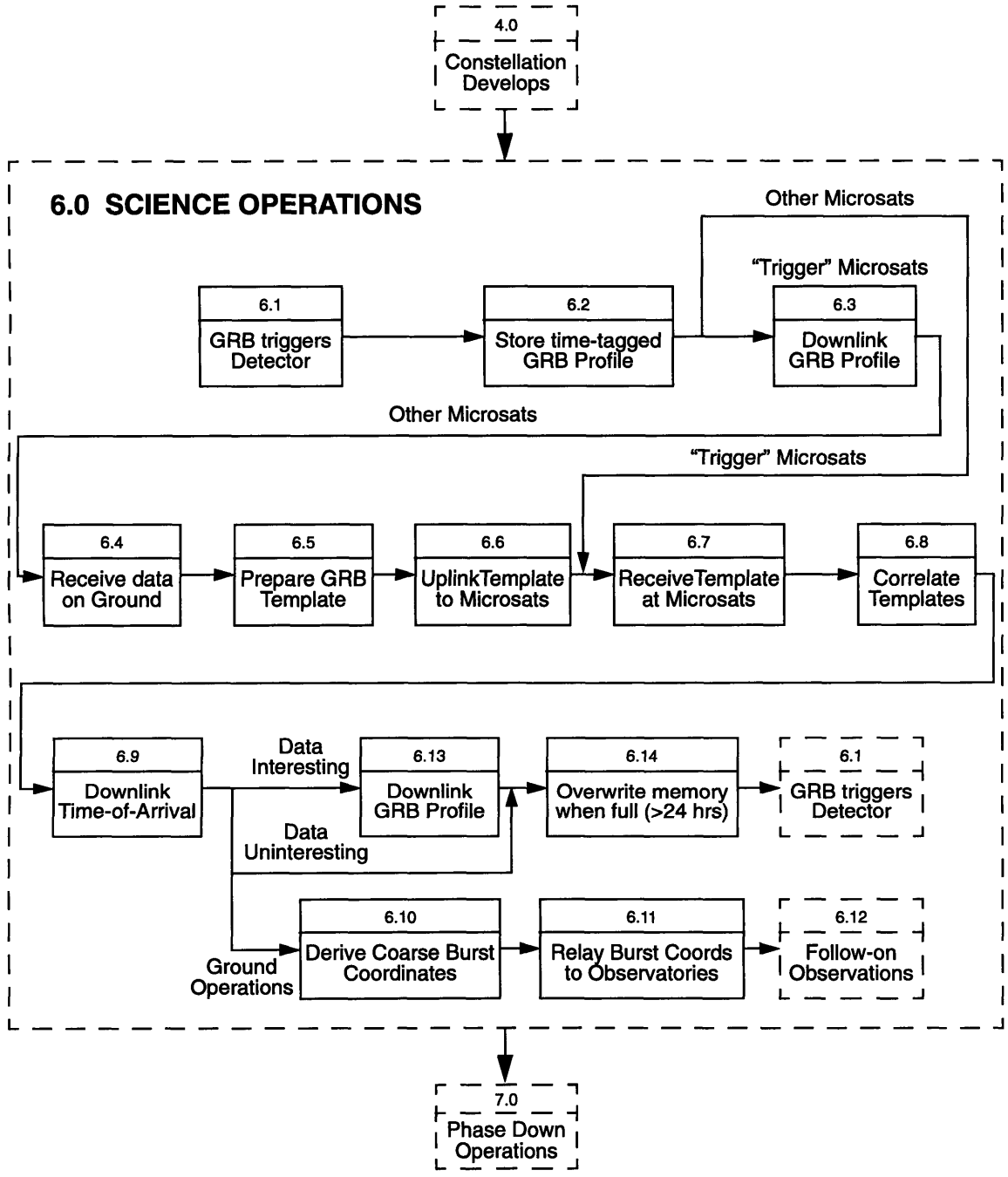

Figure 3-9: ETA Operational Flow Diagram

GRB data from all microsatellites was not considered to be an option since there is a premium on incorporating a high datarate link capability in a platform that may be as far as 2 AU from Earth. The premium on power and antenna gain requirements would unnecessarily complicate microspacecraft design as well as increasing spacecraft mass, volume and cost. On the other hand, the provision of sufficient onboard storage capacity was not deemed to be a problem. The closer trigger satellites will perform the function of real-time GRB profile downlinking.

Once the GRB profile has been telemetered from the trigger microsatellites, the ground segment has to carry out the function of preparing a GRB template for uplinking to the microsatellites. The prepared GRB template is uplinked to the rest of the microspacecraft constellation. Upon receipt by the microsatellites, the template is used to derive the time-of-arrival (TOA) by correlating it with the profiles stored onboard. The TOA is the only information, together with a correlation confidence parameter, that needs to be telemetered back to Earth. GRB localization is a time critical function in that the information has to be quickly disseminated to organizations controlling other observatories so that that follow-on observations of the GRB can be undertaken.

The trade associated with the function of determining TOA for each microsatellite reduces to whether the data processing function is to be kept onboard as opposed to performing it on the ground. In this case, the large distances involved would place heavy demands on microsatellite transmitter power if a large amount of data was to be downlinked for ground processing. Efficient onboard processing is found to be easier to accomplish with current techniques. Even though the functional flow diagram has not been expanded further, it can be demonstrated how functional flow diagrams can be used to identify trades to the lowest levels of the system. For example, if the onboard correlation function were to be considered, a trade on the configuration of the command and data handling system arises. This involves deciding whether to incorporate the correlation function into the spacecraft computer or have a dedicated processor. A dedicated processor has been selected for the ETA microspacecraft since it simplifies interface and computer tasking issues as well as allowing optimization of the processing function.

The TOA downlinked from each microspacecraft platform is used by analysts to compute the localization coordinates of the GRB. These coarse coordinates are relayed to observatories for the purpose of follow-on observations of the GRB. If a particular GRB is considered to be interesting enough to warrant subsequent analysis, the microsatellites can be commanded to telemeter that specific GRB profile. The onboard memory will have the capability to store data accumulated over at least 24 hours and is overwritten when necessary. There is sufficient time over 24 hours to retrieve all interesting data from the microsatellites. The whole process from detection to template correlation and downlink of TOA is repeated whenever a GRB occurs.

The important functions of the system have been identified by the functional flow diagrams. The next issue that arises is to determine the hardware, software or any other resources necessary to accomplish these system functions.

3.2.2 Functional Block Diagram

The major system elements required to realize system functions are shown in the System Functional Flow diagram shown as Figure 3-10.

The space segment will comprise the microsatellite constellation and a dedicated carrier spacecraft, if that option is selected. The launch and ground segments will complement the space segment. It is assumed at this stage that ground stations with antennas will be functionally separate from a Mission Operations Center (MOC) which will incorporate both the spacecraft control and science data analysis functions. The hardware required for these functions will be colocated at a single facility. The other elements making up the ground segment are the relay networks and other scientific organizations. In essence, the scientific organizations are a peripheral component from the perspective of the core ETA system.

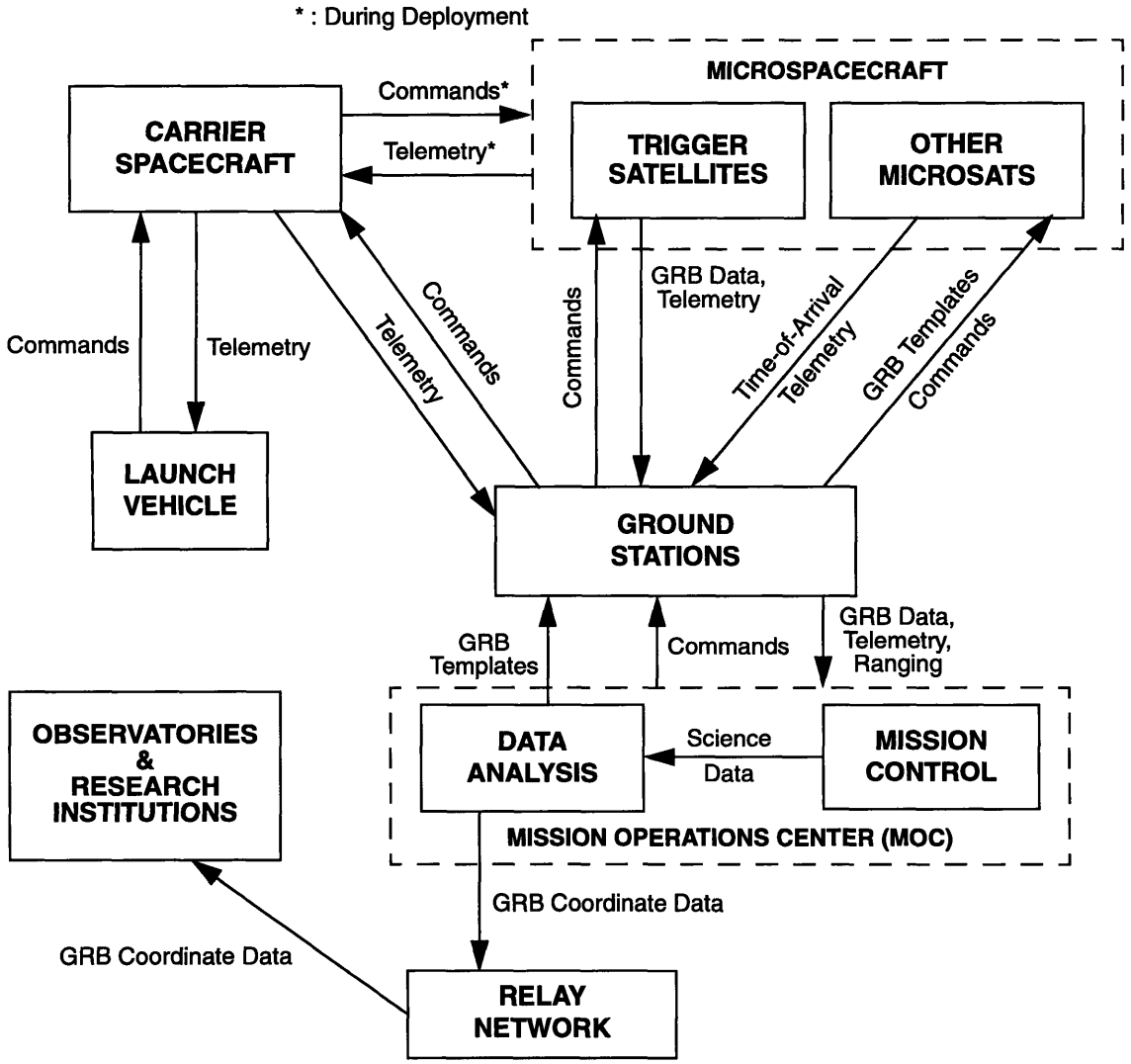

Figure 3-10: ETA System Functional Block Diagram

Major data/information interfaces between the various system elements have been identified and mainly include command and data interfaces. Other interfaces related to provision of power and mechanical functions, such as separation and deployment of spacecraft components like solar arrays and antennas, are not shown.

The launch vehicle will provide the main interfaces with the carrier spacecraft prior to and during the launch phase. Launch control will not be maintained from the ETA mission operations center, even though a monitoring capability will probably be provided; the launch vehicle will be controlled at the launch facility. The carrier spacecraft will provide communication links to the microsatellites during the deployment phase and will relay commands and telemetry during microspacecraft checkout. Commands and telemetry from the space segment will be relayed from the antenna facilities to the MOC. Ranging data, which is important from the perspective of accurate determination of spacecraft positions, will also be relayed to the MOC by whatever ground stations are implemented for Very Long Baseline Interferometry (VLBI) position determination techniques [4].

Networks set up specially to relay scientific data, will be used to disseminate GRB data to the scientific community. The BACODINE and possibly HETE networks will be employed for the rapid distribution of GRB localization coordinates. It is envisaged to utilize the Internet for making the scientific data available to interested parties worldwide [4].

The time critical interfaces during nominal mission operations are the datalinks for downlinking GRB profiles in near real-time from the trigger satellites and distributing derived GRB coordinates via the relay networks. An internal interface will exist between the mission control and data analysis elements of the MOC to transfer science data retrieved from the telemetry. Data-intensive interfaces associated with the space segment are the GRB profile downlinks from the trigger microsatellites, uplinks of GRB templates to the microsatellites and GRB profile downlinks from the rest of the microsatellites.

Functional analysis demonstrates that system functions can be allocated to system elements in a multitude of ways. The crucial point to keep in mind when defining the system functional block diagram is that the interfaces provide maximum leverage and functions should be allocated so that these interfaces are well defined and manageable. The interface managment issue thus drives the definition of the block diagram and ultimately the system architecture itself.

3.3 ETA System Architecture and Interfaces

This section develops the ETA system architecture based on the functional analysis presented previously. The system architecture is presented before elaborating upon the various interfaces and inter-relationships in the formats of the N^2 diagram and inter-relationship diagram.

3.3.1 System Architecture

Figure 3-11 incorporates the important features of the system functional flow and block diagrams presented in the previous sections. The sequence of events outlined in the functional flow diagrams is shown in addition to the hardware elements that are required to support the system functions. The distinction between the two microsatellite downlink events (Events 7 & 9), as noted before, will be in terms of the data volume. The action denoted by 7 is to downlink just the time-of-arrival and template correlation confidence factor. Action 9 represents the downlinking, if a partiular GRB is found to be interesting, of the profile stored onboard of that particular GRB.

Figure 3-12 presents the formal ETA system architecture. The system comprises the launch, space and ground segments. The launch segment will consist of the launch vehicle and the ground support facilities, including those for launch vehicle/payload integration and testing; these are not shown in the architecture for the sake of brevity.

The carrier spacecraft can be classified in a number of ways. One obvious way is the payload/bus breakdown, which is overly simplistic. In this study, the carrier spacecraft is classified into the following elements:

- **Microsatellite Storage and Separation System**
  This is the payload of the carrier spacecraft and comprises the microsatellites stacked in their stowed configuration. The trigger satellites and the rest of the microsatellites are identical in design even though the trigger satellites are different functionally. The critical component of the stack is undoubtedly the separation mechanism which will allow each microsatellite to separate from the stack. The design of the separation mechanism has to take into account constraints such as launch fairing dimensions and microsatellite configuration.

- **Propulsion System**
  This is included as a separate element since it drives the constellation design and hence influences the overall system in a strong manner. Remembering from previous discussion that the propulsion system could be an upper stage of the launch vehicle, or electric or chemical bipropellant system on a dedicated carrier spacecraft, the broad definition of "carrier spacecraft" in the architecture encompasses both these options. The utilization of an electric propulsion system will add a new dimension to the consideration of the system and justifies the inclusion of the propulsion system in the system architecture as a separate element of the carrier spacecraft.

- **Bus**
  This includes all the other standard systems of the carrier spacecraft. The more important ones are the power, attitude control, launch adaptor, thermal control and command and data handling subsystems.

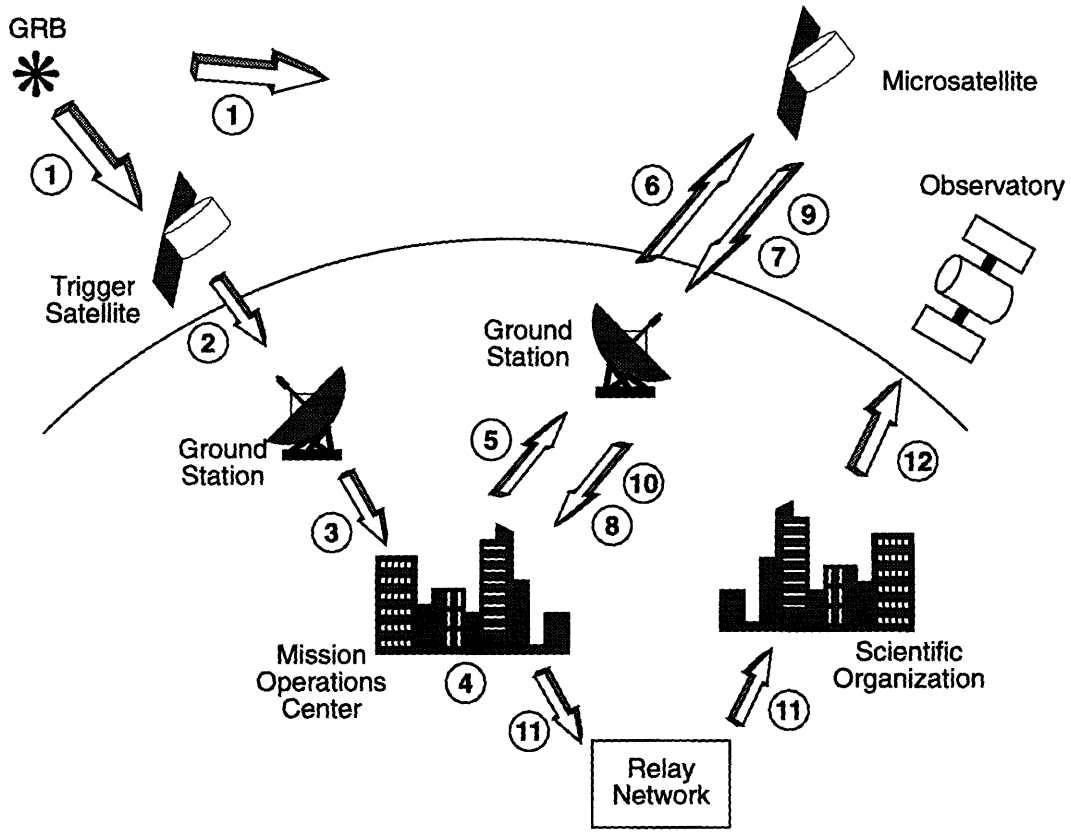

SEQUENCE OF EVENTS

(1) GRB triggers detectors, profile stored onboard
(2) Trigger satellite(s) downlinks GRB profiles
(3) Ground station relays profiles to Mission Operations Center
(4) Data Analysis Center prepares GRB template
(5) GRB template relayed to ground station
(6) GRB template uplinked to microsatellites where onboard processing determines Time-of-Arrival (TOA)
(7) Time-of-Arrival downlinked
(8) Time-of-Arrival relayed to Mission Operations Center
(9) Stored GRB template downlinked (if required)
(10) GRB template relayed to Mission Operations Center (if required)
(11) Coordinates relayed to scientific organizations
(12) Coordinates uplinked to spaceborne observatories

Figure 3-11: ETA System Concept

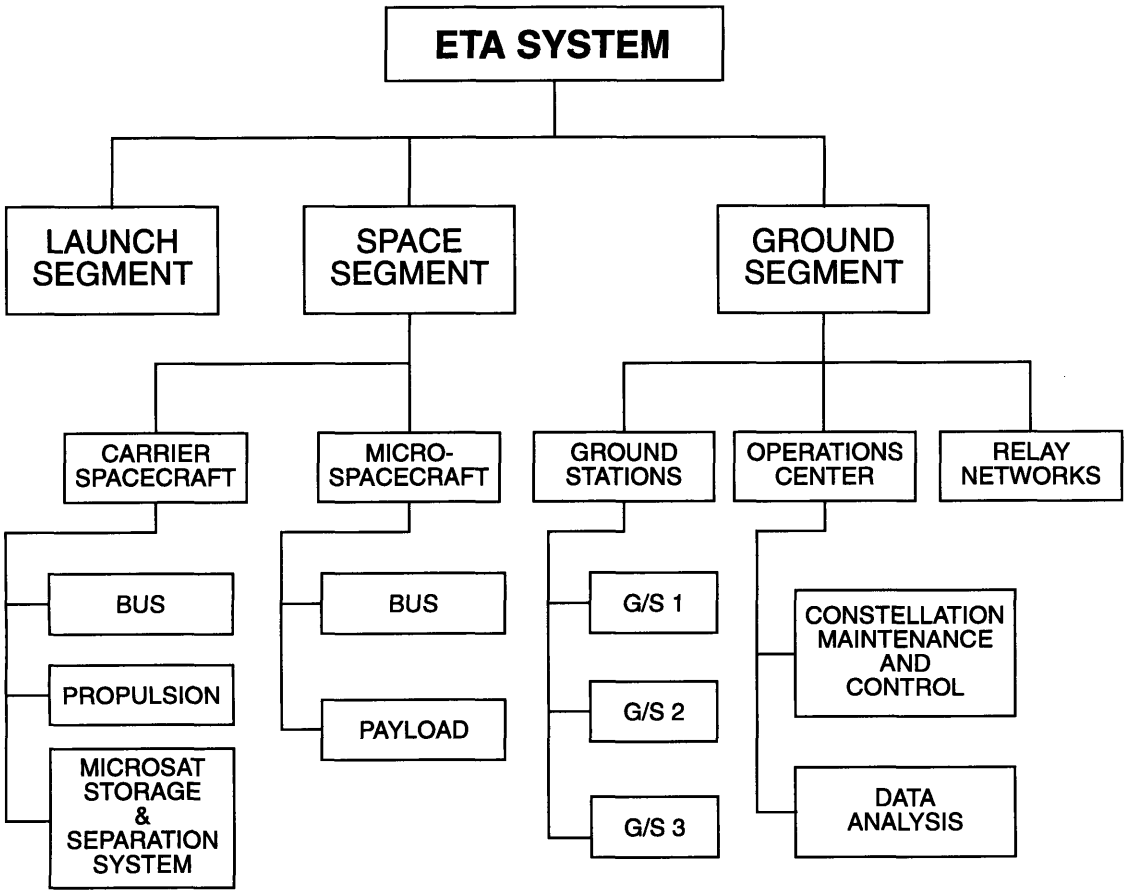

Figure 3-12: ETA System Architecture

The microsatellites are classified in a payload/bus manner. The payload includes the GRB detectors, payload electronics and the computer and associated software for onboard data processing. Standard subsystems related to power, attitude control, thermal control and so forth make up the microsatellite bus.

The ground segment will consist of a number of separate ground stations. Current considerations point towards using three ground stations for VLBI ranging (details presented in Chapter 8). The extra ground stations are also required to maximize link availability with the microsatellite constellation as well as providing redundancy in the ground segment.

The Mission Operations Center (MOC) is functionally divided into the constellation control and science data analysis sections. These will be colocated, but will probably be distinct in terms of software.

3.3.2 N^2 Diagram

The system interfaces, identified in the system functional block diagram previously, are presented in a more organized manner in the N^2 diagram in Figure 3-13. Even though the

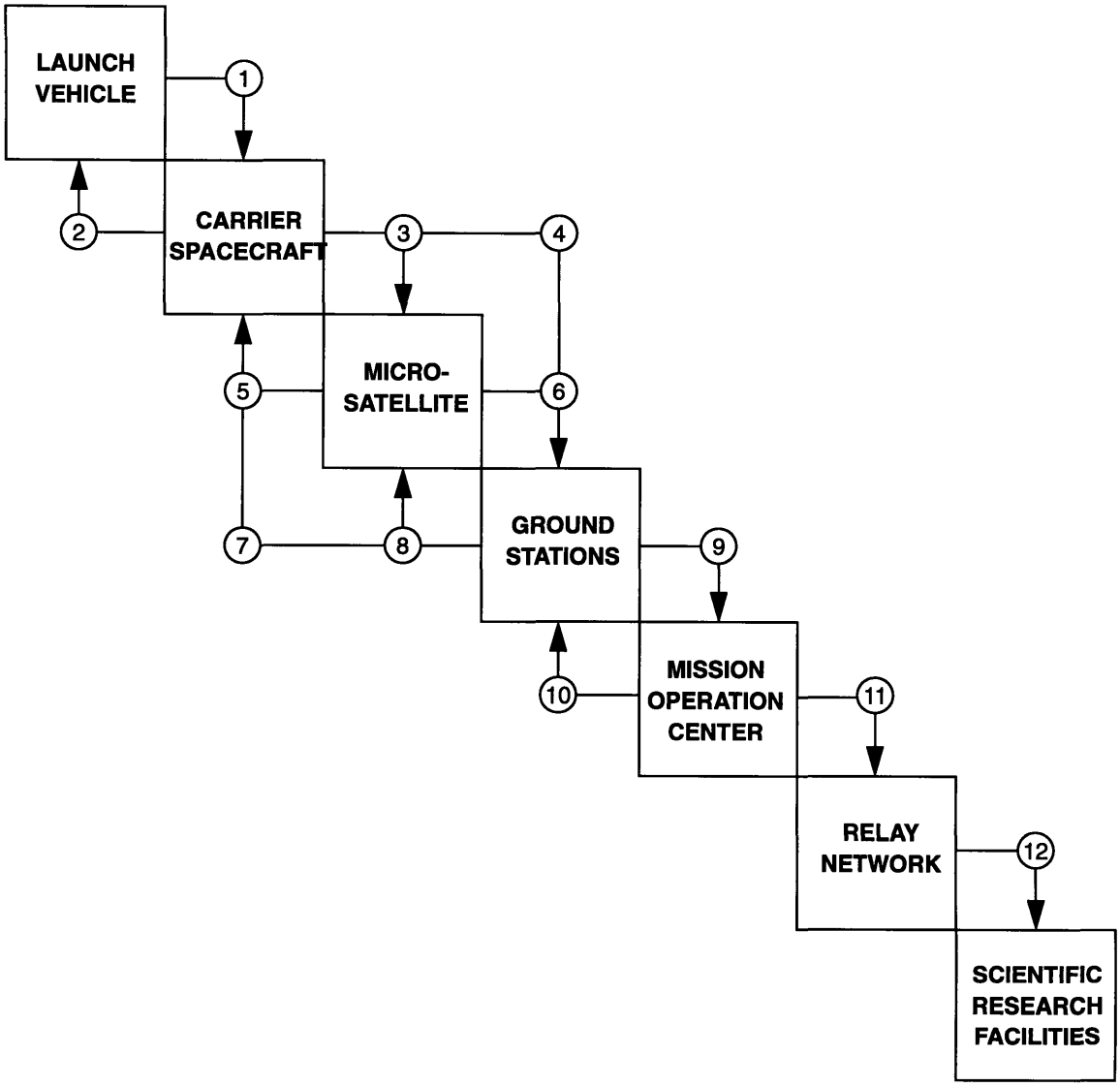

INTERFACES

(1)	Commands, Power	(launch phase)
(2)	Status (Telemetry)	(launch phase)
(3)	Power, Commands, Separation	(deployment)
(4)	Telemetry	
(5)	Status (Telemetry)	(deployment)
(6)	Status, GRB Data (time of arrival, profiles)	
(7)	Commands	
(8)	Commands, GRB Templates	
(9)	Spacecraft Telemetry, GRB Data, Ranging Data	
(10)	Commands (Carrier & Microsats), GRB Templates	
(11)	GRB Coordinate Data	
(12)	GRB Coordinate Data	

Figure 3-13: ETA System N^2 Diagram

scientific research facilities are not directly part of the ETA system, they have been included since the associated interfaces (Interfaces 11 & 12) are nevertheless very important to the effectiveness of the ETA system.

It is evident that the systematic mapping of interfaces facilitates the design of the system since redundant interfaces, for example, are easily identified. Alternate interface options, which can be used in backup modes or contingencies, are also readily determined. The complementary nature of most interfaces (command/telemetry) is clearly shown.

3.3.3 Inter-Relationship Diagram

The inter-relationships between various system elements are shown in Figure 3-14. The shaded boxes contain the main system elements with the first box including system features or characteristics such as accuracy, real-time alert capability and so forth. The characteristics of any particular element are listed in that respective row. For example, the real-time alert capability of the system depends on, among other factors, the proximity of the trigger satellites from Earth, which is a feature of the constellation design. The inter-relationship diagram is adept at identifying subtle inter-relationships. To illustrate the point, the area of the GRB detector is related to the ranging accuracy of the ground segment, through the system requirement on localization accuracy, which is a function of factors such as ranging accuracy and detector area. A trade thus exists between these two elements.

The utility of the inter-relationship diagram in the requirements flowdown process can be shown by considering the most important system performance requirement, GRB localization accuracy. The diagram reveals that accuracy depends on

- baselines provided by the microsatellite constellation
- accuracy of spacecraft locations
- timing uncertainties associated with the hardware and software of the microsatellite
- area of the GRB detector

All these factors are taken into account when flowing down the accuracy requirement. The allocation of this important requirement is performed in the next section.

3.4 ETA System Requirements

Having performed the analysis to define ETA system support requirements and baseline system architecture, it is now possible to list the ETA system requirements and allocate the driving requirements such as error box accuracy to lower levels of the system architecture.

3.4.1 Scientific Requirements

The scientific requirements stated in Chapter 2 are repeated here for the sake of completeness. The major requirements are:

SYSTEM FEATURES	1) Accuracy 2) Realtime Alert 3) Redundancy 4) "Wait-time" for Science Operations	1) Redundancy, Reliability 2) "Wait-time" for Science Operations	1) Accuracy 2) Realtime Alert 3) Reliability 4) Data Volume	1) Accuracy 2) Redundancy 3) Data Volume 4) Realtime Alert	1) Accuracy 2) Realtime Alert 3) Reliability/ Redundancy
1) Baselines 2) Proximity to Earth, Deployment Strategy 3) No. of S/Craft 4) Rate of "Spread"	**CONSTELLATION**	1) "Spread" over lifetime 2) Rate of "Spread" 3) Proximity from Sun 4) C_3 Reqmt	1) Proximity from Sun 2) Proximity from Earth 3) C_3 Reqmt 4) Rate of "Spread"	1) Maximum Range to Earth 2) Trajectory Declination	1) Earth Range 2) Deployment Strategy 3) Earth/Sun/S/c geometry 4) Trigger Sat. Orbits
1) Carrier Mass, Reliability 2) ΔV capability of propulsion system	1) Propulsion System 2) Carrier Mass, Thrusting Strategy 3) Power, TCS 4) Carrier Mass	**CARRIER SPACECRAFT**	1) Carrier Mass (based on LV) 2) Microsat Stack Separation Mechanism 3) Configuration	1) Microsat Separation Strategy	1) Power, G/T 2) Autonomy 3) Comms Interference 4) Antenna, Solar Array Directions
1) Timing Errors (H/w, S/w) 2) Datarates 3) System Reliability 4) Onboard Storage	1) Power, TCS 2) Comms Datarates 3) Microsat Mass 4) Microsat Mass	1) Microsat Mass 2) Separation Mechanism 3) Configuration	**MICROSAT**	1) Mass 2) Configuration 3) Power 4) Onboard Storage 5) Datarates	1) EIRP, G/T 2) Power Sizing 3) Autonomy
1) Sensitivity, Detector Area 2) No. Detectors 3) Compression Algorithm 4) Onboard Processing	1) Data Compression 2) Sensitivity, Quality of Measurements	1) Volume, Aperture Size, Placement on Microsat	1) Mass 2) FoV, Size 3) Power Reqmts 4) Resolution 5) Compression Technique	**PAYLOAD**	1) Correlation Accuracy 2) Detector Area
1) Ranging Accuracy 2) Data Analysis, Relay Network 3) No. of Ground Stations	1) Power, G/T 2) Command/ Tracking 3) Link Availability 4) Realtime Alert Capability	1) G/T, EIRP 2) Command Reqmts 3) Link Quality, Availability 4) Noise Background	1) EIRP, G/T, Link Quality 2) G/T 3) Command Reqmts	1) Ranging Accuracy 2) Ranging Accuracy	**GROUND SEGMENT**

Figure 3-14: ETA System Inter-relationship Diagram

- detect a sufficiently large number of GRB's with accuracies of 1-100 arcsec. Th exact number will depend on GRB characteristics and is necessary for statistical analysis to derive GRB positions. The ETA system will need to detect between 800-1,000 GRB's over its mission lifetime.
- provide a rapid trigger alert for ground-based and Earth-orbiting observatories
- provide accurate burst profiles
- ensure a constellation of at least 4 operational spacecraft over mission lifetime
- provide 100% temporal and spatial coverage of the sky over mission lifetime.
- provide a minimum constellation spread of 120^{o} with spacecraft at ranges of ~1 AU from the Sun. Such a constellation will provide the minimum baselines for GRB localization measurements.

3.4.2 Technical/Programmatic Requirements

Functional analysis provides insights into what system support requirements are necessary. Furthermore, there are other program related requirements and constraints that are imposed on the system. The major system requirements and constraints are listed below [4]:

- Nominal mission lifetime: 4 years, including data collection period
- Data collection period: 2 years minimum, implying constellation development time of 2 years for minimum baselines specified in scientific requirements
- Launch: 1st quarter 2000
- Launch vehicle: MEDLITE series, DeltaLite version
- System cost (including contingency): < $ 70M (FY'94 dollars)
- Total Timing Error limit: < 0.7 msec
- Minimum Number of Operational Microsatellites: 4
- Multiple ground stations for VLBI spacecraft location determination
- Microsatellite position knowledge: +/– 90 km
- Data logging capacity on Microsatellite: 24 hours minimum

3.4.3 Requirements Flowdown

Once the system requirements are defined and understood, the next step is to flow down the requirements to lower levels by the process of allocation. The flowdown process can be thought of in two complementary ways: the flowdown of all relevant system requirements to a particular system level or the flowdown of a given system requirement to all levels of the system. The former is discussed in Chapter 4, where system requuirements are flowed down to the constellation "level". An example of the latter is presented here in

the form of the flowdown of the requirement for system accuracy. Figure 3-14 illustrates the flowdown of the requirement for system accuracy.

The system accuracy requirement is signified by the error box size, which in turn can be related to performance measurables such as timing uncertainty. The accuracy requirement is thus an example of an indirectly allocable requirement according to the classification presented in Section 3.1.4. GRB localization accuracy depends strongly on the accuracy of the Time-of-Arrival (TOA) measurements as this is the most important measurable parameter. Timing uncertainty, as elaborated upon in Chapter 2 and revisited in the previous section, has a number of individual sources which contribute to the overall timing uncertainty of the system. Figure 3-14 identifies the major sources, with particular emphasis on the errors originating in the microsatellite system. Errors are introduced through clock errors, command execution, databus and onboard processing delays.

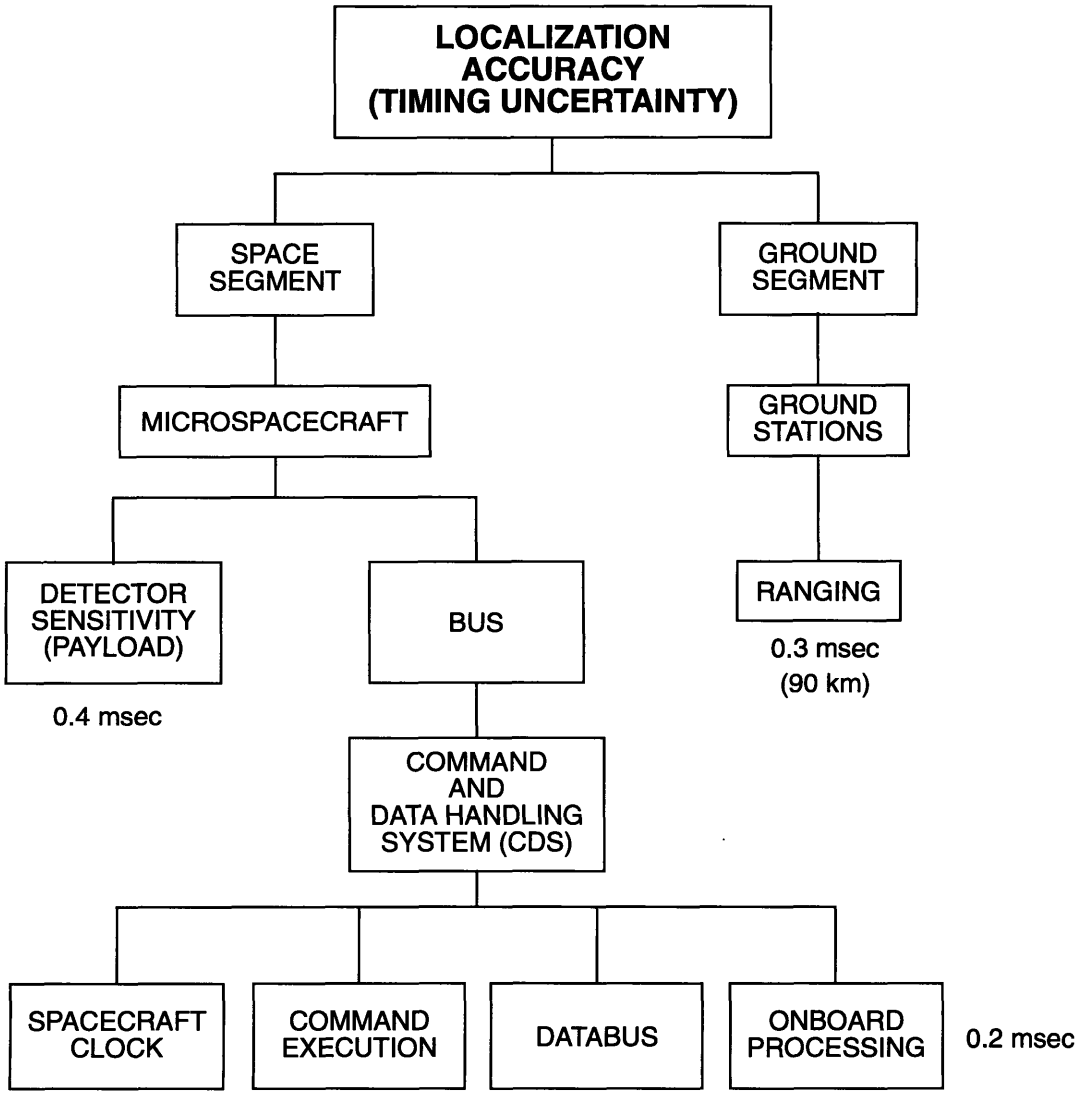

Figure 3-15: Flowdown of Accuracy Requirement

Overall timing accuracy is affected by statistical burst timing errors and systematic timing errors [15]. Burst timing errors are a function of the size of the GRB detectors as well as the characteristics of the burst itself. Shorter, brighter bursts are found to result in higher localization accuracies. Simulations have shown that the brightest bursts will result in a timing match of about 0.4 msec, which results in a localization acuracy of ~ 0.10 arcsec [4]. This is the allocation made for the payload (GRB detectors) of the microsatellites. It is important to minimize the contribution of systematic errors in order to achieve localization accuracies of the order of 0.1 arcsec.

Systematic errors can be controlled through design. The primary contributors to systematic errors are timing errors due to spacecraft hardware and those due to uncertainties in spacecraft location. Spacecraft position uncertainty directly translates into timing errors with respect to light travel time. Spacecraft position accuracy of 90 km (or 30 km in each coordinate) translates to 0.3 msec light time. These location accuracies can be achieved but will require VLBI techniques in addition to ranging [4].

Assuming that spacecraft location and timing errors are uncorrelated, a timing uncertainty of 0.2 msec due to onboard errors will result in an overall timing uncertainty of about 0.65 msec [4]. This translates to a GRB localization accuracy of about 0.15 arcsec. The choice of 0.2 msec and 0.3 msec for hardware timing and spacecraft location accuracy respectively was based on a trade between minimizing overall timing error and the cost of achieving the requisite accuracies [4]. The improvement in performance therefore had to be traded against the cost of attaining that improvement.

The allocation of the 0.2 msec error between contributing spacecraft elements does not need to be performed at this stage of the design process. This is because the system has not been analyzed to that level and allocation will depend on trade studies performed to determine the specifications of components like the onboard clock, flight computer, databus and so forth. The more important consideration at this point is the identification of contributing error sources rather than absolute allocation of requirements.

Flowdown of system requirements to lower system levels, in the manner outlined above, allows the initiation of the analysis and design of the rest of the system. The system accuracy requirement flowdown was as example of "single requirement-to-all system levels" allocation. The converse allocation process, "all system requirements-to-single level", is illustrated in the flowdown of applicable system requirements to the constellation "level" in the next chapter.

Chapter 4

Propulsion System Trade Study

The accuracy of GRB localization measurements is a function of the inter-spacecraft baselines. In order to realize a constellation in which the microsatellites are angularly spread out around the Sun, it is necessary to deploy each of the microsatellites into distinct heliocentric orbits. This translates into requiring different orbit energies, which is accomplished by imparting a differential velocity (ΔV) to each microsatellite prior to deployment. A variety of propulsion options exist to perform this important function. This chapter presents the top level trade study performed to assess these options and select the one which was deemed optimal with respect to a number of criteria.

Relevant system requirements are flowed down to determine the associated requirements and constraints placed on the constellation design. The methodology adopted for this trade study is then elaborated upon. In particular, the assumptions and criteria for selection are discussed, together with the method used to estimate the performance of the propulsion systems. After identifying the propulsion options available, a comparison is made based on the established criteria. The selected option is discussed in the summary at the end.

This chapter serves as a "bridge" between the requirements development phase (Chapter 3) and the commencement of both mission and system design. The selection of the propulsion system for constellation deployment constitutes an integral step towards the analysis necessary to develop the constellation deployment strategy.

4.1 Requirements Flowdown

The requirements flowdown process, as discussed in the previous chapter, is vital to the design of the system. It provides a means to translate top level system requirements into forms which facilitate the design of lower levels of the system. In addition to enabling trade studies, the flowdown also establishes the traceability of top level system requirements. In the event that low level requirements are found to be difficult to meet, the traceability established by the requirements flowdown process allows designers to "push back"

on the relevant top level requirements. The discussion here deals with the flowdown of relevant system requirements to the constellation "level" so as to form the basis for the propulsion system trade study. Propulsion system options have to comply with the objectives and constraints identified by the requirements flowdown process. Even though some of the requirements may not be of direct consequence to the trade study considered here, they are nevertheless included on account of their impact on the constellation analysis and design carried out later.

The major requirements applicable to the constellation, and hence to the propulsion system trade, are discussed hereafter. The type of the requirement, according to the classification presented in Chapter 3, is mentioned. The system requirements from which the constellation level requirements originate, are also identified.

- **Provide a constellation angular "spread" of 120^0 in 2 years**
  This indirectly allocable requirement results from a combination of scientific and programmatic requirements. Microsatellites orbiting at ~1 AU from the Sun and angularly spread out in a 120^0 arc about the Sun provide baselines which can localize GRB's to specified minimum accuracies. From the perspective of scientific operations, it is ideal if the constellation can be designed to develop these minimum baselines in the shortest possible time. However, this requires large ΔV's which would substantially impact spacecraft design. This requirement is somewhat fuzzy and is essentially an "eyeball" compromise between system design and programmatic considerations.

  This requirement defines, in effect, the rate at which the constellation must develop to achieve the minimum baselines in the given time. The requirement has to be converted into a performance variable which is more directly related to the propulsion system; the performance variable appropriate in this case is the net ΔV required. The derivation of ΔV from the requirement is done in a later section in this chapter.

- **Launch Vehicle: DeltaLite version of the Medlite Series**
  The ETA mission is constrained in terms of the choice of launch vehicle due to a programmatic requirement associated with the type of NASA-sponsored mission ETA is being proposed for. DeltaLite, a variant of the Delta launcher, is a member of the Medlite series which is to be procured by NASA [24].

  The launch vehicle requirement is a non-allocable system requirement applicable to the entire system. While specifications such as launch environment and payload fairing sizes will impact the spacecraft design, it is the payload lift capability of the DeltaLite that is of importance here. In particular, the escape (C_3) performance is relevant as it defines trajectory velocity conditions and places limits on available mass for the carrier spacecraft and microsatellites.

The payload capability of the DeltaLite to a range of C_3's is tabulated in Table 4-1; data are estimated from performance curves in Reference [24].

Table 4-1: C_3 Capability of DeltaLite Launch Vehicle [24]

C_3 (km^2/sec^2)	Payload Mass[a] (kg)
-2	600
-1	587
0	570
1	560
2	550
3	540
4	530
5	520

a. Uncertainty in Mass estimates is 7 kg.

Noting that payload mass for the launcher constitutes both the carrier spacecraft and the microsatellites, assumptions have to be made on the carrier spacecraft and microsatellite masses when performing the trade study. The assumptions for the trade study are outlined later.

- **Minimum number of microsatellites in constellation: 4**
  A lower constraint of 4 is placed on the microsatellites in the constellation based on the minimum number required for unambiguous GRB localization, as discussed in Chapter 2. This requirement is hence a direct flowdown of a non-allocable scientific requirement. The number of microsatellites is also related to the mass available from the launch vehicle. There is a related requirement for one or two microsatellites to perform the function of the trigger satellites in the vicinity of Earth.

- **Mission lifetime of 4 years**
  This non-allocable system requirement applies to the constellation in a manner which is different compared to how it is applicable to hardware. Two years will be allowed for the constellation to develop before nominal scientific activities commence. Current plans call for a further two years of scientific data gathering based on funding availability.

The specified mission timeline affects the design of the microsatellite deployment strategy and subsequent constellation deployment. The

constellation will develop over time and provide maximum baselines when the microsatellites cover the complete 360° arc around the Sun. The angular spread will continue to increase beyond 360° but this will create an "overlap" and as a result, the effectiveness of the constellation to localize GRB's will degrade relative to the maximum baselines. This effect will be illustrated by the time history of the constellation figure of merit, η_{const}, in Chapter 6, where the constellation analysis is performed.

It follows that the deployment strategy should be designed such that the constellation creates the minimum baselines two years after launch and provides better η_{const} at least until about 4 years after launch.

- **Reliability/Redundancy**
  Like any other complex system, the ETA system has a requirement for reliability/redundancy, even though it has not been stated explicitly before. The system has to be reliable while providing redundancy in the form of backup options for critical mission and system elements.

  The flowdown of the reliability requirement to the constellation can be understood in terms of the propulsion system employed for the deployment phase. The propulsion system has to be highly reliable and should incorporate redundancy in one form or another. Partial failure of the propulsion system should not compromise the mission in its entirety but provide a "graceful degradation". For example, if a partial failure occurs, the propulsion system should still be able to provide a substantial fraction of the required ΔV to each microsatellite. This will enable the constellation to provide at least some reasonable baselines, albeit later in the mission than originally planned.

  The number of microsatellites in the constellation is also affected by the redundancy requirement. More microsatellites provide a higher level of redundancy but there is an upper constraint based on available launch mass, launch stacking, cost and so forth.

4.2 Top Level Trade Methodology

This section outlines the basic framework for conducting the top level trade study concerning the choice of propulsion system for the deployment phase of the mission. Relevant assumptions are identified and the criteria for the selection process are established before going into the details of the estimation of performance in terms of constellation "spread" and launch mass required.

4.2.1 Overview

The goal of the trade study was to identify the propulsion system that best satisfies the var-

ious criteria for performing perhaps the most important phase of the mission. The results of this particular trade study are based on a number of identified criteria. Some of these, such as risk and availability, are not easily quantifiable. As a result, some degree of "arm-waving" is necessary and justified for this stage of the top level design phase. It also turns out that performance is not the primary criterion for assessment. As is so often the case, programmatic issues dictated that other criteria like cost and availability were deemed to be more important than performance. A simple method was developed to provide reasonable estimates of constellation performance.

The simple approach to compare performance of the various options was basically to estimate the ΔV required to achieve the required spread in the specified time (120^{o} in 2 years). An estimate of the launch mass could then be arrived at using the Rocket Equation. This could be compared against the payload capability of the DeltaLite for a given C_3. Details of the method are presented later. A number of assumptions had to be invoked to facilitate the comparison of options.

4.2.2 Assumptions

The assumptions that were made for the purposes of the propulsion system trade are discussed below:

- **$C_3 = 1.0\ km^2/sec^2$**
  Even though the C_3 affects the rate of "spread" of the constellation, its effect was nullified under the condition that the assumed value would be consistently used for all propulsion options. In that respect, the utility of the C_3 was merely to provide a launch mass benchmark against which to compare the actual launch mass required for each propulsion option. Launch masses for the various propulsion options will be compared against 560 kg (DeltaLite capability to C_3=1).

- **Core Mass of Adaptor/Carrier Spacecraft = 70 kg [25]**
  The trade study considered two different schemes for deploying the microsatellites. These were microsatellites with their own propulsion systems ("dedicated" microsatellites) or microsatellites deployed by a carrier spacecraft with a propulsion system. In the case of the dedicated microsatellites, an "adaptor" spacecraft would be required to stack the microsatellites onto. The adaptor would require some power for telemetry and guidance. This was assumed to be the same as the corresponding "core" mass of the carrier spacecraft (everything except power and propulsion systems). 70 kg was selected based on estimates from the spacecraft contractor.

- **Microsatellite Mass = 50 kg [25]**
  Microsatellite mass is one design parameter which will fluctuate over the design period. The mass is assumed to include all mass except that of any propulsion system that may be utilized for providing the

"spread" ΔV prior to deployment (as in the cases of dedicated microsatellites). 50 kg was based on a conservative preliminary estimate of the spacecraft mass required to support the payload.

- **Number of Microsatellites in Constellation: 4-8**
  The number of microsatellites was undecided at the time of the trade study. The rationale was that the number of microsatellites would be determined by the available mass for microsatellites after subtracting the carrier spacecraft mass from the launcher capability. For example, if the carrier and microsatellite masses were found to be 250 kg and 50 kg respectively, then 6 microsatellites would be used for a C_3 of 2 km^2/sec^2 (550 kg payload capability). Therfore, the analysis was performed for 4-8 microsatellites, the upper limit set by considering the minimum achievable microsatellite mass. A minimum of 4 spacecraft are required for science operations; a five spacecraft system thus provides redundancy against loss of one spacecraft. With dual trigger satellites, six microsatellites are required for the system to function with the loss of one trigger satellite and one other microsatellite. This is the minimum number to provide redundancy against both trigger satellite and "general" microsatellite failures.

4.2.3 Criteria for Selection

The criteria established for assessing the trade options are outlined below:

- **Compliance with Requirements**
  Any propulsion system alternative must first and foremost satisfy system and constellation-related requirements and constraints. Even though it has not been explicitly stated in the Section 4.1, the propulsion system must not, during the course of the ΔV burn, create conditions that could potentially damage the microsatellites.

- **Performance**
  Performance here is meant to be the launch mass required to achieve the required angular spread in the specified time. Trade options will be compared in terms of launch mass required and the optimal option, in the context of performance, will be the one with the lowest launch mass. It is important to note, however, that performance is not the sole criterion for selecting the propulsion system.

- **Flight Experience/Heritage**
  Since ETA is being proposed as a scientific mission, it is imperative that any technology that is utilized have an established flight heritage with extensive flight experience. The incorporation of unproven technology would only serve to create doubt in the minds of NASA proposal reviewers and jeopardize the chances of the mission being

selected. This criterion is complementary to technical risk.

- **Availability**
  This is a very important aspect from the standpoint of the successful endorsement of the proposed mission. The selected propulsion system should be readily available, without complications associated with procurement or qualification testing. Other factors like political or regulatory constraints may prohibit the utilization of hardware that may otherwise satisfy ETA mission requirements.

- **Cost**
  It is relatively difficult to estimate the costs related to utilizing a specific system. In certain cases, contractor information may be available but more often than not, such information would be proprietary. Nevertheless, a relative comparison of costs can be made with the aim of identifying and discarding prohibitively expensive options.

- **Reliability/Redundancy/Flexibility**
  While any propulsion system will have to be highly reliable, it should also incorporate a level of redundancy and allow a fair degree of flexibility to allow for unexpected circumstances or failures. If possible, there should be no possibilities for single point failures, since this can potentially lead to complete mission failure. Such a failure of the propulsion system would leave the microsatellites undeployed and seriously endanger the chances of mission success.

With the exception of performance, most of the criteria are difficult to quantify and some degree of "arm-waving" is necessary, based on information that can be gleaned from available manufacturer literature and opinions of industry experts. A simple method of estimating propulsion system performance is outlined next.

4.2.4 Estimation of Propulsion System Performance

The process of estimating propulsion system performance involves linking the constellation "spread" requirement with the payload capacity of the launch vehicle, through the net ΔV required. Figure 4-1 outlines the process adopted.

The requirement for the constellation to have developed a certain angular "spread" in a specified time is translated into an equivalent net ΔV requirement on the propulsion system. Keplerian orbit theory is invoked to facilitate this translation. Once the net ΔV requirement is known, it is allocated to each microsatellite, depending on the scheme being considered (dedicated microsatellites or carrier spacecraft). The Rocket equation is then used to determine the total propellant mass required by the propulsion system to impart the allocated ΔV to each microsatellite. Launch mass is calculated via the summation of the various component masses for each propulsion option and these are compared against the payload capability of the launcher to the assumed C_3. The optimal option is

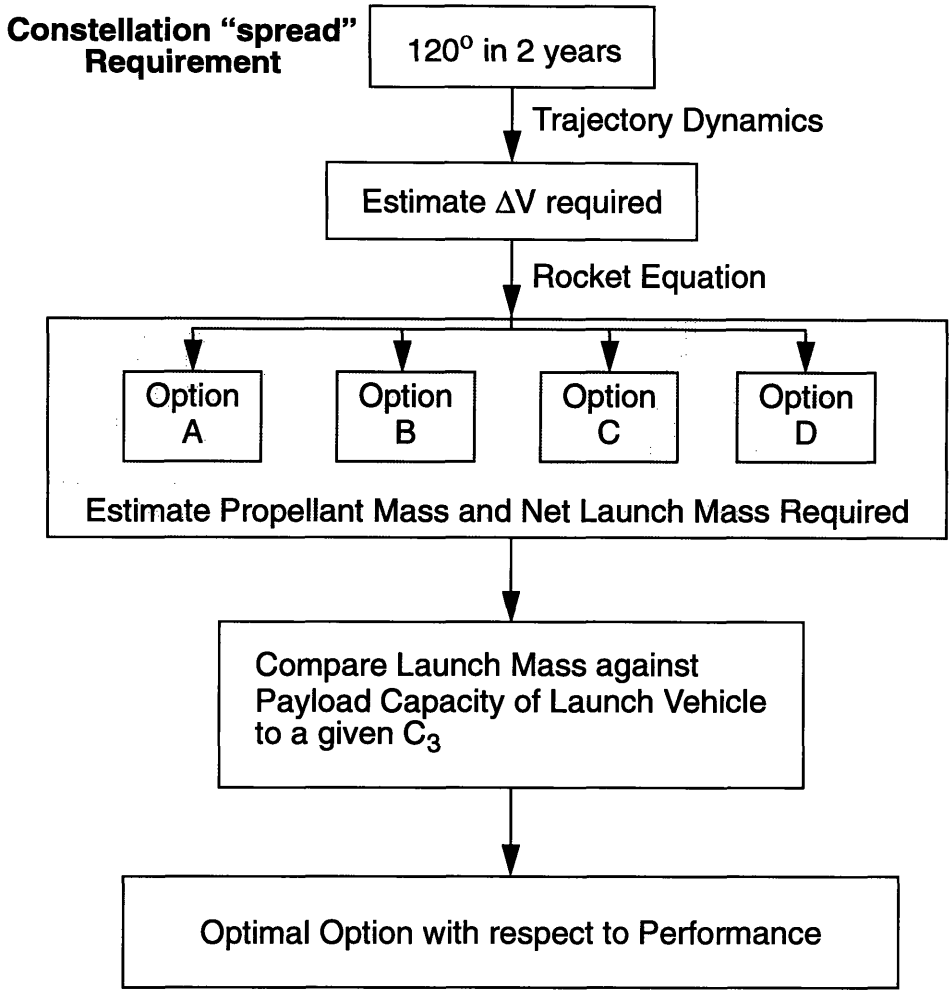

Figure 4-1: Methodology for Estimation of Propulsion System Performance

that which results in the minimum launch mass.

The relationship between constellation angular spread and required ΔV is established by starting off with Kepler's Third Law in the form of the mean motion, n:

$$n = \sqrt{\frac{\mu_{Sun}}{a^3}} \qquad \text{Eqn (4-1)}$$

where μ_{Sun} is the gravitational parameter of the Sun and a is the semimajor axis of the orbit. Differentiation of Eqn (4-1) yields

$$\Delta n \approx -\frac{3}{2}\left(\frac{\mu}{a^5}\right)^{0.5} \Delta a \qquad \text{Eqn (4-2)}$$

By assuming, for the purposes of this preliminary trade study, that the velocity V, in the orbit is approximated by that in a circular orbit of equal semimajor axis, it is possible to relate Δa to ΔV as follows:

$$V \approx \sqrt{\frac{\mu_{sun}}{a}} \qquad \text{Eqn (4-3)}$$

Differentiating and rearranging,

$$\Delta a \approx -\frac{2a^2}{\mu} V \Delta V \qquad \text{Eqn (4-4)}$$

Substituting Eqn (4-4) into Eqn (4-2) and using Eqn (4-3) to substitute for V, the azimuthal spread $\Delta\theta$ is related to ΔV in the form

$$\Delta V \approx \frac{a\Delta n}{3} \qquad \text{Eqn (4-5)}$$

Δn can also be approximated by

$$\Delta n \approx \frac{\Delta\theta}{T_s} \qquad \text{Eqn (4-6)}$$

where $\Delta\theta$ is the angular azimuthal spread around the Sun and T_s is the time over which that spread is achieved. Substituting Eqn (4-6) into Eqn (4-5) finally results in an approximate relationship between constellation spread and required ΔV:

$$\Delta V_{net} \approx \frac{\bar{a}\,(\Delta\theta)}{3T_s} \qquad \text{Eqn (4-7)}$$

where $\bar{a}$ is the "average" value of the semimajor axis of the orbit. For achieving a spread of 120^0 in 2 years, and assuming orbits of ~1 AU, the net ΔV required is approximately 1650 m/s. This is the differential velocity, relative to first microsatellite, that must be imparted to the last microsatellite in order that the angular separation between them is about 120^0 after 2 years.

The next issue is with regard to the distribution of the net ΔV to the microsatellites, and this depends on the scheme of deployment being considered, namely dedicated microsatellites or carrier spacecraft with propulsion system.

Considering the scheme of dedicated microsatellites, the distribution of ΔV assumed in this study depends on the type of propulsion system being used, the types being either solid propellant or liquid/electric propulsion systems. The distribution was based on the strategy outlined in Figure 4-2.

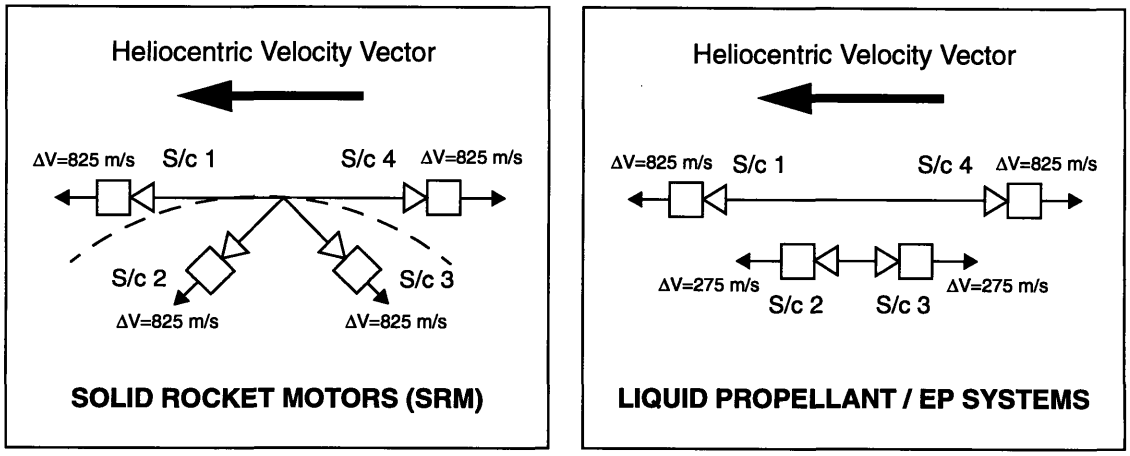

Figure 4-2: Deployment Strategy for Dedicated Microsatellites

The spread can be attained by providing the ΔV's in the +/- heliocentric velocity directions as shown.

Thus, the ΔV for the first and last microsatellites is effectively half of the net ΔV in order to achieve the total "spread" ΔV. It was further assumed, for solid propellant systems, that the rest of the microsatellites would have the same propellant load and are fired at angles to the heliocentric velocity vector to achieve the spread. As a result, all microsatellites have a propulsive ΔV of $0.5\Delta V_{net}$, even though the final heliocentric velocities will be different. The rationale behind this approach is that the SRM's are all the same and the spacecraft masses are the same, easing system design. Furthermore, the cost of procuring the SRM's is less since the they do not have to be customized differently from each other. Note, however, that this strategy is inefficient in terms of propellant utilization since the maximum ΔV is only obtained if the burn is parallel to the velocity vector. As an example of this strategy, for a 4 microsatellite constellation, the net "spread" ΔV of 1650 m/s could be achieved by ΔV's of 825 m/s to each microsatellite but at angles of 0, 60, 120, 180 degrees to the heliocentric velocity vector.

If the dedicated microsatellites have a liquid propellant system, it is possible to have a common design (propellant tank and hardware). The propellant load can be varied at the same time as performing the ΔV only in the +/- directions to get maximum change in heliocentric velocity. The first and last microsatellites have ΔV's of $0.5\Delta V_{net}$ in the +/- velocity directions, with the rest of the microsatellites' ΔV's equally distributed in between. For example, a 4 microsatellite constellation would have ΔV's of +825, +275, -

275, -825 m/s respectively.

The distribution of net ΔV for a constellation deployed by a carrier spacecraft with propulsion system is as follows. The ΔV's to each microsatellite are imparted in the same direction (prograde or retrograde but not both) since a single propulsion system is being used. It is assumed that the first microsatellite is deployed immediately after escape without any imparted ΔV from the propulsion stage. For ease of calculation, it is further assumed that each of the rest of the microsatellites is given an equal ΔV increment. Thus, for a constellation of N microsatellites, the incremental ΔV imparted to each microsatellite is

$$\Delta V_{\mu sat} \approx \frac{\Delta V_{net}}{(N-1)} \qquad \text{Eqn (4-8)}$$

For constellations of between 4-8 microsatellites, $\Delta V_{\mu sat}$ could thus range between 250-300 m/s.

The next step in determining launch mass is to calculate the propellant mass required for each ΔV burn and hence the net propellant mass required to deploy the entire constellation. Keeping in mind that the effective payload for each ΔV burn is the total mass of the carrier spacecraft and all other microsatellites still undeployed, the net propellant mass is calculated by starting with the last microsatellite and working back to the first microsatellite. The Rocket Equation can be written as

$$\Delta V = g I_{sp} \ln\left[\frac{M_a + M_{prop}}{M_a}\right] \qquad \text{Eqn (4-9)}$$

where g is the acceleration due to Earth's gravity, I_{sp} is the specific impulse of the propulsion system, M_a is the accelerated mass and M_{prop} is the propellant mass required to impart the ΔV to M_a. M_a for the ΔV burn of the i'th microsatellite of an N microsatellite constellation is given by

$$M_{a\,(i)} = M_{carrier} + (N+1-i)\,M_{\mu sat} + \sum_{i+1}^{N} M_{prop\,(i)} \qquad \text{Eqn (4-10)}$$

where $M_{carrier}$ is the dry mass of the carrier spacecraft, $M_{\mu sat}$ is the mass of each microsatellite and $M_{prop(i)}$ is the propellant mass required to impart $\Delta V_{\mu sat}$ to the i'th microsatellite. The expression for $M_{prop(i)}$ is derived by rearranging Eqn (4-9):

$$M_{prop\,(i)} = M_{a\,(i)}\left[\exp\left(\frac{\Delta V_{\mu sat}}{gI_{sp}}\right) - 1\right] \quad i = 1, 2, \ldots N \qquad \text{Eqn (4-11)}$$

Note that $M_{prop(1)} = 0$, by assumption.

Starting off with the last microsatellite, $M_{a(N)}$ is calculated from Eqn (4-10). $M_{prop(N)}$ is then determined from Eqn (4-11) after which Eqn (4-10) is used again to evaluate $M_{a(N-1)}$ and the process continues until $M_{a(1)}$ is determined; this is the launch mass required for that specific propulsion system.

Note that the carrier mass includes propulsion system mass which has to be estimated. Under the assumption that propulsion system mass is a certain fraction of total propellant load, it follows that the above procedure for calculating the launch mass is iterative. Since the core mass is known (assumed to be 70 kg), the goal of the iteration should be to estimate the net carrier mass which includes the core, propellant and propulsion system mass. Propulsion system/propellant mass ratios were assumed to be 0.20 and 0.25 for chemical and Electric Propulsion (EP) systems respectively.

Additionally, EP systems also have extra power system mass which has been estimated based on power requirements. Power system mass was based on required power and includes solar array mass (at 17 kg/kW) and power electronics mass. The total power requirement was estimated by assuming a power conversion efficiency of 85% and knowing the input power to the EP thruster.

4.3 Propulsion System Options

Two different schemes of deployment were considered:

- **Dedicated Propulsion for Microsatellites**
  This is an obvious option. Small Star-type solid motors for each microsatellite would provide the ΔV independently. The advantages of this approach are the redundancy and protection against single point failures that could potentially plague a single propulsion stage providing ΔV's to all microsatellites. A major disadvantages is the no-restart capability. Another disadvantage is the overhead on each microsatellite for Guidance, Navigation and Control (GNC). This translates not only into increased spacecraft complexity but also into increased ground control during the deployment phase. A Star 13 motor has been assumed for this study. Even though this motor gives extra ΔV, the propellant charge is assumed to be reduced to the necessary amount to give a ΔV of 825 m/s.

  Liquid bipropellant systems could be used for restartability. This is

especially useful when considering the trigger satellites which may need to be injected into different orbits. A monopropellant hydrazine system has been assumed for this study. For purposes of comparison, an EP system is also assessed with a 100 W stationary plasma thruster (SPT); note that this thruster is currently unavailable. This thruster is assumed to be scaled from the SPT-70 which is available.

- **Dedicated Carrier Spacecraft with Chemical Propulsion System**
  The notion of using a dedicated carrier spacecraft is attractive since it allows the microsatellite masses to be constant, allowing simpler and common designs. This is so because the final microsatellite to be deployed accumulates a large fraction of its needed ΔV while the other microsatellites are being accelerated. Obviously, the carrier spacecraft dry mass has to be accelerated all the the way but this apparent penalty can be mitigated through the use of propulsion systems with higher I_{sp} than solid propellants. A restartable chemical bipropellant system is one such option.

  Liquid bipropellant technology has been well proven over the years and is readily available. The issue is whether it can provide sufficient performance to provide the required ΔV to all the microsatellites as well as the carrier spacecraft.

  Another plus point of the dedicated carrier spacecraft concept is that the carrier would, at the end of the deployment phase, provide a platform in heliocentric orbit that would be ideal for a secondary mission which requires just such an environment. This is especially attractive in the context of potential cost-sharing to reduce program cost for each of the participating parties.

- **Dedicated Carrier Spacecraft with Electric Propulsion**
  Alternatively, the dedicated carrier spacecraft could employ an electric propulsion system. The substantial improvement in I_{sp} over chemical systems would alleviate the problem of having to accelerate the carrier spacecraft. The disadvantage of Electric Propulsion systems is the need for larger solar arrays and extra power processing equipment. Moreover, the low thrust of such systems results in a prolonged deployment period of the order of months, incurring ground operations costs.

  Skepticism regarding the application of EP systems is still rife within the community despite the fact that a number of EP technologies have demonstrated operational feasibility over the years. It is thus imperative, with regard to acceptance of the proposed mission, that if selected, the EP system should have substantial flight experience and be readily available.

One feature of Electric Propulsion often overlooked is the flexibility it offers in operation. EP systems can operate over a range of operating conditions without substantial degradation in performance, allowing fallback options for mission design. Additionally, it is easier to protect against single point thruster failures by including redundant thrusters since the mass penalty is quite small.

Of the various EP thrusters, this trade study considers the arcjet, Stationary Plasma Thruster (SPT) and Ion engine. The discussion of the attributes of each of these is beyond the scope of this study and the reader is referred to related literature for details [26,27]. Suffice it to say that the typical I_{sp}, which is the important parameter for this trade study, of the arcjet, SPT and Ion engine is of the order of 300-600 sec, 1400-1600 sec and 2000-3000 sec respectively.

Typical performance characteristics of the propulsion alternatives considered are outlined in Table 4-2. [26,27,28,29]

Table 4-2: Performance Characteristics of Propulsion Options

	Propulsion Option	Performance Characteristics			
		Isp (sec)	Thrust (N)	Power (W)	Efficiency
Dedicated Microsats	Solid RocketMotor(SRM)	286	3800	N/A	N/A
	Monopropellant Hydrazine: MR-50	~230	22.2	N/A	N/A
	100 W SPT (not available yet)	1510	~0.006	100	0.46
Carrier Spacecraft	Chemical Bipropellant: KM-R4D	312	490	N/A	N/A
	Arcjet : MR 508	502	0.225	~1600	0.35
	Plasma Engine: SPT-70	1510	0.04	660	0.46
	Ion Engine : XIPS	2585	0.018	439	0.51

The Star 13 motor was found to be the most suitable motor for ETA. The relatively high thrust is typical of solid propellant systems. The Kaiser Marquardt R-4D is actually an attitude control thruster with over 800 built [28]. For the EP systems, the driving constraint was availability since the mission can only be implemented with available technology. Thus, even though a lower power arcjet is under development, a higher power version was selected because it is available. The lowest power available was 1800 W for the MR 508. The Stationary Plasma Thruster (SPT-70) is a Russian thruster used for stationkeeping functions on their spacecraft. The larger SPT-100 was not considered since it requires

1350 W. XIPS, which stands for Xenon Ion Propulsion System, is an ion engine developed by Hughes for stationkeeping on their HS 601 spacecraft buses [27]. Of the options listed in Table 4-2, only the 100 W SPT is not available; this was included for comparative purposes.

.

4.4 Comparison of Propulsion Options

This section presents the comparison of the trade alternatives in a criterion-wise fashion. The motivation behind this manner of presenting the results is because it enables one to assess all propulsion options against one criterion at a time. It also facilitates the elimination of options which fail to meet minimum criteria. The criteria are not ordered in terms of relative importance or priority. A summary of the trade results is presented at the end.

4.4.1 Compliance with System Requirements

All the propulsion options can be configured to meet the requirement for constellation "spread", albeit at higher launch masses for some options. This is however addressed in the comparison of performance. The other system related requirements such as the use of the DeltaLite, minimum number of microsatellites and mission lifetime are met by all options.

4.4.2 Performance

This section discusses the results of the evaluation of the performance of the propulsion options, according to the procedure outlined previously. Launch mass estimates for the different propulsion options are presented.

Figure 4-3 summarizes the results for the propulsion options considered, plotting launch mass as a function of number of microsatellites. The carrier propulsion alternatives are plotted as lines while dedicated microsatellite cases are plotted as points.

Launch mass varies linearly with number of microsatellites for all options. The lowest launch masses are achieved by EP systems such as the SPT-70 and XIPS systems for the carrier spacecraft. The chemical and arcjet systems for the carrier spacecraft require the highest masses. Despite its relatively high specific impulse, the arcjet has the highest launch masses, primarily because of the high power requirements, which subsequently translate into higher carrier masses. This seems to indicate that the arcjet's power is too high for this application; a lower power system is required. Currently, the MR-508 is the lowest power arcjet available, even though sub-kilowatt arcjets are under development [30]. The chemical bipropellant carrier system also has too high a launch mass, being unable to deploy 6 microsatellites to a C_3=1.

As might be expected, dedicated microsatellite propulsion systems result in lower launch masses compared to the bipropellant or arcjet carrier options because of the absence of a bulky carrier spacecraft. The interesting thing to note, however, is that the monopropellant systems have better performance than solid propellant systems which have a higher spe-

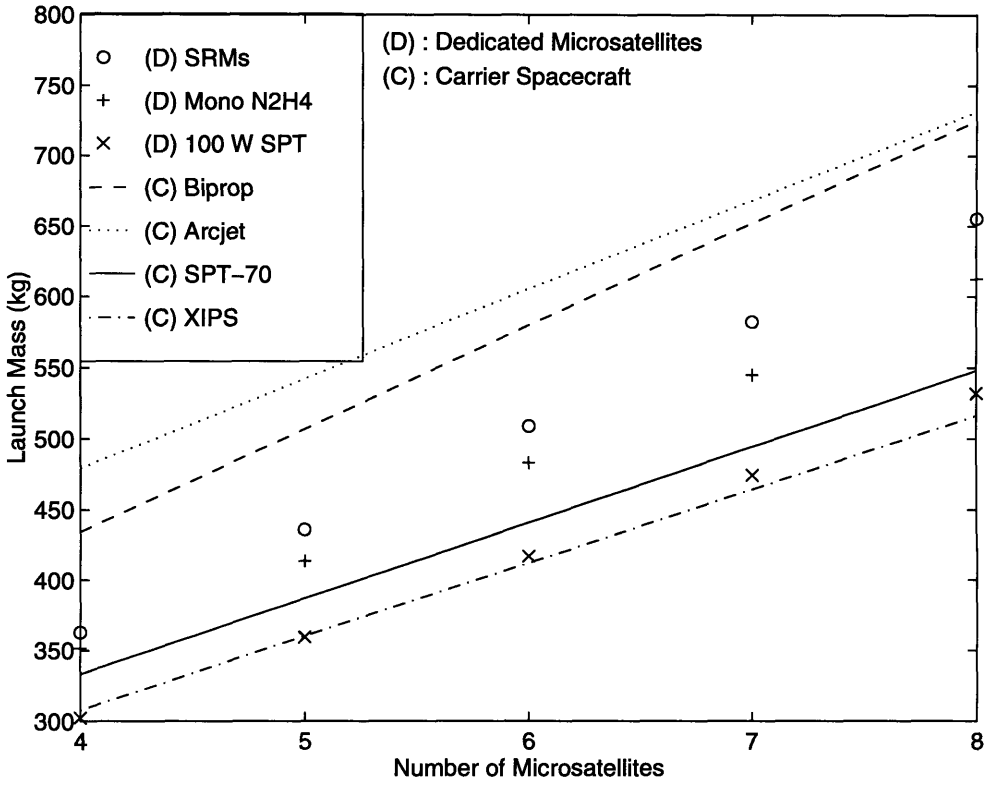

Figure 4-3: Launch Mass Requirements for Propulsion System Alternatives

cific impulse. This is attributable to the fact that the SRM systems have the same propellant load, using vectoring with respect to the heliocentric velocity vector to achieve the ΔV spread. On the other hand, the monopropellant systems get maximal ΔV by firing parallel to the velocity vector and reducing the propellant load for lower ΔV's. The restartability of monopropellant systems is another advantage, even though SRM's are easier to integrate into spacecraft design than monopropellant systems.

The SPT-70 propelled carrier system does not perform as well as the XIPS system which has a higher specific impulse, although, because of the higher Isp and lower power, the deployment time with XIPS would be about twice as long as with the SPT-70. The improvement in performance is marginal and both systems can potentially deploy 8 microsatellites within DeltaLite constraints. It is interesting to note that the dedicated microsatellite scheme with 100 W SPT's performs equally with the XIPS propelled carrier system. Again, the bulkiness of the carrier spacecraft overrides the lower I_{sp} of the SPT as compared to XIPS. If a 100 W SPT system could be developed, then it would be optimal for ETA.

The arcjet and bipropellant carrier options can be discarded on the basis of very high launch masses and the fact that they can't deploy the minimum 6 microsatellites (based on redundancy requirements) within DeltaLite constraints. The 100 W SPT is discounted on the basis of unavailability. This leaves the solid and liquid options for dedicated microsatellites and SPT-70 and XIPS options for carrier spacecraft schemes. The dedicated sys-

tems have a higher launch mass requirement but provide some redundancy in the system.

However, the issue of launch vehicle fairing compatibility has also got to be considered. For example, the SRM systems would need to be stacked in some fashion in the fairing. Based on the height of the SRM, estimated height of microsatellite and maximum allowable launch fairing height of ~4 m [24], it was found that 4-5 microsatellites can be stacked vertically. The monopropellant systems might allow 6 spacecraft to be stacked since the propulsion system can be integrated within the microsatellite. Another method of stacking the spacecraft may be necessary and this adds to design complexity. Since there are other carrier options which have lower launch masses and are easier to integrate with the launch vehicle, the dedicated microsatellite options were discounted at this stage. However, these options need to be studied in more detail before being discarded completely. Some aspects that need to be looked at include the constellation development, launch vehicle stacking and spacecraft design impacts.

The XIPS system provides the best performance on the basis of launch mass requirements, although the performance advantages are small in comparison with the SPT-70 system and the deployment time is larger. Other criteria such as cost, availablity and flight experience have to be taken into account before selecting a particular system.

It is interesting to analyze the impact of thrusters which are not currently available. In particular, it is likely that scaled versions of the arcjet and XIPS may become available in future. These systems were considered by scaling their power to achieve the same thrust as the SPT-70. This was under the assumption that the same efficiency and specific impulse are possible at the different power level. The rationale behind scaling to the same thrust was to achieve the same acceleration and have the same deployment time. The performance of these options is presented in Figure 4-4, together with the other baseline carrier spacecraft options.

Because the arcjet has a higher thrust level than the SPT-70, its power level goes down when it is scaled to the SPT-70 thrust level. This results in lower power conversion/solar array mass, ultimately resulting in substantially improved performance compared to the nominal arcjet. On the other hand, XIPS has a lower thrust level than the SPT-70 and scaling would require higher power, degrading performance compared to the nominal XIPS. These trends are illustrated in the plot. Interestingly, the SPT-70 gives the same performance as the powered-up XIPS. The arcjet is seen to provide better performance than the chemical system. This confirms the fact that the currently available MR-508 is not power-optimized for the ETA mission.

4.4.3 Flight Experience/Heritage

Chemical propulsion systems have had a long history of successful operation and in this regard, there is no question concerning the heritage of the solid motors or the liquid bipropellant systems. The Star 13 has been used in NASA's Anchored Interplanetary Monitoring Platform program and more recently on the Freja scientific platform [28]. About 800 units of the Kaiser Marquardt R-4D have been manufactured for use on satellites such as

Milstar, Intelsat VI, Olympus and Superbird [28].

The arcjet is finding increasing application onboard satellites and the MR-508 has flown on Telstar 4. By the time of launch of ETA in 2000, arcjets are anticipated to be standard features on satellites. The SPT-70 first flew in the early 1970's and over 50 SPT flight units have been flown since. SPT units are currently the normal means of stationkeeping for Russian spacecraft [29]. More recently, increasing interest in using SPT technology onboard Western spacecraft has resulted in extensive ground testing by experts in the US and Space Systems Loral (SS/L) is in the process of developing the SPT-100 for use on one of its spacecraft buses [29].

XIPS, which has been developed by Hughes Research Laboratories [28], is expected to become a standard feature of the HS-601 bus in the years to come. However, the current flight experience of the system is limited and this is detrimental from the standpoint of NASA officials who will assess the ETA proposal. The general feeling is biased towards conservatism and a scientific mission utilizing well proven technology fares better than one which employs hardware which is not comprehensively flight-tested. Despite its marginally better performance, as identified in the performance comparison, XIPS was not selected for ETA on the grounds of, among other factors, lack of flight experience.

4.4.4 Availability

Because of their flight heritage and utilization in recent spacecraft programs, the Star 13

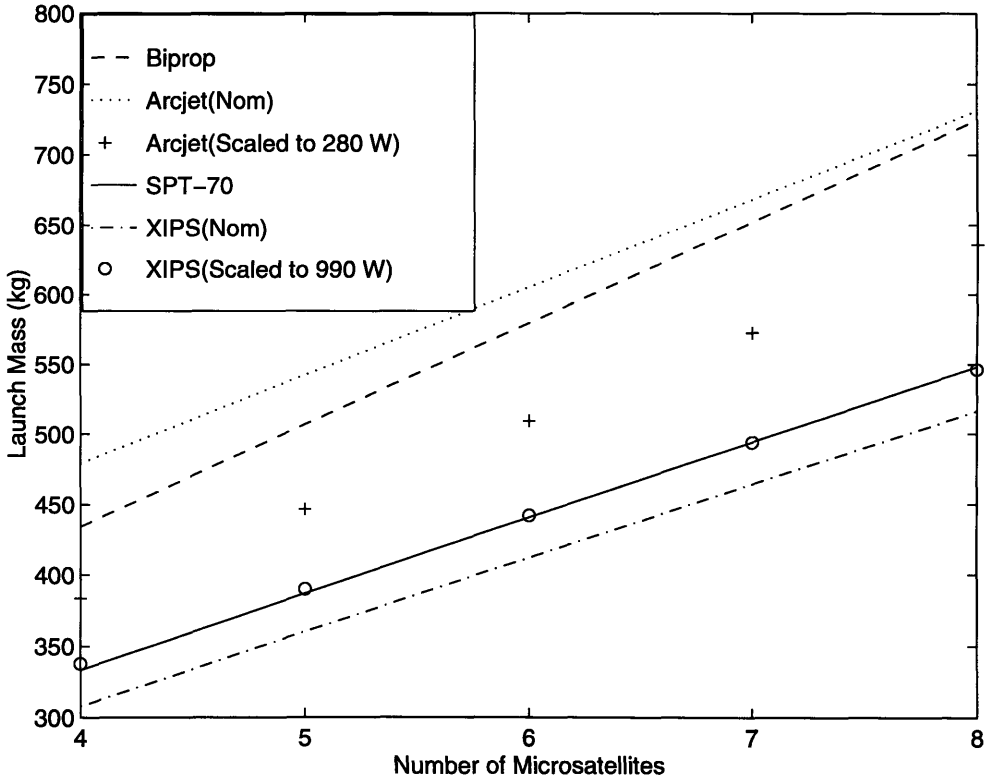

Figure 4-4: Launch Mass Requirements for Scaled Propulsion Systems

solid motor and Kaiser Marquardt R-4D bipropellant engine are readily available. Moreover, it is possible to modify, if necessary, the grain charcteristics of the solid motor to cater for the specific needs of the ETA mission; there is of course an associated cost penalty. Although a bipropellant with better performance than the KM R-4D is under development by TRW [30], its availability is uncertain at this stage. For that reason, the KM R-4D has been selected and represents a conservative choice, although the improvement in I_{sp} of the new system will probably be a few percent at most and will not affect the trade results significantly.

The MR-508 arcjet is manufactured by Olin Aerospace company and is also readily available. The issue here, is the availability of an arcjet operating at power levels of under 1000 W and, even though development testing is underway on such low power arcjets, they will not be commercially available for at least a few years [30].

The SPT-70 is available through the International Space Technology International (ISTI) consortium of Russian and Western companies. Specifically, Atlantic Research Corporation (ARC) is responsible for marketing the SPT in the the US [31]. The availability of the SPT-70 for potential use for ETA is unique. The Air Force Phillips Laboratory at Edwards AFB had previously procured two flight units and one engineering unit of the SPT-70 for their Miniature Sensor Technology Integration (MSTI) spacecraft program. SPT-70 units were scheduled for flight onboard MSTI-3 but were not flown due to budgetary considerations [32,33]. These units are now available to the ETA program. Additionally, Phillips Laboratory have also offered to actively participate in the integration and testing of the system if the SPT-70 is selected for the carrier spacecraft. This is a strong advantage for the SPT-70 alternative.

The availability of XIPS is uncertain at this stage. XIPS may not be commercially available yet although it may be possible to procure the system with some difficulty and extra cost. While XIPS demonstrates slightly better performance, the SPT-70 does provide sufficient performance for the purposes of ETA. Availability then becomes of crucial importance and XIPS has been discounted for ETA primarily on the basis of ready availability of the SPT-70. Availability was thus a driving criterion in this case.

4.4.5 Cost

Even though it is difficult to make an absolute assessment of costs, a relative comparison is possible. The acquisition of separate solid motors for each microsatellite may increase system cost. While the unit cost of SRM's may be lower, procurement of a larger number for each microsatellite may add up to a lot. This of course, depends on the number of microsatellites selected.

Electric Propulsion systems are normally more costly but the cost depends a lot on the availability of the hardware. For instance, the SPT-70 system could be obtained at a reasonably low cost because of the unique arrangement with Phillips Laboratory and the willingness of the Russians to aggressively market the SPT through ISTI. On the other hand, XIPS would probably cost a lot more, especially since it is not in commercial production.

The large number of SPT's manufactured in Russia also result in lowering costs whereas that is not true for XIPS. The same probably applies to a lesser extent to arcjets but the larger solar arrays will add to the cost.

There are other elements apart from hardware that affect propulsion system cost. System development, integration and testing incur cost both from the standpoints of facilities and manpower. Rigorous testing is necessary to ensure that the propulsion system is compatible with the rest of the spacecraft. In this regard, the flight experience of the SPT-70, as well as development work done already by Phillips Laboratory, may help to reduce propulsion system-related costs.

4.4.6 Reliability/Redundancy/Flexibility

With several years of operational experience, chemical propulsion technology has attained a high level of reliability which is thus not a source of concern normally. Achieving redundancy is somewhat trickier. It is difficult to incorporate redundancy or flexibility in solid motors which cannot be stopped once started. Liquid propellant systems allow a certain level of redundancy and operational flexibility. Flexibility can provided in terms of thrusting times or impulses.

Electric propulsion systems are known for their operational flexibility. The low thrust, high I_{sp} systems are more flexible in operations since it is easier to adjust operational parameters like imparted impulse and thrust levels. Furthermore, the low thrust, long duration nature of EP systems enables backup mission or trajectory options if partial system failure necessitates changes in mission strategy. It is easy to incorporate redundancy into the system as well since redundant thrusters can utilize common power processing and propellant management systems which are themselves redundant. The redundancy and flexibility provided by EP systems is a major advantage over chemical systems.

4.5 Summary of Trade Results

The major conclusions derived from the trade study are summarized here. The rationale behind each decision is given and a direct comparison is made with the selected system where possible.

The SPT-70 has been selected to provide the propulsive capability required for constellation deployment. The microsatellites will be stacked on a carrier spacecraft which will deploy each microsatellite after providing the required ΔV through SPT-70 thrusting. In addition to requiring a relatively low launch mass, the SPT-70 has over 20 years of failure-free flight experience, is readily available at low cost and provides operational flexibility. The availability of hardware as well as system integration and testing expertise from the Phillips Laboratory was one of the major reasons for selecting the SPT-70. The SPT-100 was not selected, despite its higher I_{sp}, on account of requiring higher power for operation.

Dedicated microsatellite propulsion systems are attractive in that they provide the redundancy that cannot be achieved with a single proopulsion system employed by a carrier

spacecraft. The major drawbacks are the higher launch masses compared to the carrier EP systems and potential difficulties associated with integrating the microsatellites with the launch vehicle. There is also concern that, while incorporating an SRM does not pose a big problem, integrating a monopropellant hydrazine system into the microspacecraft design may require redesign of the standard bus being proposed by the spacecraft contractor. The dedicated microsatellite options need to be looked at with more detail before discarding them altogether.

A liquid bipropellant system for the carrier spacecraft was attractive from the perspective of cost, availability and flight heritage. The system would push on volume constraints within the carrier spacecraft due to the larger propellant load but this was deemed to be manageable too. The main drawback is the performance, in comparison to the SPT-70 and XIPS, and was the reason for discarding this option. This is further justified by the fact that the launch mass required is in excess of DeltaLite capability.

The arcjet was eliminated due to high power and larger solar array requirements. Currently available technology has too high a power requirement and there is development risk associated with a new sub-kilowatt thruster, that a mission like ETA cannot afford to take. Even though a sub-kilowatt arcjet is under development, it is not currently available commercially and would still have lower I_{sp} performance compared to the SPT-70.

The XIPS ion engine provides marginally better I_{sp} performance over the SPT-70. The power requirements are also lower than the SPT-70. Lower thrust levels imply a longer constellation deployment phase but this is offset by the performance increase. However, XIPS is still yet to accumulate sufficient flight experience. The marginal performance improvement of XIPS over the SPT-70 does not justify the lack of flight experience, increased constellation deployment time and difficulties pertaining to procurement of XIPS. This constitutes the rationale behind not selecting XIPS for ETA.

The selection of the SPT-70, based on the reasons stated above, enables the initiation of the detailed analysis of the constellation deployment and development. Prior to this, it is necessary to better understand the performance capabilities of the system as well as fully comprehend the constraints imposed on its operation and the rest of the system design. To this effect, the next chapter describes the SPT-70 system and serves to set the stage for the constellation analysis presented in a later chapter.

Chapter 5

SPT-70 Electric Propulsion System

> *"Perhaps with the help of electricity, it will in time be possible to give tremendous velocity to particles thrust out of the reactive apparatus....." - Konstantin Tsiolkovsky [34]*
>
> *"The use of Electric Propulsion to accomplish a wide range of planetary and interplanetary missions has long been advocated.....one of the primary advantages in the use of Electric Propulsion is the degree of flexibility it introduces in the selection of mission options. In addition to the usual flight-time/payload trade-offs, there is a great deal of flexibility in the selection of mission parameters. Operation at off-optimum power, specific impulse or efficiency seems to carry no overwhelming penalty....." [35]*

The suitability of electric propulsion, with its inherently high specific impulse, for high ΔV missions has never been doubted. Application of Electric Propulsion (EP) technology to missions, though, has been minimal over the years but is encouragingly on the increase currently. The utilization of the Russian SPT-70 thruster for the ETA mission stands to reap significant benefits both in terms of performance and enhancing the credibility of the practical applicability of Electric Propulsion to interplanetary missions.

Having selected the SPT-70 system in the previous chapter, the purpose of this chapter is to elaborate upon how the SPT-70 system will be implemented for ETA, what its requirements, interfaces/interactions are with respect to the rest of the system and what levels of performance it will provide. The chapter thus facilitates consideration of both mission and spacecraft design aspects discussed in later chapters. It is appropriate to note that the treatment of the propulsion system in this chapter is primarily in the context of the application to the mission; theoretical details may be found in the references.

Commencing with an introduction to the application of Electric Propulsion to space mis-

sions and the history and flight experience of the Stationary Plasma Thruster (SPT), the discussion then moves onto a brief overview of the physical principles associated with the operation of the SPT. This is necessary to comprehend the operational characteristics presented next. The section on operational characteristics serves to identify important constraints such as lifetime, which are imposed on both mission and spacecraft system design. Spacecraft design inputs are further augmented, in terms of mass and power requirements as well as interfaces, by a description of SPT-70 system hardware. SPT-70/carrier spacecraft interactions which could potentially affect the overall system are identified so as to ensure that system design is carried out with these issues in mind.

5.1 Introduction

The potential of Electric Propulsion for high ΔV missions was recognized as early as the dawn of this century by pioneers such as Goddard and Tsiolkovsky [34]. Their ideas spawned numerous concepts, some of which were practically implemented; some of which, unfortunately, never made it beyond theoretical studies. This section provides an overview of the past history of applications of Electric Propulsion technology and reviews the development and flight experience of the Stationary Plasma Thruster (SPT). No attempt has been made to include all details and the reader is referred to the literature for a more complete treatment of the subject.

5.1.1 Background

Researchers have always appreciated the advantages of high specific impulse (I_{sp}) and endeavored to develop systems which could provide these high exhaust velocities. The theoretical principles governing electromagnetic and electrostatic phenomena were recognized to be useful towards this goal. It was in the Soviet Union, in the years 1929-1933, that Valentin Glushko, later to become a famous figure in Soviet Rocketry, developed the world's first electric thruster [34].

Interest in electric propulsion grew over the years and system studies by Ernst Stuhlinger revealed that Electric Propulsion could indeed provide substantial benefits [36]. Hardware was developed for different types of thrusters, including ion engines, plasma accelerators and resistojets. The practical application of such thrusters was, however, constrained by a number of factors and these issues have plagued the space industry ever since, even though some of these have been mitigated in recent years by advances in technology.

The primary hurdle, from the technical standpoint, was associated with the electrical power necessary to operate the electric thrusters. Some of the thrusters required kilowatt-megawatt levels of power which could not be achieved without resorting to nuclear power sources or unduly large solar arrays. Furthermore, the power processing equipment required was heavy and cumbersome. Since then, space power technology has developed to the extent of providing a few kW with solar arrays, although nuclear sources have almost been discarded. The rapid advances in power electronics have also resulted in the reduction of the mass of power processing equipment. The difficulty associated with power levels of a few kW is thus not so much a concern now.

A more important hindrance to the application of EP technology has been the reluctance of mission managers to use electric propulsion on the grounds of high risk and lack of flight operation and testing. This trend is still prevalent these days and unfounded skepticism within the aerospace community continues to deter the accelerated application of EP and other advanced technologies for all sorts of space missions. A few exceptions exist and missions have been flown to test EP, primarily in the mode of auxiliary propulsion for stationkeeping and attitude control.

The Space Electric Rocket Test (SERT) series of missions is the best example of dedicated EP missions [37]. SERT I and SERT II were flown to test mercury ion thrusters developed at NASA Lewis Research Center (LeRC) in the 1960's. SERT I demonstrated that broad beam ion thrusters could operate in space. SERT II's main objective was to test long duration operation of the thrusters. Even though the thrusters initially operated for 5 months instead of the intended 6 months, SERT II was reactivated in 1973 and the thrusters were tested for restart capabilities until thruster propellant supplies were exhausted in 1981. The mission established the resilience of EP systems, logging over 3,000 hrs of thruster operation and over 15,000 hours for the power conditioning equipment [37].

The utility of EP in the role of auxiliary propulsion has recently renewed interest in utilizing EP technology for satellites. The lifetime of satellites, geostationary spacecraft in particular, is normally limited by the amount of stationkeeping propellant available onboard. In their pursuit to develop longer lived satellites, manufacturers have been looking at EP technology. The Europeans have developed ion propulsion systems for the experimental ARTEMIS satellite [38]. Hughes have developed the Xenon Ion Propulsion System (XIPS) and are planning to use these thrusters for stationkeeping on some of their HS-601 spacecraft buses [27,28,39]. The feasibility of using Ion engines onboard INTELSAT VII has also been favourably explored [40]. Arcjets have been performing stationkeeping functions since 1994. It has been a standard feature of Soviet spacecraft to utilize SPT thrusters for stationkeeping and Space Systems Loral is currently developing the hardware to implement the SPT-100, a larger version of the SPT-70, on one of their spacecraft buses [29].

It is ironic that EP technology has never really been applied to the types of missions that would clearly underline its potential, namely interplanetary primary propulsion missions. The utilization of the SPT-70 for the ETA mission is, in that respect, one of the first missions to use EP for the primary propulsion of an interplanetary spacecraft. Before going into the technical details of the SPT-70, it is instructive to briefly note the heritage of the SPT-70 and its flight experience to date.

5.1.2 Overview of SPT Development and Flight Experience

Ever since Glushko's development work in the early 1930's, the Soviet Union (and later the CIS) has continued with its Electric Propulsion research and development to the point where today, electric thrusters are a standard feature of their spacecraft.

Even though development work has been carried out for a number of types of electric propulsion systems, the most widespread application has been that of plasma engines such as the Stationary Plasma Thruster (SPT). Plasma engines can be classified into closed Hall current engines and high current engines. Within the closed Hall current category, there exists a type called the linear Hall Accelerator, of which the SPT is an example.

The concept of accelerating ions in crossed electric and magnetic fields was first developed by Morozov and his colleagues at the Kurchatov Institute of Atomic Energy in the 1950's [34]. Morozov went on to design what was called the SPT-50, which was first tested on the Meteor spacecraft in 1971. The technical point of interest in Morozov's design was the incorporation of a magnetic field which increased axially. This field decreased ion flow near the electrically insulating walls, thereby minimizing recombination losses. The SPT-50 consumed 400 W and operated for about 170 hours.

Since then, the SPT family of thrusters has grown to include the SPT-70, SPT-100 and other larger versions. The number in the thruster designation stands for the diameter, in mm, of the discharge chamber of the thruster. The SPT-70 has been most commonly used, with SPT-70 thrusters used for stationkeeping aboard several spacecraft such as Meteor-Priroda, Gorizont, Kosmos and Ekran. More than 50 SPT-70 units have been flown without failure and lifetimes of over 3,000 hours have been demonstrated [41]. The fact that no failures have occured is testimony to the robustness of the SPT.

Eight units of the larger SPT-100 have been flown on the GALS spacecraft. The West has been interested in using these proven thrusters and as a consequence, an American team of specialists conducted a series of tests on the SPT-100, both in Russia and in the US to validate its performance [42,43]. Extensive testing in the US has demonstrated the performance of the SPT-100, including testing to up to 7,000 hrs.

To market the SPT in the West, an international venture, the International Space Technology, Inc (ISTI), was founded with partners including Space Systems Loral (SS/L) of the US and Fakel of Russia. SS/L is in the process of developing power processing hardware for implementation of the SPT-100 onboard one of their spacecraft buses. Furthermore, the US Air Force Phillips Laboratory acquired a few SPT-70 thrusters for testing on their Miniature Sensor Technology Integration (MSTI) spacecraft [32,33]. The thrusters could not be flown on MSTI-3 as planned and are thus available for the ETA mission through a mutual agreement [4].

The utilization of the SPT-70 for the ETA mission is thus accompanied by the heritage of a flight proven thruster which has not failed and is backed by extensive testing of a derivative thruster. An example of the SPT is shown Figure 5-1.

5.2 Operating Principles of the SPT

The Stationary Plasma Thruster (SPT), also called a closed-drift Hall thruster, is an electromagnetic plasma device which achieves high I_{sp} at low power with long electrode life. Figure 5-2 shows a schematic of the SPT. A typical SPT thruster consists of

Figure 5-1: Stationary Plasma Thruster (SPT-70)

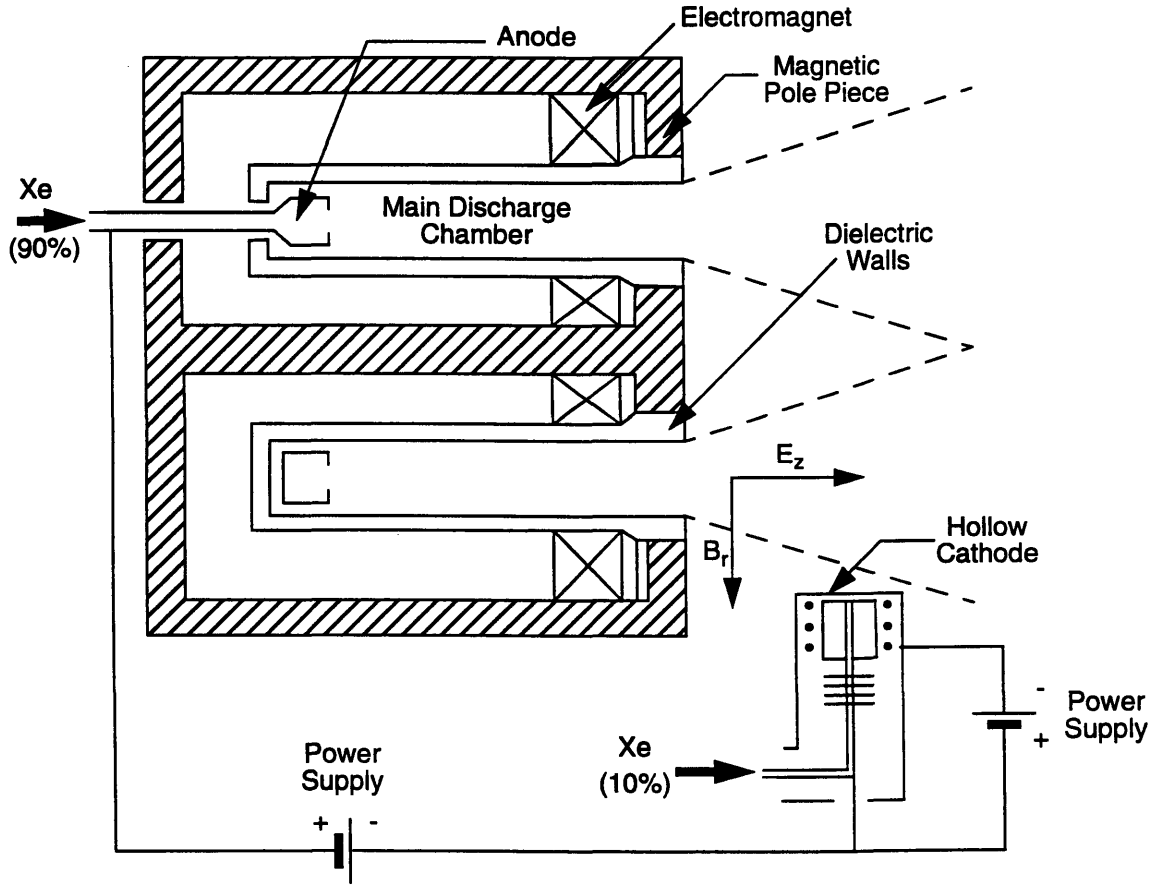

Figure 5-2: Schematic of Stationary Plasma Thruster (SPT)

- annular anode
- hollow cathode placed externally
- discharge chamber lined with dielectric material (ceramic)
- radial magnetic field established by electromagnets, coils or yokes.

Xenon (Xe) gas is injected into both the hollow cathode and the main discharge chamber. Prior to initiation of discharge, the cathode is heated by an external heater; subsequent operation is in self-heating mode. A radial magnetic field is established across the annular channel of the main discharge region by electromagnets. The magnetic system comprises an internal electromagnetic coil and four external coils.

A discharge voltage of 300-400 V is applied across the anode and cathode. The heated cathode emits electrons which accelerate towards the anode. However, the radial magnetic field acts as an impedance to direct electron flow. As a result, the electrons undergo cyclotron motion, tracing out trajectories which spiral azimuthally around the magnetic field lines. The electrons can thus diffuse to the anode via collisions with Xenon atoms which are subsequently ionized. The heavy Xe ions are not so much affected by the magnetic field and are electrostatically accelerated to the nearly the full applied voltage by the axial field set up by the potential difference across the electrodes. The ion beam exits the chamber at high velocities producing the thrust. The positively charged ion beam is neutralized by extra electrons from the cathode, thereby maintaining charge balance.

Electron drift in a direction mutually perpendicular to both the electric and magnetic fields, in the azimuthal direction for the geometry shown, constitutes the ExB Hall effect and hence the name Hall thruster. The relatively low power requirements are enabled by the Hall accelerator geometry and low mass flow rate [44]. Ions and electrons have similar concentrations in the acceleration zone. As a result, the medium is quasi-neutral and there is no space charge limitation on the ion current density, unlike classical electrostatic thrusters [45]. The absence of an acceleration grid also implies longer lifetime, even though there is some limitation due to erosion of the insulation lining through stray ion collisions. The discharge chamber is composed of a Boron Nitride (BN) and Silicon Dioxide (SiO_2) ceramic unit that insulates the thruster body from the plasma [45].

Even though the ion trajectories are largely unaffected by the magnetic field, there is some bending of ion trajectories, resulting in a torque which attempts to roll the thruster. This roll torque has to be negated in some manner, either by using pairs of thrusters or firing roll control thrusters to cancel torque buildup.

One source of losses in the thruster is attributable to the recombination of ions that occurs at the walls [39]. These losses are minimized in the SPT by tailoring the magnetic field to mitigate wall recombination. Moreover, the ionization of Xe atoms takes place in a region of maximum electric field so that the ions are accelerated out of the chamber as soon as they are generated. The recombination of energetic ions at the walls creates another problem in that the insulator walls erode away, leading to reduced thruster lifetime and contamination of sensitive surfaces. The minimization of wall recombination thus has

widespread benefits.

Some of the challenges that had to be overcome when designing the SPT included instabilities and materials problems with the electrodes and insulators. The non-uniform magnetic field was key to resolving some of these problems [44] and is also instrumental in reducing convective instabilities. This constitutes one of the major differences between Russian SPT's and earlier American designs.

5.3 Operational Characteristics

This section presents details of the performance of the SPT under various operating conditions. Performance curves are presented and descriptions of startup transients and steady state operation are given. The lifetime and cycling limitations of the SPT are elaborated upon so that the constellation design takes these issues into account.

5.3.1 Performance

Thruster performance depends upon a number of design characterisitics, including discharge channel geometry and magnetic field [46]. The performance of the SPT-70 can be characterized by parameters such as thrust, specific impulse (I_{sp}) and efficiency. Figure 5-3 presents plots of these parameters derived from experimental measurements [33,47,48]. The data are plotted as a function of input power. Power input was at a constant discharge voltage of 300 V. Uncertainty in the data is at most 10% [48]. When the SPT-70 is operated in the voltage-regulated mode, the discharge current is found not to be a strong function of discharge voltage, but more of propellant flow rate and the magnetic field. Different input power levels would thus be realized by varying the propellant flow rate. The ratio of current-to-propellant flow rate, which is an indicator of propellant utilization efficiency, is nearly unity. The SPT is thus very fuel efficient.

At the nominal operating point of 660W, the SPT-70 produces 40 mN of thrust at an efficiency of ~45% and I_{sp} of ~1510 sec. Thrust, I_{sp} and efficiency increase with input power. It is important to determine performance variations with respect to power since the range of the carrier spacecraft from the Sun, and hence the generated power by the solar array, will vary during the deployment process. It is imperative that the range variations are not so much as to compromise the performance of the SPT-70. The ideal strategy would be to make use of the extra power available when the carrier spacecraft is closer to the Sun. Conversely, it is necessary to provide a minimum power level when the carrier spacecraft is further away from the Sun, since SPT-70 performance degrades markedly with lower power levels. Performance variations within 550-750 W are not that much, providing a range of operating points while maintaining a reasonable level of thrust and I_{sp}.

Furthermore, the design of the Power Processing Unit (PPU) for the SPT-70 has to take into account the Sun range variations during the deployment phase since that will determine the range of power levels that it will have to operate over. The PPU is designed for constant 300 V operation with variable current levels [49], since incorporating variable voltage capability would be expensive. The design of the solar array of the carrier space

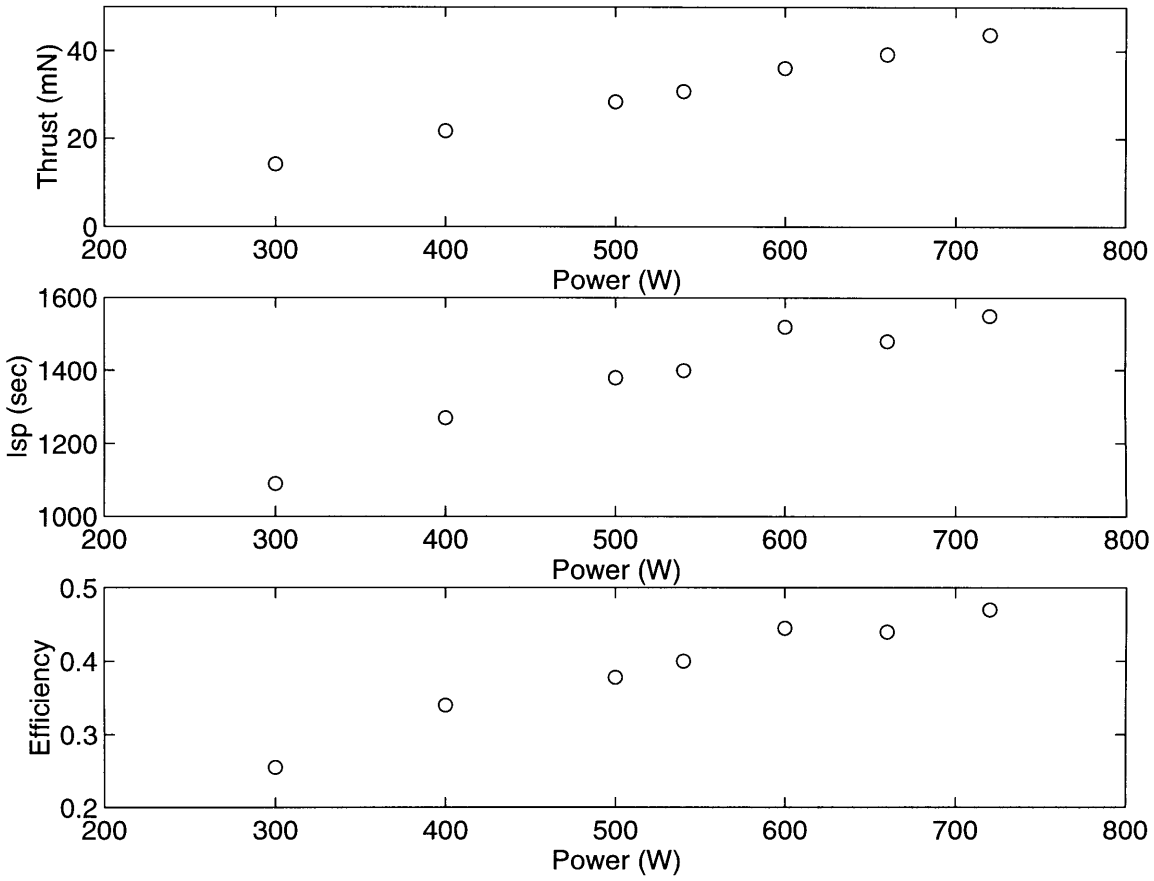

Figure 5-3: SPT-70 Performance Curves [47,48]

craft will also be heavily influenced by the same issue because the SPT-70 is the heaviest power load on the carrier spacecraft solar array.

A lot of data exists from the extensive testing that has been carried out on the larger SPT-100 [42,43]. Since the SPT family of thrusters is scalable, and not that much performance data exists on the SPT-70 itself, it would be useful to see if analysis of SPT-100 data reveals any unknown performance traits. Of course, more testing of the SPT-70 is required nevertheless in order to understand better the impacts on the rest of the carrier spacecraft system.

5.3.2 Transient/Steady State Operation

Nominal operation of the thruster is preceded by a startup sequence which is necessary to initiate the discharge. The startup sequence is commenced with the turning on of the cathode heater supply. This is necessary to enable the hollow cathode to attain a temperature that is high enough for the emission of electrons. The cathode heater consumes about 80 W nominally and is powered for approximately 2.5 min [33].

Once the cathode has reached a suffuciently high temperature, a valve is opened to inject propellant and then a high voltage pulse train is applied to the ignitor electrode to initiate the discharge. The duration of the pulse is normally of the order of 5 msec and the thruster typically starts up on the first series of pulses. The thruster, thereafter, rapidly attains steady state operating conditions. The time required to attain steady state from heater power-up is usually less than 4 min [33]. Power to the cathode heater has to be cut off at discharge initiation to avoid over-temperature conditions on the cathode [49]. The startup sequence will be managed by the PPU.

Due to the inherently quasi-stable plasma conditions, steady state operation is characterized by oscillations in discharge voltage and current at frequencies in the 20-30 kHz range [49,50]. While this issue does not seem to have severe impacts on the performance of the thruster, it does have implications on the design of the power electronics associated with the thruster. The oscillations are dampened by a matching network which is essentially an inductive filter circuit [49,51]. Care must also be taken to ensure that the thruster oscillations are isolated from the rest of the spacecraft power subsystem.

5.3.3 Lifetime and Cycling Issues

Lifetime considerations have always been a major concern with electric thrusters. Despite the fact that the SPT-70 has been proven in flight and in ground tests in Russia, the longer lifetime requirements of Western spacecraft have meant that extensive lifetime and associated environmental testing has had to be undertaken in the US [29,42,43]. Even though the tests were carried out on the SPT-100, the observations and results are applicable to the SPT-70. Over 40,000 hours of time have been accumulated on the SPT-70 and SPT-100 [29]. The SPT-100 has been tested to over 7,000 hours and includes 6,000 on/off cycles. The performance of the thruster has been as expected [29,42,43].

For the purposes of the ETA mission, cycling (stop/start) performance is not so much a concern since the thruster has to be started and stopped only for the deployment of the few microsatellites. The more important issue is that of thruster lifetime since that primarily determines the total time the thruster can be fired. Analyses for the constellation deployment, which require SPT-70 thrusting time constraints, were done with the conservative assumption that the SPT-70 has an effective lifetime of 3,000 hours. However, the SPT-70 can be expected to operate for greater than 3,000 hours since it has had no failures so far and the similar SPT-100 has been successfully tested to over 7,000 hours. Relaxing this assumption will only serve to provide more thrusting time which may be utilized for the microsatellite deployment phase or post-deployment testing of the SPT-70 system, if extra propellant is loaded. Other tests associated with long duration operation, such as environmental, degradation tests are planned or underway [29,43,52].

5.4 SPT-70 System Hardware and Interfaces

This section describes the architecture and associated hardware developed to support the operation of the SPT-70 during the ETA mission [48]. Interface issues are discussed together with a description of the salient aspects of the system components.

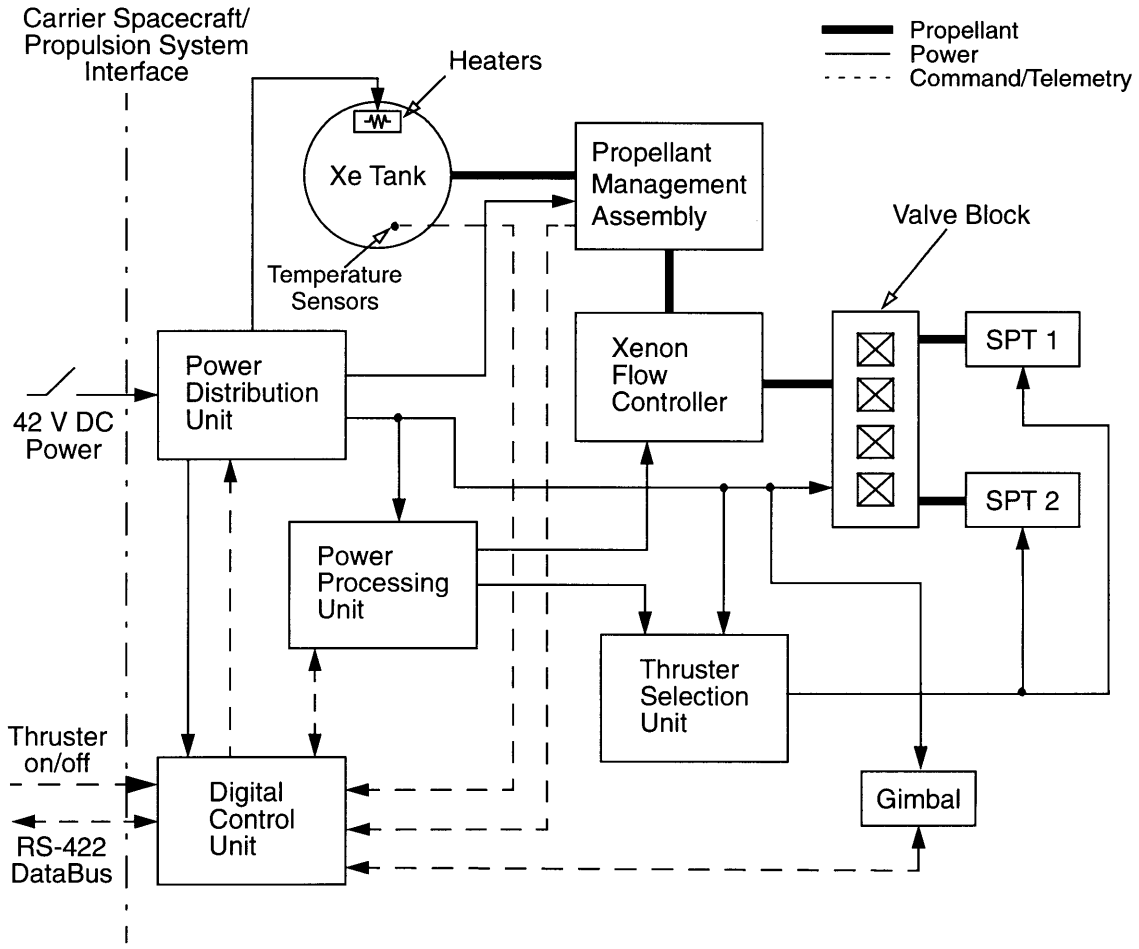

Figure 5-4: SPT-70 Propulsion System Block Diagram [48]

5.4.1 System Configuration

Figure 5-4 is the block diagram of the SPT-70 propulsion system [48]. Primary command/ telemetry, power and plumbing interfaces are shown. The major components making up the system are briefly described hereafter.

- **Thruster**
  Two thrusters are to be used. The operation of these thrusters will not be in parallel but will serve to double the thrusting time available. This is necessary since the lifetime of the SPT-70 is uncertain beyond 3,000 hours. The trade associated with the number of thrusters is dealt with in more detail in the next chapter. Suffice it to say that the primary drawback of operating the two thrusters in parallel is the size of the solar array and Power Processing unit (PPU) required to generate the necessary input power. A single SPT-100 could also be used but this requires over a kilowatt of power. The thrusters will be mounted on a gimbal to align the thrust vector along the carrier spacecraft's center-of-gravity (c.g). Thermal control is an important issue since a lot of power is dissi-

pated as heat. Each thruster will have two redundant cathodes. The dimensions of the thruster are 16 cm x 10.5 cm x 10 cm and mass is approximately 1.5 kg for each thruster.

- **Power Processing Unit (PPU)**
  The PPU for the SPT-70 is a derivative of the PPU being developed by SS/L for the SPT-100 [29,48]. The PPU is the central component of the system and provides power to the anode, magnet, cathode heater, ignitor and Xenon flow controller supplies and has an efficiency of 93% [48]. It is also responsible for a number of control functions and general monitoring of thruster operation. Two separate channels will be provided for the two cathodes of each thruster. The unit is internally redundant. The capability of the PPU to handle a range of power levels will have an impact on the performance of the thruster and consequently on the constellation deployment strategy. Details of the PPU design can be found in Reference [51]. The PPU weighs about 6.6 kg and has dimensions 29 cm x 13.3 cm x 18.8 cm.

- **Digital Control Unit (DCU)**
  The DCU acts as the Command/Telemetry interface unit for the propulsion system and is the main controlling unit for the propulsion system. It accepts control commands from the spacecraft computer and command decoder unit and routes them to appropriate units such as the Propellant Management Assembly (PMA) and PPU. Telemetry, in the form of voltages, currents, temperatures, pressures and flow rates, from the various units is fed to the DCU which converts the data into a form appropriate for channeling to the spacecraft computer. The DCU weighs about 4.5 kg and has dimensions 25.4 cm x 17.8 cm x 12.7 cm.

- **Power Distribution Unit (PDU)**
  The PDU receives power from the main spacecraft bus at 42 V DC and distributes it to various components, notably the PPU, DCU, PMA and propellant tank heaters and valves. Efficiency of the unit is estimated to be about 90% [48]. The PDU weighs about 7.5 kg and has dimensions 27.9 cm x 20.3 cm x 12.7 cm.

- **Propellant Tank**
  The spherical tank is sized for about 60 kg of Xe propellant which will be stored at 1000-1500 psi, depending on temperature. It is necessary to maintain pressure under 2100 psi for the proper operation of the regulator. There is thus a constraint on how small the propellant tank can be made. The tank is fabricated from stainless steel with graphite overwrap and is fitted with heaters for maintaining the propellant within the optimum temperature range of 290-333 K. Temperature sensors are used for monitoring the temperature. The tank is 48.3 cm (19 inches) in diameter and weighs about 11.3 kg [48].

- **Propellant Management Assembly (PMA)**
  The PMA consists of a series of valves, regulators, filters and pressure transducers to channel propellant from the tank to the Xenon Flow Controller (XFC) at the right flow conditions. Two independent paths are provided for redundancy and ports are included for testing purposes. The tank is filled using a fill/drain valve in the PMA. Most of the components for the PMA are flight qualified and readily available [29]. The PMA weighs about 2.8 kg and has dimensions 26.7 cm x 15.5 cm x 9.4 cm.

- **Xenon Flow Controller (XFC)**
  The XFC is the flow control unit which serves a number of functions associated with thruster operation. Some of these include isolation between thruster firings, selection of the redundant cathode, flow throttling for regulation of discharge parameters and providing appropriate mass flow between anode and cathode (~ 90/10%) [53]. Redundancy is provided by two flow paths which can supply either of the thruster's cathodes. A thermothrottle is used to regulate propellant flow. Taking advantage of the viscosity variations of Xenon with respect to temperature, the thermothrottle, which is essentially a capillary tube, controls flow rate by varying the temperature of the tube. Heating the tube heats up the gas which increases its viscosity, reducing the flow rate and vice versa. Each "half-XFC" weighs about 0.3 kg and has dimensions 2.3 cm x 9.4 cm x 10.2 cm.

- **Thruster Selection Unit (TSU)**
  The function of the TSU is to provide the capability to switch between either of the thrusters. A relay network channels power to the thrusters as required. Note that there are two power inputs to the TSU. The PPU provides the power to relays which feed the thrusters. The PDU provides power to the relay drivers which switch the relays [29]. The TSU weighs about 2 kg and has dimensions 15.2 cm x 12.7 cm x 10.2 cm.

- **Gimbal**
  The two thrusters will be mounted on a gimbal in order to facilitate a limited degree of thrust vectoring to align the thruster through the spacecraft c.g. Microsatellite deployments will shift the carrier spacecraft's c.g and uncertainties in thrust vector direction and spacecraft c.g necessitate a gimballing requirement of approximately (+/–) 15 degrees [48]. The allocation for the mass of the gimbal is currently 6 kg.

A preliminary system configuration is graphically illustrated in Figure 5-5 [48]. The system is mounted on a honeycomb plate, on one side of which are mounted the two thrusters and gimbal. The other side is dominated by the propellant tank with the rest of the hardware placed around and underneath the tank. The placement of the entire propulsion system in relation to the rest of the spacecraft is shown in Chapter 7.

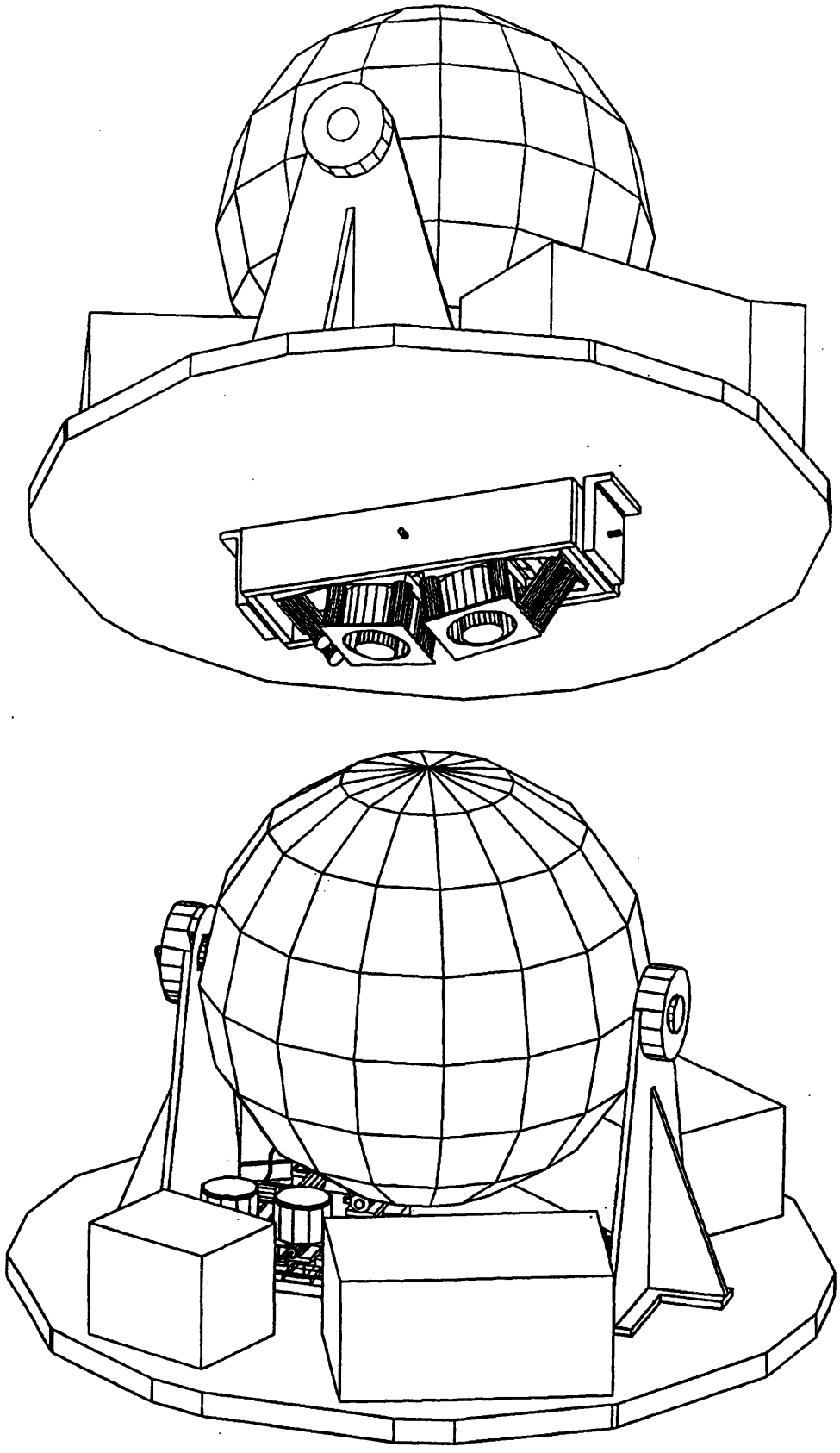

Figure 5-5: SPT-70 Propulsion System Configuration

Power requirements of the propulsion system are dependent on the operating point of the thruster and the power efficiencies of the PDU and PPU. Assuming a nominal operating point of 660 W for the thruster and efficiencies of 93% and 90% for the PPU and PDU respectively, the power required is about 790 W. Adding on about 30 W for heaters, transducers, DCU and so forth gives a net power input to the PDU from the spacecraft power bus of about 820 W [48]. It is important to note that other components such as the TSU and certain valves will only be operated when the thruster is off.

Table 5-1 includes the current mass budget for the propulsion system [48]. Masses for

Table 5-1: SPT-70 Propulsion System Mass Budget [48]

	Quantity	Mass (kg)
Stationary Plasma Thruster	2	3.0
Power Processing Unit (PPU)	1	6.6
Digital Control Unit (DCU)	1	4.5
Thruster Selection Unit (TSU)	1	2.0
Propellant Management Assembly (PMA)	1	2.8
Power Distribution Unit (PDU)	1	7.5
Propellant Tank	1	11.3
Gimbal	1	6.0
Half- Xenon Flow Controller (XFC)	2	0.6
Latch Valves	4	0.4
Structure		5.0
Harness, Plumbing, Miscellaneous		5.0
Total Dry Mass		54.7
Margin		4.5
Xenon propellant load		60.0
Total Wet Mass		119.2

most of the main component includes a 15% margin. The dry mass of the system is under 55 kg which adds up to a wet mass of about 120 kg with the 60 kg propellant load. Estimates are based on actual or breadboard hardware.

5.4.2 System Interfaces

The propulsion system is fairly well defined in terms of individual components. The important aspect of the design at this point is to clearly define the interfaces, both externally with the rest of the spacecraft and internally within the propulsion system itself.

The main external interfaces are for power and data (commands/telemetry). The power interface is between the PDU and the spacecraft power bus with power supplied at 42 V. Data interfaces are managed through an RS-422 databus [48] with the DCU controlling the thruster as well as gimbal.

Internal interfaces are mainly power and data between various components, as shown in Figure 5-4. Plumbing between propellant handling hardware is also shown. Thermal interfaces are very important since the thruster dissipates about half the input power. Further design work is necessary to model the thermal environment. Even though the thruster faces cold space, the internal thermal environment for the power electronics and so forth may be fairly constrained in terms of access to space. Thermal control for the propulsion system will thus have to be integrated with the thermal control system for the carrier spacecraft.

5.5 SPT-70/Carrier Spacecraft Interactions

The issue of spacecraft-thruster interactions is important in the sense that lack of attention to possible impacts can jeopardize the operation of the spacecraft. Even though most of the possible interactions can be avoided or mitigated through careful design, the sources of these interactions must nevertheless be investigated in detail.

The SPT-70 may, as a result of its unique operating characteristics, induce a variety of unwanted interactions on the carrier spacecraft. Some of the major ones include

- spacecraft charging
- sputtering
- contamination due to material deposition
- disturbance torques
- electromagnetic interference (EMI)

This section goes into a brief discussion of each of the interactions, outlining how it affects the carrier spacecraft for ETA.

5.5.1 Spacecraft Charging

The highly ionized and energetic plume of the SPT can be expected to charge the spacecraft [54]. However, since the SPT-70 generates equal numbers of positive and negatively charged particles, charge balance will be maintained unless the particles exit what is termed the Debye sheath around the spacecraft in unequal numbers. Even if a large negativ charge does build up on the spacecraft, it may be large enough to slow down exiting ions and attract them back to the spacecraft, thereby canceling the charge. In this context,

the SPT can be though to act as a plasma contactor which minimizes the possibility of spacecraft charging [54]. It is thus highly unlikely that SPT operation will lead to spacecraft charging.

5.5.2 Sputtering

Sputtering is the removal of surface material due to the impact of high energy plume ions. Exposure of surfaces such as solar cell anti-reflective coatings and cell interconnect material to the energetic SPT plume, can result in degradation of solar array performance . The sputtering erosion rate at a given surface is a function of distance from thruster, angle of beam impingement with respect to surface normal and angle of beam impingement with respect to thrust centerline [55]. Simulation of a geostationary satellite over a 15 year lifetime has revealed a 1% degradation in the power generation capability of the solar array at end of life [55]. Experimental evidence suggests that over 90% of the ion current is concentrated within 45^{o} of the thrust centerline [56]. Russian flight experience also confirms that sputtering effects can be minimized by designing the spacecraft such that sensitive surfaces such as solar arrays are not exposed to the plume.

5.5.3 Contamination due to Material Deposition

Contamination deposition occurs as a result of erosion of discharge chamber insulation material and redeposition of this material on sensitive surfaces. This can change the optical or thermal properties of the material. Once again, contamination can be mitigated by ensuring that sensitive surfaces such as solar cells or optical instrument apertures are not in the line-of-sight of the thruster plume. However, there is a possibility that contaminants could be ionized, for example by charge exchange, and accelerated by potentials prevailing in the beam. The ETA carrier spacecraft has to be configured with these aspects in mind.

5.5.4 Disturbance Torques

SPT operation, as discussed earlier, produces a "swirl" torque, due to bending of ion trajectories by the magnetic field, which tends to roll the thruster. This is a disturbance torque on the spacecraft which has to be cancelled. Other sources of disturbance torques can be moments due to changes in thrust level or thrust direction or plume impingement on surfaces [57]. Equivalent forces of 2-8% of nominal thrust have been reported in the literature [42,57]. The problem can be overcome by using momentum wheels to take up the momentum and desaturating these with monopropellant or bipropellant thrusters. The ETA carrier spacecraft will use cold gas thrusters to perform this function. Propellant mass estimates for this function are presented in the discussion on the carrier spacecraft in Chapter 7. Yet another method could be the periodic reversal of the magnetic field to reverse torque direction but the reversal could impact the PPU/SPT interface and perhaps also thruster operation as well.

5.5.5 Electromagnetic Interference (EMI)

The operation of the thruster and PPU can give rise to an electromagnetic environment that could potentially affect spacecraft subsystems such as communications; guidance,

navigation and control; or even payload instruments. Flight experience over the last 35 years or so indicates that electromagnetic interference from electric propulsion units has not been a critical concern [58]. RF communications through the SPT plume have resulted in slight degradation of the signal but not large enough to jeopardize signal transmission or receipt. Furthermore, recent tests on the SPT-100, carried out at NASA Lewis Research Center, show no apparent effects of SPT operation on RF transmission [59]. Experiments have shown that the level of interference is highly dependent upon propagation path, carrier signal frequency and thruster discharge current oscillations [60]. The planned utilization of X-band (7-9 GHz) frequencies for ETA should thus mitigate interference. Incorporation of a filter circuit in the discharge power supply also serves to reduce phase noise levels [60]. EMI does not seem to be a problem, but it is important to characterize the electromagnetic environment by ground testing. Integrated simulations of carrier antenna and thruster directions during the constellation deployment phase would assist in identifying potential situations when transmissions have to be carried out through the SPT plume. Even though this issue is not a design "driver", the constellation design should take it into account and minimize the chances of having to transmit through the plume.

Chapter 6

Constellation Analysis

Unprecedented source localization accuracies are what distinguish ETA from current GRB detection systems. To this effect, it is the dedicated network of microsatellites that enables such accuracies to be attained. Inter-spacecraft baselines are a critical component of the system accuracy, as identified in Chapter 2. Overall mission success hence requires the deployment and subsequent development of the constellation of microspacecraft in a manner that not only provides the required baselines at the appropriate time but also facilitates space and ground system design. This chapter presents the analysis performed to develop the constellation deployment and development phase of the ETA mission.

Commencing with the scope and approach of the analysis and a redefinition of constellation-related requirements, the discussion then moves onto the details of the model which was developed to simulate constellation dynamics. Noteworthy aspects of the model are presented together with the definition of the constellation figure of merit which is used as a metric for the trade studies. The most important trade studies and results are next discussed, as well as the associated sensitivity analysis. The focus then shifts to the orbit design of the trigger spacecraft, which are an integral element of the constellation. The chapter is rounded off with a summary of the ETA baseline mission scenario which results from the analysis.

6.1 Introduction

Before going into the analysis, it is necessary to specify the scope of the work. The purpose of this section is to clarify the scope of the trade studies together with the methodology adopted for conducting the analysis. Constellation requirements and constraints are restated in order to stipulate, at the outset, the framework for constellation design.

6.1.1 Scope

This chapter presents the analysis performed during the concept development phase of the ETA mission to develop a constellation deployment strategy. The main objective of the

analysis was to support the ETA team in understanding the dynamics of the constellation and assist in developing an overall mission scenario that would enable the satisfaction of system requirements.

The emphasis at this stage of the design process is normally to gain a better understanding of the system and its ability to meet system requirements by exploring options and design parameter sensitivities. A high level of detail and accuracy is not so much required as is the ability to model the system to sufficient accuracy in order to conduct top level system trades. The constellation is a central component of the ETA system since it melds the scientific aspects into the system design. There is thus a need for a tool which can simulate the constellation fairly quickly and lends itself to the assessment of various trade options while providing inputs to the system design process.

Such a simulation tool was developed and a number of important trade studies were carried out to resolve issues which affected the rest of the system development. The analysis was geared towards assessing the impacts of important system parameters, determining the ability of various mission options to meet system requirements and synthesizing a baseline scenario for the constellation deployment phase of the mission.

Since the constellation affects a multitude of system aspects such as measurement accuracy, cost, schedule, carrier spacecraft and microsatellite design, an attempt is made, where possible, to relate the analysis to these system considerations.

6.1.2 Approach

The approach adopted for the constellation analysis is outlined in Figure 6-1.

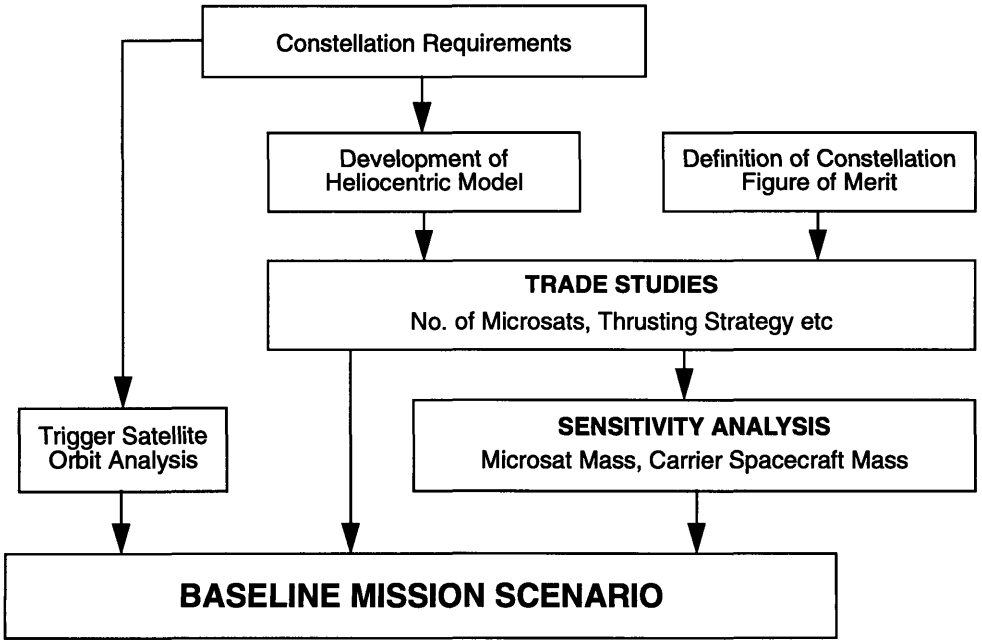

Figure 6-1: Constellation Analysis Approach

The analysis involved the development of two functionally different models, namely

- **General Model (Heliocentric Model)**
  This general model was developed first and characterizes the dynamics of the constellation in the heliocentric frame of reference. It is the main tool utilized for the trade studies and concept exploration since the effectiveness of the constellation towards scientific operations (GRB localization) is best quantified within this frame.

- **Trigger Satellite Orbit Model (Geocentric Model)**
  This model was developed during the latter phase of the constellation analysis to refine the orbit design of the trigger microspacecraft. The main purpose of the model was to explore the various orbit options that were available for the trigger satellites. The relevant trajectory dynamics were more easily simulated and understood in an Earth-centered reference frame. Additionally, the heliocentric model was not developed to have the fidelity necessary to model such trajectories.

While the general model was being developed, a figure of merit was also defined which quantified the ability of the constellation to provide the baselines for GRB astrometry. This constellation figure of merit, η_{const}, was developed by ETA scientists and was based on scientific considerations [17].

It was then possible to conduct trade studies using the general model and assess options against η_{const}. Some of the more important trades involved the number of microsatellites within the constellation and the thrusting strategy for the SPT-70, both in terms of thrust direction and duration. Analysis was also performed to determine the sensitivity of constellation performance to design parameters such as microsateliite and carrier spacecraft mass, which are bound to change as the system design is refined.

At that stage, scientific and communications issues necessitated addressing the analysis of the trigger satellites in more detail. This led to the development of the trigger satellite orbit model which was used to refine the trigger satellite orbits.

The general deployment and subsequent development of the constellation, as identified from the general model and trade studies, was combined with the trigger satellite orbit analysis to synthesize the ETA baseline mission scenario.

While every effort has been made to include important details, not all the simulation and analysis carried out can be presented in the thesis. Therefore, the emphasis has been on showing selected results of the most important trades as they impact the ETA system.

6.1.3 Constellation Requirements and Constraints

The major constellation-related requirements that have to be taken into account when designing the constellation are listed here. Even though some of these requirements have already been noted in Chapter 4, they are nevertheless included here for the sake of completeness.

- **Provide a constellation "spread" of 120° in 2 years**
  This requirement was addressed in Chapter 2 for the top level propulsion system trade to estimate the net ΔV required. While it was used to derive an indirect requirement then, it is now used in the opposite sense in that any scenario being analyzed will be checked to see if this spread is achieved in the specified time.

- **Launch Vehicle: DeltaLite version of the Medlite series**
  The launch vehicle constraint was also dealt with in Chapter 2 with launch mass constraints, as defined in Table 4-1. Net system mass, including that of the microsatellites and carrier spacecraft, will have to comply with this constraint.

- **Minimum Number of Microsatellites in Constellation: 4**
  A minimum of 4 microspacecraft are required for science operations. Redundancy requirements necessitate more spacecraft but the exact number has to be decided upon through a trade study, taking into account not only performance but also other issues such as cost.

- **At least one Trigger Satellite near Earth for real-time alert capability**
  This requirement complements the previous requirement. Two trigger satellites may be required to provide redundancy for the real-time alert capability, which is an important attribute of the ETA system. This requirement is somewhat fuzzy in that the proximity to Earth was initially unspecified. Communication link capability, and hence the time taken to downlink GRB templates, was the determinant here. While initial range-to-Earth values of up to 0.2-0.3 AU were considered, these were reduced to values in the region of 0.01-0.05 AU later as the scientific requirements and microsatellite capabilities were better understood. The reduced ranges to Earth result in over a 16-fold increase in datarates (since datarate varies inversely with square of range). This requirement shift was one of the reasons for developing the Trigger Satellite Orbit model in order to simulate the orbits more accurately.

- **Provide at least 2 years of data collection**
  Scientific and programmatic issues combine to give this requirement. This period is necessary for acquiring the specified amount of GRB event data in addition to the fact that current funding allocations allow 2 years for scientific operations.

- **Nominal Mission Lifetime of 4 years**
  Mission lifetime complements the data collection period requirement since they collectively specify the time available for the constellation to be deployed and develop the minimum angular spread to commence scientific operations.

- **Maximize baselines over mission lifetime**
  This is another fuzzy requirement which is currently not quantified. It will be interpreted as the need to maximize the constellation figure-of-merit, η_{const}, as much as possible. For example, given two deployment strategies, the one with maximum η_{const}, integrated over mission lifetime, will be selected.

- **SPT-70 operating time: 3,000 hours**
  The SPT-70 has a limitation on lifetime, as discussed in the previous chapter. It is conservatively assumed that an SPT-70 thruster wil have an effective thrusting time of 3,000 hrs. This number is important because it sets a constraint on the thrusting time available between microsatellite deployments.

- **Constellation to be in the ecliptic plane**
  This requirement is brought about by scientific considerations to ensure that GRB measurements have the highest accuracy for GRB's originating for the directions of the ecliptic poles. Ecliptic plane orbits also allow the GRB detectors to be shielded from solar radiation.

These requirements have to be taken into account at all stages of the constellation analysis. Other requirements or constraints imposed by spacecraft design issues, for example, were introduced at different stages of the conceptual design phase and are introduced at the appropriate stages of the analysis. Examples of such requirements or constraints include spacecraft Earth/Sun look angles for Antenna/Solar Array placement and Earth ranges for communication link design.

6.2 Simulation Model

This section deals with the general constellation dynamics model (heliocentric model) that was developed and used for simulation. Model assumptions are identified before developing the trajectory and thrusting models. The constellation figure-of-merit is defined and a brief description of the MATLAB code is given. Sample results, in the form of plots, are presented.

6.2.1 Assumptions

A number of assumptions were made to simplify the implementation of the constellation dynamics model. Some of the pertinent ones are

- **"Patched Conics" approximation**
  The model was developed using the "patched conics" method to convert Earth referenced escape trajectories onto the heliocentric frame. This simplifying assumption is justified for the preliminary, exploratory phase of conceptual design [61,62].

- **Earth's heliocentric orbit is circular**
  Even though the Earth's orbit about the Sun is slightly eccentric, it is assumed to be circular here. This avoids having to use an ephemeris to keep track of the Earth and is a simplification that is consistent with the overall accuracy of the model.

- **All trajectories are in the ecliptic plane and the launch vehicle injects the carrier spacecraft in the ecliptic plane**
  The general constellation model does not deal with the launch vehicle's trajectory, except vectorially adding the hyperbolic excess velocity to Earth's orbital velocity to determine the carrier spacecraft's initial velocity in the heliocentric frame. The only other consideration of the launch vehicle is with regard to its throw weight to the specified launch energy (C_3). The net mass of the carrier spacecraft, including the microsatellite stack, is correlated with the launcher capabillity.

- **All trajectory perturbations, except those due to Earth, are neglected**
  Incorporating perturbations due to Jupiter and other sources would make the simulation computationally intensive and that level of accuracy is not required at this stage of the analysis. Detailed simulations can be carried out after the baseline mission scenario has been developed.

- **SPT thrusting is along the +/- velocity vector heliocentric direction**
  Thrusting is assumed to be vectored in the positive or negative heliocentric velocity direction. Other thrust control laws may be more effective but were not considered in this study.

- **Trade Baseline Case**
  While the design parameters were varied over quite a range during the analysis, it is not possible to present all of the results here. Selected cases will be compared with the assistance of a trade baseline case which was assumed and used as a benchmark. The parameters assumed for this trade baseline are

  - Number of Microsatellites: 6
  - Carrier Wet Mass: 250 kg (including ~60 kg propellant)
  - Microsatellite Mass: 50 kg
  - DeltaLite C_3: 1 km^2/sec^2 in the retrograde direction to Earth's orbital velocity

- Total thrusting time: 6,000 hrs (Two SPT-70's operating serially)
- Equal thrusting times between microsatellite deployments with first microsatellite deployed without any thrusting
- SPT thrusting in the positive heliocentric velocity direction
- Carrier spacecraft thrusts for a further 10 days after deployment of the final microsatellite.

It is important to note the distinction between this trade baseline case and the ETA baseline scenario that was synthesized from the results of the trade studies. Other minor assumptions that were made will be identified at the appropriate points in the analysis.

6.2.2 Trajectory and Thruster Model

A trajectory model was derived to simulate the constellation, based on the simplifying assumptions outlined previously. Since a large portion of the model is based on standard astrodynamics and trigonometry, only the general details of the model are presented here. The reader is referred to specialized texts on Celestial Mechanics and Astrodynamics for the formal derivation of the equations [61,63,64,65].

Figure 6-2 below illustrates the geometry of the trajectory problem.

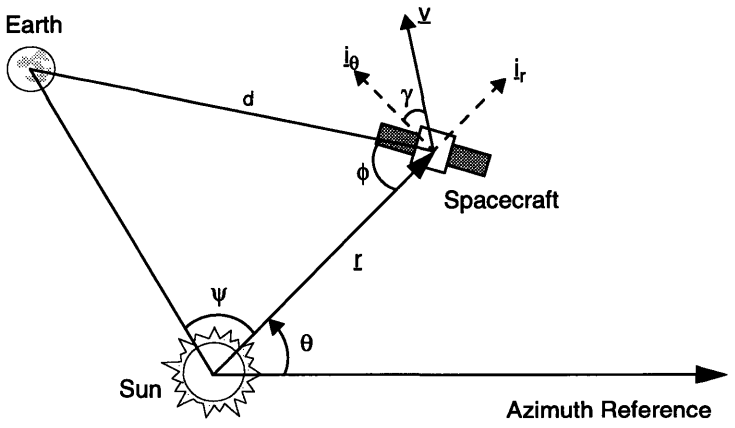

Figure 6-2: Trajectory Geometry

The range of the spacecraft from the Sun is r and that to the Earth is d. The angle θ is the angular coordinate measured with respect to a reference direction. The azimuthal difference between the spacecraft and the Earth is denoted by ψ. The "look" angle φ, is the angular separation between the Sun and Earth, as seen from the spacecraft. A polar coordinate frame (r,θ) was selected for the model. The general equation of motion in this coordinate frame can be shown to be

$$\underline{a} = \left(\ddot{r} - r\dot{\theta}^2\right) \underline{i}_r + \left(r\ddot{\theta} + 2\dot{r}\dot{\theta}\right) \underline{i}_\theta \qquad \text{Eqn (6-1)}$$

where the radial and tangential components are given Noting that the thrust, F, of the thruster is along the velocity vector (+/-), it is easy to show that the radial and tangential components of thrust are given by

$$F_r = F\,Sin\,\gamma = \frac{F\dot{r}}{V} \qquad \text{Eqn (6-2)}$$

$$F_\theta = F\,Cos\,\gamma = \frac{Fr\dot{\theta}}{V} \qquad \text{Eqn (6-3)}$$

where γ is the flight path angle, as defined in Figure 6-2, and V is the velocity magnitude of the spacecraft.

The gravitational force due to the Sun is in the radial direction while that due to the Earth has to be resolved into radial and tangential components. Care has to be taken to ensure that the tangential component has the correct sign, depending on whether it assists or retards the angular motion. For example, if the spacecraft is azimuthally ahead of the Earth, then Earth's gravitational attraction retards the angular motion and vice versa. Taking these force terms into account together with thrusting, the equations of motion become

$$\ddot{r} - r\dot{\theta}^2 = \frac{F\dot{r}}{MV} - \frac{\mu_{sun}}{r^2} - \frac{\mu_{earth}}{d^2}Cos\,\phi \qquad \text{Eqn (6-4)}$$

$$r\ddot{\theta} + 2\dot{r}\dot{\theta} = \frac{Fr\dot{\theta}}{MV} \pm \frac{\mu_{earth}}{d^2}Sin\,\phi \qquad \text{Eqn (6-5)}$$

where μ_{sun} is the Sun's gravitational parameter, μ_{earth} is the Earth's gravitational parameter, d is the range of the spacecarft from the Earth, ϕ is the "look" angle, M is the instantaneous mass of the spacecraft and V is the spacecraft velocity magnitude given by

$$V = \sqrt{(\dot{r})^2 + (r\dot{\theta})^2} \qquad \text{Eqn (6-6)}$$

The rate of change of mass is related to the thrust and I_{sp} through

$$\dot{M} = -\frac{F}{gI_{sp}} \qquad \text{Eqn (6-7)}$$

where g is the acceleration due to Earth's gravity and I_{sp} is the specific impulse of the propulsion system. The range to Earth, d, and the look angle can be determined simply through trigonometric relations.

Equations (6-4), (6-5) and (6-7) are integrated numerically to compute the trajectory. The simulation performs these integrations and presents the data in the form of plots. Thrust terms are not included for the microsatellites' orbits. The variation of thrust with respect to the range from the Sun (hence power) was modelled in a simple way, in the form of a $1/r^2$ law. The tacit assumption here was that the specific impulse and efficiency were constant. It was necessary, however, to specify a maximum limit on the power that could be utilized when the carrier spacecraft was closer to the Sun. This constraint was determined by the capabilities of the SPT-70 PPU.

The computation of the carrier spacecraft trajectory involves the reinitialization of the system after each microsatellite deployment since the carrier mass has to be initialized.

Some of the main design parameters in the computations are

- C_3 (direction is pure +/- heliocentric velocity direction)
- Carrier Wet Mass (excluding microsatellite stack but including propulsion system mass)
- Microsatellite mass
- Number of microsatellites
- Thrusting direction (pure +/- heliocentric velocity directions only)
- Thrusting times between each microsatellite deployment

The carrier and microsatellite masses were not changed for most of the analysis but a sensitivity analysis was carried out. Trade studies were performed on the number of microsapececraft , thrusting direction and thrusting times between deployment. The impact of varying each of these parameters was assessed in terms of the constellation figure-of-merit.

6.2.3 Constellation Figure of Merit

The effectiveness of the constellation towards GRB source localization can be quantified by a figure-of-merit which is a function of the positions of the microsatellites. This figure-of-merit, η_{const}, is used as a metric for the trade studies related to the constellation. As shown by Eqn (2-3), η_{const} contributes to the system level figure-of-merit, η_{sys}, through

$$\eta_{sys} = C_{burst} A_{det} \eta_{const} \qquad \text{Eqn (6-8)}$$

where C_{burst} is a natural GRB characteristic and A_{det} is the effective area of the GRB detector. η_{const} is a function of the positions (X_i , Y_i , Z_i) of the microspacecraft, where the subscript i denotes the i'th microsatellite in the constellation. The coordinates are conveniently selected to be in the heliocentric frame to facilitate integration with the rest of the heliocentric simulation model. Given the assumption that the constellation will be in the ecliptic plane and taking that as the reference, it follows that the Z-component will be negligible.

The centroid (X_c , Y_c) of an N microspacecraft constellation is given by

$$X_C(t) = \frac{1}{N}\sum_{1}^{N} X_i(t) \quad , \quad Y_C(t) = \frac{1}{N}\sum_{1}^{N} Y_i(t) \qquad \text{Eqn (6-9)}$$

The time-varying coordinates of the microsatellites with respect to the constellation centroid, (x_i , y_i), are simply

$$x_i(t) = X_i(t) - X_C(t) \quad , \quad y_i(t) = Y_i(t) - Y_C(t) \qquad \text{Eqn (6-10)}$$

Having determined the relative coordinates, the next step is to define the covariance matrix

$$\begin{bmatrix} \sum x_i^2 & \sum x_i y_i \\ \sum x_i y_i & \sum y_i^2 \end{bmatrix} \qquad \text{Eqn (6-11)}$$

η_{const} is then related to the determinant of the covariance matrix by

$$\eta_{const} = \frac{1}{c^2}\sqrt{\sum x_i^2 \sum y_i^2 - \left(\sum x_i y_i\right)^2} \quad , \quad \text{Units: sec}^2 \qquad \text{Eqn (6-12)}$$

where c is the speed of light. The units of η_{const} are square seconds. In effect, η_{const} , denotes the "area" in square light-seconds covered by the constellation. The larger the spread area, the larger the value of η_{const} . Since the microsatellite positions are a function of time, it follows that η_{const} is a time-varying function as well.

The constellation figure-of-merit can be calculated over the mission lifetime, as will be shown later. This can be integrated over time and time averaged over mission lifetime, if necessary. Since there is no defined goal as to the value of η_{const}, it follows that a logical manner of using the figure-of-merit is to maximize its integrated (or time averaged) value over mission lifetime. This quantification of the "spread" of the constellation is very useful, as shall be seen, in assessing trade options.

6.2.4 Simulation Code

A simulation code was developed based on the formulations described previously for the constellation dynamics and figure-of-merit. The model was coded for implementation on MATLAB 4.2c, which provides superior data handling and graphics quality at the expense

of a slight loss in computation speed.

The code consists of three main modules, namely

- Computation
- Data plotting
- Dynamic Simulation

Figure 6-3 outlines the flow of events in a typical simulation run.

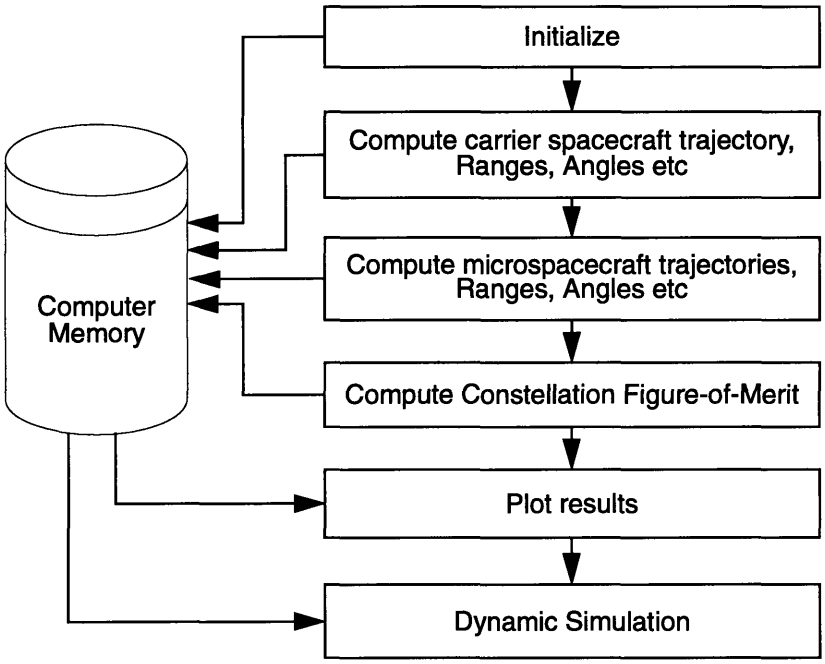

Figure 6-3: Constellation Simulation Flow

The computations are carried out first before plotting the data and dynamically simulating the constellation. The rationale behind the serial approach is that it enables a flexibility in plotting and interpreting the data, something which would not be possible if the computation and data presentation were carried out concurrently. Moreover, there are many important parameters that need to be tracked and it would have been difficult to present all these simultaneously while the computation was going on. MATLAB stores all the data internally so that data from different simulation runs can be retrieved and plotted for comparison without recourse to accessing datafiles which are also generated.

After initializing the model with input data such as deployment times, launch conditions and thrusting direction, the carrier trajectory is computed, taking into account the reinitialization after each deployment. The initial conditions for the microsatellite trajectories, as established by the carrier trajectory, are used to compute the microsatellite trajectories. Once the time histories of the microsatellite positions are known, it is a formality to compute the time history of the constellation figure-of-merit (η_{const}).

Even though any data can be easily plotted, the code automatically generates plots of the time histories of the following parameters

- Carrier Mass
- Range to Sun
- Range to Earth
- Azimuth with respect to azimuth reference
- Azimuthal difference between spacecraft and Earth (ψ)
- "Look" angle (ϕ): Angular separation of Earth/Sun as seen from spacecraft
- Constellation figure-of-merit (η_{const})

Except for the carrier mass and η_{const}, all the other parameters are plotted for the carrier spacecraft and all microsatellites. In addition to these plots, the code can plot the positions of the entire constellation at up to four different instants in time. These snapshots are useful to visualize the development of the constellation.

A further enhancement of great utility is the dynamic simulation. This plots in succession, the snapshots of the constellation at specified intervals over the mission lifetime, giving a visualistic impression of the dynamic development of the constellation. The dynamic simulation facilitates the understanding of the dynamics at the same time as assisting in validating the data of the simulation.

Because the computations are done and data stored beforehand, it is possible to plot other interesting data, replot and modify the standard plots and rerun the dynamic simulation. This flexibility is crucial in the analysis since it facilitates data analysis without having to redo the time-intensive computations. The easily accessible data structures provided by MATLAB were also enabling elements to this effect.

Typical results of the simulation are presented in the next section where the dataplots and constellation snapshots are included for the trade baseline case.

6.2.5 Sample Results

The results shown here are for the trade baseline case, as outlined in the discussion on the assumptions. The microsatellites are deployed at 50 day intervals with the first microsatellite being deployed immediately after escape. The purpose of this section is to familiarize the reader with the formats for the presentation of data in later sections.

Figure 6-4 plots the variation of carrier mass during the constellation deployment period. The net mass of the carrier, including the microsatellite stack, at the beginning is 550 kg but 500 kg is plotted at T=0 days since the first microsatellite is deployed immediately after escape. Time is referenced to the time at escape or transfer to the heliocentric frame. The interim period for the launch and escape trajectory is not included here but is simply added on when necessary. The other microsatellite deployments are portrayed by the 50 kg

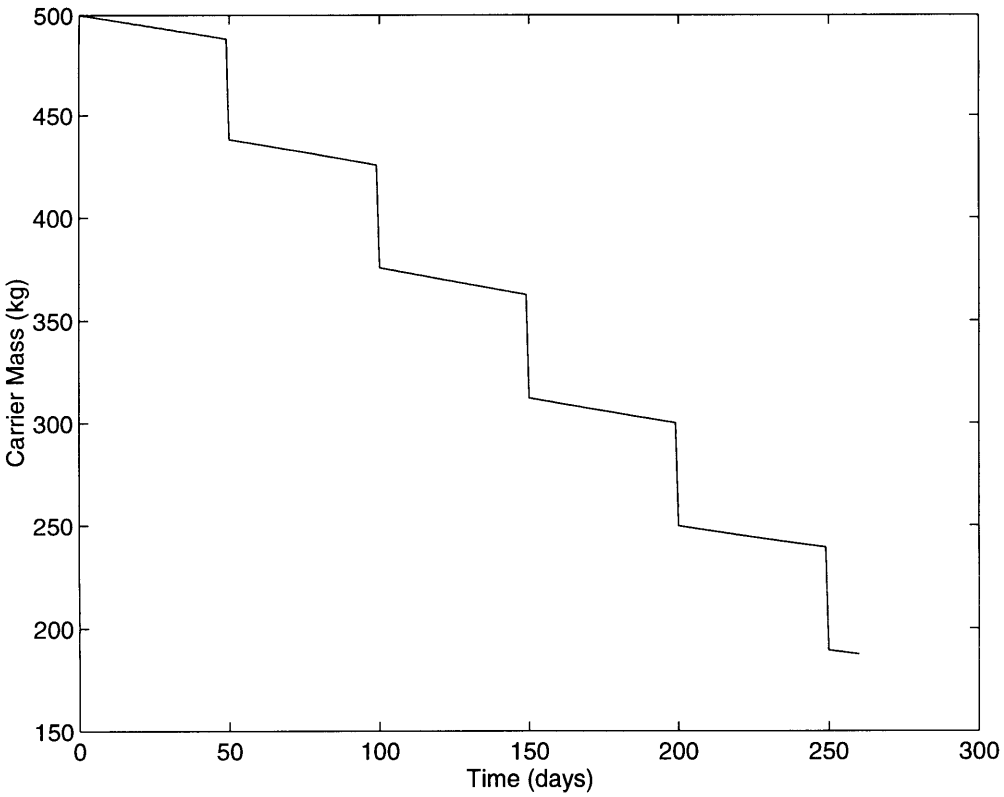

Figure 6-4: Variation of Carrier Spacecraft Mass

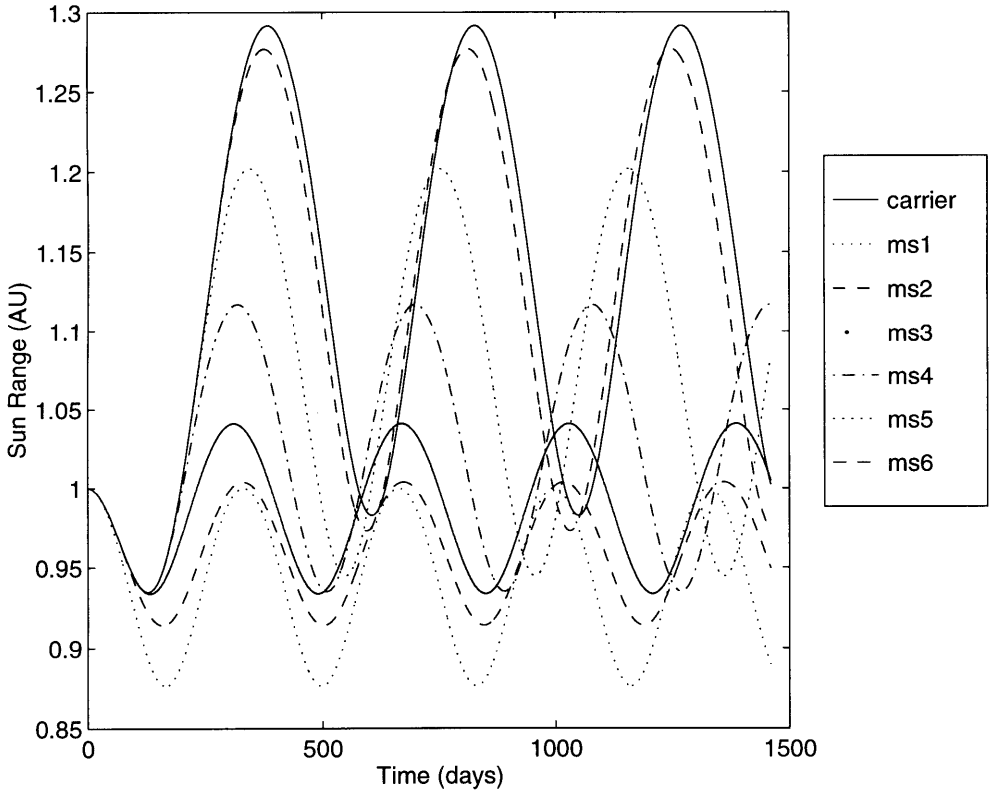

Figure 6-5: Variation of Range from Sun

drops at 50 day intervals. Consumption of propellant in the interim periods is shown by the steady decrease in mass. One use of such data to spacecraft designers is in center-of-gravity (c.g) movement considerations.

Figure 6-5 displays the variation of the distance from the Sun of the carrier spacecraft and all microsatellites. This plot is only for illustration purposes and, while it is relatively difficult to plot so much on paper clearly, the use of color greatly enhances the distinct curves. The periodic nature of the orbits is evident as are the perihelions and aphelions. The carrier spacecraft orbit is shown for illustrative purposes. The utility of the carrier after the deployment phase is, as of now, undecided upon. One possible use would be to continue thrusting with the SPT-70; the model enables the exploration of such scenarios. Proximity from the Sun drives the design of the power and thermal subsystems and the variation of Sun range is thus an important consideration for the spacecraft designer.

Figure 6-6 shows the variation of range from Earth for all the spacecraft. This plot is integral to the design of the communications system of the carrier spacecraft and microsatellites. Link analysis requires a knowledge of maximum and minimum ranges which can be provided by such data plots. This plot is also quite useful in checking the proximity of the trigger satellites.

Figure 6-7, which shows azimuth angle (θ) histories for all spacecraft, was primarily used as a check to verify the simulation and cross check against the dynamic simulation.

Figure 6-8 plots the angular separation (ψ) with respect to the Sun of the spacecraft and Earth. This gives an indication of whether the angular separation increases over time and whether or not a spacecraft is "ahead" or "behind" Earth in an azimuthal sense. The angle was arbitrarily defined not to exceed 180 degrees.

The angular separation of the Sun and Earth (ϕ), as seen from the spacecraft, is plotted in Figure 6-9. Again, the angle was defined so as not to exceed 180 degrees. Knowledge of the look angle is an important consideration for the configuration of the spacecraft. The positioning of the solar array and communication antenna on the carrier spacecraft and microsatellites were driven by the look angle variations. This graph was used to a large extent, especially since there was a constraint placed, at one time, on the range of the look angle. The constraint was due to the desire to simplify spacecraft design if the look angle range could be minimized by constellation design itself. It normally turned out initially that the microsatellite closest to Earth had very large look angle variations and this was a source of concern for spacecraft design. Furthermore, the look angle gives an indication of the periods when the Sun will appear in the backgound of the spacecraft or Earth and degrade communications links due to radio noise. Mission planners need this type of information to schedule command uplinks and telemetry downlinks, taking into account "outage" periods, as identified by the look angles. This is a very good example of how the constellation and spacecraft design affect each other.

In the context of the trade studies presented in this thesis, the constellation figure-of-merit is perhaps the most important element and Figure 6-10 presents the time history of the fig-

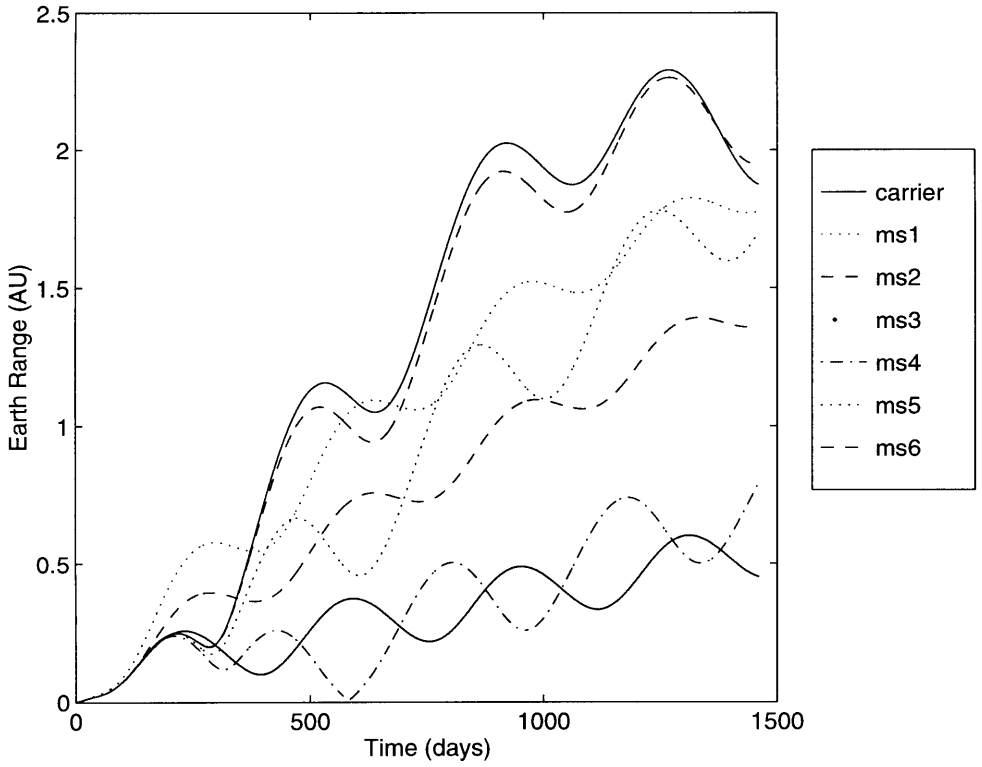

Figure 6-6: Variation of Range from Earth

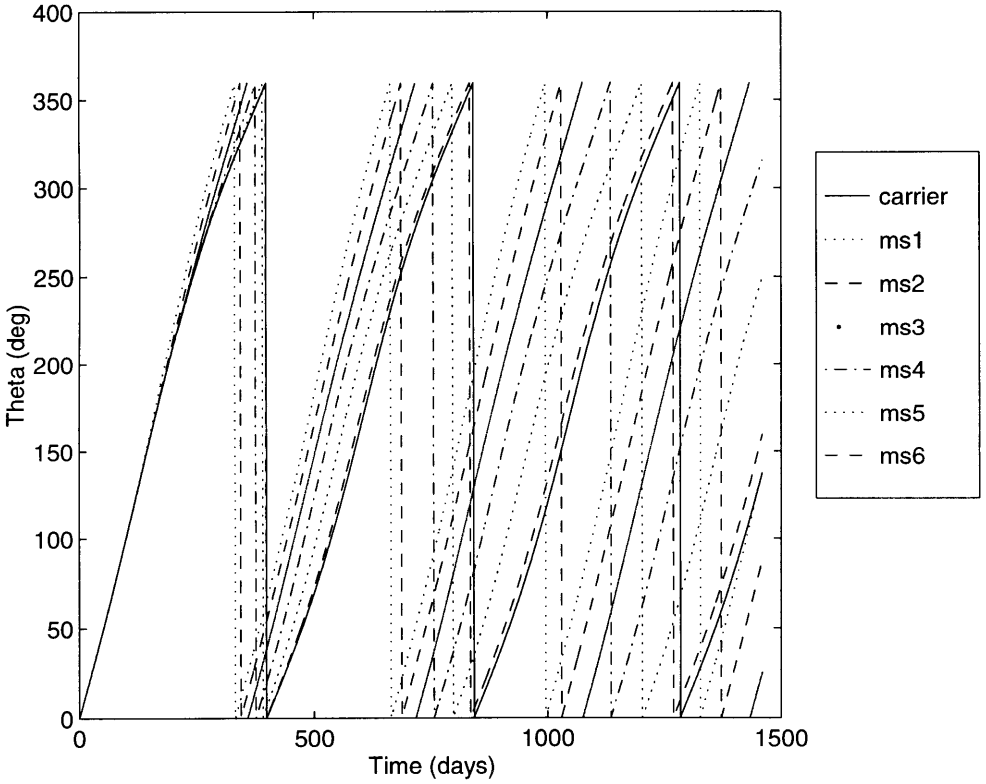

Figure 6-7: Variation of Azimuth

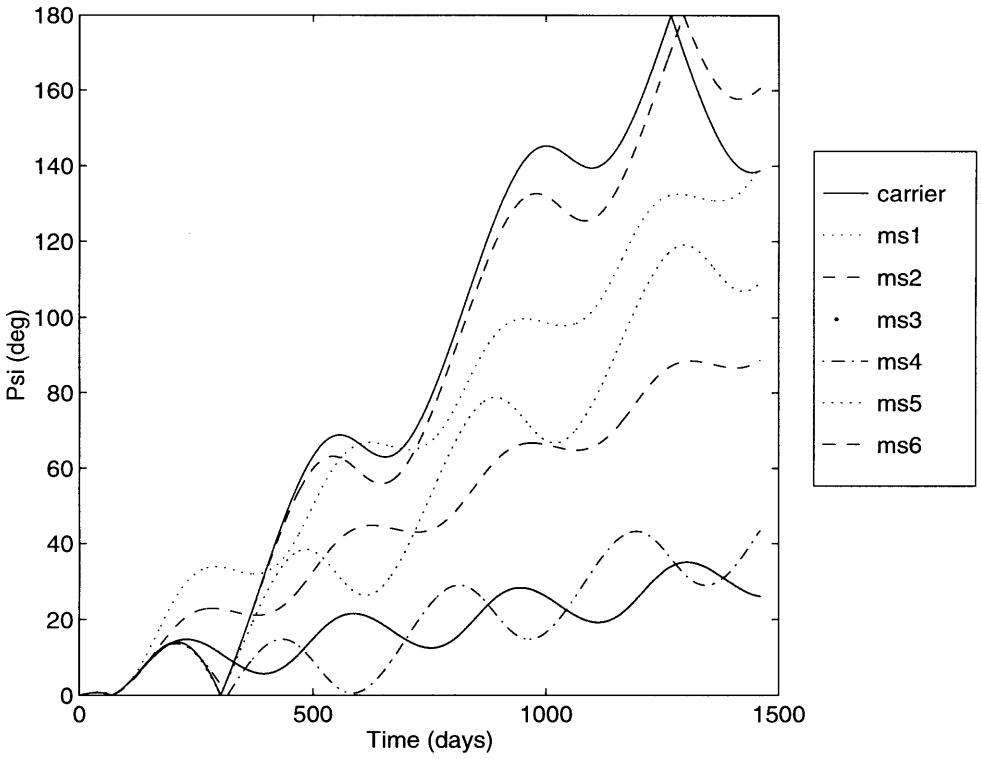

Figure 6-8: Variation of Azimuthal Difference

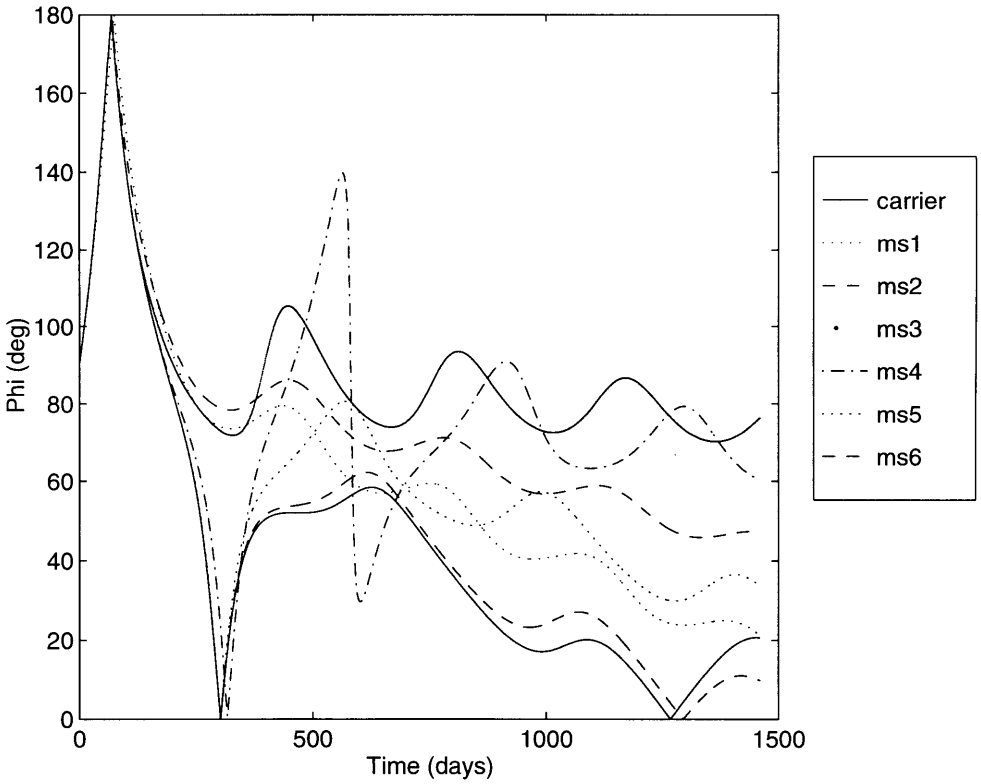

Figure 6-9: Variation of Look Angle

ure-of-merit, η_{const}, over the mission lifetime. The capability of the constellation to contribute towards the GRB astrometry is summarized by the graph. A high value indicates better performance. A single "number" that could summarize the performance could be the time-averaged value of the figure-of-merit, which could be calculated by computing the area under the graph and averaging it over the mission lifetime. The constellation takes time to develop and it is obvious that the low values of η_{const} over the first year do not justify the commencement of science operations then. Thereafter, the constellation rapidly starts providing good baselines. The interesting thing to note is that η_{const} starts degrading after about 40 months.

The intuitive explanation behind the degradation of the figure-of-merit would be that the microsatellites have spread around the entire 360 degree arc and started "bunching" up. This is confirmed by Figure 6-11, which presents the state or "spread" of the constellation at the end of each year. Indeed, at the end of the fourth year, the first microspacecraft has caught up with the carrier and last microsatellite. The revolution of the bodies is in an counterclockwise fashion. The Sun and Earth are also shown. There is no way of displaying the dynamic simulation on paper, except for these "snapshots". The code allows one to plot the state of the constellation at any instant. Plots of the type of Figures 6-10 and 6-11 are most frequently used in the thesis to present the results.

As shown above, the data generated by the simulation could be visualized in a number of ways to facilitate the understanding of the system and the presentation of trade study results. Having familiarized the reader with the data plots, it is now appropriate to move onto the trade studies and develop the constellation deployment strategy.

6.3 Trade Studies

This section presents a discussion of some of the trade studies that were performed for the constellation. The major ones included the number of microspacecraft, thrusting strategy and launch energy. The motivation for this analysis was to decide upon the first order considerations pertaining to the constellation and its deployment.

6.3.1 Introduction

The design of the constellation deployment strategy, such that it provides the necessary baselines for scientific operations, involves a large number of variables that have to be optimized. The optimization is not solely based on the capability to support scientific operations, as quantified by the constellation figure-of-merit. More often than not, the decisions were driven by other factors such as cost, programmatic constraints and so forth. Therefore, it is imperative to keep all such non performance-related issues in perspective while conducting the trade studies and presenting the results.

The general methodology adopted to conduct the trade studies has been to simulate the alternatives, using the code described before, and compare their performance in terms of the constellation figure-of-merit, η_{const}. Trade options are also compared qualitatively on cost, schedule and program risk. It is recognized that some of the parameters traded off

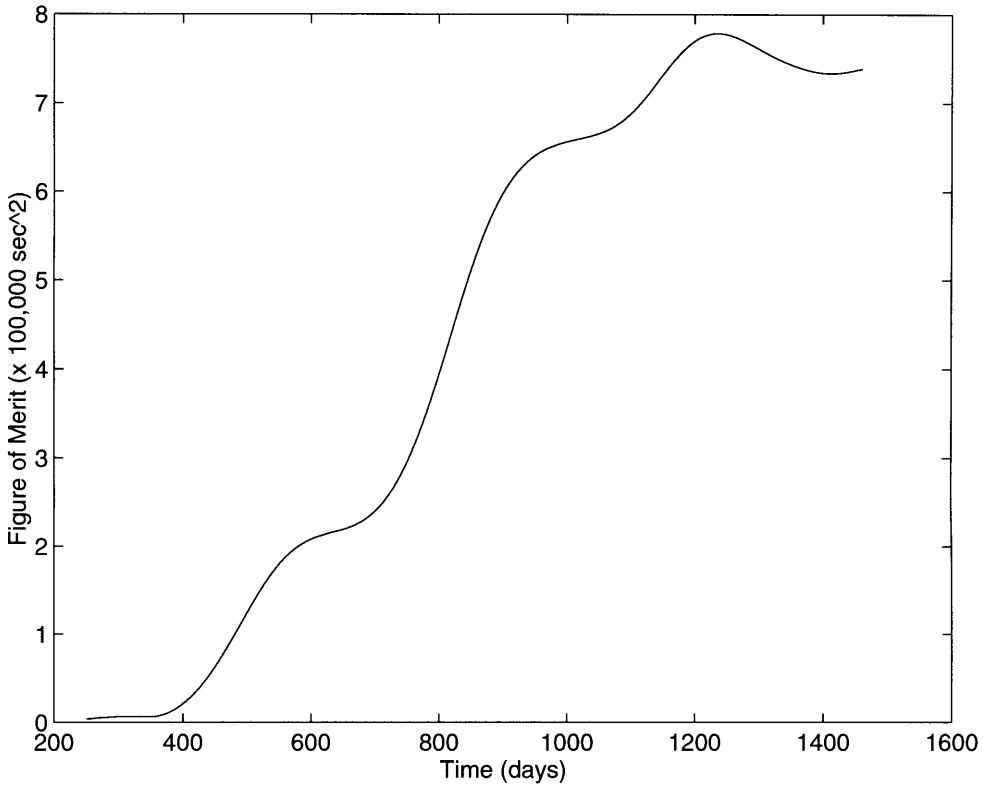

Figure 6-10: Time history of Constellation Figure-of-Merit

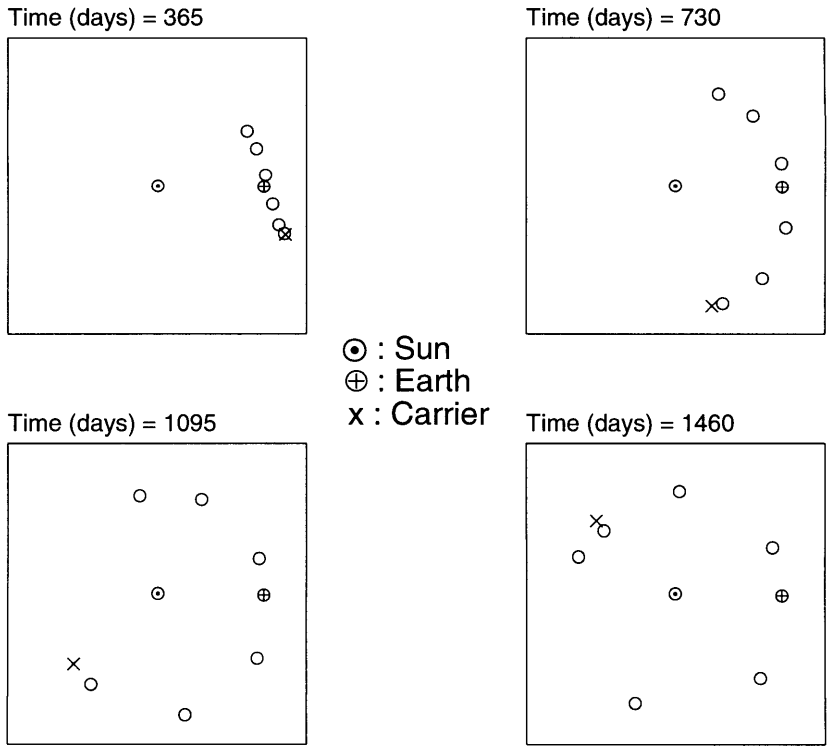

Figure 6-11: Constellation Development Over Mission Lifetime

here are inter-related and the trade studies, in effect, were carried out in a more integrated manner. The approach to analyzing the effect of various design parameters was to assess them while the other major factors were constant or their effect on the results negated in some fashion. For example, the impact of number of microsatellites was analyzed assuming the same thrusting strategy. The "sequential" treatment here is only to facililtate the orderly presentation of the rather interwoven analysis that went into the design of the constellation.

A large number of trade studies performed but only the major ones are addressed here. These are

- Number of Microspacecraft
- Number and mode of operation of SPT-70 thrusters
- Thrusting direction
- Launch energy (C_3) magnitude and direction
- Distributiion of total available thrusting time between each deployment.

The effect of these design parameters was analyzed assuming the trade baseline case and assessing the options for the particular parameter being considered. For example, when assessing the impact of the number of microsatellites, all options were differentiated from the trade baseline by the number of microsatellites and any other directly related parameter such as microsatellite mass.

6.3.2 Number of Microsatellites

The number of microspacecraft within the constellation has wide-ranging impacts on the rest of the system. Not only are spacecraft design and cost affected but the capability of the constellation to support GRB astrometry is also dependent on the number of microsatellites.

The effect of the number of microsatellites on the constellation figure-of-merit was analyzed by assuming that there was a constant mass allocation for the total mass of the microsatellites. That is, the carrier mass was assumed to be 250 kg and an allocation of 300 kg was made for the microsatellites. Thus, for a 6 microsatellite constellation, the mass of each microsatellite was 50 kg while a 4 spacecraft constellation had the spacecraft weighing 75 kg each. Because of the larger spacecraft mass for a constellation with fewer microsatellites, the GRB detector area A_{det}, in Equation (6-8), would be expected to be larger. This would contribute to increasing the overall system figure-of-merit. Figure 6-12 plots the time history of η_{const} for constellations comprising 4-8 microspacecraft.

The thicker plot is for the trade baseline 6 microsatellite case. The general trend is for a better η_{const} with increasing number of spacecraft.The interesting point to note is that the 4 microsatellite constellation develops at a faster rate over the first 600 days or so. This is explained by the relatively heavier spacecraft being deployed earlier. The spread over 4 years is however not so favourable. In general, the constellations do not provide sufficient

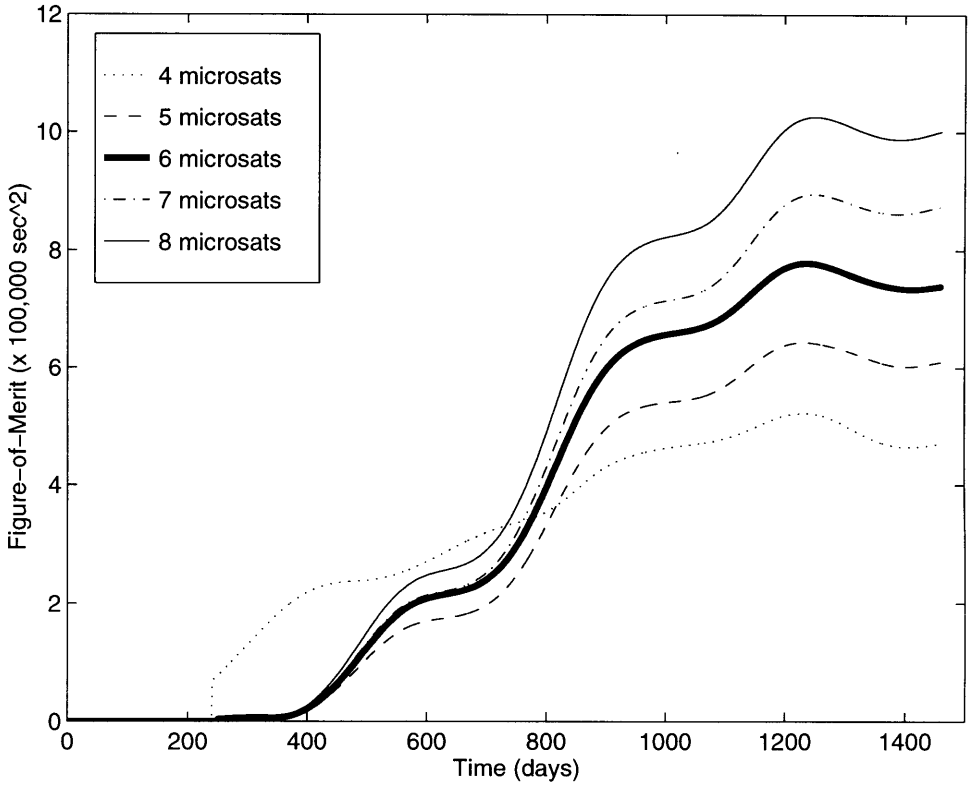

Figure 6-12: Effect of Number of Microsatellites in Constellation

baselines until after about 600 days. If programmatic issues forced scientific operations to be commenced at the end of the first year, then the 4 microsatellite constellation is the best option. It also serves as a fallback option for a "minimum science" mission if, for example, microsatellite mass increased to about 75 kg. However, there is also a requirement for redundancy in the system and a 4 microsatellite constellation would not provide any redundancy since a minimum of 4 spacecraft are required for GRB localization. Network timing inconsistencies can be detected by a 4 spacecraft constellation but correction is not possible since the spacecraft in error cannot be identified unambiguously. A 5 microsatellite network has the capability to both detect and correct for such timing inconsistencies. The 4 microsatellite alternative was discarded on these grounds.

The 8 microsatellite constellation would require the spacecraft to weigh approximately 37.5 kg. Initial estimates of the microsatellite mass indicated that, with the GRB detectors weighing about 18 kg themselves, spacecraft designers would be hard pushed to go for a net mass of 37.5 kg, including margins [66]. It was thus not feasible to select the 8 microsatellite alternative at this stage.

A 50 kg microspacecraft was deemed to be feasible and hence a 6 microsatellite constellation is possible. It is thus not necessary to go for a 5 microspacecraft design due to the better performance of the 6 spacecraft option. Moreover, a 6 spacecraft network allows the loss of one microsatellite while still retaining the capability to detect and correct timing errors. If a constellation comprising two trigger satellites (instead of the trade baseline one trigger satellite configuration) is considered, then a 6 spacecraft constellation allows a

redundant trigger satellite for the important real-time alert capability. There is no argument for discarding the 7 spacecraft constellation at this stage. For the sake of conservatism, a 6 spacecraft design has been selected and it is envisaged that if microsatellite mass and carrier mass are lower than current estimates, a seventh spacecraft will be added to the constellation [66].

One issue that has not been addressed here is the cost of building the spacecraft. The cost is a function of the number of spacecraft produced depending on the spacecraft manufacturer. Budgetary considerations were also a contributing factor to the selection of 6 as opposed to a 7 microsatellite design, since it was felt that at this stage, the proposed mission would rather have a conservative design with the potential for growth.

6.3.3 Number of Thrusters

The effect of the propulsion system on the constellation has to be assessed and the available options traded off. In this respect, primary consideration was given to how many thrusters to use. The number of thrusters to use was an option, if somewhat limited, since the source of the SPT-70 thrusters, Phillips Laboratory, has two flight units. Hence it was necessary to assess the impact of the various methods in which these thrusters could be used. Lifetime was of course the major factor here. Considering either one or two thrusters to be available and assuming that each thruster can only be operated for 3,000 hrs, the following options arise:

- Single SPT-70 operating for 3,000 hrs (second thruster flown as a reserve)
- 2 SPT-70 units operating "serially", that is only one is operated at a given time. The serial operation essentially doubles the available thrusting time to 6,000 hrs.
- 2 SPT-70 units operating in parallel, so that even though the available thrusting time is still 3,000 hrs, the thrust is doubled to a nominal value of 0.08 N.

Figure 6-13 displays the performance of each of these alternatives. It is quite clear that a single SPT-70 thruster has inferior performance since it does not have the gain of either thrust level or thrusting time that two thrusters would have.

The question of how to use the two thrusters is intriguing. Operating them in parallel provides slightly improved performance, as indicated by Figure 6-13. However, this performance advantage has a premium on power since at least twice the power is required to operate the thrusters in parallel. The estimate of power required for single thruster operation presented in Chapter 5 shows that about 820 W are required; this translates into a need for over 1650 W (power losses would also increase) if the two thrusters were to be operated in parallel. The doubling of solar array area results in at least a doubling of cost, if not more. This does not take into account the additional hardware (power processing unit and so forth) that would be required. Operation of the thrusters serially doubles the lifetime and does not require the additional hardware. In this case, the trade between per-

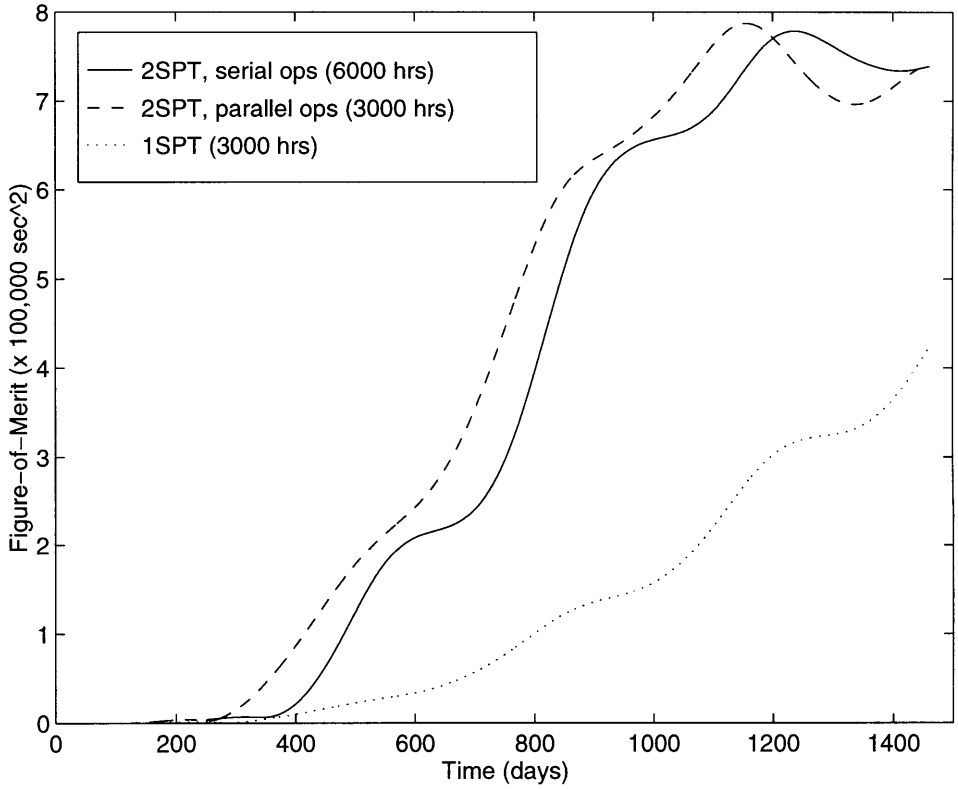

Figure 6-13: Effect of Number of SPT-70 thrusters

formance and cost is best assessed by a metric which incorporates both.

For the purposes of this top level trade, it is convenient to define a metric, $\eta_{p/c}$, as

$$\eta_{p/c} = \frac{\eta_{const}}{C_{power}} \qquad \text{Eqn (6-13)}$$

where C_{power} is the cost of power in dollars. The units of $\eta_{p/c}$ are thus $sec^2W/\$$ and the higher the value of $\eta_{p/c}$, the better. The easiest way to determine $\eta_{p/c}$ is to divide the time-averaged value of η_{const} with the cost of power since the cost is not a function of time. The time-averaged values of η_{const} for the parallel and serial operational modes are 4.770×10^5 and 4.3721×10^5 sec^2 respectively. Assuming a cost of 1500 \$/W [22] for the solar arrays (not taking into account any other hardware), the values of $\eta_{p/c}$ for the parallel and serial modes are 0.1927 $sec^2W/\$$ and 0.3554 $sec^2W/\$$ respectively. Clearly, the doubling in cost for the parallel mode is not compensated for by a doubling in the performance and operating the two thrusters is not justified based on just this issue.

Furthermore, the failure of one thruster for a parallel operation architecture would render

half the solar array useless and this would constitute an expensive overdesign. Serial operation allows flexibility without the need for additional hardware. Most of this hardware is redundant already, as described in Chapter 5, and there is no need for the dual string redundancy that is provided by a parallel operation architecture. Power is a major cost element and it is imperative that cost be minimized unless the improvement in performance overrides and is deemed necessary.

Both the trade baseline and ETA baseline scenarios adopt a serial mode of operation with each thruster providing at least 3,000 hrs so that a total of 6,000 hrs are available. More importantly, the solar array can be sized for ~820 W rather than ~1650 W.

6.3.4 Thrusting Direction and Launch Energy (C_3)

Having decided upon using 2 SPT-70 thrusters to provide 6,000 hrs of thrusting time, the next issue to be addressed is the strategy for the thrusting, in terms of thrusting direction and thrusting time. Simulations revealed that the thrusting direction and the magnitude and direction of the hyperbolic excess velocity at escape are inter-related with regard to their impact on the "spreading" of the constellation. The SPT-70 can be thrusted in the positive (prograde) or negative velocity (retrograde) direction, by assumption. The Earth escape trajectory can be configured such that the excess velocity adds to or subtracts from Earth's orbital velocity. These two alternatives are termed, in this report, as prograde C_3 (positive) and retrograde C_3 (negative) cases respectively. There are thus four possible combinations of C_3 and SPT thrusting directions. The performances of these alternatives are plotted in Figure 6-14 for a C_3 of 1 km^2/sec^2.

The trade baseline case of retrograde C_3 and prograde SPT thrusting is plotted as a solid line and provides the best performance after about 2.5 years. The time-averaged figure-of-merit for each alternative is listed in Table 6-1 below.

Table 6-1: Comparison of C_3 and SPT thrusting direction alternatives

Case #	C_3[a] direction	SPT Thrusting Direction	Time-Averaged Figure-of-Merit (x 100,000 sec^2)[b]
1	Retrograde	Prograde	4.3721
2	Retrograde	Retrograde	3.7289
3	Prograde	Prograde	2.8507
4	Prograde	Retrograde	3.5522

a. C_3=1 km^2/sec^2

b. Figure-of-merit is averaged over mission lifetime of 4 years

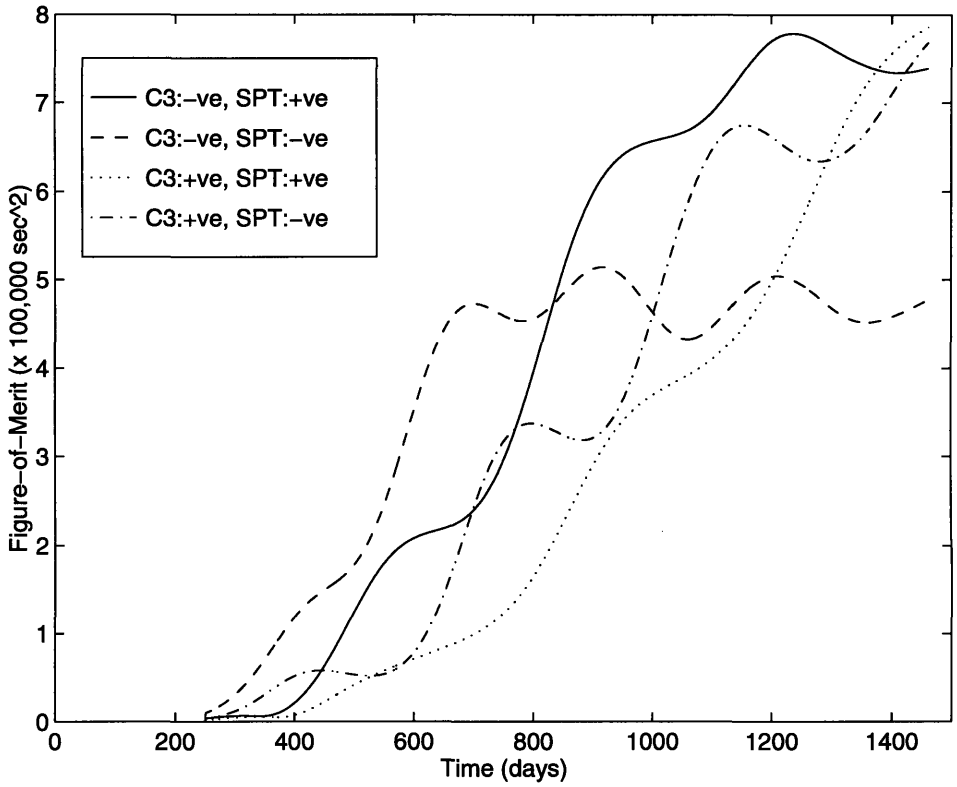

Figure 6-14: Effect of SPT Thrusting and C_3 Direction

Prograde SPT thrusting provides better performance for retrograde C_3 cases. The trend, however, is reversed for prograde C_3 cases, with retrograde SPT thrusting providing better performance. This indicates that C_3 direction and SPT thrusting are coupled with regard to their impact on the spread of the constellation.

The understanding of the trends shown in Figure 6-14 can be facilitated by attempting to develop a first order comprehension of the effect of C_3 and SPT thrusting as follows. Since the C_3 will either increase or decrease the spacecraft velocity in comparison to Earth's orbital velocity, a retrograde C_3 leads to a lower initial heliocentric velocity, causing the carrier spacecraft to fall in towards the Sun; the converse applies for prograde C_3. A prograde C_3 has the effect of initially increasing the radial distance and vice versa for retrograde C_3. SPT thrusting in the prograde (positive velocity) direction has the effect of increasing the net energy of the orbit, which results in an increase of semimajor axis and hence distance from the Sun. Again the converse applies for retrograde thrusting. Retrograde SPT thrusting has the effect of increasing the angular velocity and vice versa for prograde thrusting. There are thus two effects which determine the "spread" of the constellation:

- Increase of distance from Sun increases the radial separation of the microsatellites, thereby increasing the figure-of-merit
- Increase in angular separation brought about by higher angular

velocities results in an increase in the figure-of-merit.

The issue is therefore to see which of these effects is dominant. Moreover, power variations due to Sun range also affect SPT-70 performance, and hence constellation development.

Considering the (retrograde C_3, prograde thrusting) case, the carrier will initially fall in towards the Sun due to the lower heliocentric velocity, which increases the angular rates of the microsatellites which are deployed during this period. However, the prograde thrusting of the SPT adds velocity and the carrier spacecraft "pulls" out, gradually increasing radial distance from the Sun. Any microsatellite deployed during this phase has a larger semimajor axis. This results in a constellation in which one of the interim microsatellites ends up in the vicinity of the Earth. The overall spread of the constellation is also greater.

For the (retrograde C_3, retrograde SPT thrusting) case, the retrograde thrusting keeps on reducing the velocity all the time. The end result is that, while the microsatellites have larger angular velocities and are thus angularly spread out to a greater extent, the radial (with respect to the Sun) separations are much smaller and the overall effect at a later time is a smaller figure-of-merit. This ties in with the trends in Figure 6-14 where, in general, retrograde SPT thrusting has a faster rate of increase of η_{const} initially but a smaller value towards the end of the mission.

The effect of prograde C_3 is to initially increase the distance from the Sun since the initial heliocentric velocity of the carrier spacecraft is greater than Earth's and the semimajor axis increases. Prograde SPT thrusting will keep on increasing the range from the Sun but this also means that the angular velocities decrease. The maximal performance seems to be achieved by a combination of the actions that cause an increase in radial distance and angular separation, as exemplified by the (retrograde C_3, prograde SPT thrusting) and (prograde C_3, retrograde SPT thrusting) cases. (prograde C_3, retrograde SPT thrusting) also places one intermediate microsatellite near Earth.

Note also that prograde and retrograde C_3 cases depend on the magnitude of the C_3, with degeneration when C_3 is zero. The performance is hence a function of the magnitude as well. Figure 6-15 presents the η_{const} time histories for C_3 values of 0,1,2 km^2/sec^2, with C_3 adding onto Earth's orbital velocity (prograde C_3).

There is a large difference between the C_3=0 case and all others, as shown by the time histories as well as time-averaged values of figure-of-merit tabulated in Table 6-2.

There is a relatively smaller increase in performance when the C_3=2 km^2/sec^2. The general observation is that while performance increases with C_3, the relative improvements become less and less as C_3 increases. Hence, it might be be more effective to design for a lower C_3, which gives more mass from the launcher. The extra mass could be used to

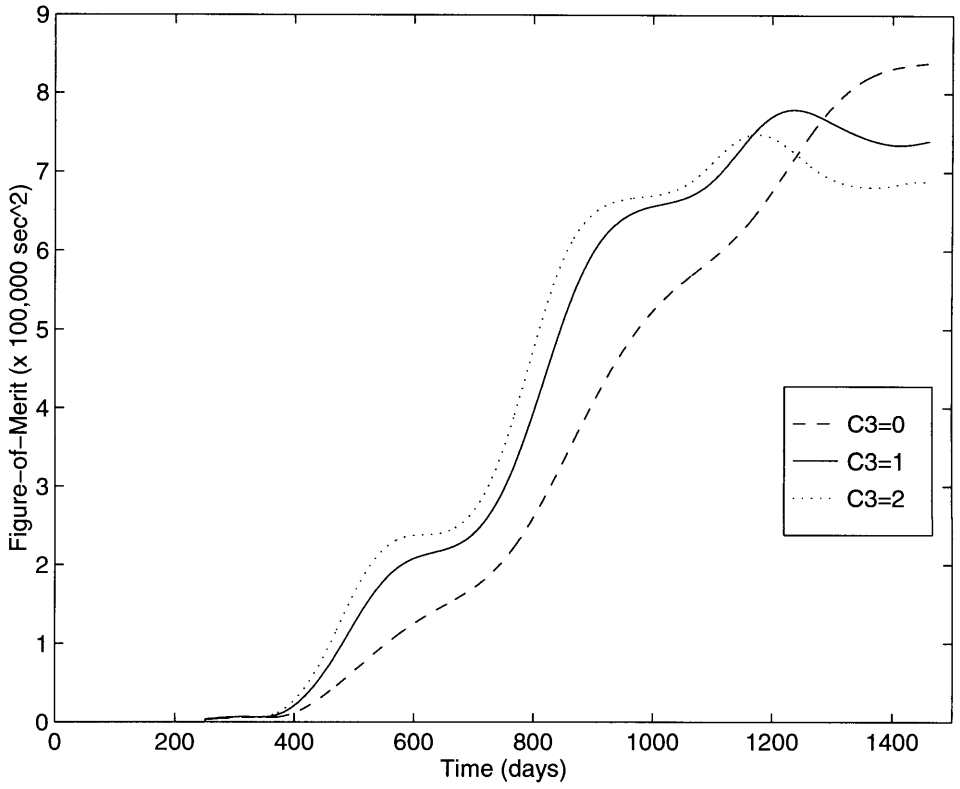

Figure 6-15: Effect of Magnitude of Launch Energy

increase the area of the GRB detectors since they also contribute to the system figure-of-merit, of which η_{const} is one component. The case of C_3=0 is interesting and worth investigating further because it represents the "boundary" between two different effects.

Table 6-2: Effect of C_3 on Constellation Figure-of-Merit

Case #	C_3 (km^2/sec^2)	Time-Averaged Figure-of-Merit (x 100,000 sec^2)
1	0	3.7586
2	1	4.3721
3	2	4.4667

The effect of SPT thrusting direction on the constellation figure-of-merit is illustrated in Figure 6-16 which plots the time histories of η_{const} for C_3=0..

As mentioned before, retrograde thrusting initially provides a higher angular rate and hence figure-of-merit, but then has lower values towards the end of the mission due to the relatively smaller radial distances from the Sun. The opposite applies for prograde thrusting. The time-averaged figure-of-merit for the prograde and retrograde options is

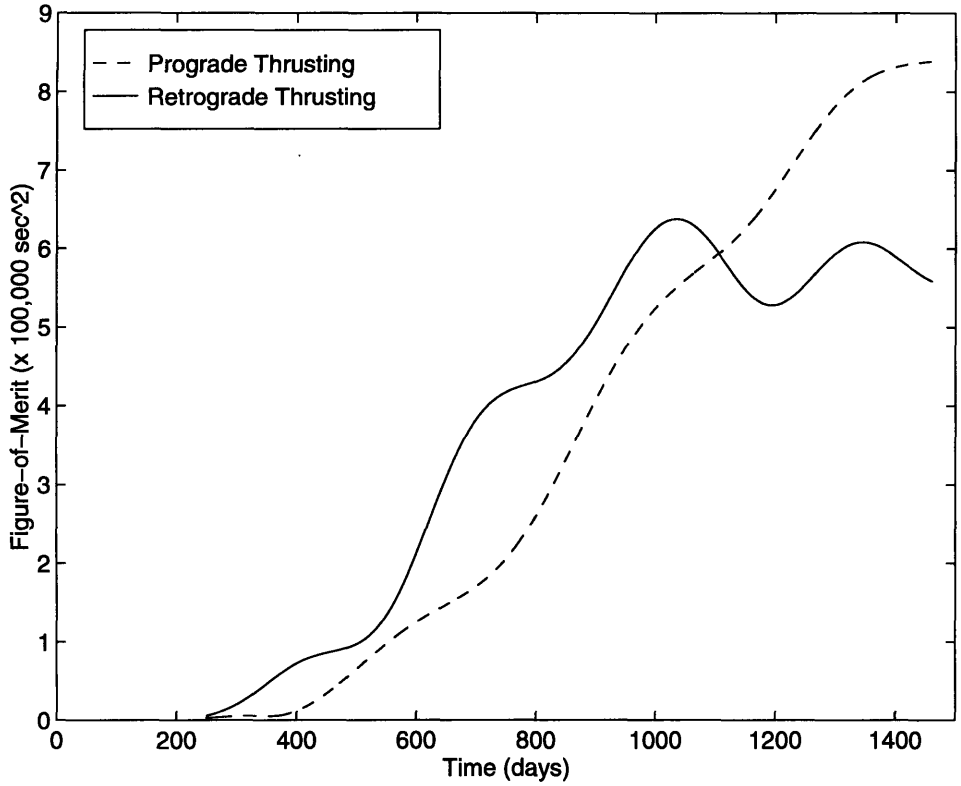

Figure 6-16: Effect of SPT thrusting Direction for C_3=0

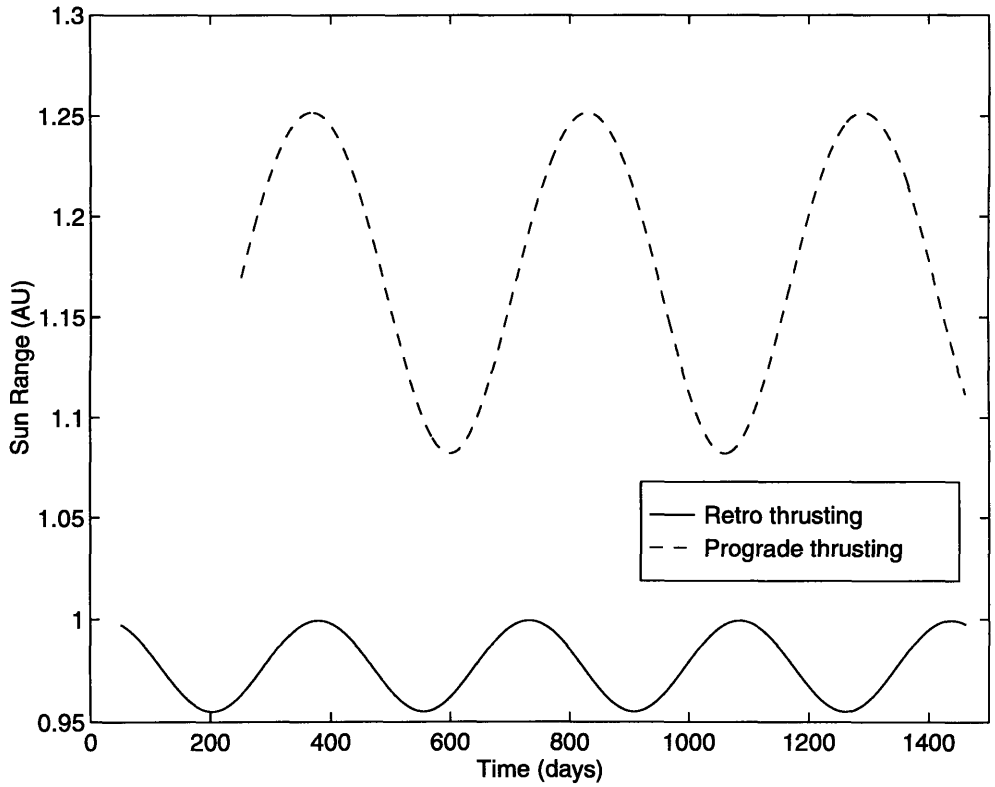

Figure 6-17: Effect of SPT thrusting Direction on maximum Sun range for C_3=0

3.7586×10^5 sec^2 and 3.9013×10^5 sec^2 respectively, indicating that the retrograde thrusting strategy offers better performance. Apart from performance, the impact of these alternatives on spacecraft design needs also to be addressed.
Spacecraft design is affected in many ways by the thrusting strategy adopted. Some of these are related to the range of the spacecraft from the Sun and Earth. Solar array sizing and thermal control are dependent on the distance from the Sun. Communication link design is affected by the range to Earth and a preliminary link analysis is presented in the next chapter. It is worthwhile here to do a top level analysis of the impact of the thrusting strategy on solar array sizing, which is a function of the range from the Sun. This will serve to demonstrate that constellation design is integrated with the design of the rest of the system and that it is necessary to have an appreciation of all the system elements that can be affected.

Figure 6-17 presents the range to the Sun for the furthest microsatellites for the prograde and retrograde SPT thrusting for C_3=0. The furthest microsatellite for the prograde thrusting case is the sixth and final one. Discounting the first one, the second microsatellite is furthest for the retrograde thrusting case. Prograde SPT thrusting has an effect on the semimajor axis of the orbit and this is evident from the plot of the Sun range of the sixth microsatellite. The maximum range is about 1.25 AU. In comparison, retrograde SPT thrusting results in the furthest spacecraft having an aphelion of about 1 AU. The solar power available per unit area is inversely proportional to the square of the range from the Sun. For a given electrical power requirement, the solar array area is thus directly proportinal to the square of the range to the Sun. As a result, the prograde option would require the microsatellites to have solar arrays that are 56% larger than those required for the retrograde alternative. This is further accentuated by the fact that all the microspacecraft will have a common design. When solar array degradation effects are taken into account, the retrograde option is even more attractive since the degree of oversizing required is smaller than for the prograde option, as degradation losses can be compensated for by the increase in power generation due to closer proximity to the Sun. The impact on cost is significant and it is evident that the retrograde option will have advantages in the context of spacecraft design while also providing comparable, if not better, performance with respect to prograde SPT thrusting for low values of C_3.

To summarize, preliminary analysis indicates that the strategy that should be adopted for ETA is to use the minimum possible prograde C_3 to maximize available spacecraft mass while providing sufficient η_{const}. Thrusting of the SPT-70 should be in a retrograde direction to facilitate spacecraft design and reduce costs.

6.3.5 Thrusting Time

So far, the simplifying assumption, regarding distribution of the total available thrusting time, has been to equally distribute the time between each microsatellite deployment. It is obvious that this does not result in a symmetric angular distribution of the microsatellites as shown for the trade baseline case, in Figure 6-18.

The angular separation between adjacent spacecraft increases with the maximum separa-

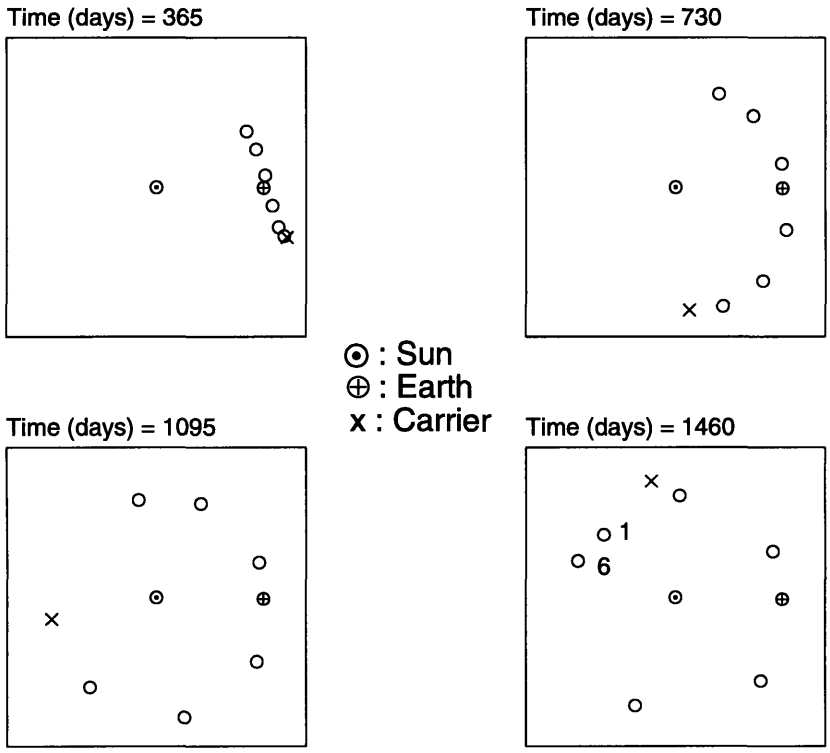

Figure 6-18: Constellation Development for Trade Baseline Scenario

tion between the 5th and 6th microsatellites. This is to be expected since the SPT-70 accelerates increasingly smaller masses for the same thrusting periods. The accelerations are smaller for the heavier masses earlier in the deployment period and as a result, the ΔV imparted to the earlier microspacecraft is less compared to later microsatellites. The increase in ΔV between subsequent microsatellites results in increasing angular separations, as predicted by the approximate equation derived to quantify constellation dynamics, in Chapter 4 (Eqn (4-7)).

One advantage of having a constellation in which the microsatellites are uniformly spread in azimuth is that mission control can maintain regular contact with the spacecraft. Outages due to communication noise from the presence of the Sun in the background would occur at regular intervals. This has the obvious advantage of facilitating the scheduling of mission operations. More importantly, a uniformly spread constellation ensures that no more than one spacecraft is unavailable due to an outage, as might be the case if microsatellites are angularly close to each other. This is illustrated in Figure 6-18, where chances are that both the 1st and 6th microsatellites, in the fourth year, may be simultaneously unavailable at some time or other.

A uniformly spread constellation can be achieved by adjusting or "tailoring" the deployment times such that the ΔV between adjacent spacecraft is more or less equal. Figure 6-19 displays the constellation distribution over the mission lifetime for such a case. The angular separation between adjacent microsatellites is approximately equal and the closest

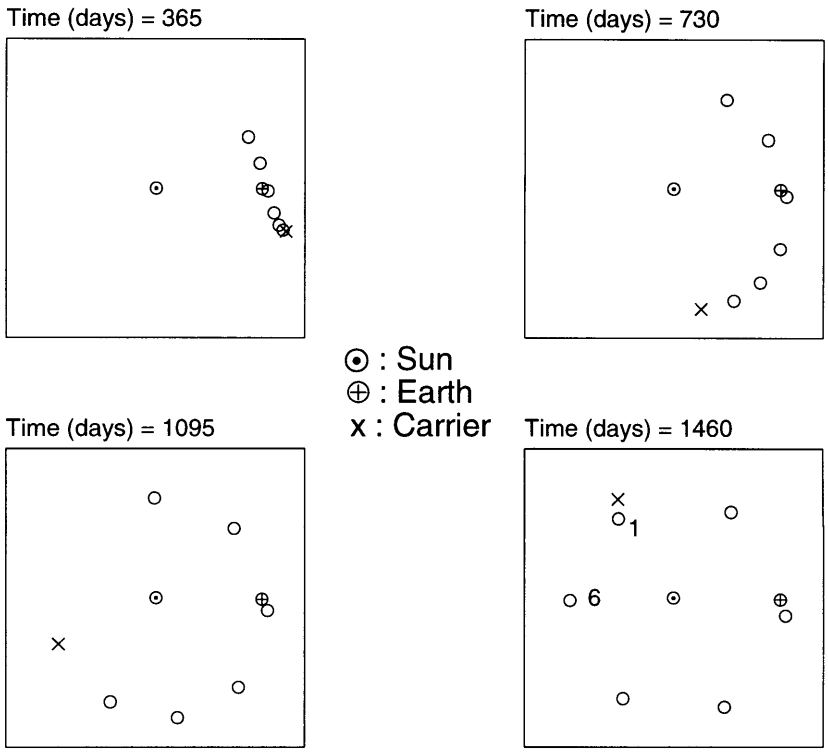

Figure 6-19: Constellation Development for "Tailored" Deployment Time Scenario

microsatellite to Earth is, for this case, closer to the Earth than the trigger satellite for the baseline case. The deployment times are presented for comparison in Table 6-3.

Table 6-3: Deployment Times for "Tailored" Constellation Deployment

SCENARIO	MICROSATELLITE DEPLOYMENT TIME (DAYS)					
	Microsatellite Order					
	1	2	3	4	5	6
Baseline	0	50	100	150	200	250
"Tailored"	15	80	130	175	215	250

The thrusting times between subsequent microspacecraft deployments are shorter. Since more time is being spent accelerating larger masses at the beginning of the deployment phase, the net ΔV would be expected to be less and as a consequence, the "spread" of the constellation, as quantified by η_{const}, would be lower. This is confirmed in Figure 6-20 which plots the η_{const} time histories for the trade baseline and tailored cases. The slight degradation in performance may be justified if a uniformly spread constellation is advan-

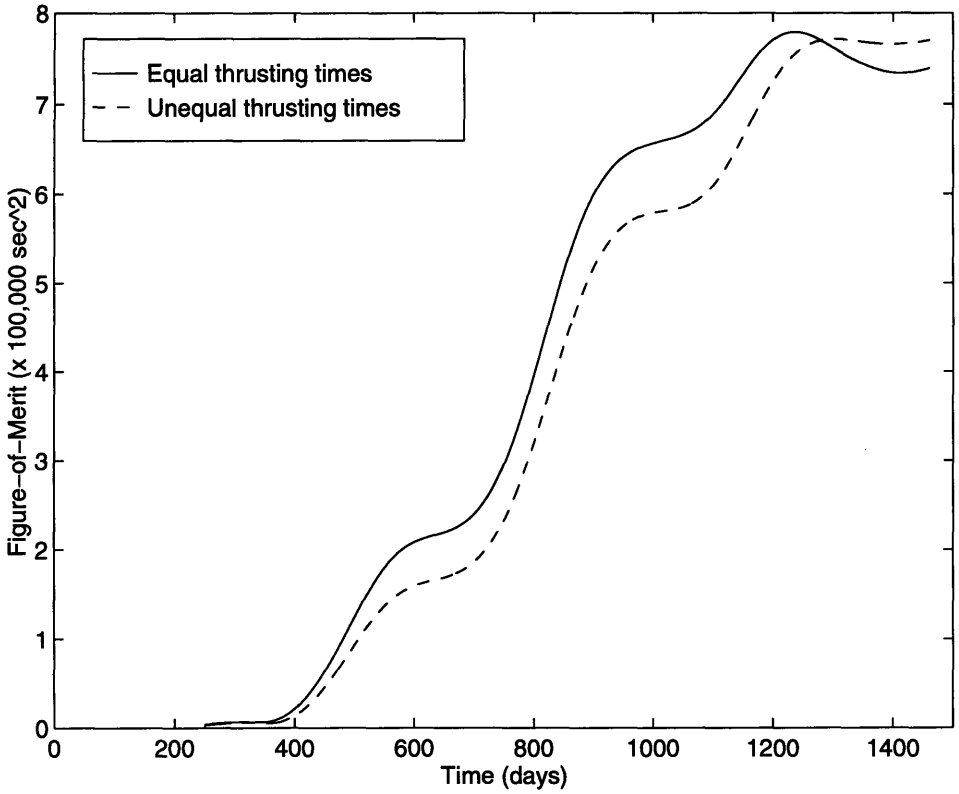

Figure 6-20: Impact of "Tailoring" Deployment Times on Figure-of-Merit

tageous with regard to other aspects such as microsatellite availability.

An important issue that has not been discussed in detail so far has been the utility of the carrier spacecraft after the constellation deployment phase. It is almost certain that the SPT-70 units will provide extra thrusting time after the deployment. Provided that there is enough propellant onboard, the carrier could continue thrusting to continue going closer towards the Sun (for retrograde SPT thrusting). Not only could a secondary scientific mission be carried out, but the thrusting would also provide data on long term operation of the SPT-70, something that would be of immense interest to the Electric Propulsion community. This issue needs to be addressed in more detail during later stages of system development.

Another aspect that has not been addressed here, but is of vital importance, is the development of alternate thrusting strategies. These would include fallback strategies in the event of SPT-70 failure or strategies that would take advantage if the thrusters perform better than expected in terms of lifetime. The trade between using the extra thrusting time for constellation deployment involves considering trading off the obvious increase in performance against the mass penalty of extra propellant and, perhaps more importantly, the extra mission operations costs that would be incurred over that extra thrusting period. The mission schedule is also affected significantly, especially in the context of funding profiles. Fallback strategies for scenarios where one SPT-70 fails need to be developed to provide at least the minimum constellation spread.

6.3.6 Summary

The trends and results of the various trade studies discussed in this section are summarized below.

- **Number of Microsatellites in Constellation**
  Increasing the number of microspacecraft improves the constellation figure-of-merit. A 4 microsatellite constellation does not provide redundancy and the microsatellite mass for an 8 spacecraft constellation is difficult to achieve. A 4 microsatellite constellation provides better performance over the first 2 years and can be used for a minimum science mission. The current ETA baseline is a 6 spacecraft constellation with the intention of adding a seventh spacecraft if the system mass is lower than current estimates.

- **Number of SPT-70 thrusters**
  A single SPT-70 provides neither the performance nor the redundancy to warrant application. The availability of two thrusters allows parallel or serial operation. Parallel operation doubles the nominal thrust while serial operation doubles the available thrusting time to 6,000 hrs, based on the assumed time of 3,000 hrs per thruster. Even though parallel operation provides better performance, its application is not justified since the extra cost of providing the extra power is not offset by the performance improvement. The ETA baseline case thus uses two SPT-70 units in serial operation, which essentially provide 6,000 hrs of thrusting time.

- **Magnitude and Direction of C_3**
  The direction of C_3 is important depending on the magnitude, with the difference minimal for small C_3's. A prograde C_3 results in an initial increase in radial distance from the Sun and vice versa. The constellation figure-of-merit improves with increasing C_3, with improvements getting smaller as C_3 increases. The goal should be to maximize available launch mass by minimizing the C_3 as much as possible. The slight degradation in performance can be compensated for by the appropriate SPT thrusting direction. Current ETA planning is for a C_3 close to zero.

- **SPT-70 Thrusting Direction**
  SPT thrusting direction has wide-ranging implications on the system. Prograde thrusting increases velocity and hence the energy and radial distances for the orbit and vice versa for retrograde thrusting. Retrograde thrusting leads to increased angular velocities which result in a faster "spreading" rate, even though the figure-of-merit in the later stages is not so good. Another important consideration is the impact on spacecraft design aspects such as power and thermal control. The closer

proximity to the Sun provided by retrograde thrusting can result in solar arrays which are upto 35% smaller than those required for prograde thrusting. Retrograde thrusting has been selected for the ETA baseline mission for these reasons.

- **Thrusting Time**
  The trade baseline assumption was for equal thrusting times between deployments. This resulted in a non-uniform angular spread of the microsatellites, since the last microsatellites acquired a comparatively greater ΔV due to the smaller accelerating masses. Advantages of a uniform angular spread include improved microsatellite availability and ease of mission operation scheduling. A uniform spread can be achieved by "tailoring" the deployment times such that more thrusting time is available for the intial phases when the carrier spacecraft is heavier. The goal is to provide the same ΔV between adjacent spacecraft deployments. However, the net ΔV in this case is lower compared to equal thrusting times and the overall constellation spread is slightly less. The need for a uniform spread is deemed to outweigh the slight degradation in constellation figure-of-merit and the current ETA mission scenario thus incorporates a "tailored" deployment strategy.

6.4 Sensitivity Analysis

The trade studies discussed in the previous section were based on current estimates of the carrier spacecraft and microsatellite masses. However, it is inevitable that these masses are bound to change for a number of reasons. The design would grow and as it becomes more refined, the mass may be found to be different from, what are after all, the approximations used for the trade studies. Moreover, carrier mass would change depending on the post-deployment phase selected. If a secondary science mission is planned, then another scientific payload has to be incorporated, of course within the launch vehicle constraints. Or if the post deployment phase is to be dedicated for Electric Propulsion experiments, there would be additional propellant and instrumentation. The microspacecraft mass could change as well, primarily due to design growth.

To incorporate these possible changes and others into the trade analysis carried out before, it is necessary to perform a sensitivity analysis with respect to these design parameters. This section deals with two of the more important parameters, namely carrier spacecraft and microsatellite mass. The impact of variations in these parameters on the constellation figure-of-merit is analyzed. The following general assumptions apply for both sensitivity analyses:

- 6 microsatellite constellation
- equal thrusting times between deployments
- C_3=0
- retrograde SPT-70 thrusting

Other assumptions are stated where applicable. Even though the carrier and microsatellite masses are related through the launch vehicle mass limit, an attempt has been made to invoke such assumptions that the effects of each on the constellation figure-of-merit are separated. This is possible within a certain range, as shall be demonstrated hereafter.

6.4.1 Carrier Mass

The number and mass of microsatellites were assumed to be 6 and 50 kg respectively. The carrier spacecraft wet mass was varied from 220 kg to 270 kg. The maximum limit was set by the throw weight of ~570 kg of the DeltaLite to a C_3 of zero. In the event that total mass was less 570 kg, it was assumed that the spacecraft would nevertheless be given a C_3 of zero. This was neccessary in order to avoid the introduction of the effect of C_3 into the sensitivity analysis. Figure 6-21 plots the variation of constellation figure-of-merit time histories for carrier masses in the range 220-270 kg.

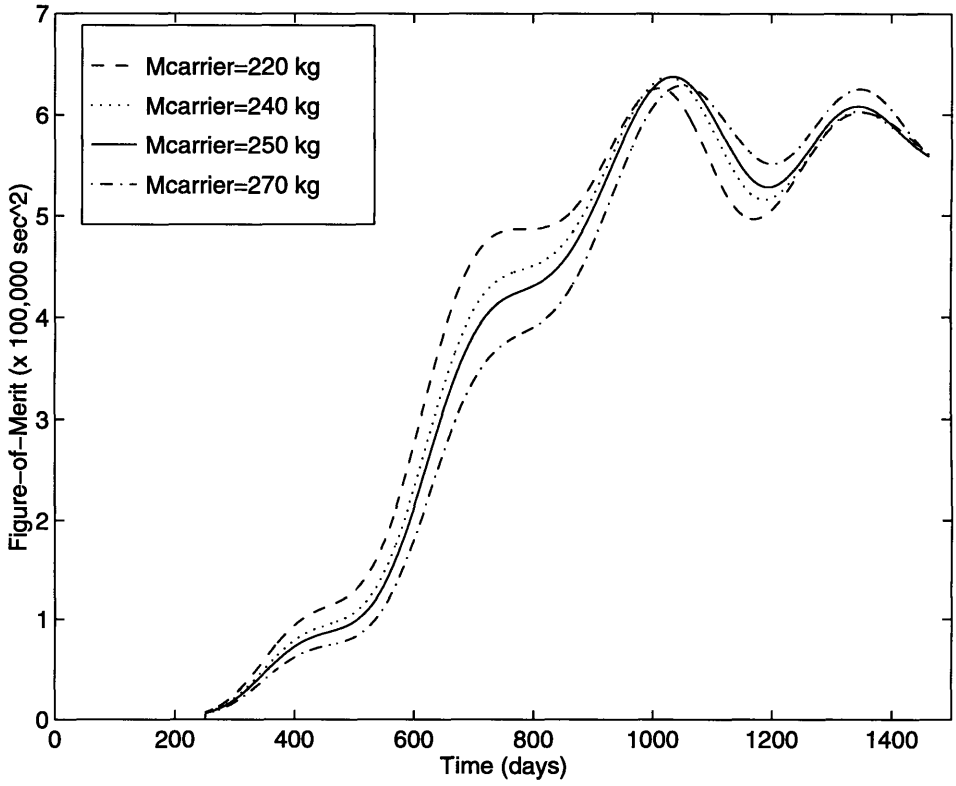

Figure 6-21: Sensitivity to Carrier Spacecraft Mass

The performance of the baseline mass of 250 kg is plotted as a solid line for comparison. As might be expected, a lower carrier mass provides better performance in terms of the spread of the constellation since the smaller accelerated mass results in a larger net ΔV. There is not a significant degradation in performance over the wide range of 50 kg for the carrier mass. Figure 6-22 compares the time-averaged value of constellation figure-of-merit for this range of carrier masses.

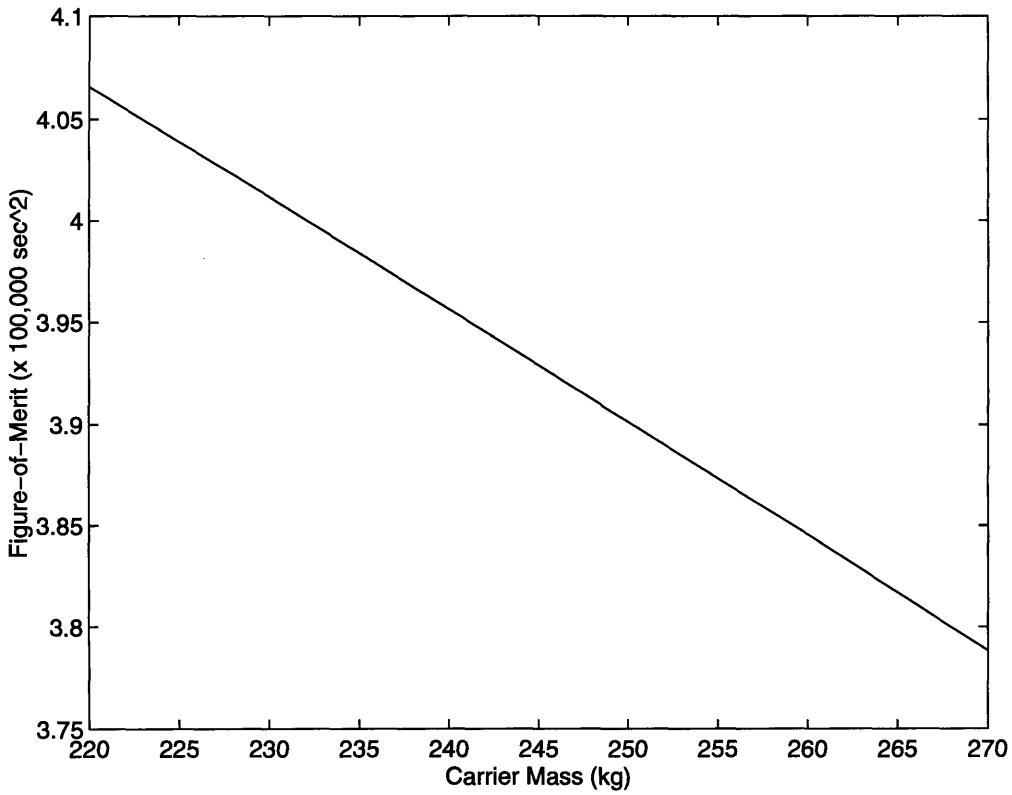

Figure 6-22: Average Figure-of-Merit as a function of Carrier Spacecraft Mass

The average figure-of-merit decreases linearly with increase in carrier mass over the range being considered. The slope is -556 sec^2/kg. Thus the constellation's capability to support GRB astrometry is not substantially affected by variations in carrier spacecraft mass.

The baseline assumption of 250 kg for the carrier spacecraft wet mass is conservative since the current estimates of carrier mass are towards the lower end of the range under consideration here [4]. Some of the reasons which may lead to variations in carrier mass are

- increase in mass as design gets more refined and hardware masses are more accurately known.
- decrease in mass brought about by innovative lightweight technology that has not been under consideration currently.
- increase in mass due to a larger Xenon propellant load for extra thrusting, either for the deployment or post-deployment phases of the mission.
- increase in mass with the incorporation of secondary payload for post-deployment phase. This could be a scientific payload or additional propulsion hardware for Electric Propulsion experiments.

Preliminary analysis shows that the ability of the constellation, as quantified by the figure-of-merit, to support scientific operations is not strongly dependent on the wet mass of the carrier spacecraft. A slight performance degradation occurs with increasing carrier mass.

6.4.2 Microsatellite Mass

The underlying assumption for this analysis was to assume that the wet mass of the carrier, excluding microsatellite stack, is constant at 250 kg. The only exceptions occur when carrier mass may have to be decreased in order to remain within the 570 kg limit imposed by the DeltaLite launch vehicle. These exceptions are noted where applicable. The baseline mass assumed so far has been 50 kg and the range selected for this analysis is 40-55 kg. Note that the total microspacecraft mass for a unit mas of 55 kg is 330 kg, leaving 240 kg for the carrier spacecraft. This deviation from the carrier mass of 250 kg will undoubtedlly distort the results slightly. Hence this datapoint should be considered with that fact in mind. The performance of the constellation for the assumed range of microsatellite masses is presented in Figure 6-23. The case of the baseline mass of 50 kg is plotted as a solid line.

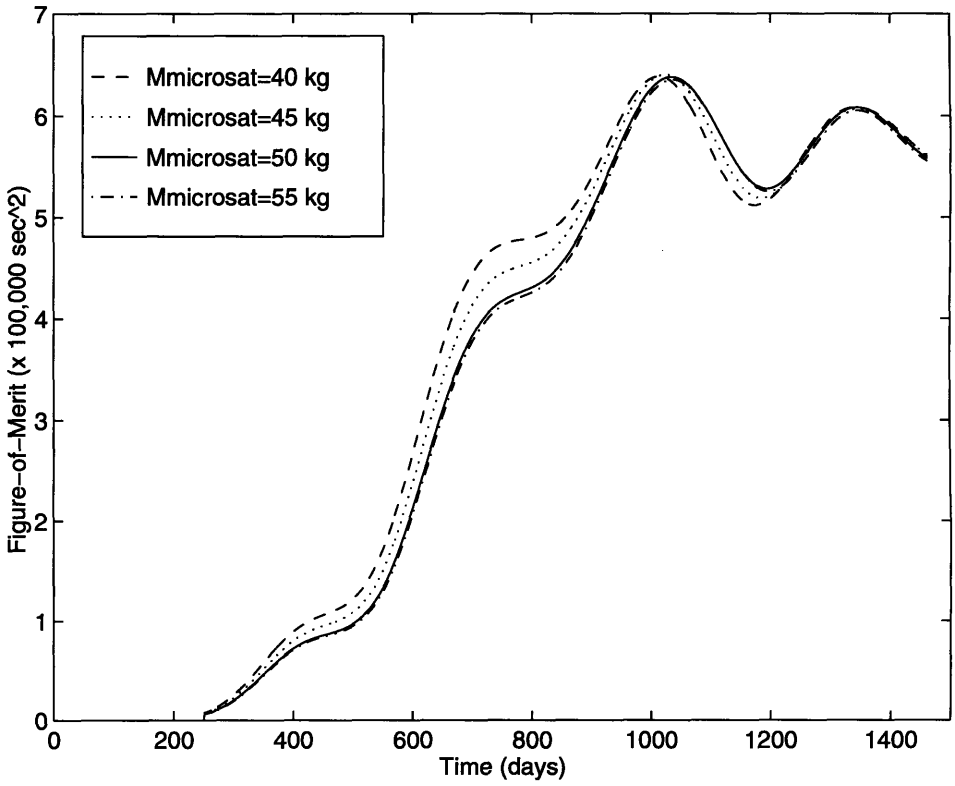

Figure 6-23: Sensitivity to Microsatellite Mass

A smaller mass provides better performance since the net ΔV acquired is greater for the same thrusting time. As expected, the performance of the 55 kg microsatellite mass is very similar to the baseline 50 kg case. This is due to the smaller mass of the carrier spacecraft imposed by the assumptions. Figure 6-24 plots the time-averaged constellation figure-of-merit as a function of microsatellite mass.

Time-averaged constellation figure-of-merit decreases linearly with increase in microsatellite mass in the range 40-50 kg. The deviation of the 55 kg datapoint was expected. The

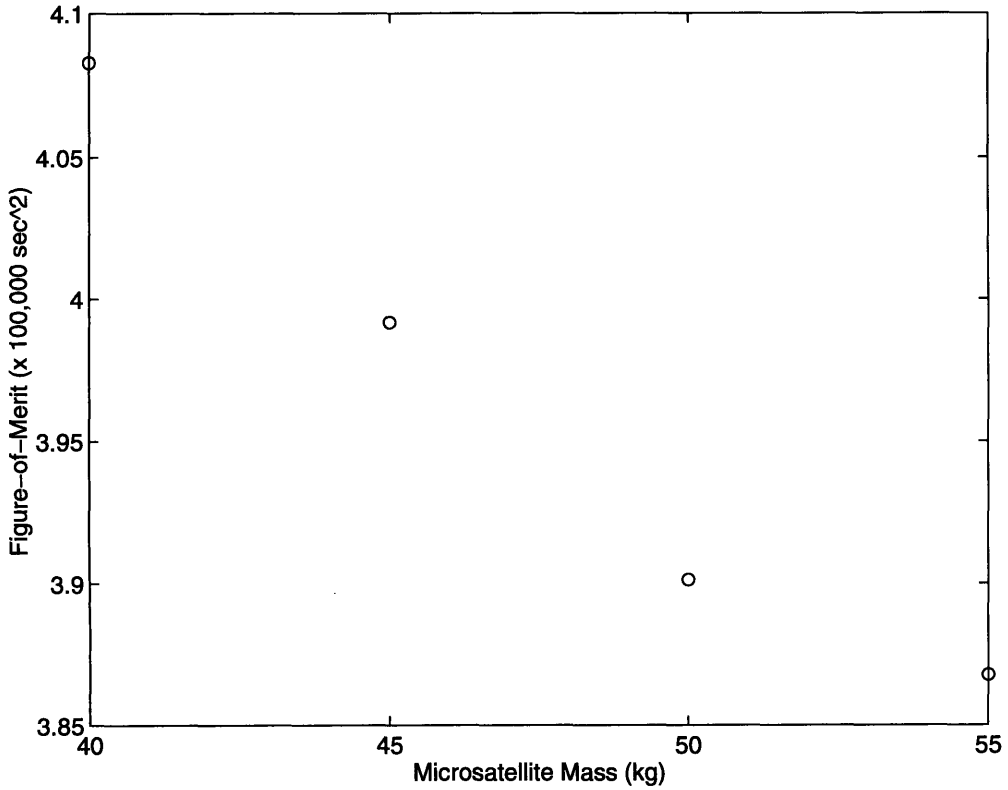

Figure 6-24: Average Figure-of-Merit as a Function of Microsatellite Mass

slope of the linear region is -1820 sec^2/kg. Before comparing this value with the corresponding slope for the carrier mass, it is important to realize that every kilogram increase in microspacecraft mass results in a net increase of 6 kg for the assumed 6 microsatellite constellation.

Comparing the two slopes, the values for the carrier spacecraft and microsatellite are -560 sec^2/kg and -1820 sec^2/kg respectively, giving the indication that controlling the microspacecraft mass is of prime importance to the spacecraft designer. The constellation is relatively insensitive to variations in carrier mass.

Variations in microspacecraft mass may be attributed to

- increase in mass as design is refined and component masses are more accurately known.
- design changes in the GRB detector. About 50% of the current microspacecraft design mass is allocated to the GRB detectors.
- increased propellant load for attitude control. The microspacecraft has a cold gas system for attitude control. Details are presented in the next chapter.
- reduction in mass brought about by incorporation of innovative lightweight technology that is not under consideration currently.

Summarizing the sensitivity analysis, it is found that constellation figure-of-merit is more sensitive to microsatellite mass and the need for controlling this critical design parameter cannot be overemphasized both from performance and cost standpoints.

6.5 Trigger Satellite Orbit Analysis

This section presents a brief treatment of the design of a trigger satellite orbit which is as close to the Earth as possible. While such an analysis requires a high accuracy model to account for moon perturbations and so forth, time constraints did not permit the development of such a model. Instead, a simplified Hill model was developed to assess the feasibility of these near-Earth orbits.

After introducing the problem, the motivation for the need to have a trigger satellite is elaborated upon and preliminary communications link performance estimates are presented in order to gain an understanding of range requirements. Having identified these, the possible orbits that can provide such ranges are identified. The Hill frame model is briefly introduced before presenting the trigger satellite orbits that are currently baselined.

6.5.1 Introduction

The analysis presented so far did not address in detail the requirement to have a "trigger" satellite in the vicinity of the Earth to provide the real-time alert capability for the ETA system. There are a number of reasons for this approach. First, the primary goal of the analysis in the previous section was to acquire a better understanding of the dynamics of the constellation and the impact of various system parameters on scientific operations and system design. In essence, the objective was to develop a "feel" for the system and come up with a baseline which would form the basis for more detailed analysis and design. Secondly, the requirement for the trigger satellite was not clearly defined at that stage of the analysis. Hence, the requirement on maximum distance of the trigger satellite from the Earth ranged up to 0.1 AU and the analysis was performed on that basis.

However, as the system requirements, especially the scientific ones, were better understood, it became clear that the trigger satellite would need to be closer to the Earth than previously thought. Ranges of as low as 0.01 AU were suggested to support the high rate links. This necessitated a deeper analysis to assess the feasibility of such orbits and their stability over the mission lifetime. Even though a preliminary analysis was performed, time constraints did not allow a detailed analysis of this very interesting problem. It is important to note, however, that the results of analysis in the previous section are still applicable since the impact of the more stringent Earth range requirement on the constellation figure-of-merit is minimal. This is because the relative change in the location of the trigger satellite is negligibly small compared to the interplanetary separations of the other microspacecraft.

The requirement for close proximity to Earth implies that the long term stability of the orbits under consideration is a major issue. In this regard, the analysis would ideally require accurate modelling of perturbation sources such as Jupiter, the Moon and so forth.

It was not possible to develop such a model within the timeframe of this thesis project but a simplified model was developed, primarily to see if it is feasible to have the trigger satellite within 0.01-0.05 AU over the four year mission.

This section summarizes the work done to date on the orbits of the trigger satellite. But before going into the analysis itself, it is instructive to comprehend the motivation behind this requirement. Moreover, it is crucial to have a good understanding of the requirement. If the requirement is found to be difficult to satisfy, it should be "pushed back" upon the source, especially if it could potentially drive the mission and system design.

6.5.2 Motivation

Real-time alert capability is an important attribute of the ETA system. To enable this, there is a requirement on the constellation to have at least one microspacecraft in close proximity of Earth. The function of this microsatellite is to downlink in real-time, the profile of the GRB that has been detected. This informs the mission operation center (MOC) of the occurence of a GRB. The MOC prepares a template for uplinking to the rest of the microsatellites for deriving the times-of-arrival via onboard template matching. The key here is to uplink the template rapidly and receive the times-of-arrival from the microsatellites as soon as possible, so that coarse GRB coordinates can be derived and relayed to observatories for follow-on observations.

In order to provide the real-time alert capability, there is a need for the trigger satellite to have a high rate downlink. The GRB profile has to be downlinked in the minimum time, implying a high datarate. The relationship between the distance from the Earth and datarate is given by considering the standard communications link equation [67,68]. The details of the link analysis are not presented here for the sake of conciseness; Appendix A provides a brief introduction to communications link analysis. The next chapter also goes into more detail with regard to the link design. Suffice it to say here, that assuming that all other communication parameters are assumed constant, the datarate is a function primarily of

- **Microsatellite Transmitter Power and Antenna Gain**
  The datarate is directly proportional to transmitter RF power and transmitting antenna's gain. Increasing either would provide higher datarates. The spacecraft designer's goal is to have a standard design for both trigger satellites and the other microsatellites, in order to simplify design and reduce development costs. In that context, it is unwise to provide more power to the trigger satellite or increase its antenna gain, unless all other microsatellites are to be overdesigned. This is so because the other microsatellites do not require that much power or gain to accomplish their communication requirements. Hence, the high rate link for the trigger satellite cannot be provided for by changing these parameters.

- **Gain and Noise temperature of receiving system**

A high gain and low noise temperature are ideal and efforts should be made to increase the (G/T) of the receiving system. This is actually being planned for the MIT Haystack Antenna facility which will serve as the primary receiving facility for the ETA system. A low noise amplifier (LNA) with a lower noise temperature is planned for installation for the ETA mission [69]. But this still does not provide the necessary datarates.

- **Range from Earth**
  Datarate is inversely proportional to the square of the distance of the spacecraft from the Earth. Given the constraint that the trigger satellite cannot be designed to provide more power or gain, reducing the range seems to be the only alternative. This can be brought about by placing the trigger satellite in an appropriate "near-Earth" orbit. Mission design incorporating such an orbit would create the minimal effect on the rest of the system. This was the approach adopted to satisfy the trigger satellite requirement.

There is a requirement on the microsatellites to support a link of 10 bits/sec at a range of 2AU. The variation of datarate as a function of range can be estimated assuming that the microspacecraft design remains the same and other communication parameters remain constant. Figure 6-25 plots the first order variation, assuming that a rate of 10 bits/sec is required at 2 AU.

Depending on how much data is within a single GRB profile, the required datarate can be estimated, based on the maximum time delay allowed for GRB coordinate relay to observatories. The datarate is also set by the time delay associated with signal processing and signal travel time. Therefore, a trigger satellite which is "far" away will not only have a lower datarate but also a longer signal travel time, resulting ultimately in a longer delay on both counts. The trigger satellite should thus be as close to Earth as possible, but not too close as to be captured back by Earth. Noting that there is a system requirement for 100% temporal coverage, it is necesary to avoid having the trigger satellite very close to Earth (like LEO) since the satellite is not visible all the time. Furthermore, the very high datarates available at smaller ranges may not be required. LEO or GEO orbits would also necessitate separate launches, adding substantially to system cost. A compromise on the range from Earth has thus got to be arrived at.

The communications link can support about 10 kilobits/sec at about 0.06 AU and 100 kilobits/sec at 0.02 AU. The datarate requirement will not exceed 100 kilobits/sec. The maximum range seems to be 0.06 AU but the design goal should be to minimize the range as much as possible.

The other issue associated with these orbits is their long term stability. Because the trigger satellite will probably have a very small propulsive capability for stationkeeping, the selected orbit should require no stationkeeping over the mission lifetime, if possible. Stationkeeping requirements might require spacecraft redesign and this has to be avoided.

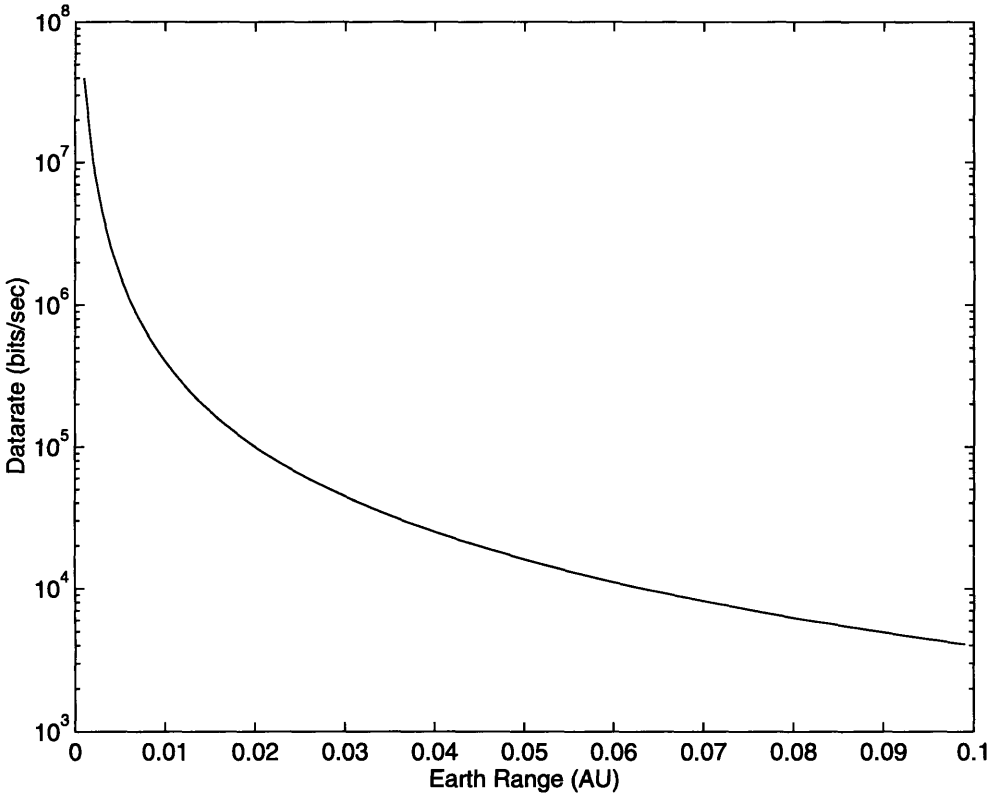

Figure 6-25: Trigger satellite datarate as a function of range to Earth

The question then arises as to whether there are any classes of near-Earth orbits which could provide high datarates and be stable over the mission lifetime so as not to require stationkeeping.

6.5.3 Orbit Options

There exist a number of orbit options which can provide the ranges mentioned in the previous section. The applicability of these orbits to the ETA mission needs to be addressed. Some of the major orbit alternatives are:

- **Low/Medium Earth orbits**
  These standard orbits are an obvious choice, especially since they can provide very high datarates and can be designed to have minimal stationkeeping over the mission lifetime. There is, however, the disadvantage that these orbits are not generally optimal from the scientific perspective. There are issues of interference as well as ground station contact. Moreover, the launch strategy would be complicated since the DeltaLite will not be able to place the trigger satellite in this orbit and also boost the rest of the stack to Earth escape. This option was not considered optimal for ETA.

- **Geostationary-type orbits (GEO)**

These orbits do not have the problems of ground station contact but the launch issue is complicated even more. It may have been possible to boost the entire stack to GEO, deploy the trigger satellite and then reboost the rest of the launch stack to escape. Apart from being inefficient, this strategy is not possible with the DeltaLite since it has the Star 37 solid motor as the upper stage and is hence not restartable.

- **Earth/Moon system orbits**
  This is an interesting option which employs lunar flybys to minimize C_3 and place the trigger satellite in an orbit within the Earth moon system. A mission scenario for ETA has been suggested [70] which could not only satisfy the trigger satellite orbit requirements, but also result in a better constellation distribution. The only disadvantage of this scenario is the need to correct for launch injection errors and the targeting and guidance required for the flybys.

- **Lissajous orbits**
  These are orbits **about** the libration points of the Earth/moon, or in this case, the Sun/Earth system. A Lissajous orbit is a quasi-periodic orbit that can exist near any of the collinear libration points, namely L_1 (between Earth and Sun) and L_2 (outside Earth and Sun). These orbits have been suggested for a number of missions [71], but their applicability to ETA is currently limited by stationkeeping requirements.

  The Lissajous orbit is unstable and even though the orbit inserion ΔV is almost zero [71], there is a ΔV requirement for stationkeeping. Unfortunately, the current design of the ETA microsatellite does not have the capability to provide this ΔV over the mission lifetime. The stationkeeping requirement for the SIRTF mission [71] has been estimated at under 6 m/s per year. Because of the close proximity of the Sun in the microsatellite's background, communications might be expected to degrade due to solar radio noise. However, previous and proposed missions using these orbits avoid this by inclining the orbit with respect to the ecliptic [71]. The out-of-plane motion allows sufficient angular separation between the Sun and microsatellite to avoid RF interference.

  At this stage, the only issue preventing the utilization of the Lissajous orbit is the stationkeeping capability of the microsatellites. Further design work should address the issue of including more propellant on the microsatellite for stationkeeping. It may turn out that the Lissajous orbit may be optimal for the ETA mission, due to its negligible orbit insertion ΔV requirement and flexibility in terms of stability since a large band of Lissajous orbits exist. Further study of this option is required.

- **Halo orbits**
  The Halo orbit is a special case of the Lissajous orbit in that it is periodic. It has been used for the ISEE-3 mission [72,73,74] previously and will also be used for the SOHO mission [75]. In comparison to the Lissajous orbit, the Halo orbit has a larger orbit insertion ΔV and larger stationkeeping costs which are about double those for the Lissajous orbit. Even though the Halo orbit is optimal for Solar observing missions and so forth, it is not as applicable to the ETA mission. Nevertheless, it would be worthwhile to explore this option with the Lissajous orbit if the constraint on the stationkeeping capability of the microsatellite is relaxed.

- **Orbits *around* L_1 & L_2 points**
  These are orbits which essentially go around the Earth but also include the L_1 or L_2 points or both within the orbit; that is, the orbit goes out as far as the L_1 or L_2 points, which are ~0.01 AU from Earth, and around them [76]. This option is currently under consideration for ETA and is discussed here. For the purposes of this thesis, such an orbit shall be termed an "Orbit Going Around a Libration point (OGAL)". The first issue to be tackled was to determine the feasibility of a stable OGAL orbit.

6.5.4 Hill Frame Analysis

It is convenient to perform the analysis for the trigger satellite orbit in an Earth-centred frame of reference, rather than the heliocentric frame used for the general simulation. In this regard, the model represented by the linearized equations of motion, called Hill's equations or Clohessy-Wiltshire equations, is approximate but appropriate for this analysis. The equations are presented below; no attempt is made to derive them. The interested reader is referred to standard astrodynamical texts [64]. The coordinate convention adopted is illustrated in Figure 6-26. The linearized equations of motion can be shown to be [64]

$$\ddot{x} = 3n^2x + 2n\dot{y} + F_x \qquad \text{Eqn (6-14)}$$

$$\ddot{y} = -2n\dot{x} + F_y \qquad \text{Eqn (6-15)}$$

$$\ddot{z} = -n^2z + F_z \qquad \text{Eqn (6-16)}$$

where (x,y,z) are the coordinates of the spacecraft in the Earth-centred frame, n is the mean motion of Earth's orbit and (F_x,F_y,F_z) are the components of any perturbation acceleration. It is assumed that Earth's heliocentric orbit is circular and serves as the orbit about

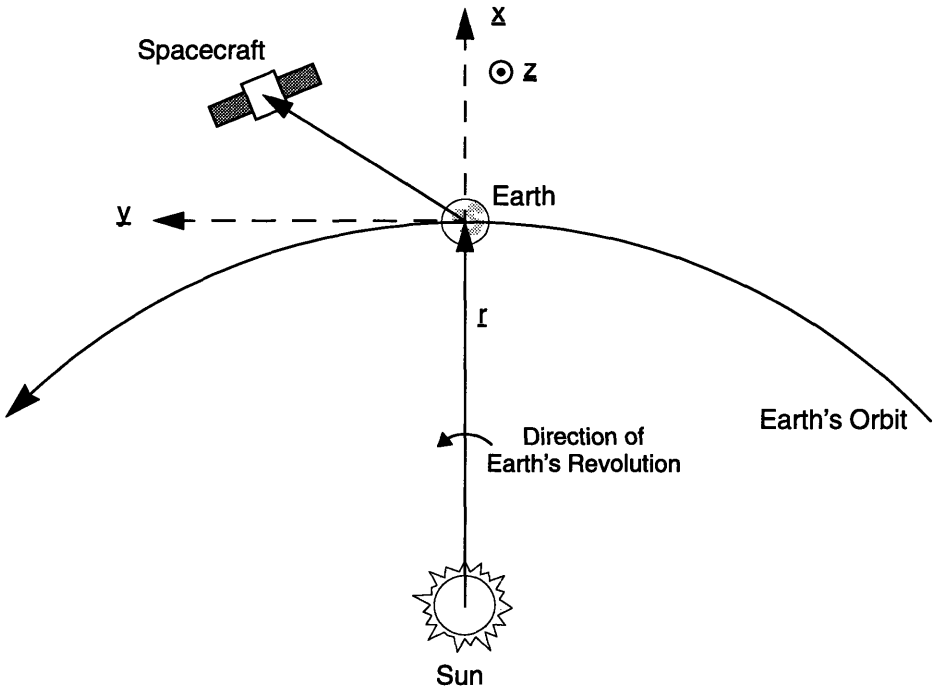

Figure 6-26: Frame of Reference for Trigger Satellite Orbit Analysis

which linearization is done.

The out-of-plane motion (z) is governed by an equation of the simple harmonic oscillator type and this motion is uncoupled from the in-plane (x-y) motion. The x-y motion is coupled and the system is somewhat akin to gyroscopic damping, where the acceleration in one coordinate is dependent on the velocity in the other coordinate. Since the constellation assumes that the trajectories are in the ecliptic plane, it is not necessary to consider the z-component. The gravitational attraction due to Earth was included as a perturbation term. Equations (6-14) and (6-15) were numerically integrated on SIMULINK, a tool available in MATLAB. The search for a stable orbit near the L_1 point was carried out by varying initial conditions.

Figure 6-27 illustrates typical results generated by the SIMULINK Trigger Satellite Orbit Model. It shows the trajectory traced out by a spacecraft starting off at 0.01 AU and shows its motion over the 4 year mission period. There are very many close passes by Earth, where lunar influence (Earth-moon distance is about 0.002 AU) would be strong and difficult to avoid in the long term. This plot demonstrates the difficulty of maintaining a stable orbit in this region around Earth.

6.5.5 Baseline Periodic Trigger Satellite Orbits

A baseline periodic trigger orbit was defined after simulations. It is shown plotted as a dot-

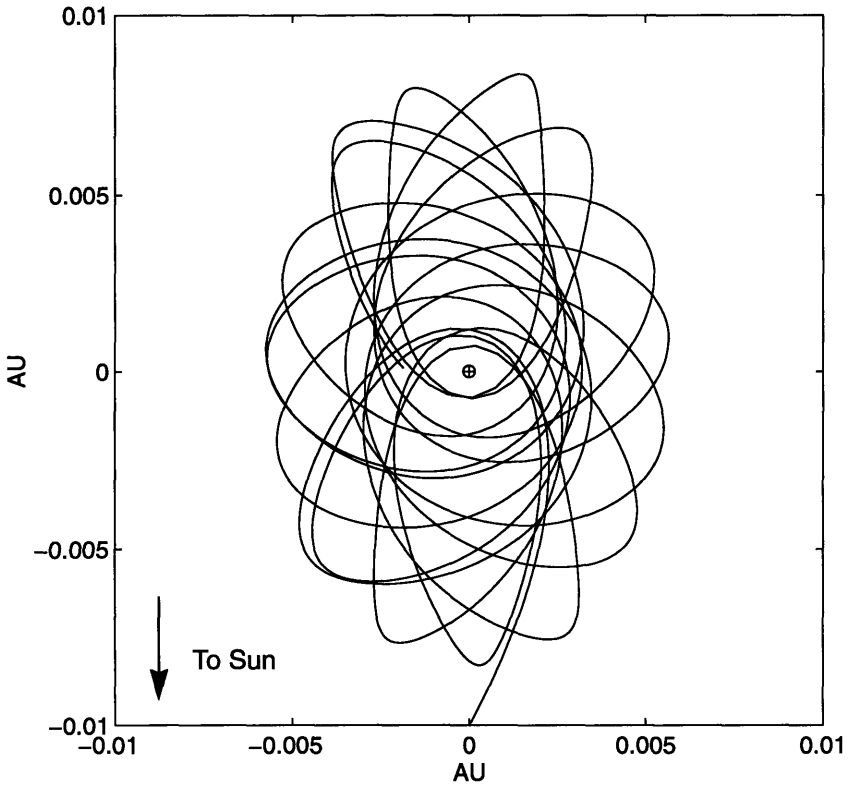

Figure 6-27: Sample Trigger Satellite Orbit Model Output

ted line in Figure 6-28. The distance to Earth is in the range 0.020-0.036 AU and hence satisfies the range constraints imposed earlier. This orbit should enable the trigger satellite to provide the high rate communications links for downlinking the GRB profiles in real-time. Similar periodic orbits can be found with any other major axis, but those whose minor axes are close to 0.01 AU are unstable to small departures from proper initial conditions. The selected baseline orbit is robust against a wide range of initial conditions.

Having decided upon the baseline trigger satellite orbit, the next issue was to determine how to get the microspacecraft into that orbit. One possible method was to provide SPT-70 thrusting for a certain period after the DeltaLite had completed its upper stage burn [76]. The trajectory of the SPT would be designed such that the insertion ΔV into the trigger satellite orbit would be very small.

It was felt that the rapid alert capability of the ETA was a critical element of the system and there was a need for redundancy in that function. Program management decided to effect this by including two trigger satellites. The constellation was redesigned around this requirement. Figure 6-29 presents the launch trajectory and SPT-70 thrusting strategy developed to date.The baseline mission scenario is summarized in the next section.

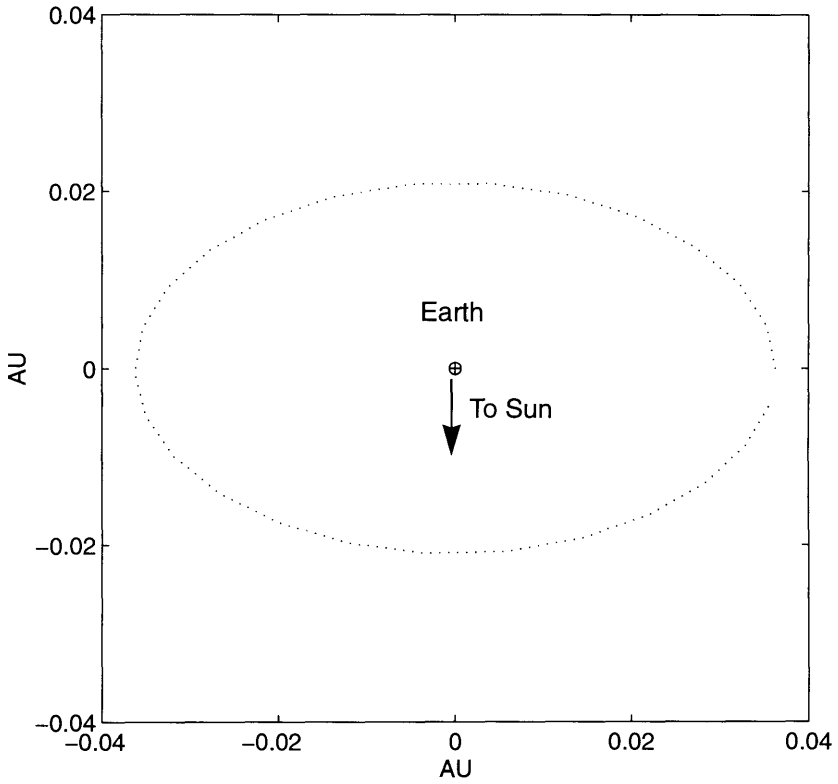

Figure 6-28: Baseline Trigger Satellite Orbit

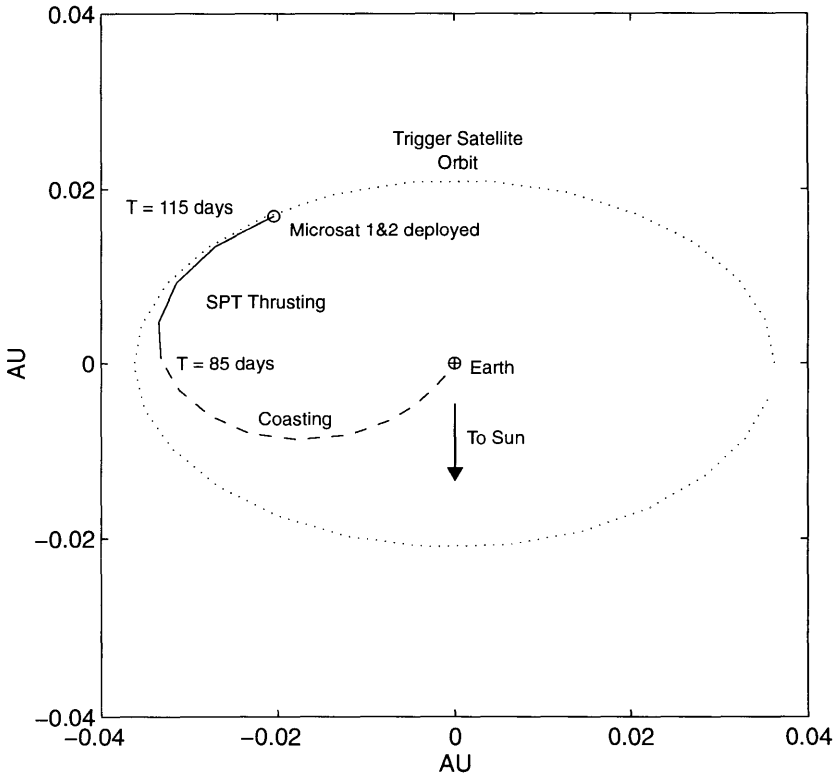

Figure 6-29: Baseline Launch Trajectory

6.6 ETA Baseline Mission Scenario

Referring to Figure 6-29, the launch is followed by upper stage burn and separation of the carrier spacecraft from the DeltaLite launcher. The carrier spacecraft, with the stack of 6 microsatellites, then coasts for about 85 days. At that point, the SPT-70 starts thrusting in a retrograde sense with respect to heliocentric motion and this continues for 30 days.

At T=115 days (referenced to launch date), the carrier spacecraft is at the point of deployment of the first two microsatellites into the trigger satellite orbit. The two spacecraft will be deployed close to one another. After the deployment, the carrier spacecraft continues to thrust for 68 days in a retrograde direction before deploying the third microspacecraft. The subsequent deployment trajectory of the carrier spacecraft is shown in Figure 6-30. Deployment times and other parameters such as Earth range at deployment are tabulated in Table 6-4.

The fourth, fifth and sixth microspacecraft are deployed 242, 292 and 335 days after launch. The deployment phase thus takes just over 11 months, after which the carrier spacecraft is available for post deployment activities such as secondary science or SPT-70 testing. SPT-70 thrusting is in retrograde direction and hence the "fall in" towards the Sun, due to decreasing heliocentric velocity.

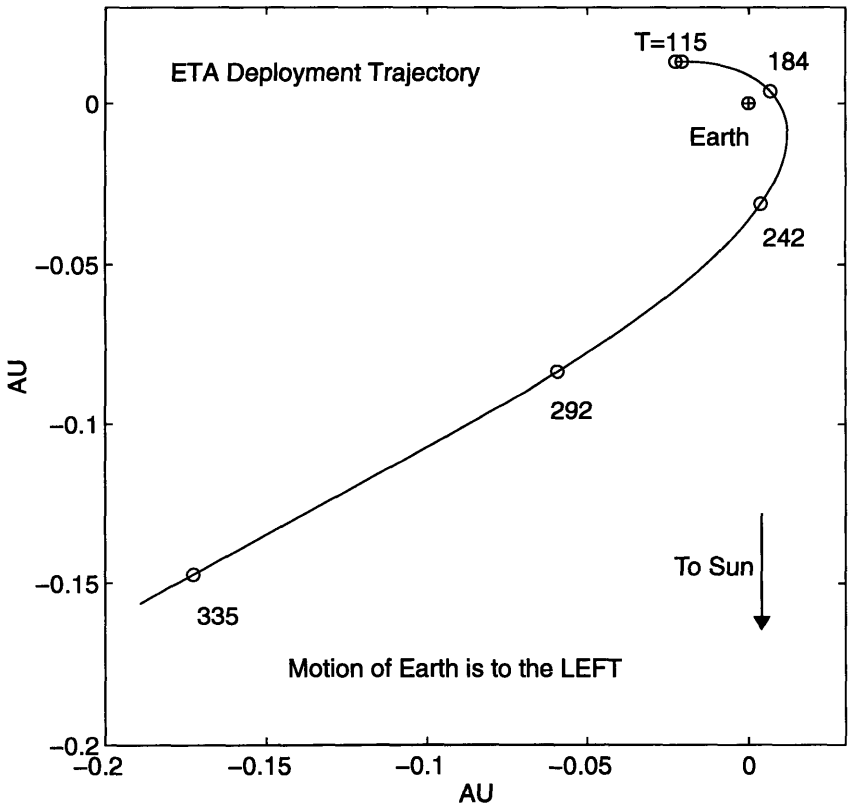

Figure 6-30: Baseline Constellation Deployment Trajectory

Table 6-4: ETA Baseline Constellation Data

Microsatellite Order	DEPLOYMENT		Microsatellite Heliocentric Orbit Period (days)
	Earth Range (AU)	Time from Launch (days)	
1	0.02618	115	370
2	0.02585	116	370
3	0.00771	184	353
4	0.03143	242	337
5	0.10228	292	320
6	0.22694	335	301

Figure 6-31 displays the positions of the microsatellites at yearly intervals. The unequal thrusting times have resulted in a constellation in which the angular separation of the spacecraft is quite uniform. Two microsatellites are in close proximity of Earth and per-

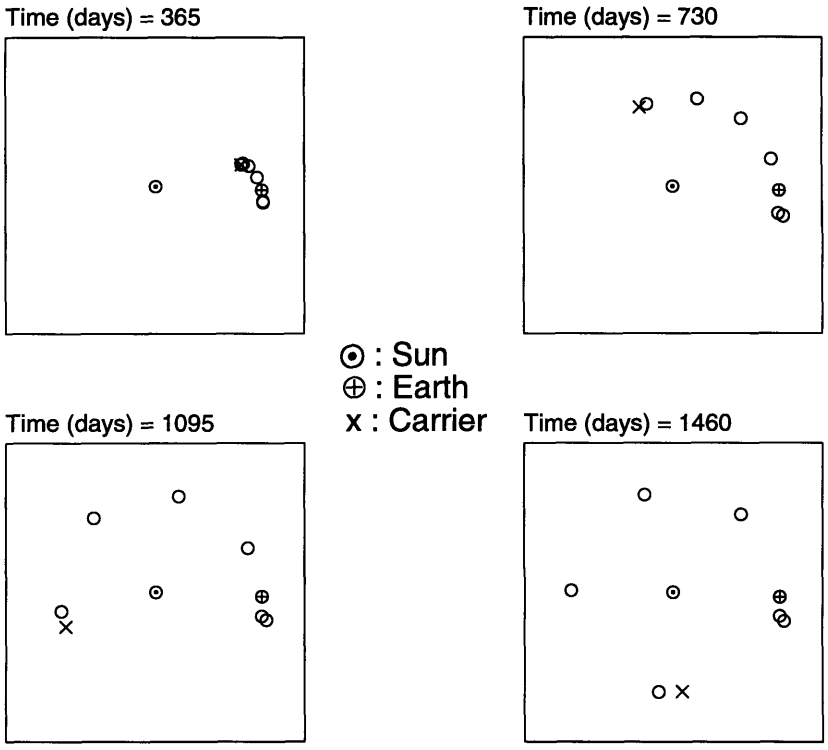

Figure 6-31: Constellation Development for ETA Baseline Scenario

form the function of the trigger satellites. Mission operations are scheduled to commence at the end of the second year when the constellation has started providing the required baselines. The accuracy of GRB source localization, which is a function of the "spread" of the constellation, will be highest in the fourth year. The constellation will, however, continue to provide similar baselines beyond 4 years, as shown in Figure 6-32, and scientific operations can be carried on, if funding is available.

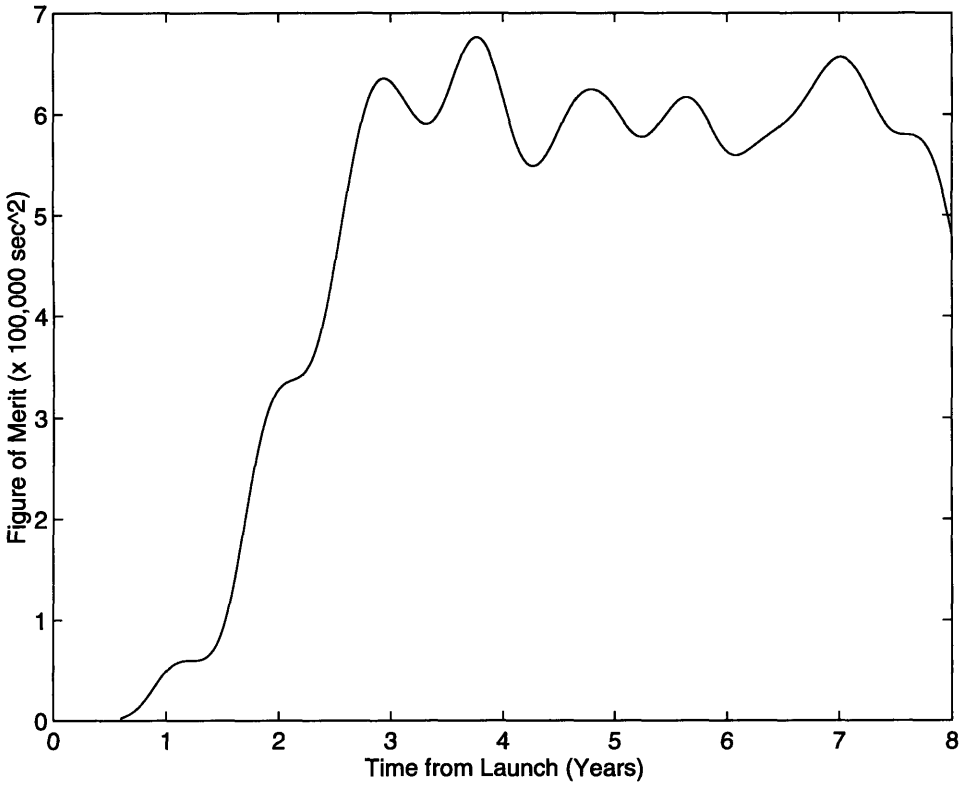

Figure 6-32: Figure-of-Merit for Baseline Mission

The carrier spacecraft is available for post-deployment operations. The presence of such a platform in interplanetary space is ideal for performing other science missions. On the other hand, experimentation and testing of hardware such as the SPT-70 system could be done. The carrier spacecraft currently has sufficient mass margin to incorporate a reasonable amount of hardware, be it scientific or technological.

The establishment of the baseline mission scenario provided some of the required design inputs for the rest of the system. This information was used to develop the system design described in the next Chapter.

Chapter 7

ETA System Design

System design is a concurrent, iterative process in which, in the context of the ETA program, both constellation (mission design) and hardware (system design) concepts are developed simultaneously with continuous refinement. In this regard, it is necessary to further establish the impacts, on the space and ground segment designs, of the constellation design presented in the previous chapter.

The main purpose of this chapter is to present an overview of the carrier spacecraft, microsatellite and ground segment designs, with the intent of determining the influence of the constellation design. The discussion is presented from the perspective of systems engineering, specifically as signified at lower level by the constellation. Additionally, this chapter also contributes towards the secondary thesis objective of presenting an overview of the ETA system.

The designs presented in this chapter constitute the work of the ETA team in developing the system [4]. While the work presented in the thesis, notably the constellation analysis, was an enabler to system design, it is acknowledged that the system design presented here was not a primary focus for the thesis work. The author is grateful to the ETA team for permission to include the system design in this thesis. With due consideration to the sensitivity of some of the information, certain details are deliberately omitted, giving the impression of an incomplete discussion. This could not be avoided in certain areas but an effort has been made to make the presentation as complete as possible within the constraints. The spacecraft designs developed for ETA are also proprietary and this company-sensitive information could not be presented in the thesis. Instead, conceptual designs are included to facilitate the discussion of pertinent points.

The chapter begins with the space segment and the microsatellite design is discussed first. This is necessary to better appreciate the carrier spacecraft design which is presented next. The ground segment discussion includes a brief treatment of ETA VLBI/Ranging techniques which motivated the specific ground segment architecture presented thereafter.

Each section sets out the relevant segment requirements before going into the configuration, mass, power and link budgets where applicable. The impacts of constellation design on each segment are discussed. The system design presented in this chapter is the version which is current at this stage of the ETA program.

7.1 Microsatellite Design

The constellation of microsatellites is one of the most crucial functional elements of the ETA system from the standpoint of scientific operations. Microsatellite design has to incorporate a wide variety of design considerations which originate from programmatic issues (cost, schedule, risk and so forth), system requirements as well as other inputs from constellation, ground system and carrier spacecraft design.

There are two types of ETA microsatellites, namely the trigger satellites and the "distant" microsatellites. The trigger satellites are in close proximity of Earth and perform the function of rapid alert of GRB events. The "distant" microsatellites, hereafter termed "general" microsatellites, are the spacecraft which make up the rest of the constellation and are normally much further away from Earth than the trigger satellites. Even though the "trigger" and "general" microsatellites are functionally different, the spacecraft designs are the same. Hence, the discussion in this section refers to both types of microsatellites, unless otherwise specified.

7.1.1 Requirements

The major requirements for the microsatellites are [4]

- **Maximum Wet Mass: 50 kg**
  This constraint originates from the constellation design and also takes into account the spacecraft contractor's assessment of what can be achieved in terms of microsatellite mass.

- **Operating Lifetime: 4 years (nominal)**
  Even though the mission duration is currently 4 years, with 2 years of nominal scientific operations, there exists the possibility of extended operations beyond 4 years. Since there are no eclipse phases and hence no need for batteries, there is no related limitation on spacecraft lifetime and it is envisaged that the microsatellites will continue to operate beyond 4 years [4].

- **Uplink Datarate: 1000 bps**
  This datarate is required to uplink the GRB templates to the microsatellites for template matching. The link will be supported at all ranges up to about 2 AU.

- **Downlink Datarate (@2 AU): 10 bps**
  The "general" microsatellites will only need to downlink GRB time-of-

arrival and template match confidence factor data most of the time. A high datarate is thus not necessary. A low rate link facilitates not only communications link design but also the rest of the microspacecraft design. Of course, when the microsatellite is closer to the Earth, the link will be able to support higher datarates.

- **Downlink Datarate (0.05 AU): 16 kbps**
  The "trigger" satellites need this high datarate to downlink GRB profiles as quickly as possible. Since the designs for the "trigger" and "general" microspacecraft are to be the same, it follws that the more stringent link requirement on design is the 10 bps link at 2 AU; the 16 kbps link is a consequence of this.

- **Contingency Uplink Rate: 5 bps**
  A contingency link will be provided to maintain contact with the spacecraft in the event of loss of attitude (Earth, Sun pointing). The link will be used to load relevant attitude sensing data, such as Earth, Sun and star positions, for the re-establishment spacecraft attitude and antenna/ solar array pointing.

- **Thermal Control: should be able to accomodate Sun range variations**
  As shown in the previous chapter, the range of the microsatellites from the Sun will vary depending on microsatellite. For the current baseline mission scenario, the Sun range variations are approximately within 0.8-1.0 AU. This constitutes almost a 36% variation in solar flux from 1 AU. The microsatellite should be able to remain within specified temperature limits irrespective of Sun range.

- **Autonomous Safe Hold Mode**
  In the event of some major failure, the spacecraft will enter a safe hold mode whereby the electronics are powered down and the spacecraft maintains Earth and Sun pointing for communications and power.

7.1.2 Configuration

Figure 7-1 illustrates a conceptual configuration of the microsatellite. The actual design could not be presented due to the sensitive nature of the information; it is sufficient to say here that the design has been proven in space. The conceptual design serves the purpose of illustrating the important issues by noting the location of important hardware such as the GRB detectors.

A flat shape was selected for the 3-axis stabilized bus to facilitate the stacking of the six microsatellites on the carrier spacecraft. Two GRB detectors are placed on each of the North/South bus faces so that they can face the ecliptic poles, as specified by scientific requirements. The bus walls shield the detectors from radiation inputs from the Sun. Pay-

NOT TO SCALE

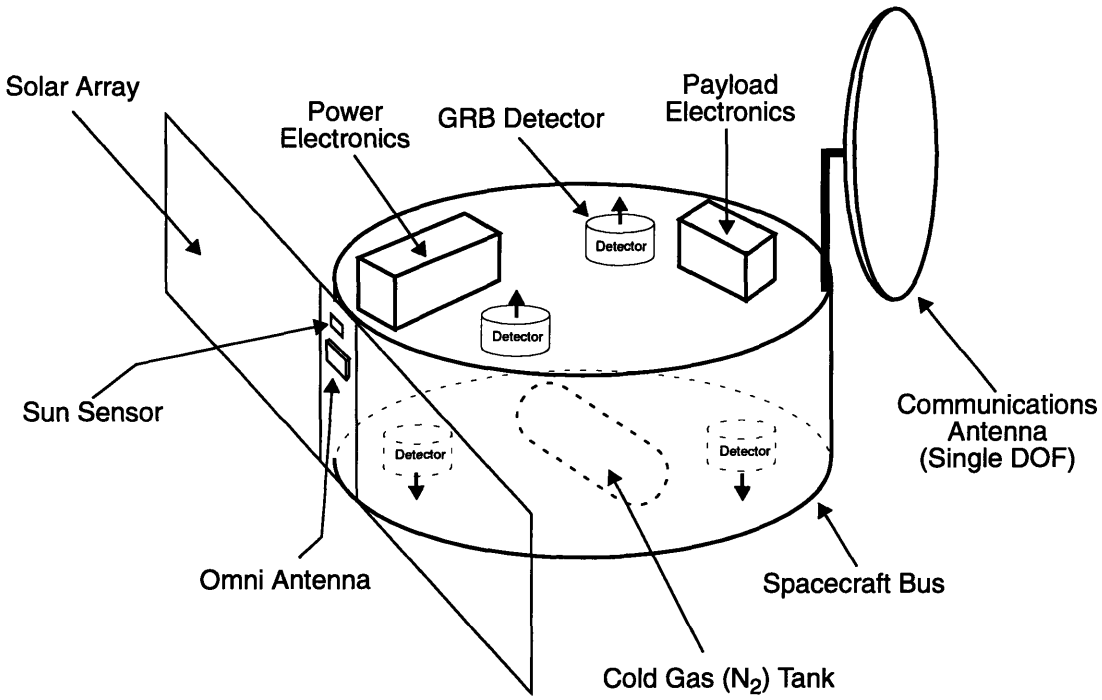

Figure 7-1: Conceptual Configuration of ETA Microsatellite

load electronics is mounted on the bus wall. The solar array is mounted parallel to the bus wall, with an omnidirectional X-band antenna and sun sensor in the central region. Power electronics, to condition the power generated by the solar array, is mounted next to the solar array, reducing cabling and associated losses.

The X-band communications antenna can be steered about one axis (ecliptic normal). When the microsatellite is in the undeployed state on the carrier spacecraft, the antenna lies flat on the top face of the bus. During deployment, the support arm unfolds and raises the antenna to a vertical orientation. The antenna can then be swivelled to any direction about the normal to the ecliptic plane. Omnidirectional antennas for contingency links are mounted on the solar array panel and the anti-sun face.

Attitude determination will be done using sun sensors and a star sensor for star field sensing. A momentum wheel will provide bias to the axis parallel to the ecliptic normal. Four cold gas thrusters are mounted on the bottom face of the spacecraft to control momentum wheel speed and orientation. Nitrogen propellant will be stored in the tank shown.

Even though the spacecraft has more than sufficient propellant to support attitude control over 4 years, it does not have enough ΔV capability to perform stationkeeping for a Lissajous or Halo orbit for the trigger satellite. As mentioned in the previous chapter, this was a major constraint which eliminated the otherwise promising orbit options of Lissajous orbits for the trigger satellites. In this context, the issue of a larger propellant load should be considered in further design work if mass considerations allow some allowance for extra propellant. This is a direct trade between mission and system design.

The ETA mission will be operational during a period of high solar activity. There is thus the possibility of radiation-related failures such as single event upsets and latchups in the spacecraft system. To counter this, an operational mode has been developed which continues to maintain the spacecraft in stable attitude and thermal modes. A Radiation Storm Monitor (RSM) will monitor radiation levels. When a very high level is detected, the spacecraft is powered down, with the exception of thermal heaters. The loss of power to the momentum wheel will spin it down, transferring angular momentum to the spacecraft. The bus will start rotating about 0.1 RPM, averaging out thermal inputs as well as disturbance torques. The slow rotation also facilitates the acquisition of Sun and Earth pointing, when the nominal operating mode is invoked.

7.1.3 Communications Links

The communications subsystem is the design driver for the microsatellite due to the extreme ranges involved. With the need to communicate from ranges of up to 2 AU, the microspacecraft has to have a relatively high Equivalent Isotropic Radiated Power (EIRP), which results in a high power transmitter and high gain antenna. Even though the driving link requirement is the 10 bps link at 2 AU, the common microsatellite design has also got to ensure that a 16 kbps link can be maintained at 0.05 AU for the trigger satellites. Table 7-1 includes the telemetry link budgets for both the "general" and "trigger" satellite links. Details of communications link analysis are presented in Appendix A.

The X-Band telemetry link will be at 8.4 GHz with the antenna providing a gain of about 29 dB at this frequency. A Solid State Power Amplifier (SSPA) will provide 4 W RF power at an power efficiency of 25%. The low mass, small volume and high linearity of the SSPA are advantageous to the design. The data will be transmitted using Differential Binary Phase Shift Keying (DBPSK) modulation with a Bit Error Rate (BER) of 10^{-5}, which is necessary for retaining data accuracy.

Hardware changes at the MIT Westford Antenna facility will enable a system noise temperature of 50 K to be achieved. This is conservative in light of the fact that the installment of a new Low Noise Amplifier (LNA) would reduce system noise temperature to about 20 K. The link should therefore have at least a 2 dB improvement over the 7 dB link margin that is currently available for both "general" and "trigger" links.

Table 7-1: Microsatellite Telemetry Link Budgets [4]

	General 10 bps, 2 AU	**Trigger** 16 kbps 0.05 AU	
TRANSMITTER PARAMETERS			
Transmitter RF Power (4 W)	6.02	6.02	dBW
Circuit Losses	-1.00	-1.00	dB
Antenna Gain	28.94	28.94	dB
EIRP	33.96	33.96	dBW
PATH PARAMETERS			
Free Space Loss (8.4 GHz)	-280.45	-248.41	dB
Atmospheric Loss	-0.50	-0.50	dB
RECEIVER PARAMETERS			
Antenna Gain (MIT Westford 18 m)	61.40	61.40	dB
System Noise Temperature (50 K)	-(17.00)	-(17.00)	dB/K
Losses	-2.00	-2.00	dB
Boltzmann's Constant	-(-228.60)	-228.60	dBJ/K
C/N_0 Received	**24.01**	**56.05**	**dBHz**
DATA CHANNEL PERFORMANCE			
E_b/N_0 (DBPSK, Bit Error Rate=$1x10^{-5}$)	7.06	7.06	dB
Losses			dB
Datarate	10.00	42.04	dBHz
C/N_0 Required	**17.06**	**49.10**	**dB**
Link Margin	**6.95**	**6.95**	**dB**

Noting, from the discussion of the trigger satellite orbit in the previous chapter, that the current orbit has a maximum range of about 0.036 AU, the "trigger" satellite link should be able to support higher rates higher than 16 kbps. Conversely, the flexibility could be incorporated into the mission design for the trigger satellite orbit by allowing maximum ranges of upto 0.05 AU.

It may be necessary to downlink a particular stored GRB profile aboard the microsatellite. The low rate at 2 AU will prolong this process but taking advantage of the spread of the constellation, profiles will first be downlinked from the nearer spacecraft. Moreover, the GRB profile onboard the microsatellite will be compressed using an algorithm implemented by onboard computers. In any case, there is sufficient time to downlink interesting GRB profiles from the microsatellites since they are stored onboard for at least 24 hrs before being overwritten. Command links budgets are presented in Table 7-2; both the nominal 1000 bps general link and the contingency 10 bps link are included.

Table 7-2: Microsatellite Command Link Budgets [4]

	General 1000 bps, 2 AU	**Contingency** 10 bps 2 AU	
TRANSMITTER PARAMETERS			
Transmitter RF Power (10 KW)	40.00	40.00	dBW
Circuit Losses	-1.00	-1.00	dB
Antenna Gain (MIT Westford 18 m)	60.29	60.29	dB
EIRP	99.29	99.29	dBW
PATH PARAMETERS			
Free Space Loss (7.4 GHz)	-279.35	-279.35	dB
Atmospheric Loss	-0.50	-0.50	dB
RECEIVER PARAMETERS			
Antenna Gain	3.00	28.90	dB
System Noise Temperature (450 K)	-(26.53)	-(26.53)	dB/K
Losses	-2.00	-2.00	dB
Boltzmann's Constant	-(-228.60)	-228.60	dBJ/K
C/N_0 Received	**22.51**	**48.41**	**dBHz**
DATA CHANNEL PERFORMANCE			
E_b/N_0 (DBPSK, Bit Error Rate=$1x10^{-6}$)	11.60	11.60	dB
Losses			dB
Datarate	10.00	30.00	dBHz
C/N_0 Required	**21.60**	**41.60**	**dB**
Link Margin	**0.91**	**6.81**	**dB**

The ground station will transmit 10 kW to provide an EIRP of almost 100 dBW at the uplink frequency of 7.4 GHz. The low rate (10 bps) link is essentially a contingency link, whereas the 1000 bps link is used for uplinking commands and GRB templates to the microsatellites. The spacecraft will use a low gain 3 dB omnidirectional antenna for the contingency link. Spacecraft receiver noise temperature is assumed to be 450 K.

Template matching requires a very accurate GRB template that is uplinked to the microsatellite. Distortion of the template during transmission could result in an inaccurate determination of GRB time-of-arrival. A low BER of 10^{-6} is required to avoid this loss of accuracy.

7.1.4 Mass, Power Budgets

The current version of the microsatellite mass budget is presented in Table 7-3 [4].

Table 7-3: Microsatellite Mass Budget [4]

Subsystem	Mass (kg)
Payload: GRB Detectors (4) and Electronics	18.20
Communications	3.45
Power	5.91
Attitude Control	3.95
Flight Computer	1.30
Thermal Control	0.86
Structure and Mechanisms	10.61
Microsatellite Dry Mass	44.28
Nitrogen Propellant	0.83
Microsatellite Wet Mass	45.11

Payload constitutes 41% of the spacecraft dry mass. Total wet mass, including a nitrogen propellant load of 0.83 kg, is below the 50 kg constraint used for the constellation analysis presented in Chapter 6. Even though mass margins are not explicitly indicated, they have been included at the subsystem level [77].

The microsatellite nominal power budget at 1 AU is presented in Table 7-4. As might be expected, the largest power load is the communications X-band transmitter. Operation of the cold gas thrusters will require over 7 W for valves and so forth. The solar array can provide 55 W after 4 years, providing a power margin of 13 W over the nominal spacecraft power requirement of 42 W. From the standpoint of extended operation beyond 4 years, the solar array will provide lower power levels but, because the payload only takes

up 5 W, it will be possible to continue operations, albeit at lower datarates.

Table 7-4: Microsatellite Nominal Power Budget at 1 AU [4]

	DC Power (W)
Payload Computer	4.00
GRB Detectors and Interface Electronics	1.00
X-Band Transmitter/Receiver	20.00
Flight Computer	2.00
Canopus Sensor	1.00
Momentum Wheel	1.80
Cold Gas Thruster (One Operating)	7.20
Power Conversion Losses	5.13
Total Power	42.13
Solar Array Output, 4 years	55.32
Power Margin	13.19

7.2 Carrier Spacecraft Design

The role of the carrier spacecraft is essentially to deploy the constellation of microsatellites into the distinct, heliocentric orbits. To this effect, it has to provide the propulsion, the separation mechanism and command and control relay to the microsatellites before they are deployed. The deployment phase of the mission is a serial phase and failure of the carrier spacecraft could lead to loss of the mission. High reliability is thus a major issue with the design of the carrier spacecraft.

7.2.1 Requirements

Key requirements pertaining to the carrier spacecraft are [4]

- **Maximum Wet Mass (excluding microsatellite stack): 250 kg**
  This requirement is based on constellation analsysis and preliminary mass estimates by the spacecraft contractor. The mass allocation includes the current estimate of 60 kg for Xenon propellant.

- **Operating Lifetime: 1 year**
  Even though the carrier spacecraft's primary mission, microsatellite deployment, is over a period of about one year, the post-deployment phase could include a secondary scientific payload or extended SPT-70

thruster operation and other experiments. There is currently nothing that precludes the carrier spacecraft from supporting such operations beyond 1 year, even though some power degradation is inevitable.

- **Mission Reliability: 90%**
  Because the carrier spacecraft's mission is a serial element, the reliability of the spacecraft has to be high in order to accomplish the mission. This aspect has not been looked into in great quantitative detail in the design work to date.

- **Uplink Datarate: 5 bps**
  The operation of the carrier spacecraft does not require a high rate uplink since only commands are required as well as occasional updates for attitude determination and so forth.

- **Downlink Datarate: 10 bps**
  Again, the carrier spacecraft has no data intensive operations that require a high rate downlink. This requirement could potentially change depending on what the post-deployment scenario is. A secondary scientific payload may require a higher rate, but electric propulsion experiments can be carried out with the current datarate capability.

- **Power to SPT-70: 660 W @ 42 V DC**
  This is the nominal operating point of the SPT-70. However, as pointed out in Chapter 5, the SPT-70 is tolerant to available power, with graceful degradation in performance with lower power. The more important issue here is the capability of the power electronics to operate over a range of powers.

- **Spacecraft should be able to counteract "swirl" torque from SPT operation**
  Operation of the SPT-70 creates a "swirl" torque which will tend to roll the carrier spacecraft. This has to be negated in some fashion by using roll control thrusting.

- **Attitude pointing control: 0.25 deg (3 axis)**
  Antenna pointing, microsatellite deployment attitude, thrusting direction and so forth necessitate attitude pointing control to the specified accuracy.

- **Autonomous Safe Hold Mode**
  This is similar to the microsatellite safe hold mode in that the carrier should, in the event of a contingency, be able enter a safe operating mode in which the chances of losing the spacecraft are minimized.

7.2.2 Configuration

Figure 7-2 illustrates a conceptual configuration of the carrier spacecraft. Again, the actual configuration could not be presented due to its proprietary nature but the design is based on space-proven designs. It comprises the following main elements:

- Microsatellite stack
- Bus containing electronics, propellant tank and other hardware
- Solar arrays
- SPT-70 propulsion system

The flat bus of the microsatellite is seen to facilitate the compact stacking of the microsatellites. The separation and deployment mechanism for separating each microsatellite from the stack is an innovative design developed by the spacecraft contractor for one of their commercial products. This mechanism minimizes shock effects on the microspacecraft from hard release and also allows checkout of the microsatellite before it is deployed. Note that the solar arrays of the microsatellites are already in deployed state but there is sufficient rigidity to avoid damage at launch [77]. An adaptor between the carrier bus and microsatellite stack provides interfaces with the microsatellites prior to deployment.

The cylindrical honeycomb bus is large enough to accomodate the Xenon propellant tank, electronics as well as other hardware associated with the carrier spacecraft. The SPT-70

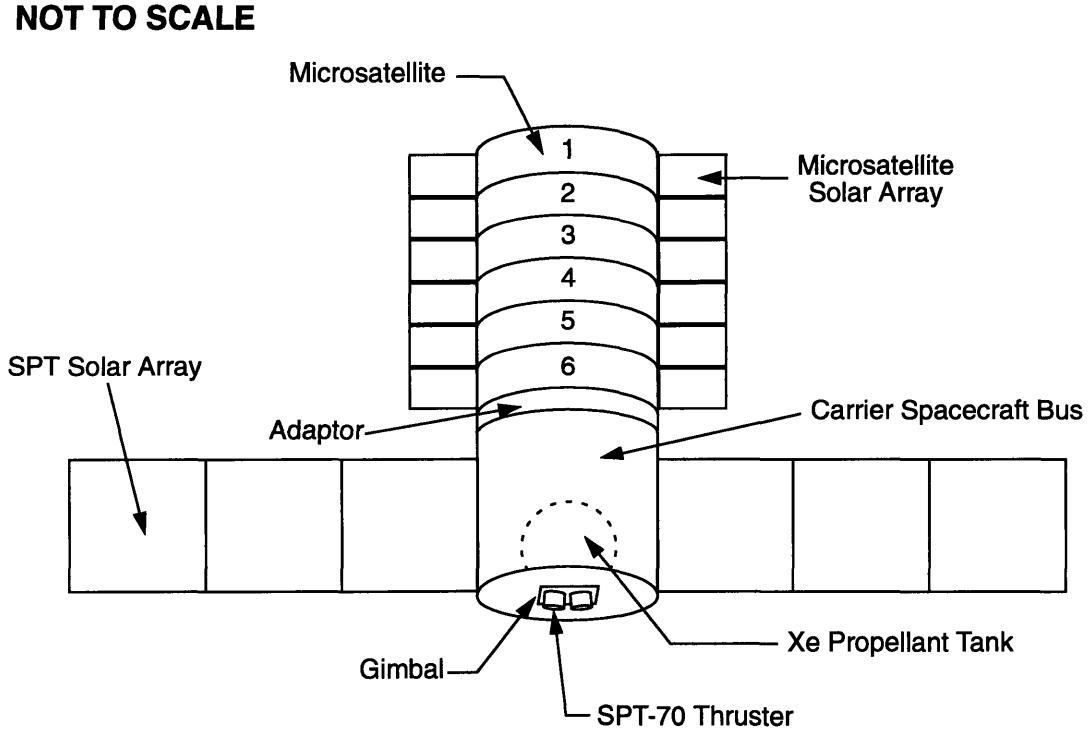

Figure 7-2: Conceptual Configuration of Carrier Spacecraft

module is mounted at the lower end with the thrusters mounted on a gimbal.

The SPT-70 system imposes the largest power load (power budget presented later) on the system and a separate solar array, comprising 2 wings of 3 panels each, is provided to genrate this power. The rest of the spacecraft power, which is small compared to the SPT-70 load, is provided by a small solar array (Bus array), which is the same as that used on the microsatellites, but is not shown in Figure 7-2 for the sake of clarity. A discussion of the SPT-70 system, in the context of the carrier spacecraft, is presented in a later subsection.

The carrier spacecraft architecture incorporates dual string redundancy for all major hardware elements, except the SPT-70 system, which incorporates internal redundancy for critical components such as the PPU.

When the SPT-70 is thrusting, the attitude of the carrier is such that the SPT solar array is normal to the ecliptic plane. Retrograde thrusting necessitates the carrier spacecraft to be in a "reverse" attitude with the microsatellite stack at the "aft" end and the thrusters facing the direction of motion. Prior to deployment of a microsatellite, the SPT-70 will stop thrusting and the carrier spacecraft will rotate by 90 degrees such that the microspacecraft stack faces the ecliptic north pole. The microsatellite can then be deployed with its solar array facing the Sun and the bus in its operational orientation. Such a strategy minimizes the extent of initial attitude acquisition operations required of the microsatellite. The carrier spacecraft reacquires its thrusting attitude after microsatellite deployment to commence the next thrusting phase.

7.2.3 Communications Links

Table 7-5 presents the carrier spacecraft command and telemetry link budgets. The link budgets are presented for a range of 0.25 AU because this is the maximum range during the constellation deployment phase which is the main mission for the carrier spacecraft.

The carrier spacecraft uses the same communications hardware used for the microsatellites and this is reflected in the same EIRP and required E_b/N_o. The commonality in harware not only simplifies system design but also reduces system costs. Spacecraft system noise temperature is assumed to be 450 K. Utilization of the MIT Westford facility provides large margins and these are beneficial in that communications links can still be maintained when the carrier spacecraft is further away from Earth. For example, it will still be possible to support a 20 bps telemetry link at 2 AU and allowing a 4 dB margin. This is very useful from the standpoint of the post-deployment carrier operations.

Table 7-5: Carrier Spacecraft Command and Telemetry Link Budgets [4]

	Telemetry Link 8.4 GHz, 10 bps, 0.25 AU	**Command Link** 7.4 GHz, 10 bps, 0.25 AU	
TRANSMITTER PARAMETERS			
Transmitter RF Power	6.02	40.00	dBW
Circuit Losses	-1.00	-1.00	dB
Antenna Gain	28.94	60.29	dB
EIRP	33.96	99.29	dBW
PATH PARAMETERS			
Free Space Loss (0.25 AU)	-262.38	-261.28	dB
Atmospheric Loss	-0.50	-0.50	dB
RECEIVER PARAMETERS			
Antenna Gain	61.40	3.00	dB
System Noise Temperature	-(17.00)	-(26.53)	dB/K
Losses	-2.00	-2.00	dB
Boltzmann's Constant	-(-228.60)	-(-228.6)	dBJ/K
C/N_0 Received	**42.08**	**40.58**	**dBHz**
DATA CHANNEL PERFORMANCE			
E_b/N_0 (DBPSK, BER=$1x10^{-5}$, $1x10^{-6}$)	7.06	11.60	dB
Losses			dB
Datarate	10.00	10.00	dBHz
C/N_0 Required	**17.06**	**21.60**	**dB**
Link Margin	**25.02**	**18.98**	**dB**

7.2.4 Mass, Power Budgets

Table 7-6 presents the current mass estimates of the various components that make up the carrier spacecraft.

Table 7-6: Carrier Spacecraft Mass Budget [4]

Subsystem	Mass (kg)
Communications	5.63
Power	50.82
Attitude Control	10.57
Flight Computer	2.39
SPT-70 Propulsion System	59.20
Thermal Control	4.83
Structure and Mechanisms	33.80
Carrier Dry Mass	**167.24**
Xenon & Nitrogen Propellants	62.50
Carrier Wet Mass	**229.74**

The SPT-70 and power subsystems dominate the mass budget and carrier dry mass is estimated to be about 167.3 kg. With a propellant load (Xenon and nitrogen) of 62.5 kg, the wet mass of the carrier spacecraft adds up to just under 230 kg. This leaves almost a 10% margin on the 250 kg assumption imposed on carrier spacecraft mass for the constellation analysis.

Table 7-7 highlights the nominal power budget for the carrier spacecraft. As mentioned before, there are two separate solar arrays for the SPT system and the rest of the carrier bus and both are presented separately in the power budget.

Since the carrier spacecraft employs essentially the same core subsystems as the microsatellites, the baseline power load is well approximated by the microspacecraft total power requirement. Power requirements for an additional receiver and star sensor result in a total bus power requirement of about 47 W.

Solar array power levels continuously change during the deployment period since Sun range changes. Over that time, the solar cells undergo degradation as well. This has to be incorporated into the power calculations. Constellation analysis reveals that the maximum Sun range of the carrier spacecraft during the deployment phase is about 1.02 AU, remembering that retrograde SPT thrusting eventually keeps on bringing the spacecraft closer to the Sun. The solar array, until then, has degraded by about 9% [4].

Table 7-7: Carrier Spacecraft Nominal Power Budget [4]

	DC Power (W)
CARRIER BUS	
Baseline Microsatellite Total Power	42.13
Secondary Receiver	3.00
Secondary Canopus Sensor	1.00
Losses	0.60
Total Bus Power Required	46.73
Bus Solar Array Output, BOL	83.00
Net Power Level Change at Maximum Sun Range (see below)	-13%
Bus Solar Array Output at Maximum Sun Range	72.21
Power Margin	25.48
SPT SYSTEM	
Nominal Power to Thruster	660.00
Power Processing Unit (PPU) Losses (Efficiency: 90%)	73.33
Power Distribution Unit (PDU) Losses (Efficiency: 93%)	55.20
Miscellaneous Power for Heaters, Valves etc	30.00
Net Power Required for Thruster Operations	818.53
SPT Solar Array Output, BOL	870.00
Power Loss at Maximum Sun Range (1.02 AU)	4.0%
SPT Solar Array Degradation at Maximum Sun Range	9.0%
SPT Solar Array Output at Maximum Sun Range	756.90
Power Available to Thruster at Maximum Sun Range	608.40

Taking into account the 4% power loss due to Sun range (with respect to 1 AU), the net reduction in array power is about 13%. Thus, about 72 W are available from the carrier bus array but this still leaves a margin of over 25 W, which is useful to accomodate temperature variations and other unanticipated effects.

The SPT array, which has two wings with 3 panels each, is sized to generate 870 W at

BOL. SPT-70 operation at nominal operating power of 660 W requires 789 W from the array. This is to account for the power losses in the PDU and PPU which can be considered to be serial elements between the carrier power bus and the SPT thruster. Adding on another 30 W for other propulsion system components [48], the nominal power requirement of the SPT-70 system is about 819 W. Accounting for the 13% degradation in available power due to Sun range and array degradation, the SPT array can generate 757 W at maximum Sun range. Working back, this implies that the power input to the thruster itself is about 608 W. The operating point, as Figure 5-3 shows, does not result in substantial performance degradation.

Beyond maximum Sun range point, the retrograde thrusting of the SPT-70 will bring the carrier spacecraft closer to the Sun and array degradation losses can be offset by the power gains due to decreasing Sun range. Prograde SPT thrusting would have resulted in increasing Sun ranges well beyond 1.02 AU and this would have necessitated a larger solar array to provide SPT-70 power, increasing size as well as cost. The strong inter-relationship between constellation design and spacecraft design is clearly illustrated by this example.

7.2.4 SPT-70 Issues

The SPT-70 thruster module is mounted on the lower end of the carrier spacecraft. The thrusters have an unobstructed area in front of them. Spacecraft charging is not considered to be an issue since the thruster acts like a plasma contactor, minimizing the chances of spacecraft charging.

Contamination of solar array surfaces is expected to be minimal, if any, since the arrays are placed behind the thruster and, moreover, since the panels have the solar cells on the sides which face away from the thruster. Likewise, sputtering is not deemed to be a concern.

There is the possibility that power-related effects of SPT thruster operation may feedback to the carrier spacecraft power system through the PPU and PDU. While these power electronics units will be designed to minimize such feedback, the utilization of a separate solar array for SPT power will also assist in isolating SPT power-related feedback.

With regard to electromagnetic interference, the placement of the communications antennas serves to minimize signal transmission through the thruster plume. However, there may be instances during the deployment phase when the thruster plume is in the line-of-sight to Earth and there is the possibility of having to communicate through the plume. Signal transmission can be avoided by including redundant antennas in different locations on the spacecraft or simply not communicating when signal noise levels are high. Detailed simulations are necessary to quantify the nature (directions) and extent of such phases. Past flight experience shows that electromagnetic interference has not been a design driver [58,60].

The "swirl" torque produced by SPT operation is perhaps the most pertinent of SPT/ spacecraft interactions. Unless the torque is negated, the spacecraft will start accumulating

angular momentum about its roll axis. A Nitrogen cold gas system on the spacecraft will perform the function of negating these torques. It is then necessary to ensure that there is sufficient propellant to negate the "swirl" torque over at least the deployment phase of the mission.

The equivalent thrust due to the "swirl" torque is estimated to be between 2-8% [42,57] of nominal thrust. Assuming 2%, the equivalent thrust of about 0.8 mN, acting at a distance of 35 mm from the centerline of the thruster results in a torque of 2.8×10^{-5} Nm. This gives a net torque impulse of about 605 Nms over the 6,000 hrs of thruster operation. Assuming that the cold gas thrusters are placed 0.5 m from the roll axis of the carrier spacecraft, the net impulse required from the cold gas system is 1210 Ns. Nitrogen has an I_{sp} of about 73 sec and thus the mass of nitrogen required to impart the net impulse is about 1.70 kg. An additional 0.5 kg is required for other maneuvering [4], adding up to a total Nitrogen load requirement of about 2.2 kg. The cold gas tank onboard the carrier spacecraft can accomodate 2.5 kg of nitrogen and hence there is a margin on the propellant. However, this estimation is under the assumption that the equivalent "swirl" thrust is 2%, whereas it could be as high as 8%, in which case there isn't sufficient propellant onboard. It is hence very important to obtain actual "swirl" torque estimates through testing in order to size the roll control propellant load. Such tests are planned to be performed at Lewis Research Center [4]. In the event that better estimates are not available, it will be more appropriate to incorporate a conservative propellant load, especially if there is margin on carrier spacecraft wet mass.

7.3 Ground System Design

ETA mission operations comprise spaceborne and ground operations. The ground segment provides support for both scientific operations and space segment command and control functions. Moreover, the ground segment provides a very important interface between the space platforms and the end users (scientists). Ground system architecture has to be developed in such a manner as to comply with performance requirements, cost and availability constraints.

7.3.1 Requirements

Key ground segment requirements are listed below:

- **Accurate determination of spacecraft positions**
  In order to accurately localize GRB sources, spacecraft locations need to be determined to an accuracy of 30 km in each coordinate, as outlined in Chapter 2. The ground segment is responsible for tracking the spacecraft and has to comply with this requirement. This requirement is discussed further in a later subsection.

- **Maintenance and Control of space segment**
  The carrier spacecraft and 6 microsatellites have to be controlled and monitored throughout the mission. A dedicated space segment control

function is required that will uplink commands, receive and analyze telemetry and carry out critical mission operations.

- **Analysis and Dissemination of GRB data**
  Once GRB data are received from the "trigger" and "general" microsatellites, they have to be analyzed before being relayed to interested users around the world. There are two separate functions involved. First, coarse GRB source coordinates (after times-of-arrival have been received from distant microsatellites) have to be transmitted to ground and spaceborne observatories through their controlling organizations so that follow-on observations of the GRB can be made. Secondly, GRB profiles and localization data have to be made available to the general scientific community for research. The time frames for the former are of the order of an hour or so while the time frames for the latter are of the order of weeks.

- **Daily contact with constellation: 12 hrs**
  It is necessary to maintain daily contact with the carrier spacecraft and microsatellites for a number of reasons. New commands may need to be uplinked or star field catalogues may need to be updated. The onboard clock will also need to be recalibrated if drifts are above nominal, since timing errors can degrade error box sizes significantly. The carrier spacecraft may require new commands with regard to SPT-70 thrusting or microsatellite deployment and so forth. Moreover, the microsatellites would have to downlink, within 24 hrs, required burst profiles before the onboard memory is overwritten.

- **Redundancy/Reliability**
  Since the only contact with the space segment is through the ground stations, it is necessary to incorporate some level of redundancy. This may be achieved by having more than one ground station, which also provides redundancy when weather, for example, restricts contact through a specific ground station.

7.3.2 VLBI/Ranging

ETA can accurately localize GRB sources by timing the arrival of GRB's at the microsatellites and correlating with the spacecraft positions. It follows that while timing accuracy is important, spacecraft positions also need to be determined to high accuracy.

The flowdown of the system accuracy requirement in Chapter 3 specifies a 0.3 msec timing error allocation to the ground segment. Considering light-time, the 0.3 msec accuracy translates into a distance accuracy of 90 km. Thus the spacecraft positions need to be accurate to 30 km in each coordinate.

Spacecraft position can be specified in a variety of coordinate frames. For the purposes of

measurement, it is more practical to use an inertial spherical coordinate system where the spacecraft position is specified by

- Range from Earth
- Elevation, as specified by the Declination
- Azimuth, as specified by the Right Ascension

These coordinates can always be transformed into other coordinate frames.

The ground segment has to be able to simultaneously determine these 3 coordinates for each microsatellite. Simultaneous determination is necessary so as to avoid random orbital perturbations such as solar wind from distorting the measurements [4,77].

Range measurements can be made using conventional 2-way radio ranging methods. A pseudo-random code is uplinked to the spacecraft which downlinks it back for subsequent range determination. This method can provide accuracies of under 60 km [4]. Ranging operations also assist in the synchronization of onboard clocks. The more demanding problem is that of determining the directional coordinates.

The directional accuracy required to achieve an accuracy of 60 km at 2 AU is of the order of $2x10^{-7}$ radians. The ETA mission will utilize Very Long Baseline Interferometry (VLBI) methods to attain the necessary accuracy. The basic concept of VLBI, as applied to spacecraft position determination, is to measure the time difference between the arrival of a spacecraft-originated signal at two widely spaced ground stations. The time difference is derived from phase measurements of the received signals. In order to determine both directional coordinates (declination and right ascension), 3 ground stations are required.

The directional accuracy, in radians, of the VLBI method can be approximated by dividing the time-delay measurement uncertainty by the projected distance between the ground stations in light-seconds [4]. The three ground stations selected for the ETA mission are [4]

- MIT Haystack Antenna Facility in Westford, Massachusets (18 m antenna)
- National Radio Astronomy Observatory (NRAO) in Greenbank, West Virginia (26 m antenna)
- Deep Space Network (DSN) facility in Goldstone, California (34 m antenna)

The orthogonally projected baselines provided by the NRAO and DSN antennas with respect to the Haystack antenna are about 840 km and 2300 km respectively [4]. Hence, the timing accuracies required to obtain a directional accuracy of 2x10-7 radians are 0.56 nsec and 1.53 nsec respectively. An accuracy of 0.5 nsec is not difficult to achieve at the X-Band frequencies that will be used for spacecraft communications links [4]. There is however, the issue of having sufficient signal strength (Signal to Noise Ratio) and bandwidth. The spacecraft X-Band transmitter will operate over a 50 MHz bandwidth and the link will provide the requisite SNR for VLBI operations.

7.3.3 Ground System

Ground segment functions for the ETA system will be performed by the ground system illustrated in Figure 7-3.

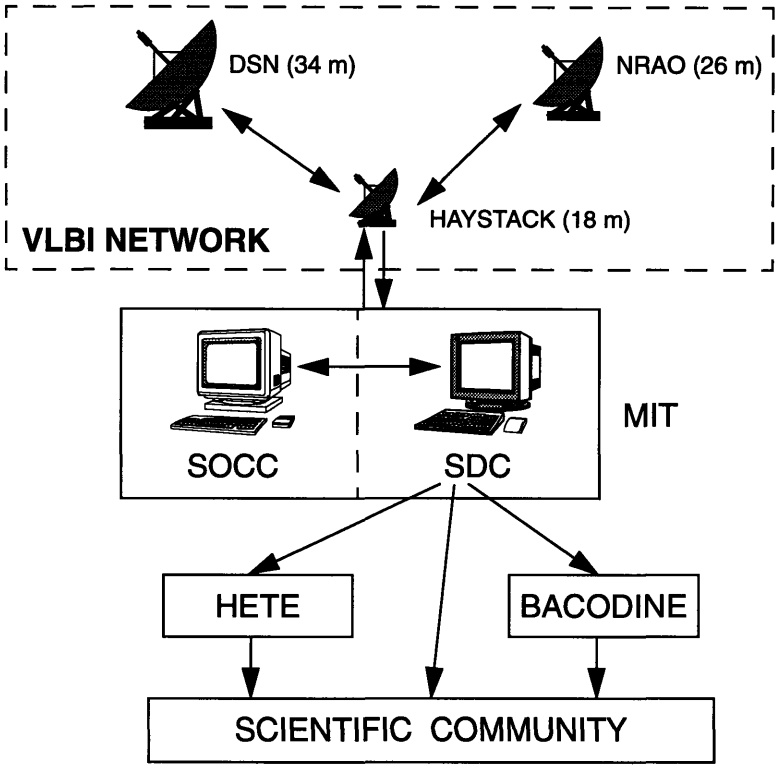

Figure 7-3: ETA Ground Segment

The hub of ground operations will be MIT where an ETA center will be set up. This will consist of the Spacecraft Operations Control Center (SOCC) and the Science Data Center (SDC) [4]. The SOCC will be responsible for command and control of the ETA space segment, namely the carrier spacecraft and the microsatellite constellation. Scientific data receipt and data reduction will be performed in the colocated but functionally different SDC. The SDC will also provide the interface with the scientific community.

MIT's Haystack antenna facility will be the main ground station for ETA. It will coordinate VLBI operations with the NRAO and DSN antennas. Trigger satellite communications will be through the smaller 1.8 m antenna at Westford, providing a degree of redundancy. The DSN antennas will serve as backup in the event that communications cannot be maintained with the constellation due to an outage at the Westford facility. VLBI correlation will be carried out at Haystack since it has the necessary hardware. This also avoids the MIT center from having to coordinate VLBI operations.

The scientific community will receive the scientific data in a number of ways. The HETE and BACODINE networks will be used to relay coarse coordinate information for follow-on observations with other observatories. The time delay for this information is expected

to be in the region of one hour. Accurate GRB data will be made available to the general scientific community and public by means of the Internet. Preliminary data will be available within 24 hrs, but final updated versions will require incorporating VLBI measurements into the calculations and may not be available until about a month after the GRB occurs [4]. Additionally, data will also be available to the general public through an ETA World Wide Web (WWW) site, which will contain a regularly updated database. The WWW site will facilitate downloading of GRB profiles, images, error boxes and other formats which would normally be difficult to acquire.

7.4 System Mass Budget

Having described the carrier spacecraft and microsatellite designs, it is now possible to draw up the system mass budget and compare the total system mass with the launch vehicle capability to see how much margin is available. Table 7-8 presents the system mass budget [4].

Table 7-8: ETA System Mass Budget [4]

	Mass (kg)
Microsatellite Dry Mass	44.28
Nitrogen Propellant	0.83
Microsatellite Wet Mass	**45.11**
Carrier Payload (6 Microsatellites)	270.66
Carrier Bus Mass (Dry)	167.24
Xenon & Nitrogen Propellants	62.50
Carrier Wet Mass (excluding Microsatellites)	**229.74**
System Mass (Carrier + Microsatellites)	**500.40**
DeltaLite Capacity to C_3=0	570.00
Launch Margin	**69.60**

The wet mass of the microsatellite is 45.1 kg. The dry mass of the carrier spacecraft is 167.3 kg which sums up to a wet mass of just under 230 kg when the propellant load is added. Taking into account the 6 microspacecraft stack, the total system mass is about 501 kg. The DeltaLite capacity to a C_3 of zero is about 570 kg so there is a margin on launch mass of about 70 kg.

The 70 kg mass margin can be used in a number of ways. However, it must be realized that the current mass estimates are based on preliminary design studies and further detailed

design may result in an increase in system mass. This will result in a reduction of the available launch mass margin. Nevertheless, there is still the possibility of including a seventh microsatellite. A 7 microsatellite constellation, as pointed out in Chapter 6, will provide better performance from the standpoint of scientific operations and the extra spacecraft will also increase the level of redundancy in the ETA system.

Post-deployment functions for the carrier spacecraft can also be defined based on the mass margins available. A small secondary scientific payload could be incorporated aboard the carrier. If extended thrusting of the SPT-70 is contemplated, there is the possibility of including more Xenon propellant and possibly some instrumentation, should the need arise. It is important to note that all this is contingent upon mass being available at the end of spacecraft design.

Constellation analysis was performed under the conservative assumptions that the carrier and microsatellite weighed 250 kg and 50 kg respectively. The current baseline masses are lower by about 10% and this means that the constellation performance, as signified by the figure-of-merit, will be better than indicated. The performance improvements are quantified in the sensitivity analysis that was presented in Chapter 6.

The system mass margin indicates that there a number of options available to ETA planners with regard to issues such as

- utility of carrier spacecraft after the constellation deployment phase
- possible inclusion of a seventh microsatellite in the constellation
- inclusion of more propellant for the microsatellites to provide a stationkeeping capability that will allow the use of Lissajous type orbits for the trigger satellites.
- inclusion of a small secondary science instrument onboard each microsatellite, supplementing the capabilities of the GRB detectors
- performing the mission to a higher C_3, leading to better performance from the constellation. Cost wise, this is probably the best option but then again, the advantage of a higher C_3 diminishes, beyond a certain value.
- enhancing the design of the GRB detector by including extra hardware or sensors. This would yield better GRB measurement data.

Experience shows that, more often than not, no mass margins are available by the time the system is ready for launch [77]. Hence, it is important to get an accurate understanding of sysem mass estimates as early into the program as possible, if the options listed above are to be explored and incorporated. The issue of increase in complexity associated with inclusion of extra hardware has also got to be considered carefully.

Of course, these options have to be assessed in terms of their impacts on scientific return, cost, schedule and program risk and this is something that would be addressed contingent upon the availability of mass margin.

Chapter 8

Programmatic Issues

Even though programmatic issues such as cost, schedule and risk are of prime concern to any program, they are even more critical from the standpoint of a proposed project such as ETA. This is so because, unlike other space programs, the ETA mission is in competition with a rather large number of other project proposals for support from NASA. The current fiscal climate dictates that cost is always a driver and more often than not, there is a likelihood that a low cost program with moderate scientific return will be selected over a program which is more costly but promises greater scientific return. In that context, ETA program planners and designers have to come up with a system concept that has the right balance of performance, cost and risk. Moreover, they have to demonstrate their ability to remain within cost and schedule limits, using a program management philosophy that facilitates the management of a complex program such as ETA. This chapter highlights some of these programmatic issues in the context of the ETA mission.

From a systems engineering perspective, cost, schedule and risk constitute areas in which program planners pay special attention all through the system development process. It is important to get a feeling for these issues early in the design process in order to identify potential hurdles and devise means of mitigating these. ETA system designers and program planners have given due consideration to these issues while developing the ETA system around the aim of maximizing system performance with a low cost system that does not incorporate an inordinately high level of risk.

This chapter discusses the programmatic issues of schedule, cost and risk in that order. A brief discussion on program management is also included at the end since the management approach adopted by ETA planners is rather unique. A lot of the pertinent information is sensitive or proprietary and cannot be included here but details are provided where possible. Cost issues are discussed qualitatively due to the sensitive nature of the information in the context of the proposal. On the whole, the purpose of the chapter is to identify the salient issues that affect program cost, schedule, risk and management.

8.1 Schedule

ETA is an Astrophysics mission that has been proposed to NASA for the MIDEX class of programs. Contingent upon selection, the ETA program has an eight year lifecycle with program start in the first quarter of 1996 and science operations currently scheduled to continue until early 2004. Launch is scheduled for January, 2000. The program lifecycle can be considered to be divided into four main phases as identified below [4]:

- **System Definition Phase**
  The system definition phase starts in April 1996 after ETA has been selected by NASA for support. The system concept, which has been developed in preparation for the proposal, will be further refined in this phase. Documentation such as system requirements documents, Interface Control Documents (ICD's), hardware drawings and so forth will be prepared. Necessary design reviews will be conducted with the participation of the hardware contractors, ETA program management and NASA reviewers. Requirements reviews, Concept reviews and other Design reviews will address all issues associated with transitioning from system definition to system development phase.

- **"Bridge" Phase**
  This phase is a short interim period of about 3 months between the definition and system development phases. Unresolved design issues, identified by the reviews during the definition phase, will be worked on at the same time as preparing for the commencement of the system development phase.

- **System Development Phase**
  ETA system hardware will be developed, procured, tested, integrated and launched during this phase which will span from initiation of system development to 30 days after launch. This phase is the most intensive both in terms of cost and schedule. The various elements of the ETA system will be developed and produced before being integrated and tested prior to launch. The major system hardware elements are payload (GRB detectors and electronics), microsatellite and carrier spacecraft, SPT-70 propulsion system and ground system elements. The development process will be punctuated with the requisite reviews, in order to ensure that system development is progressing as planned.

  This phase also encompasses final integration of the carrier spacecraft and microsatellite stack, prelaunch testing and launch. The formal definition of the system development phase includes a month after launch where system hardware, especially space system elements, is tested to the extent possible.

- **Mission Operations and Data Analysis (MODA) Phase**
  After launch and 30 day system checkout, the MODA phase is initiated and is scheduled to continue until cessation of scientific activities. During this period, the carrier spacecraft will deploy the microsatellite constellation, the system will be tested and calibrated while the constellation develops and finally, scientific operations will commence two years after launch. Current planning specifies a two year period for nominal scientific operations. There is the possibility, depending on funding availability, of extending scientific operations beyond the current two year period.

The breakdown of the ETA program into the phases outlined above was linked to the definition of the funding profiles as specified by NASA. The major aspects of the ETA program schedule are presented in Table 8-1 [4]. The dates are given in year quarters.

With program start in April 1996, there is a 10 month definition phase during which the system design is refined and reviewed through relevant reviews. The Design/Non-Advocate review is scheduled for the first quarter of 1997. Then follows the 3 month Bridge phase. The system development phase will start in the second quarter of 1997 with simultaneous development of the payload (GRB detectors and electronics), microsatellite, SPT-70 propulsion system and carrier spacecraft. These development segments are scheduled such that the integration and test of relevant subsystems (for example, payload with microsatellite, SPT-70 with carrier spacecraft) can be done without any need for "waiting". There is the issue of further characterization testing of the SPT-70 system and these will be conducted earlier on during the system definition phase. Ground system development will commence in the third quarter of 1997, with the procurement of the ground station transmitter for the MIT Haystack facility. Procurement of long lead items such as GRB detectors, solar arrays, communications systems and momentum wheels will be phased so as not to hold up the program during the later stages of development. The microsatellites will be delivered in a staged fashion over a two month period towards the end of the second year of the development phase. Hardware procurement will be phased in a manner which facilitates the incorporation of the latest technology to improve performance and reduce mass, volume and cost.

With most of the subsystems developed and tested by the end of 1998, a large portion of 1999 will be devoted to overall system integration and test. There is a 3 month contingency between system integration and prelaunch operations which will serve as a buffer against any delays that may potentially be caused earlier on in the program. Launch is scheduled for January 2000 and on-orbit checkout and testing of the system will be carried out in the month after launch, marking the formal culmination of the system development phase. Note that the current mission scenario calls for no specific constraint with regard to launch windows, except perhaps the need to avoid close proximity to the moon during the launch and escape phase.

The Mission Operations and Data Analysis (MODA) will begin immediately after on-orbit system checkout, with the beginning of the constellation deployment phase which

Table 8-1: ETA Program Schedule [4]

PHASE		START DATE (Qtr, Yr)	END DATE (Qtr, Yr)
Program Start		Q2, 1996	
SYSTEM DEFINITION	System Definition and Reviews	Q2, 1996	Q1, 1997
	Design/Non-Advocate Review	Q1, 1997	
BRIDGE	Preparation for Development Phase	Q1, 1997	Q2, 1997
SYSTEM DEVELOPMENT	Payload Production, Integration and Test	Q2, 1997	Q3, 1998
	Microsat Development, Integration, Test	Q2, 1997	Q4 1998
	SPT Characterization	Q3, 1996	Q4, 1996
	SPT System Development, Test	Q2, 1997	Q4, 1998
	Carrier S/c Development, Integration, Test	Q2, 1997	Q4, 1998
	System Integration (Carrier/SPT/Microsats)	Q1, 1999	Q3, 1999
	Ground System Development and Test	Q3, 1997	Q3, 1999
	Contingency, Final Readiness Review	Q3, 1999	Q4, 1999
	Launch Integration, Launch	Q4, 1999	Q1, 2000
	On Orbit Testing	Q1, 2000	
MODA	Constellation Deployment	Q1, 2000	Q4, 2000
	Constellation Development, System Testing	Q4, 2000	Q4, 2001
	Nominal Scientific Operations	Q1, 2002	Q1, 2004

will continue until the end of 2000. The next year will be allowed for the constellation to develop and no operations will take place except general upkeep of the space segment, validation and testing of the software for GRB data analysis and testing of the ground system. The carrier spacecraft may be used for a secondary mission during this period, depending on what is planned.

Nominal science operations will begin in 2002 and will continue for a minimum of 2 years, with extended science operations a possibility contingent upon funding availability.

The program schedule reflects a conservative approach to the development of the ETA system. All the major subcontractors (spacecraft, payload) are well experienced to remain within schedule but the incorporation of a 3 month contingency before launch serves to minimize the risk of schedule overruns.

8.2 Cost

The ETA program is competing with a large number of proposals for NASA funding support. Because the staged proposal evaluation process is still underway at the time of writing this thesis, cost information is deemed to be sensitive and cannot be presented here. As a result, the following discussion on programmatic cost issues is essentially qualitative in nature.

It is interesting to consider the perception of proposal reviewers to program costs. Even though a formal cost constraint is normally imposed, the current trend is that cost almost always overrides scientific returns. Thus, a low cost program with reasonable scientific return is likely to be selected over a more scientifically ambitious mission which is more costly. However, in their efforts to minimize program costs, program planners have to guard against underquoting proposals because NASA will not provide additional support in the event of cost overruns. Balance between cost and scientific return can be hard to achieve and, while the scientific merits of ETA are exceptional, program costs have got to be minimized to improve the chances of program selection. Hence, it is imperative that systems engineers work in concert with scientists in trading off scientific return and program cost to come up with the right balance.

Proposal considerations dictated that the ETA program would have to be developed under a cost cap of around $70 million (M) (FY'94). This cost is assumed to be up to the end of the system development phase and does not include operations costs incurred during the MODA phase. It is interesting to note that, even though some hardware is to be procured on an "organization participation" basis, the would-be cost of procuring it has nevertheless got to be included in the final cost estimate. Similarly, the cost of the participation of a number of NASA and DOD research centers has to be included in the final accounting, even though the ETA program office will not directly pay for that. This philosophy of including all "potential" program costs into the final estimate is presumably to impart a degree of fairness to all proposals that are submitted, without biasing any proposal that would have acquired a lot of external support.

The ETA program is estimated to cost under $70M, through the system development phase which includes a 30 day post-launch period. Cost estimates include reserve and contingency margins for all phases of the program. All cost contributing elements such as personnel wages, travelling expenses and so forth are included. The incorporation of a large cost margin minimizes the risk of cost overruns.

System overall cost can be broken down in a number of ways including breakdown by program phases or by program functions. Considering cost breakdown by program phases, it is found, as expected, that almost three quarters of system costs are incurred during the system development phase. The high cost of mission operations is reflected by MODA costs approaching almost a fifth of total cost. Mission operations costs are always an issue for long missions like ETA. Moreover, there is a limit on the funding available from NASA for operations. It is up to program planners to make best use of the available funding and tailor their spending profiles such that scientific returns are maximized within the

funding constraints. In the context of the ETA mission, this issue boils down to when scientific operations should be commenced.

Funding is available for two years of nominal scientific operations and the ETA mission scenario has to be designed with regard to that constraint. Specifically, the constellation deployment and development scenario have to be designed to incorporate at least two years of optimal scientific operational conditions within the current 4 year mission lifetime. To that effect, the baseline ETA mission scenario, as discussed in Chapter 6, allows one year for constellation deployment, one year for the constellation development phase and two years of scientific operations after that. Inter-spacecraft baselines during the second year are not sufficiently large to support high accuracy GRB astrometry and hence no scientific operations are planned for this year. Requesting funding for scientific operations during this period would not result in maximum scientific return for the dollar. Instead, current planning calls for requesting operational funding support for the third and fourth years of the mission, when the constellation best supports scientific operations, resulting in maximal scientific return per dollar. Such a strategy also portrays to proposal reviewers, the ETA team's commitment to yielding scientific returns in the most cost-effective manner.

Hardware development costs are attributable to the spacecraft (carrier and microsatellites), payload and ground segment elements. The spacecraft will cost the most while ground system costs are expected to be comparatively small since infrastructure from current programs such as HETE will be utilized. Research and Development (R&D) costs will also be reduced because most of the hardware is either already in an advanced stage of development or is derived from designs already built and tested. The payload (GRB detectors and electronics) are heritaged from BATSE hardware while the spacecraft designs are derived from spacecraft buses already developed by the spacecraft contractor.

The NASA MIDEX program for which ETA is being proposed includes the provision of launch vehicle for the mission. The support package will include the availability of the MEDLITE family of launchers which will be procured by NASA. Launch vehicle costs are thus not included in the $70M cost constraint. ETA spacecraft will be launched aboard the DeltaLite version of the MEDLITE launcher family.

Looking at program costs from the perspective of programmatic functions, it is found that almost 10% of total cost is taken up by program management and systems engineering functions. This highlights the importance of these functions for the success of the program.

In summary, the ETA program cost budget is well within the cost cap specified by NASA and the risk of overruns is minimized by the inclusion of cost margins for each cost element, as well as other program-related cost management measures.

8.3 Risk

In order to compete favourably against other program proposals, the ETA program has to demonstrate to proposal reviewers that the mission is manageable with respect to technical, cost and schedule risk, to name the major ones. ETA system definition to date has incorporated a number of aspects within the program structure to mitigate risk in the areas of performance, technology, cost, schedule and management. It is important to realize that these areas are inter-related and there is a tendency that an overrun in one area may cause an overrun in another. Some of the salient issues associated with the various areas of risk are discussed below.

- **Performance**
  While the aim of any mission is to maximize return, there is always the need to demonstrate the ability to descope the mission and still manage reasonable scientific returns. ETA has incorporated this descoping facet into the mission design by adopting a constellation deployment strategy which can provide baselines for a minimum science mission in which science operations are commenced a year earlier than planned. The adoption of the retrograde thrusting strategy, as discussed in Chapter 6, can provide minimum baselines early into the mission if there is a need to descope the mission in terms of time. Error box sizes will not be as small as the baseline mission, but will nevertheless be better than current systems. There is also sufficient flexibility to achieve similar performance if there is a need to reduce the number of microsatellites within the constellation. Furthermore, the ability of the SPT-70 to provide similar levels of performance over a wide range of operating conditions will ensure that performance is not substantially degraded during contingency periods.

- **Technology**
  Technology risk is mitigated by the use of hardware that has already been proven in space. The GRB detectors are based on the highly successful BATSE detectors developed for CGRO [4]. The carrier and microsatellite buses are derived from flight proven platforms developed over the years by the spacecraft contractor. Even the selection of the Russian SPT-70 electric thruster is backed by extended flight experience of over 20 years as well as extensive testing, both in Russia and in the US. The ground system is designed around existing facilities which will require only standard equipment upgrades. There is a large mass margin which will absorb mass increase due to design growth.

- **Cost**
  The risk associated with cost overruns is always of prime concern and ETA program planners have managed this risk in a number of ways. First and foremost, the inclusion of margins in the cost budget provides a buffer against cost escalation. Contracts for hardware development

and production will be administered in a manner as to cut down the risk of cost overruns on the part of hardware contractors. More often than not, cost overruns can be attributed to the inability of program management to accurately estimate program costs in the early stages of program development. To this effect, ETA program planners have used a cost-estimation methodology that has been successfully proven for the HETE program and is an accepted accounting method from the perspective of NASA [4]. The utilization of this accounting method is justified since the program management philosophy adopted for ETA is similar to the HETE program. This should provide an accurate estimation of program cost and minimize the risk of cost overruns attributable to inaccurate cost estimation Another factor that contributes to the reduction of cost-associated risk is the use of flight proven hardware which does not incur normal research and development (R&D) costs. The most expensive hardware elements namely, the GRB detectors, the carrier spacecraft and the microsatellites all have a design heritage and there should thus be minimal incurrence of R&D costs.

- **Schedule**
  Schedule overruns have wide ranging impacts on the rest of the system. While schedule slips delay mission operations and the acquisition of science data, they ultimately lead to overruns in cost as well. The system development phase is most prone to schedule overruns and in order to minimize this, a 3 month contingency period has been included in the program schedule. Delays in hardware procurement or system integration and testing can be buffered by the contingency period. Furthermore, selection of the prime and subcontractors took into account their ability to deliver hardware on schedule. The program schedule for ETA was developed based on inputs from these contractors on how long it would take to develop, integrate and test the various hardware elements. Utilization of flight proven hardware should reduce the chances of hardware procurement delays.

- **Management**
  Program management techniques play a crucial role in the accomplishment of program objectives. The management of a complex program such as ETA, where the efforts of over ten different organizations have to be coordinated, requires an effective management philosophy which can keep the program on cost and schedule. The ETA program will be managed in the Principal Investigator (PI) mode. The PI mode essentially vests full program responsibility on a Principal Investigator who has full authority over all program-related issues. While details of this unique management approach are presented briefly in the next section, suffice it to say here that the PI mode has been successfully implemented by the same ETA/MIT management team for NASA's HETE program.

8.4 Program Management

Over the years, MIT's Center for Space Research (CSR) has managed a large number of space projects for NASA, ranging from the plasma instruments on the Voyager interplanetary spacecraft to CCD instruments on the Adavanced X-Ray Astrophysical Facility (AXAF). Moreover, complete management of the HETE program in the PI mode serve to demonstrate the expertise of CSR in managing complex space programs such as ETA.

ETA is planned to be managed in PI mode, whereby a single Principal Investigator controls and oversees the entire program with the assistance of a designated Program Manager. The unique aspect of PI mode is that, while funding for the ETA program comes from NASA, the PI is given the authority over all program issues, including contracts, system development and budgetary control. PI mode is advantageous in that it frees program management from complex and often time-consuming processes with NASA and other organizations which only delay program development. Of course, PI mode incorporates both NASA and other peer reviews into the overall management but adoption of PI mode streamlines a lot of processes and as a result, the program is more effectively controlled in all aspects. HETE is one program which employs PI mode and is being managed by the same CSR team that will manage ETA. In that regard, ETA stands to gain a lot from the HETE experience. Some of the pertinent issues related to ETA program management are briefly discussed below.

- The participation of the large number of organizations ranging from universities, commercial companies, government research laboratories and NASA centers will be managed by MIT/CSR through contracts, Memoranda of Understanding (MOU), Inter-Agency Transfer of Funds (ATF) and Space Act Agreements. It is not within the scope of this thesis to go into the details of these contractual issues. These agreements will provide for the formal transfer of funds, facilities and expertise, as necessitated by ETA program requirements.

- A team of co-investigators has been selected, the members of which will assist the PI and PM in carrying out the numerous responsibilities of the ETA program. These include instrument development, mission planning, educational outreach and data analysis.

- An ETA program office will be set up at both MIT and the prime contractor's facilities to coordinate ETA efforts. Even though the prime contractor will be responsible for spacecraft development, the PI will oversee the effort with the assistance of the PM. There will also be peer reviews at all stages of spacecraft development.

- Design reviews will be conducted at appropriate stages of system development and these will include both ETA management and NASA reviewers.

Chapter 9

Summary and Conclusions

This chapter summarizes the findings, design results, conclusions and recommendations as derived from the analysis and design work presented in this thesis. The scope of the project is reiterated briefly. Systems engineering was one of the prime study areas and accomplishments in this important area are discussed. The findings of the constellation analysis are summarized. Pertinent issues related to the implementation of the SPT-70 are addressed. A summary of the baseline ETA mission scenario, developed as a result of this project, is presented before thesis accomplishments and general lessons learnt during the course of this study are discussed in the form of final remarks. Suggestions for further work are included for the benefit of future design work for the ETA mission.

9.1 Scope of Study

The work presented in this thesis was performed to assist the ETA planning team in developing a mission and system design to accomplish ETA scientific objectives. Even though the responsibilities lay mainly in the areas of constellation design and SPT-70 implementation issues, this study took the opportunity to address the ETA design problem from a systems engineering perspective.

The main objective of the thesis was thus to perform a systems analysis of the ETA mission, with primary focus on the constellation design and SPT-70 propulsion system issues. A secondary objective was to provide a system level overview of all the major aspects of the ETA program. The results of the study were expected to be

- a better understanding of the ETA system through the application of systems engineering methodologies,
- the development of an ETA mission scenario through constellation analysis and design,
- an understanding of the implementation aspects of the SPT-70 propulsion system and

- an overview of the major aspects of the ETA program.

9.2 Systems Engineering

This study has demonstrated the application of systems engineering methodologies in designing a system that meets customer requirements. The systematic derivation of system support requirements from customer (scientific) requirements enabled system design, while providing a better understanding of system requirements, capabilities and limitations.

The overall study focus was on the Systems Engineering Process, which is a subset of Systems Engineering. Specifically, the study addressed the Functional Analysis aspects of the Systems Engineering Process. The application of Functional Analysis tools was found to be very useful in defining system elements, trade options, system architecture, support requirements and interfaces.

Lower levels of the system, the constellation in this case, could be designed after requirements flowdown. Trade studies were conducted to assess available options based on a metric or figure-of-merit. The propulsion system for accomplishing system propulsive requirements was selected based on the results of a top level trade study.

Programmatic issues related to cost, schedule, risk and management were addressed to better understand the relationships between the technical and management elements of Systems Engineering.

9.3 Constellation Analysis

Simulations of carrier and microsatellite trajectories were used to develop the baseline mission scenario described previously. Trade studies were conducted to assess the impact of various design variables, using a constellation figure-of-merit directly linked to the scientific performance of the mission. Some of the major findings were as follows:

- **Number of microsatellites**
  Increasing the number of microsatellites improves overall performance. Constellations with fewer spacecraft develop faster initally but result in lower figures-of-merit later on in the mission. Six microsatellites have been selected for the baseline scenario, taking into account the minimum requirement for redundancy and a maximum number from the perspective of mass, cost and design complexity. The capability to detect and correct for timing errors was also important.

- **Number of SPT thrusters**
  Two thrusters were found to provide substantially better constellation performance than a single thruster. Even though parallel operation of the two thrusters resulted in best performance, power (and hence cost) requirements and the need for extra hardware were overriding con-

cerns. The two thrusters will be operated serially for 3,000 hours apiece.

- **Launch energy (C_3)**
  Simulations showed that constellation performance improves with increases in C_3 but the improvements diminish for C_3 values beyond 1 km^2/sec^2. The baseline scenario employs a near zero escape trajectory.

- **Thrusting direction**
  The impact of thrusting direction on constellation figure-of-merit is related to launch energy. For near-zero launch energy cases, prograde thrusting provides better overall performance while retrograde thrusting strategies provide faster constellation development in the early stages. Retrograde thrusting has been selected for the baseline for this reason, simplifying spacecraft design, since all spacecraft are closer to the Sun.

- **Distribution of available thrusting time**
  In order to achieve regular angular separations between the microsatellites, it is necessary to impart similar ΔV's to each microsatellite. Carrier spacecraft mass diminishes with each microsatellite deployment and thus thrusting times have to be decreased accordingly. A regularly spread constellation has been designed by setting the inter-microsatellite thrusting periods.

- **Sensitivity Analysis**
  A sensitivity analysis with respect to carrier and microsatellite mass was performed to assess their effects on constellation performance. It has been found that constellation development is more sensitive to changes in microsatellite mass than it is to carrier spacecraft mass.

- **Trigger satellite orbits**
  Preliminary Hill model simulations identified a candidate orbit which is stable over the mission duration and provides Earth distances in the 0.020-0.036 AU range to support high rate communications links. Application of Lissajous type orbits about the L_1 Sun-Earth libration point has been limited by the inability of the microsatellite to provide a stationkeeping ΔV of about 30 m/s over mission lifetime.

9.4 SPT-70 Issues

This study has looked at the implementation aspects of the SPT-70 and noteworthy details are discussed below.

- **Suitability of the SPT-70 for the ETA mission**
  A top level trade study conducted to assess various propulsion options

revealed that the SPT-70 is the optimal system for ETA, based on performance, mass and power requirements, cost, availability, reliability and flight heritage. Chemical systems require a launch mass beyond the capability of the DeltaLite launcher while the marginally better performance of ion engines was not enough to justify high cost and little flight experience.

- **Performance**
  The SPT-70's performance in terms of thrust, specific impulse and power requirements has been found to be ideally suited for ETA. The low thrust and power simplify mission and system design and the high specific impulse enables system launch mass to be within DeltaLite constraints. SPT performance degrades gracefully over a wide power range, allowing flexibility in mission and system design.

- **Interfaces**
  Interfaces between the thruster and Western-developed power electronics as well as propellant management systems are well defined. Power, command and telemetry interfaces of the SPT-70 system with the carrier spacecraft will require more attention in further design work.

- **Characterization of SPT-70/Spacecraft Interactions**
  Integration of the SPT-70 system on the carrier spacecraft is such as to minimize the chances of spacecraft/thruster interactions like plume contamination, sputtering and electromagnetic interference. Even though these are not deemed to be driving issues, they should nevertheless be characterized to the fullest extent possible. SPT-generated "swirl" torques will be managed by a cold gas roll control system on the spacecraft. There may be a need to size the cold gas propellant load in a more conservative manner since the "swirl" torque is not accurately known.

9.5 ETA Baseline Mission Scenario

The ETA carrier spacecraft and six microsatellites will be launched in January 2000 aboard a DeltaLite launcher, which will place the stack onto an Earth escape trajectory. The carrier spacecraft with microsatellite stack will then coast for 85 days before the SPT-70 propulsion system is fired for approximately 30 days.

The 30 day thrusting period places the carrier spacecraft on a trajectory from where the two trigger satellites are deployed into their operational orbits. The trigger satellites orbit around the Earth at ranges between 0.020-0.036 AU, which facilitate high rate communications links for rapid GRB alert capability.

Having deployed the trigger satellites, the carrier spacecraft then thrusts in the retrograde

(anti-velocity) direction for 69 days, after which the third microsatellite is deployed. Retrograde thrusting of the SPT-70 results in the carrier spacecraft getting closer to the Sun while it deploys microsatellites. The fourth, fifth and sixth microsatellites are deployed after inter-deployment thrusting periods of 58,50,43 days respectively. The shorter thrusting periods for later microsatellites are necessary to impart similar differential ΔV's in order to result in a regularly spread constellation.

After deployment of the sixth and final microsatellite about 11 months after launch, the carrier spacecraft is in a heliocentric orbit and can be utilized for post-deployment operations such as a secondary science mission or SPT-70 propulsion system testing. The post-deployment function of the carrier spacecraft is undecided as of now.

The differential ΔV's imparted to the microsatellites cause the separation of the microsatellites to increase angularly relative to each other. As a result, the constellation spreads out and begins to establish significant inter-spacecraft baselines. About two years after launch, the constellation will have developed into a configuration which provides the minimum baselines to commence nominal scientific operations.

Nominal operations will consist of GRB detection, rapid alert through the trigger satellites in the close proximity of the Earth and determination of times-of-arrival at the other microsatellites via onboard template matching. Current plans call for science operations to continue for at least two years, resulting in a nominal mission duration of four years, including the two year launch, constellation deployment and development phase. The constellation has the capability to support GRB localization measurements to high accuracy beyond the nominal mission duration if extended science operations are contemplated.

9.6 Final Remarks

This study has demonstrated the application of systems engineering methodologies in designing a system that meets customer requirements. A trade study was conducted to select the propulsion system to meet system propulsive requirements. Implementation aspects of the selected SPT-70 system have been addressed. The results of the constellation analysis have been the development of a baseline mission scenario for ETA and an understanding of constellation dynamics and impacts of design parameters. An overview of the system design has been presented with the intention of identifying the impacts of constellation analysis on hardware design. Programmatic issues such as cost, schedule, risk and management have also been discussed in the context of the ETA program.

In summary, this project has addressed the problem of space system design from a systems perspective, utilizing systems engineering methodologies to facilitate the design of a lower system level, namely the ETA constellation. The study has also provided an appreciation of the inter-relationships between system elements, while giving insights into cost, schedule, risk and other programmatic issues that are characteristic of complex space programs such as ETA.

9.7 Further Work

Time constraints, imposed on the project, did not allow a number of issues to be addressed in sufficient detail. Furthermore, the study itself identified certain aspects that need to be looked into. Some of the more important ones are highlighted below.

- **More accurate constellation simulations**
  The simulation model developed in this project was based on a number of simplifying assumptions and was sufficiently accurate for conceptual design. Further design work will require a more accurate simulation tool which models all types of perturbations.

- **Trigger satellite orbits**
  This study has identified a number of orbit options such as Lissajous orbits and Halo orbits which need to be anlyzed further. Additionally, suggestions have been made [70] to use Earth-Moon system orbits with lunar flybys; these should be analyzed as well.

- **Microsatellite stationkeeping capability**
  Certain trigger satellite orbit options had to be discarded because the current microsatellite design cannot support the small stationkeeping requirements (~30 m/s). The possibility of including more propellant onboard the microsatellite should be analyzed. The requisite stationkeeping capability would greatly simplify mission design.

- **SPT-70 Thrusting strategies**
  Optimal thrust direction control laws can be devised and a more detailed approach to the optimization of thrusting strategies is required. SPT-70 performance variations need to be characterized and incorporated to a greater level of detail.

- **"Swirl" torque control propellant**
  The current propellant load sizing is based on the assumption that the equivalent "swirl" thrust is 2% of nominal thrust, whereas it can be as much as 8% [42,57]. This wide range can significantly affect propellant mass. A more accurate estimation of this parameter is required and the propellant load for the carrier spacecraft designed accordingly.

- **SPT-70 testing**
  Post-deployment operations of the carrier spacecraft may include dedicated SPT-70 system testing. Experiments should be designed for long duration thrusting, cyclic endurance performance, plume characterization, surface contamination and electromagnetic interference characterization. Another interesting experiment would be with regard to high voltage, direct solar array power for the SPT-70 [78]. This could potentially reduce power electronics mass.

Appendix A

Communications Link Analysis

This appendix presents a brief overview of communications link theory, as applicable to space systems. Specifically, the focus is on the link equation/link budget. It is easy to derive the link equation and, since derivations are given in all standard texts on communications and space systems engineering [67,68], this appendix only deals with the link equation from the applications perspective. The reader is referred to the listed texts for details.

When attempting to transmit information, it is inevitable that the signal wil be corrupted by unwanted signals, more commonly known as "noise". The parameter most commonly used to characterize communications signals is the ratio of signal power to signal noise or signal-to-noise (S/N) ratio. One would ideally like to maximize signal power, while minimizing the level of noise in the signal, that is maximize S/N so as to retrieve the information from the composite signal (information plus noise). An equivalent term for S/N is the carrier-to-noise (C/N) ratio which is mathematically the same as S/N; C/N is just used to indicate that the information signal is modulated onto a carrier signal and hence, it is actually the carrier signal which is being considered.

It can be shown that the C/N ratio of a signal received at the receiver end of a transmitter/ receiver pair is given by [67,68]

$$\left(\frac{C}{N}\right)_{recd} = \frac{P_T G_T G_R}{kTB}\left(\frac{\lambda}{4\pi S}\right)^2\left(\frac{1}{L}\right) \qquad \text{Eqn (A-1)}$$

where the subscripts T and R denote Transmitter and Receiver ends of the communications link with the main terms defined as

P_T : Transmitted RF power
G_T : Gain of transmitting antenna

G_R : Gain of receiving antenna
λ : Wavelength of carrier signal
k : Boltzmann's constant (1.38×10^{-23} J/K)
T : Noise temperature of the receiver
B : Signal bandwidth
S : Distance between transmitter and receiver
L : Losses in the link attributable to any source other than free space loss.

Equation (A-1) is the basic form of what is commonly termed the "link equation". Signal power is directly proportional to the transmitted RF power and transmitting and receiving antenna gains and inversely proportional to losses. The non-dimensional term, $(\lambda/4\pi S)^2$, represents the isotropic spreading of signal power over the distance and is termed "free space loss". Noise power in the composite signal is represented by the product, kTB, and is a function of signal bandwidth. It is sometimes convenient to express signal strength in terms of the carrier-to-noise density (C/N_0) ratio, which is simply the product of C/N and signal bandwidth, and is essentially a normalization with respect to bandwidth. C/N_0 is thus given by

$$\left(\frac{C}{N_o}\right)_{recd} = \frac{P_T G_T G_R}{kT}\left(\frac{\lambda}{4\pi S}\right)^2\left(\frac{1}{L}\right) \qquad \text{Eqn (A-2)}$$

The use of C/N_0 is especially convenient in digital communications systems since it can be related to datarates and modulation schemes. Before discussing the important terms in the link equation, it is helpful to rewrite Equation (A-2) as

$$\left(\frac{C}{N_o}\right)_{recd} = (P_T G_T)\left(\frac{G_R}{T}\right)\left(\frac{\lambda}{4\pi S}\right)^2\left(\frac{1}{k}\right)\left(\frac{1}{L}\right) \qquad \text{Eqn (A-3)}$$

A brief description of the terms is given below from the standpoint of both the uplink (ground-to-spacecraft) and downlink (spacecraft-to-ground).

- **($P_T G_T$): Equivalent Isotropic Radiated Power (EIRP)**
  EIRP is a term characterizing the contribution of the transmitting system to the overall link. A spacecraft with a high power transmitter and high gain antenna will have a high EIRP. EIRP is very important from the perspective of spacecraft design. Top level link requirements will normally specify an EIRP requirement and it is then upto the spacecraft designer to trade off spacecraft power against antenna types and sizes (in terms of gain). EIRP on the uplink is not so much a concern for the ETA mission because the ground stations will normally have kilowatt level transmitters as well as large antennas.

- **(G_R/T): Receiver system figure-of-merit**
  This is a measure of the performance of the receiving system. G/T is maximized by having high gain antennas and low-noise amplifiers in the receiver. Ground stations will usually have these hardware elements and so G/T on the downlink will be high. G/T is more an issue again for the spacecraft on the uplink due to limitations of spacecraft design (mass, volume and so forth). For example, the spacecraft cannot have a cryogenically cooled parametric amplifier like a ground station would. However, this difficulty is slightly alleviated by the low datarates on the uplink.

- **$(\lambda/4\pi S)^2$: Free Space Loss**
  Due to the interplanetary distances involved, space losses for ETA links will be high but this is slightly offset by the use of high frequencies (X-Band).

- **(1/k): Inverse of Boltzmann's constant**
  Calculation of noise power in the signal leads to the inclusion of this thermodynamic constant.

- **(1/L): Loss terms**
  These constitute all loss sources with the exception of free space loss. Some of the major ones include atmospheric attenuation, circuit losses, polarization losses, demodulation losses and other hardware-related sources. Because some of these losses are highly dependent on specific hardware components, top level link analyses usually assume conservative values for these sources, with refinements as the design gets more defined.

In order to incorporate datarates and modulation schemes into the link equation, the following expression is utilized, linking required C/N_0 to datarate and modulation scheme.

$$\left(\frac{C}{N_o}\right)_{reqd} = \left(\frac{E_b}{N_o}\right) R \qquad \text{Eqn (A-4)}$$

where R is the datarate and E_b/N_0 is the Energy per bit-to-noise density ratio. The choice of modulation scheme and Bit Error Rate (BER) will specify the minimum E_b/N_0 that is required. BER is a measure of the quality of the link in terms of errors in the information. Thus, a BER of 10^{-5} means that only one bit in one hundred thousand bits of information is in error. A lower BER signifies high quality data, but also requires a higher E_b/N_0 which translates into higher C/N_0. Transmission of Gamma Ray Burst templates will require a low BER of about 10^{-6} to maintain accuracy. The E_b/N_0 required will also depend on the

selected modulation scheme. Schemes which incorporate error correction coding will require lower E_b/N_0 but the penalty is the larger bandwidth. There is hence a trade between E_b/N_0 and bandwidth when choosing a modulation scheme.

Combining Equations (A-3) and (A-4) and incorporating a margin term yields

$$\left(\frac{E_b}{N_o}\right) R \text{ (Margin)} = (P_T G_T)\left(\frac{G_R}{T}\right)\left(\frac{\lambda}{4\pi S}\right)^2\left(\frac{1}{k}\right)\left(\frac{1}{L}\right) \qquad \text{Eqn (A-5)}$$

The margin term is the difference between the received and required C/N_0 and the link budget basically presents Equation (A-5) in an orderly fashion. Communications analysis is generally done in logarithmic or decibel units where the different terms can be added or subtracted. The decibel form of Equation (A-5) becomes

$$\left(\frac{E_b}{N_o}\right) + R + Margin = 10Log_{10}(P_T G_T) + 10Log_{10}\left(\frac{G_R}{T}\right) + 20Log_{10}\left(\frac{\lambda}{4\pi S}\right) - 10Log_{10}(kL) \qquad \text{Eqn (A-6)}$$

From the perspective of constellation or general mission design, free space loss is the term which is of major concern. Assuming that other link design parameters remain the same, the goal is to minimize free space losses by minimizing distance between spacecraft and ground station. A good example of this is the trigger satellite orbit design which is motivated by the need for a high rate communications link.

On the other hand, link analysis from the standpoint of spacecraft design normally involves trading off EIRP, G/T, E_b/N_0, datarate and available bandwidth. In the case of ETA, communications system design is further complicated by the variations in Earth range.

References

[1] G. R. Ricker, "The Energetic Transient Array - A Network of 'Space Buoys' in Solar Orbit for Observations of Gamma Ray Bursts", *High Energy Astrophysics in the 21st Century*, American Institute of Physics, 1990, p375-387.

[2] G. R. Ricker et al, "A Study of the Feasibility of a Gamma Ray Burst Astrometry Mission, the Energetic Transient Array (ETA)", Proposal for New Mission Concepts in Astrophysics, NRA 94-OSS-15, 1994.

[3] D. J. Kerrisk, Proceedings of the 6th AFOSR Symposium on Advanced Propulsion Concepts, May 1971.

[4] G. R. Ricker et al, "Energetic Transient Array (ETA) Gamma-ray Burst Astrometry Mission", Proposal in response to NASA AO-95-OSS-02, June 1995.

[5] K. Hurley et al, "Precise localizations and counterpart searches of GRBs from the 2nd Interplanetary Network", *Gamma Ray Bursts*, AIP Conference Proceedings 307, 2nd Workshop, Oct 1993.

[6] K. Hurley, "What are Gamma Ray Bursters?", *Sky & Telescope*, Aug 1990, p143-147.

[7] C. Graziani & D. Q. Lamb, "Evidence for 2 distinct morphological classes of Gamma Ray Bursts", *Gamma Ray Bursts*, AIP Conference Proceedings 307, 2nd Workshop, Oct 1993.

[8] J. C. Higden & R. E. Lingenfelter, "Gamma Ray Bursts", *Annual Review of Astronomy and Astrophysics*, 1990, 28:401-36.

[9] C. S. Powell, "Inconstant Cosmos", *Scientific American*, May 1993, p 110-118.

[10] K. Hurley, "Probing the Gamma Ray Sky", *Sky & Telescope*, Dec 1992, p 631-636.

[11] D. H. Hartmann, "Searching for a Galactic Origin of Gamma Ray Bursts", *Gamma Ray Bursts*, AIP Conference Proceedings 307, 2nd Workshop, Oct 1993.

[12] B. E. Schaefer, "Search for Gamma Ray Burst Counterparts", *Gamma Ray Bursts*, AIP Conference Proceedings 307, 2nd Workshop, Oct 1993.

[13] C. Meegan, "The Mystery that won't go away", *Sky & Telescope*, Aug 1994, p 28-32.

[14] P. V. R. Murthy & A. W. Wolfendale, *Gamma Ray Astronomy*, Cambridge Astro-

physics Series No. 22, 1993.

[15] K. Hurley & M. Sommer, "Timing Accuracy of the Ulysses GRB Experiment", *Gamma Ray Bursts*, AIP Conference Proceedings 307, 2nd Workshop, Oct 1993.

[16] K. Hurley, "Cross-correlating Gamma Ray Burst Time Histories", *Gamma Ray Bursts*, AIP Conference Proceedings 307, 2nd Workshop, Oct 1993.

[17] J. P. Doty, Center for Space Research , Massachusetts Institute of Technology, Personal Communication, March 1995.

[18] E. Rechtin, *Systems Architecting: Creating and Building Complex Systems*, Prentice Hall, 1991.

[19] P. L. Sutcliffe, "Systems Engineering on the 777 and Future Boeing Airplanes", Boeing Report, 1992.

[20] W. L. Chapman et al, *Engineering Modeling and Design*, CRC Press, 1992.

[21] 16.982 Class notes, Aerospace Systems Engineering and Product Development course, Department of Aeronautics and Astronautics, Massachusetts Institute of Technology, Fall 1994.

[22] "Project IRIS", 16.89 Space Systems Engineering class project report, Department of Aeronautics and Astronautics, Massachusetts Institute of Technology, Spring 1995.

[23] J. Denecke & B. Patel, "IRIS Global Communications", Project Report, 16.982 Aerospace Systems Engineering and Product Development course, Department of Aeronautics and Astronautics, Massachusetts Institute of Technology, Fall 1994.

[24] B. Milam, MIDEX Launch Vehicle Support Document, NASA Goddard Space Flight Center, April 1995.

[25] H. Alexander, Orbital Sciences Corporation, Personal Communication, May 1995.

[26] G. W. Butler, R. J. Cassady, D. Q. King, "Directions for Arcjet Technology Development", Olin Aerospace Company, 1995.

[27] J. R. Beattie, J. D. Williams, R. R. Robson, "Flight Qualification of an 18 mN Xenon Ion Thruster", International Electric Propulsion Conference, IEPC 93-106, 1993.

[28] Andrew Wilson (editor), "Jane's Space Directory", 10th Edition, 1994-1995.

[29] M. Day & W. Rogers, "SPT-100 Subsystem Development Status and Plan", AIAA Paper No. 94-2853, 1994.

[30] M. Martinez-Sanchez, Professor in Department of Aeronautics and Astronautics, Massachusetts Institute of Technology, Personal Communication, March 1995.

[31] Atlantic Research Corporation Information on SPT, 1994.

[32] D. Barnhart, "EPOCH: Electric Propulsion Operational Characterization Experiment", AIAA Paper No. 92-3196, 1992.

[33] D. Barnhart, J. M. McCombe, D. L. Tilley, "Electric Propulsion Integration Activities on the MSTI Spacecraft", International Electric Propulsion Conference, IEPC 93-011, 1993.

[34] J. W. Barnett, "A Review of Soviet Plasma Engine Development", AIAA Paper No. 90-2600.

[35] D. J. Kerrisk, "Planetary Mission Characteristics of Solar Electric Propulsion Systems", Proceedings of the 6th AFOSR Symposium on Advanced Propulsion Concepts", May 1971.

[36] J. Lazar & J. P. Mullin, "A Review of the Role of Electric Propulsion", AIAA paper No. 66-1025.

[37] W. R. Kerslake & L. R. Ignaczak, "Development and Flight History of SERT II Spacecraft", AIAA Paper No. 92-3516.

[38] H. Bassner et al, "Ion Propulsion Package IPP for N/S Stationkeeping of the ARTEMIS Satellite", International Electric Propulsion Conference, IEPC 91-055, 1991.

[39] Advanced Space Propulsion class notes, Department of Aeronautics and Astronautics, Massachusetts Institute of Technology, Spring 1994.

[40] M. L. Day et al, "INTELSAT VII Ion Propulsion Subsystem Implementation Study", AIAA Paper No. 90-2550.

[41] C. Clauss, Atlantic Research Corporation, ETA meeting, November 1994.

[42] J. R. Brophy, "Stationary Plasma Thruster Evaluation in Russia", JPL Publication 92-4, March 15, 1992.

[43] C. E. Garner et al, "Cyclic Endurance Test of a SPT-100 Stationary Plasma Thruster", 3rd Russian-German Conference on Electric Propulsion Engines and Their Technical Applications, July 1993.

[44] J. R. Wetch, J. L. Lawless, A. S. Koroteev, "Application and Review of the Development of the Closed Drift Hall Thruster", International Electric Propulsion Confer-

ence, IEPC 91-149, 1991.

[45] A. I. Bugrova et al, "Physical Processes and Characteristics of Stationary Plasma Thrusters with closed Electron Drift", International Electric Propulsion Conference, IEPC 91-079, 1991.

[46] V. M. Gavryushin et al, "Study of the Effect of Magnetic Field Variation, Channel Geometry Change and its Walls Contamination Upon the SPT Performance", AIAA Paper No. 94-2858.

[47] C. Clauss, Atlantic Research Corporation, 1995.

[48] D. Tilley, Personal Communication, Phillips Laboratory, Edwards AFB, May-June 1995.

[49] J. A. Hamley, G. M. Hill, J. M. Sankovic, "Power Electronics Development for the SPT-100 Thruster", NASA Technical Memorandum 106488, Sept 1993.

[50] T. Randolph et al, "Mitigation of Discharge Oscillations in the Stationary Plasma Thruster", AIAA Paper No. 94-2857.

[51] G. Fischer et al, "Design of a High Efficiency Power Processor for the Russian Stationary Plasma Thruster", International Electric Propulsion Conference, IEPC 93-043, 1993.

[52] C. E. Garner et al, "A 5730 hr Cyclic Endurance Test of the SPT-100", AIAA Paper No. 95-2667.

[53] K. N. Kozubsky et al, "Plan and Status of the Development and Qualification Program for the Stationary Plasma Thruster", AIAA Paper No. 93-1787.

[54] A. C. Tribble et al, "Analysis of Spacecraft-Thruster Interactions for the SPT-70 and SPT-100 Stationary Plasma Thrusters", AIAA Paper No. 94-0330.

[55] T. Randolph, E. Pencil, D. Manzella, "Far-Field Contamination and Sputtering of the Stationary Plasma Thruster", AIAA Paper No. 94-2855.

[56] S. K. Absalamov et al, "Measurement of Plasma Parameters in the Stationary Plasma Thruster (SPT-100) Plume and its effect on Spacecraft Components", AIAA Paper No. 92-3156.

[57] K. N. Kozubsky et al, "Disturbance Torques Generated by the Stationary Plasma Thruster", AIAA Paper No. 93-2394.

[58] J. S. Sovey et al, "Electromagnetic Emission Experiences Using Electric Propulsion Systems", *Journal of Propulsion*, Vol. 5 No. 5, 1987, p 534-547.

[59] R. Myers, NASA Lewis Research Center, ETA Videoconference, 12 June 1995.

[60] J. Dickens et al, "Impact of Hall Thrusters on Communication System Phase Noise", AIAA Paper No. 95-2929.

[61] R. Battin, *An Introduction to the Mathematics and Methods of Astrodynamics*, AIAA Education Series, 1987.

[62] G. Horvat, NASA Lewis Research Center, Personal Communication, June 1995.

[63] R. R. Bate, D. D. Mueller, J. E. White, *Fundamentals of Astrodynamics*, Dover Publications, 1971.

[64] J. E. Prussing, B. A. Conway, *Orbital Mechanics*, Oxford University Press, 1993.

[65] Rimrott, Introductory *Orbit Dynamics*, Braunschweig, Vieweg, 1989.

[66] H. Alexander, Orbital Sciences Corporation, Personal Communication, April 1995.

[67] W. J. Larson & J. R. Wertz (editors), *Space Mission Analysis and Design*, Microcosm Inc, 1992.

[68] G. D. Gordon & W. L. Morgan, *Principles of Communications Satellites*, John Wiley, 1993.

[69] P. Ford, ETA Meeting, 18th April 1995.

[70] G. Horvat, NASA Lewis Research Center, July 95.

[71] M. Lo, "The Application of Lissajous Orbits for the SIRTF Mission", *Advances in the Astronautical Sciences*, AAS 91-521, 1991.

[72] R. W. Farquhar et al, "Mission Design for a Halo Orbiter of the Earth", *Journal of Spacecraft*, Vol 14 No. 3, 1976.

[73] D. L. Richardson, "Halo Orbit Formulation for the ISEE-3 Mission", *Journal of Guidance and Control*, Vol 3 No. 6, Nov-Dec 1980.

[74] R. W. Farquhar et al, "Trajectories and Orbital Maneuvers for the First Libration-Point Satellite", *Journal of Guidance and Control*, Vol 3 No. 6, Nov-Dec 1980.

[75] S. Stalos et al, "Optimum Transfer to a Large-Amplitude Halo Orbit for the Solar and Heliospheric Observatory (SOHO) Spacecraft", *Advances in Astronautical Sciences*, AAS 93-294, 1993.

[76] M. Martinez-Sanchez, Professor in Department of Aeronautics and Astronautics, Massachusetts Institute of Technology, Personal Communication, May-July 1995.

[77] H. Alexander, Orbital Sciences Corporation, Personal Communication, July 1995.

[78] R. R. Lovell, Visiting Professor, Department of Aeronautics and Astronautics, Massachusetts Institute of Technology, Personal Communication, April 1995.

2556-30